ISSN 1881-7815 Online ISSN 1881-7823

BST
BioScience Trends

Volume 17, Number 6
December, 2023

IRCA
BSSA

IACMHR

www.biosciencetrends.com

BST
BioScience Trends

ISSN: 1881-7815
Online ISSN: 1881-7823
CODEN: BTIRCZ
Issues/Year: 6
Language: English
Publisher: IACMHR Co., Ltd.

BioScience Trends is one of a series of peer-reviewed journals of the International Research and Cooperation Association for Bio & Socio-Sciences Advancement (IRCA-BSSA) Group. It is published bimonthly by the International Advancement Center for Medicine & Health Research Co., Ltd. (IACMHR Co., Ltd.) and supported by the IRCA-BSSA.

BioScience Trends devotes to publishing the latest and most exciting advances in scientific research. Articles cover fields of life science such as biochemistry, molecular biology, clinical research, public health, medical care system, and social science in order to encourage cooperation and exchange among scientists and clinical researchers.

BioScience Trends publishes Original Articles, Brief Reports, Reviews, Policy Forum articles, Communications, Editorials, News, and Letters on all aspects of the field of life science. All contributions should seek to promote international collaboration.

Editorial Board

Editorial and Head Office

Pearl City Koishikawa 603,
2-4-5 Kasuga, Bunkyo-ku, Tokyo 112-0003, Japan
E-mail: office@biosciencetrends.com

BioScience Trends

Editorial and Head Office

Pearl City Koishikawa 603, 2-4-5 Kasuga, Bunkyo-ku,
Tokyo 112-0003, Japan

E-mail: office@biosciencetrends.com
URL: www.biosciencetrends.com

Editorial Board Members

CONTENTS

Volume 17, Number 6, 2023

Review

Original Article

Brief Report

Correspondence

Corrigendum

Review

DOI: 10.5582/bst.2023.01322

Conversion therapy for initially unresectable hepatocellular carcinoma: Current status and prospects

Ya-nan Ma[1,2], Xuemei Jiang[1], Hui Liu[3], Peipei Song[2,*], Wei Tang[4,5]

[1] Department of Gastroenterology, Hainan General Hospital, Hainan Affiliated Hospital of Hainan Medical University, Haikou, China;
[2] Center for Clinical Sciences, National Center for Global Health and Medicine, Tokyo, Japan;
[3] Department of Interventional Radiology, Haikou Affiliated Hospital of Central South University Xiangya School of Medicine, Haikou, China;
[4] International Health Care Center, National Center for Global Health and Medicine, Tokyo, Japan;
[5] Haikou Affiliated Hospital of Central South University Xiangya School of Medicine, Haikou, China.

SUMMARY Research has shown that locoregional and/or systemic treatments can reduce the tumor stage, enabling radical surgical resection in patients with initially unresectable hepatocellular carcinoma. This is referred to as conversion therapy. Patients who undergo conversion therapy followed by curative surgery experience a significant survival benefit compared to those who receive chemotherapy alone, those who are successfully downstaged with conversion therapy but not treated with surgery, or those who are treated with upfront surgery. Several treatments have been studied as conversion therapy. However, the success rate of conversion varies greatly, ranging from 0.8% to 60%. Combined locoregional plus systemic conversion therapy has demonstrated significant clinical advantages, with a conversion rate of up to 60%, an objective remission rate of 96% for patients, and a disease control rate of up to 100%. However, patients who underwent conversion therapy experienced significantly more complications than those who underwent direct LR without conversion therapy. Conversion therapy can cause hepatotoxicity, bone marrow suppression, local adhesions, increased fragility of blood vessels and liver tissues, and hepatic edema, which can increase the difficulty of surgery. In addition, criteria need to be established to evaluate the efficacy of conversion therapy and subsequent treatment. Further clinical evidence in this area is urgently needed.

Keywords TACE, TARE, TKI, immunotherapy, clinical trial, adjuvant therapy

1. Introduction

Hepatocellular carcinoma (HCC) is the most common primary liver malignancy and the third leading cause of cancer-related deaths worldwide. The majority of HCC cases occur in Asian countries (*1*). Treatment allocation is a critical step in managing patients with HCC due to the high heterogeneity of the disease at the clinical, pathologic, and molecular levels. Surgical resection is considered the most effective treatment for primary HCC. However, many patients may not be eligible for liver resection (LR) initially due to anatomical limitations, multifocal disease, insufficient functional hepatic reserve, extrahepatic metastases, or comorbidities (*2*). Unresectable hepatocellular carcinoma (uHCC) is defined as HCC confined to the liver but not suitable for surgical or radical treatment, according to the latest guidelines worldwide. The treatment of uHCC remains a challenge in this field.

Conversion therapy is a treatment aimed at downstaging initial uHCC to resectable HCC, providing the opportunity for subsequent curative resection (*3,4*). According to one study, patients who underwent a liver resection (LR) after tumor downstaging had a 5-year survival rate ranging from 24.9% to 57% (*5*). According to recent studies, conversion therapy has been found to increase tumor-free survival (TFS) and overall survival (OS) of patients with uHCC. However, the conversion rate from unresectable to resectable disease varies widely, ranging from 0.8% to 60% (Table 1). The surgical conversion rate with locoregional therapy alone ranges from 5.6% to 28.6%, that with systemic therapy alone ranges from 4.9% to 52%, and that with combined locoregional and systemic therapy ranges from 12% to 60%. Conversion therapy for HCC is performed in Asia with reported conversion rates ranging from 0.8% to 60% in China, 6.8% to 20% in South Korea, and 4.6% to 31.8% in Japan. In the US, locoregional or systemic therapy conversion rates ranged from 9% to 33%. Transarterial radioembolization (TARE) conversion rates

Table 1. Clinical trials on conversion therapy for initially unresectable hepatocellular carcinoma

District	Conversion rate	Conversion therapy	Study design	Patients	ORR	DCR	Median PFS	Median OS
China								
Zhang *et al.* (*6*)	60.0%	Angiogenesis inhibitors+PD-1 inhibitors + HAIC (FOLFOX)	Retrospective	BCLC C	96.0%	100%	NR	NR
He *et al.* (*7*)	57.6%	PVE+TACE	Retrospective	Unresectable HCC (≥5 cm) with ipsilateral PVTT	N/A	N/A	8 months	29.4 months
Zeng *et al.* (*8*)	53%	Hepatic artery ligation+intra-arterial 131I-Hepama-1 MAb	Retrospective	Unresectable HCC	72%	N/A	N/A	N/A
Wu *et al.* (*9*)	53%	Lenvatinib+PD-1 inhibitors+TACE	Retrospective	BCLC A/B/C	77.4%	91.9%	NR	NR
Zhang *et al.* (*10*)	52.6%	TACE+PD-1 inhibitors+TKI	Prospective, multi-center	BCLC B/C	84.2%	94.7%	12 months (91.7%)	12 months (96.4%)
Zhang *et al.* (*11*)	51.0%	Lenvatinib+PD-1 inhibitor	Non-randomized, phase IV	BCLC B/C	53.1%	N/A	12 months	12 months
Qu *et al.* (*12*)	50%	Lenvatinib+TACE+toripalimab	Retrospective	BCLC B/C	76.7%	80%	NR	NR
Li *et al.* (*13*)	48.8%	HAIC (FOLFOX)+TACE	Retrospective	BCLC A/B	14.6%	92.7%	NR	NR
Liu *et al.* (*14*)	46.7%	HAIC (FOLFOX)+sintilimab+IBI305	Prospective, single-arm, phase-II	CNLC IIb/IIIa/IIIb	66.7%	N/A	N/A	N/A
Liu *et al.* (*14*)	42.4%,	Lenvatinib+PD-1 inhibitors	Prospective	Unresectable HCC	45.5%	N/A	N/A	N/A
Gan *et al.* (*15*)	40.5%	Lenvatinib+sintilimab+arterially directed therapy	Retrospective	Potentially resectable HCC	75.7%	86.5%	25 months	NR
Wu *et al.* (*16*)	38.7%	TACE+lenvatinib+PD-1 inhibitors	Retrospective	BCLC A/B/C	N/A	N/A	NR	NR
Li *et al.* (*17*)	34.0%	Lenvatinib+TACE+PD-1 inhibitors	Retrospective	BCLC A/B/C	87.2%	93.6%	NR	NR
Wang *et al.* (*18*)	33%	Sintilimab+lenvatinib	Prospective, single-arm, phase-II	BCLC B/C	35.0%	94.4%	NR	NR
Yi *et al.* (*19*)	28%	Lenvatinib+PD-1 inhibitors	Retrospective	BCLC A /B/C	50%	100%	12 months (61.6%)	12 months (95.7%)
Chen *et al.* (*20*)	25.7%	Pembrolizumab+lenvatinib+TACE	Retrospective	BCLC B /C	47.1%	70.0%	9.2 months	18.1 months
Zhu *et al.* (*21*)	23.8%	TKI+ PD-1 inhibitor	Retrospective	BCLC B /C	49.5%	79.2%	12 months (75%)	12 months (95.8%)
Zeng *et al.* (*8*)	23%	TACE+EBRT	Retrospective	Unresectable HCC	86%	N/A	N/A	N/A
Qu *et al.* (*12*)	19%	Lenvatinib+TACE	Retrospective	BCLC B/C	47.7%	57.2%	8 months	20.6 months
Luo *et al.* (*22*)	18.6%	HAIC+PD-1 inhibitor+TKI	Retrospective	BCLC B/C	57.2%	89.7%	9.7 months	N/A
Sun *et al.* (*23*)	18.3%	PD-1 inhibitor+TKI	Prospective, cohort	BCLC A /B/C	N/A	N/A	N/A	N/A
Leung *et al.* (*24*)	18%	PIAF	Prospective, Phase II	Advanced HCC	N/A	N/A	N/A	N/A
He *et al.* (*25*)	16.9%	Lenvatinib+ PD-1+HAIC (FOLFOX)	Retrospective	BCLC C	67.6%	90.1%	11.1 months	NR
Zhu *et al.* (*26*)	15.9%	PD-1 inhibitor+TKI	Retrospective	BCLC A /B/C	N/A	N/A	NR	NR
He *et al.* (*27*)	12.8%	Sorafenib+HAIC (FOLFOX)	Randomized, open-label	BCLC C	40.8%	N/A	7.03 months	13.7 months
Chiang *et al.* (*28*)	12%	TACE+SBRT+avelumab	Single-arm, phase 2 trial	Locally advanced HCC	N/A	N/A	N/A	N/A
Lau *et al.* (*3*)	11.8%	Doxorubicin or doxorubicin +TARE (yttrium-90)	Retrospective	Unresectable HCC	N/A	N/A	N/A	N/A
Li *et al.* (*29*)	11.5%	TACE+camrelizumab + TKI	Retrospective	BCLC B/C	71.3%	89.7%	10.5 months	NR
Chen *et al.* (*20*)	11.1%	Lenvatinib+TACE	Retrospective	BCLC B/C	27.8%	52.8%	5.5 months	14.1 months
Zhang *et al.* (*30*)	9.8%	TACE	Retrospective	Unresectable HCC	100%	N/A	N/A	49 months
Li *et al* .(*13*)	9.5%	c-TACE	Retrospective	BCLC A/B	2.4%	54.8%	9.2 months	13.5 months
Lau *et al* .(*3*)	5.6%	TARE (yttrium-90)	Retrospective	Unresectable HCC	N/A	N/A	N/A	N/A
Lau *et al.* (*3*)	4.7%	PIAF or PIAF+TARE (yttrium-90)	Retrospective	Unresectable HCC	N/A	N/A	N/A	N/A
Zhang *et al.* (*31*)	3.1%	Systemic+locoregional treatment	Retrospective	Unresectable HCC	76.9%	100%	12.9 months (86.9%)	11.4 months
He *et al* .(*27*)	0.8%	Sorafenib	Randomized, open-label	BCLC C	2.46%	N/A	2.6 months	7.13 months

Abbreviations: BCLC, Barcelona Clinic Liver Cancer staging system; CCRT, concurrent chemoradiotherapy; CNLC, Chinese Liver Cancer staging system; c-TACE, conventional lipiodol-based chemoembolization; DCR, disease control rate; EBRT, external beam radiotherapy; FOLFOX, folinic acid, fluorouracil, and oxaliplatin; HAIC, hepatic arterial infusion chemotherapy; HCC, hepatocellular carcinoma; LR, liver resection; LT, liver transplantation; N/A, not available; NR, not reached; ORR, objective response rate; OS, overall survival; PD-1, programmed cell death protein 1; PFS, progression-free survival; PIAF, cisplatin/interferon alpha-2b/doxorubicin/5-fluorouracil; PVE, portal vein embolization; PVTT, portal vein tumour thrombus; RT, radiotherapy; SBRT, stereotactic body radiotherapy; TACE, transcatheter arterial chemoembolization; TARE, transarterial radioembolization; TKI, tyrosine kinase inhibitor.

Table 1. Clinical trials on conversion therapy for initially unresectable hepatocellular carcinoma

District	Conversion rate	Conversion therapy	Study design	Patients	ORR	DCR	Median PFS	Median OS
Japan								
Kudo *et al*. (*32*)	31.8%	Atezolizumab+bevacizumab	Retrospective	BCLC A/B	36.4%	81.8%	NR	NR
Kudo *et al*. (*33*)	28.7%	Atezolizumab+bevacizumab	Retrospective	BCLC B	N/A	N/A	N/A	N/A
Takeyama *et al*. (*34*)	12.5%	Sorafenib	Retrospective	Advanced HCC	N/A	N/A	NR	NR
Shimose *et al*. (*35*)	10.9%	Atezolizumab+bevacizumab	Retrospective	BCLC B/C	32.0%	84.0%	NR	NR
Tomonari *et al*. (*36*)	5.3%	Atezolizumab+bevacizumab	Retrospective	BCLC B/C	20.4%	79.6%	12.6 months	40.3 months
Tomonari *et al*. (*36*)	4.6%	Lenvatinib	Retrospective	BCLC B/C	26.7%	89.3%	12.6 months	40.3 months
South Korea								
Byun *et al*. (*37*)	20% (≥ 72 Gy), 12%(< 72 Gy)	RT (≥72 Gy or <72 Gy) +HAIC (fluorouracil)	Retrospective	BCLC C	N/A	N/A	N/A	104 months
Lee *et al*. (*38*)	16.9 %	CCRT+HAIC (FOLFOX)	Retrospective	Advanced HCC	N/A	N/A	N/A	23 months
Lee *et al*. (*39*)	12.8%	TACE+CCRT or TACE+RT	Retrospective	BCLC B/C	68.0%	N/A	24.9 months (LR), 30.6 months (LT)	166 months (LR), 62.5 months (LT)
Yoon *et al*. (*40*)	11.1%	TACE+RT	Randomized	BCLC C	N/A	N/A	7.75 months	13.75 months
Lee *et al*. (*41*)	6.8%	CCRT	Retrospective	Unresectable HCC	83.3%	N/A	N/A	N/A
USA								
Kaseb *et al*. (*42*)	33%	Modified PIAF	Retrospective	Unresectable HCC with no hepatitis or cirrhosis	36%	N/A	N/A	21.3 months
Meric *et al*. (*43*)	16%	HAI	Retrospective	Unresectable HCC	N/A	N/A	NR	NR
Labgaa *et al*. (*44*)	9%	TARE (yttrium-90)	Retrospective	BCLC A/B/C	N/A	N/A	N/A	47 months
Spain								
Inarrairaegui *et al*. (*45*)	28.6%	TARE (yttrium-90)	Retrospective	BCLC A/B	N/A	N/A	N/A	NR
Italy								
Tabone *et al*. (*46*)	20%	TARE (yttrium-90) (454 or 248 or 138 Gy)	Retrospective	BCLC C	N/A	N/A	N/A	54, 30 and 11 months

Abbreviations: BCLC, Barcelona Clinic Liver Cancer staging system; CCRT, concurrent chemoradiotherapy; CNLC, Chinese Liver Cancer staging system; c-TACE, conventional lipiodol-based chemoembolization; DCR, disease control rate; EBRT, external beam radiotherapy; FOLFOX, folinic acid, fluorouracil, and oxaliplatin; HAIC, hepatic arterial infusion chemotherapy; HCC, hepatocellular carcinoma; LR, liver resection; LT, liver transplantation; N/A, not available; NR, not reached; ORR, objective response rate; OS, overall survival; PD-1, programmed cell death protein 1; PFS, progression-free survival; PIAF, cisplatin/interferon alpha-2b/doxorubicin/5-fluorouracil; PVE, portal vein embolization; PVTT, portal vein tumour thrombus; RT, radiotherapy; SBRT, stereotactic body radiotherapy; TACE, transcatheter arterial chemoembolization; TARE, transarterial radioembolization; TKI, tyrosine kinase inhibitor.

were reported to be 20% in Spain and 28.6% in Italy. The variation in conversion rates is primarily related to the choice of the conversion therapy regimen and the patient's disease stage, systemic status, and response to treatment. However, there is controversy regarding the timing of conversion therapy, the new challenges faced in surgery after conversion therapy, and the establishment of endpoints for clinical studies. This paper has analyzed and summarized the current status of clinical trials on conversion therapy in patients with unresectable HCC, and it discusses the prospects for the development of conversion therapy based on the results of relevant research.

2. Conversion therapy improves the prognosis for patients with uHCC

2.1. Conversion therapy for uHCC *vs*. systemic therapy alone

Conversion therapy has been found to result in better patient outcomes and longer survival rates compared to systemic therapy for uHCC. Patients receiving transarterial chemoembolization (TACE) plus radiotherapy (RT) conversion therapy had a significantly higher 12-week progression-free survival (PFS) rate (86.7% *vs*. 34.3%, $p < 0.001$), longer median time to progression at 24 weeks (31.0 *vs*. 11.7 weeks, $p < 0.001$), and longer OS (55.0 *vs*. 43.0 weeks, $p = 0.04$) than those receiving sorafenib alone (*40*). A study found that patients who underwent conversion therapy had a significantly longer median OS of 1208 days (range: 1064 to not reach) compared to those who received chemotherapy alone with a median OS of 569 days (range: 466 to 704, $p < 0.01$) (*36*).

In classic clinical trials of systemic therapies for uHCC, such as SHARP (*52*), RELECT (*51*), CheckMate 040 (*47*), CheckMate-040 cohort 4 (*47*), IMbrave150 (*48,49*), HIMALAYA (*50*), REACH-2 (*53*), CELESTIAL (*54*), and RESORSE (*55*), results indicated the achievement of an objective response rate (ORR) ranging from 2% to 29.8%, a disease control rate (DCR) of 43–75.5%, a median PFS of 2.8–7.4 months, and a median OS of 8.5–19.2 months. As shown in Table 1, patients who underwent conversion therapy had an ORR ranging from 2.4% to 96%, a DCR ranging from 52.8% to 100%, a median PFS ranging from 2.6 to 25 months, and a median OS ranging from 7.13 to 166 months. Further comparative studies with conventional systemic therapy need to be conducted to more directly demonstrate the prognostic role of translational therapy for patients with advanced hepatocellular carcinoma.

2.2. Surgery after conversion therapy downstaging *vs*. no surgery after successful downstaging

Surgical resection can optimize the prognosis for patients with uHCC who have undergone successful conversion therapy. The OS rates at 1, 2, and 5 years postoperatively were 90%, 58%, and 42%, respectively, for patients who underwent conversion therapy (*56*). Patients with advanced HCC that was initially unresectable had a good long-term survival after undergoing concurrent chemoradiotherapy (CCRT) followed by hepatic arterial infusion chemotherapy (HAIC) conversion therapy in the curative resection group compared to the non-surgery group (49.6% *vs*. 9.8% at 5 years; $p < 0.001$) (*38*). Compared to patients whose cancer was successfully downstaged without surgery, patients who underwent conversion therapy and then received radical treatment had a significantly longer median survival. The surgery group had 2-, 4-, and 5-year survival rates of 93%, 47%, and 26%, respectively, which were significantly better than the 2-, 4-, and 5-year survival rates of 74%, 18%, and 10% in the group that refused surgery ($p = 0.019$) (*30*). In addition, patients with HCC and major vessel invasion (MVI) who underwent surgery had a significantly better median OS of 58 months compared to 30 months in the group that refused surgery ($p = 0.024$) (*30*). In patients with Barcelona Clinic Liver Cancer (BCLC) stage C advanced HCC who received liver-directed simultaneous radiotherapy, those who underwent surgery had a significantly longer median OS (104 months *vs*. 11 months, $p < 0.001$) (*37*).

Studies have reported that patients with uHCC treated with TACE alone have a median survival ranging from 19 to 38 months (*57-61*). When conversion therapy with TACE is conducted, however, the median survival can be extended to 49 months (30). Nevertheless, a study found no statistically significant difference in disease-free survival (DFS) and OS between patients who underwent surgery after conversion therapy and nonsurgical patients in whom clinical complete remission (cCR) was achieved after conversion therapy (*62*).

A comparison of surgical resection following conversion therapy and liver transplantation (LT) revealed no significant differences in median OS (166.0 months *vs*. 62.5 months, $p > 0.050$), median PFS (24. 9 months *vs*. 30.6 months, $p > 0.050$), median DFS (161.3 months *vs*. 45.1 months, $p > 0.050$), and the median intra-hepatic non-recurrence interval (96.9 months *vs*. 39.9 months, $p > 0.050$) (*39*). Several large clinical series conducted in Europe, the US, and Asia have shown that the 5-year survival rate after radiofrequency ablation (RFA) for HCC (≤ 3 cm) ranges from 33% to 55%, which is comparable to that in an LR series (*63-66*). Moreover, a recent study found no significant difference in treatment choice between conversion therapy followed by ablation and LR (recurrence-free survival (RFS), 274 days [157-not reached (NR)] in the ablation group *vs*. RFS, not available (N/A) days [447-NR] in the LR group; $p = 0.09$) (*36*).

2.3. Conversion therapy plus surgery *vs*. upfront surgery

Patients with locally advanced HCC who received

conversion therapy followed by LR had a better prognosis than those who received upfront surgery alone. A retrospective study reported that patients who received preoperative Y90-SIRT conversion therapy had a significantly better 5-year OS rate (69.0% *vs*. 47.5%, $p = 0.048$) and a significantly better 5-year RFS rate (53.5% *vs*. 27.0%, $p = 0.047$) than those who underwent upfront resection (*67*). Additional studies, particularly prospective ones, need to be conducted to verify this.

3. Strategies for conversion therapy

3.1. Locoregional therapy

The conversion rate for TACE alone is 9.5% to 10%, and the objective remission rate (ORR) for conventional TACE is low (2.4%) (*13,30,68*).Patients with HCC who undergo TACE conversion therapy have a median OS of up to 49 months (*13,30,68*). In the US, the conversion rate for previously uHCC conversion therapy with HAI alone was 16% (*43*).Conversion rates with TARE (yttrium-90) alone range from 5.6% to 28.6% (*3,44-46*). In addition, studies have shown that increasing the dosage of TARE can enhance patient survival rates. Patients with HCC who undergo TARE conversion therapy have a median OS time of up to 54 months (*46*).

Locoregional combination therapies, such as HAIC (FOLFOX: folinic acid, fluorouracil, and oxaliplatin) plus TACE (*13*), portal vein embolization (PVE) plus TACE (*7*), TACE plus external beam radiotherapy (EBRT) (*8*), RT plus HAIC (fluorouracil) (*37*), and TACE plus RT (*40*), are mainly performed in Asia and have a conversion rate ranging from 11.1% to 57.6%. A trial of RT plus HAIC (fluorouracil) revealed that the group receiving a radiation dose ≥ 72 Gy had a higher conversion rate in advanced BCLC-C HCC compared to the intensity-modulated radiotherapy (IMRT) radiation dose < 72 Gy group (20% *vs*. 12%, $p = 0.03$) (*37*). Moreover, the group receiving a radiation dose ≥ 72 Gy had a significantly higher localized 1-year failure-free survival (LFFS) (95% *vs*. 79%, $p < 0.001$) and median OS (21 months *vs*. 13 months, $p = 0.002$) (*37*).

3.2. Systemic therapy

The development of tyrosine kinase inhibitors (TKI) and immune checkpoint inhibitors (ICI) has significantly improved the survival prognosis for patients diagnosed with HCC. Treatment with cisplatin, interferon α-2b, doxorubicin, and 5-fluorouracil (PIAF) resulted in a conversion rate of 18% for patients with initially unresectable HCC (*24*). The conversion rate increased to 33% with the use of modified PIAF, which also resulted in an ORR of 36% and a median OS of 21.3 months (*42*). In comparison, sorafenib had conversion rates ranging from 0.8% to 12.5% (*27,34*), while lenvatinib had a conversion rate of 4.6% (*36*). In Japan, the conversion rates for a combination of anti PD-L1 antibodies and a vascular endothelial growth factor inhibitor ranged from 5.3% to 31.8%. Post-conversion treatments included LR, ablation, and superselective TACE, and the median OS reached 40.3 months (*32,33,35,36*). Compared to TKI monotherapy, the combination of TKI and PD-1 has a higher conversion rate. Studies have reported a conversion rate ranging from 15.9% to 51%, with a median OS of up to 12 months (*19,21,32,69,70*).

Moreover, patients diagnosed with unresectable primary HCC and severe vascular infiltration who received anti-PD-1 antibodies in combination with TKI conversion therapy had 70% (7/10) partial remission (PR) and 30% (3/10) complete remission (CR) prior to surgery. These findings demonstrate the effectiveness of anti-PD-1 antibodies in combination with TKI conversion therapy for patients with unresectable primary HCC and severe vascular infiltration, resulting in an increased long-term oncologic benefit. The 12-month RFS rate for these patients was 75% (*71*).

3.3. Combined locoregional and systemic therapy

The heterogeneity of HCC in terms of tumor number, size, and liver function can preclude some patients from being treated with TACE. Patients with good liver function and a high tumor burden who are not eligible for TACE may benefit from preoperative systemic therapy followed by TACE (*72*). Clinical trials have shown that combining TACE with TKIs for intermediate and advanced HCC can result in prolonged OS and improved PFS compared to TACE alone (*73-75*). Moreover, combination therapy with TACE and lenvatinib has resulted in conversion rates of 11.1-19%, with a median PFS of up to 8 months and median OS of up to 20.6 months (*12,20*). The use of TACE, TKIs, and ICIs has been found to increase residual liver volume in patients with intermediate to advanced HCC, thereby enhancing the safety of conversion resection (*76*). A meta-analysis of 18 studies found that the conversion rate of triple therapy (TACE+TKIs+ICIs) was 42%, which was higher than that of TACE alone (10%) and TACE combined with other therapies (19%) (*77*). The tumor response to triple therapy was superior to that of TACE alone or dual therapy (*77*).

A clinical study showed that combination therapy with sorafenib and HAIC (FOLFOX) resulted in a conversion rate of 12.8% (*27*). Treating patients with unresectable advanced HCC using HAIC locoregional therapy following CCRT not only reduced the tumor stage but also significantly increased the future remnant liver volume (FRLV) from 47.5% to 69.9% before surgery, which further improved the curative resection of HCC (*38*).

Another study found that the conversion rate of TACE combined with CCRT or combined RT was 12.8% (*39*). LR accounted for 8.9% and LT accounted for 3.9%

(*39*). The study in question revealed that patients who underwent LR had a median PFS of 24.9 months, whereas those who underwent LT had a median PFS of 30.6 months. LR patients had a median OS of 166 months, while LT patients had a median OS of 62.5 months. The combination of CCRT with HAIC (FOLFOX) resulted in a conversion rate of 16.9% (*39*), whereas the combination of TACE plus SBRT plus anti PD-L1 antibodies resulted in a conversion rate of 12% (*28*).

The conversion rate of triple therapy TACE/HAIC plus TKI plus anti-PD-1 antibodies ranged from 11.5% to 53% (*9,12,15-17,20,22,25,29*). A point worth noting is that the difference in conversion rates may be related to the patients' disease status. Specifically, the treatment group with the higher conversion rate included patients with BCLC stage A initially unresectable HCC. The combination of TACE, TKI, and anti-PD-1 antibodies resulted in a 55% rate of pathological complete remission (pCR) and an 83% rate of major pathological remission (MPR) (*9*). A study found that patients with uHCC who received HAIC in combination with TKI and anti-PD-1 antibody conversion therapy had a significant survival benefit after surgery (*78*). The median RFS was 19.3 months, and the median OS was 28.7 months. The study in question noted a significant reduction in tumor size, with a median decrease of 4.7 cm. Moreover, pCR was achieved in 23 out of 67 patients (34.3%), indicating a favorable pathological response.

A meta-analysis of 24 studies was performed to determine the conversion rates and ORR of different therapies. Results indicated that locoregional plus systemic combination therapy had the highest conversion rate at 25%, followed by TACE at 13%, chemotherapy at 12%, and systemic therapy at 10% (*56*). Locoregional plus systemic combination therapy had the highest ORR at 60%, while chemotherapy had the lowest at 19% (*56*). The other therapies had an ORR ranging from 30% to 32% (*56*). Locoregional-systemic combination therapies have a lower incidence of adverse reactions, and particularly grade ≥ 3 adverse events (AEs). The incidence of adverse reactions was 67% with chemotherapy, 34% with TACE, 30% with systemic therapies, and 40% with locoregional-systemic combination therapies (*56*). Subgroup analyses have confirmed the benefits of locoregional-systemic triple combination therapies. Combination therapy with TACE, TKIs, and ICIs resulted in a significant therapeutic advantage. The therapy resulted in a conversion rate of 33%, an ORR of 73%, and a rate of grade ≥ 3 AEs of 31% (*56*).

A point worth noting is that triple combination therapy with an anti-PD-1 antibody (sintilimab) plus an anti-PD-1 antibody analog (IBI305) plus HAIC resulted in a conversion rate of 46.7% and an ORR of 66.7% (*14*). Likewise, triple combination therapy with an angiogenesis inhibitor plus anti-PD-1 antibody plus HAIC (FOLFOX) resulted in significant clinical benefits, with a conversion rate of 60%, an ORR of 96%, and a DCR of 100% (*6*). The results suggest that locoregional-systemic combination therapies have optimal conversion rates and clinical remission benefits.

Kudo suggested that subsequent immunotherapy should follow locoregional therapy since the release of cancer antigens and cancer antigen-specific immune responses will further enhance the efficacy of systemic therapy (*33*). Combining locoregional therapy with ICIs preserves T-cell effector function. Locoregional therapy activates the innate immune system and generates durable and widespread T-cell immunity through tumor antigen release and danger signal production, driving the anti-tumor immune response (*79*). Studies have noted an increased PD-1 and PD-L1 expression in HCC after TACE (*80*). Moreover, TACE resulted in elevated levels of circulating GPC3-specific cytotoxic T lymphocytes (CTL), IL-6 (*81*), CD4+ T cells, a higher CD4+/CD8+ T cell ratio, and elevated NK cells while reducing CD8+ Treg cells (*82*). Combining TACE with immunotherapy has the potential to enhance tumor response.

4. Challenges of conversion therapy

4.1. Adverse reactions to conversion therapy

Preservation of liver function is crucial for sequential surgery following initial unresectable HCC conversion therapy. The Asia-Pacific Expert Consensus Statement on Primary Liver Cancer (APPLE) emphasizes that for intermediate stage HCC, maintaining liver function is as equally important as achieving a high rate of surgical resection, with the ultimate aim of treatment being to prolong OS (*83*). Maintaining the Child-Pugh score during conversion therapy is beneficial to the prognosis for patients with advanced HCC, and even in those with adequate hepatic function reserve (*84-86*). However, hepatic impairment after conversion therapy is often more severe than anticipated, and a single Child-Pugh score may not fully reflect hepatic reserve function.

Chemotherapeutic agents used in conversion therapy can have various effects on liver physiology, including steatosis and hepatic sinusoidal vascular changes such as sinusoidal obstruction syndrome (SOS) or nodular regenerative hyperplasia (NRH) (*87*). TKIs can cause hepatotoxicity in 23% to 40% of patients, which can manifest as hepatocellular injury, hepatocellular steatosis, or cholestasis (*88*). Over a 10-year period, 38 of 432 (8.8%) patients treated with ICIs experienced liver injury, which was primarily hepatocellular or cholestatic (*89,90*). A point worth noting is that the common terminology criteria for adverse events (CTCAE) classification may overestimate the severity of checkpoint inhibitor-induced liver injury. Therefore, attention should be paid to toxic adverse reactions that may occur during conversion therapy. Moreover, preventing and treating post-hepatectomy liver failure (PHLF) is crucial.

Conversion therapy has been associated with systemic adverse reactions. Studies have reported that 50% of patients experienced grade 3 or higher treatment-related adverse events (TRAE) during conversion therapy (*31*). A study of PIAF conversion therapy for advanced unresectable HCC found that patients had a median OS of only 8.9 months, AEs including myelosuppression and mucositis were reported, and there were two treatment-related deaths due to neutropenic sepsis (*24*). Patients in the surgery group who did not receive conversion therapy experienced significantly fewer complications of any grade compared to the triple conversion therapy group (51.2% *vs*. 82.9%, $p = 0.002$). In addition, the incidence of grade 3/4 complications was significantly lower in patients who did not receive conversion therapy compared to those who did (4.9% *vs*. 26.8%, $p = 0.013$) (*91*).

4.2. Criteria for evaluating the effectiveness of conversion therapy

Currently, there are no universally accepted criteria for evaluating the effectiveness of conversion therapy. Several studies have adopted the following criteria to classify patients as having resectable HCC after conversion therapy: (1) Adequate residual liver volume and function are needed to achieve an R0 resection., (2) The intrahepatic lesion must be assessed as partially responsive or stable for at least 2 months, (3) Systemic therapy should not cause any serious or persistent adverse effects, and (4) LR should not be contraindicated (*26*). Zhang *et al*. defined the criteria for successful conversion as follows: for a Child-Pugh score of less than 7.2, an Eastern Cooperative Oncology Group Performance Status (ECOG PS) score of 1 or less, the absence of extrahepatic lesions, and a preserved liver with structurally intact vasculature and adequate FLR (*71*).

4.3. Treatment subsequent to conversion therapy

Thorough evaluation of the timing of resection after conversion therapy for HCC is crucial. Prior to surgery, safety needs to be assessed. Perioperatively, treatment with lenvatinib or bevacizumab should be discontinued due to its antiangiogenic action, which can result in complications such as delayed healing and bleeding. Lenvatinib has a plasma clearance time of 28–35 hours (*92*). According to one study, the drug should be discontinued for at least 1 week prior to surgery or ablation (*93*). Bevacizumab, in contrast, should be discontinued for at least 4–6 weeks before LR and 3 weeks before ablation or radical TACE (*94*). Strictly adhering to the dosing instructions for preoperative discontinuation is important in order to minimize the effects on surgery. If a patient experiences severe adverse drug reactions during targeted therapy or immunotherapy, surgery should only be performed after he or she has fully recovered.

Curative treatment options include LR, LT, and ablation therapy . Studies have confirmed that both LR and ablation therapy have favorable long-term outcomes, with no significant difference in post-treatment complications or RFS (*33*). Some studies have suggested that surgery should be performed after successful downstaging through continued treatment with TKIs and/or anti-PD-1 antibodies to stabilize lesions, an interval that is typically 1–2 months. In instances of less difficult resection, LR is recommended after downstaging to meet surgical resectability criteria to minimize complications (*91*). In instances of more difficult resection and poor tumor behavior, surgery is recommended only after achieving maximum remission depth and maintaining stability for 3–4 months to improve the partial response rate (*91*).

LR after conversion therapy can be challenging due to the adverse reactions it causes, such as bone marrow suppression, decreased platelet function and count, increased fragility of blood vessels and liver tissue, localized adhesions, and hepatic edema. Compared to patients who underwent direct surgery, those in the triple conversion therapy group (HAIC/TACE+anti-PD-1 antibody+TKI) for LR conversion lost more blood during surgery (600 mL *vs*. 400 mL, $p = 0.015$), had a longer operating time (270 min *vs*. 240 min, $p = 0.02$), a higher transfusion rate, and a longer duration of hospitalization (11 days *vs*. 8 days, $p < 0.001$) (*91*).

Adjuvant therapy should be considered after conversion therapy. Repeated liver treatments may create a hypoxic microenvironment, which can make the remaining tumor more aggressive and resistant. Postoperative recurrence was noted in 42.9% (21/49) of patients who underwent salvage LR, 66.7% (14/21) of which was intrahepatic recurrence (*3*). A point worth noting is that studies have noted the significance of postoperative antiviral therapy in patients with HBV-related HCC (*95,96*). Patients with uHCC who underwent FOLFOX-HAIC conversion therapy and who received adjuvant therapy had a significantly longer median RFS compared to those who did not receive adjuvant therapy (19.2 months *vs*. 10.8 months, $p = 0.028$). The best RFS after adjuvant therapy was observed in patients with uHCC who were younger than 60 years of age, had large vessel invasion, and who were positive for hepatitis B surface antigen (*97*).

5. Future perspectives

Sixty-seven percent of HCC patients are in Asia. The majority of HCC patients are initially diagnosed with BCLC stages B or C. Most patients are not eligible for radical surgery, and the median survival time is only 23–33 months (*98,99*). For patients with initially unresectable HCC, surgery can only be undergone f

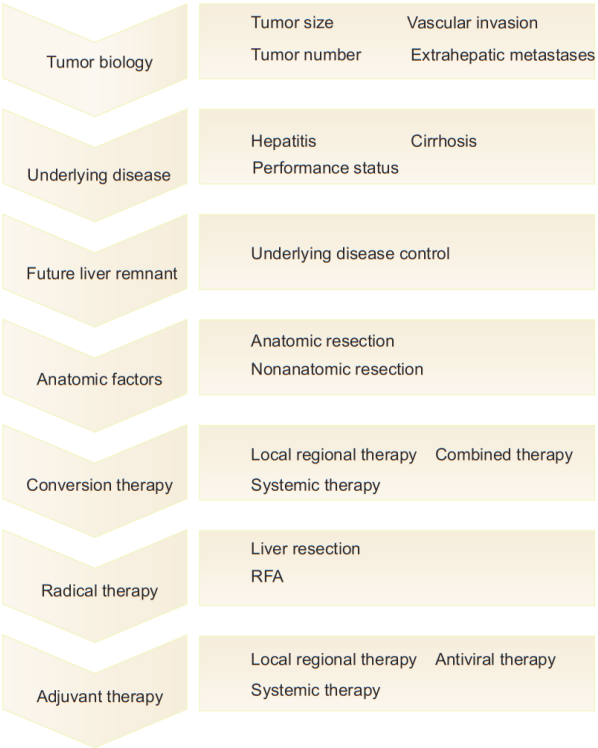

Figure 1. Conversion therapy paradigm for initial unresectable hepatocellular carcinoma. Abbreviation: RFA, radiofrequency ablation.

the tumor is shrunk or downstaged. Figure 1 shows a reference paradigm for administering conversion therapy for initially uHCC. With further development, conversion therapy could potentially yield prognostic outcomes similar to those of early HCC resection. Pathological examination can determine the tumor's sensitivity to transformative therapy and guide postoperative adjuvant therapy, potentially leading to long-term survival.

Most studies on conversion therapy focus on short-term outcomes, primarily assessing the conversion rate and ORR. Few studies have included long-term survival as a primary endpoint. In order to determine the significance of conversion surgery, the long-term outcomes of patients who underwent conversion surgery due to a positive tumor response to systemic therapy need to be compared to those who did not undergo conversion surgery despite a positive tumor response. Several clinical studies have found that a triple conversion regimen with locoregional and systemic therapy has a high conversion rate and results in significant survival benefits compared to other conversion strategies. The difficulty of LR increases after conversion therapy, and ensuring the safety of surgery requires comprehensive preoperative evaluation, appropriate selection of the procedure, and precise intraoperative technique. Emphasis should be placed on the prevention and treatment of PHLF, as well as postoperative adjuvant therapy and long-term follow-up. Due to the heterogeneity of study centers, conversion therapy protocols, and evaluation criteria, however, there is currently no unified approach to conversion therapy. Therefore, further optimization of conversion therapy would require a large prospective multicenter clinical study.

Funding: This work was supported by a grant from the National Natural Science Foundation of China (No. 81960446), the Natural Science Foundation of Hainan Province (No. 823MS167), and the 2023 Foreign Experts Program in Hainan Province (SQ2023WGZJ0002).

Conflict of Interest: The authors have no conflicts of interest to disclose.

References

1. Collaborators GBDCoD. Global, regional, and national age-sex specific mortality for 264 causes of death, 1980-2016: A systematic analysis for the global burden of disease study 2016. Lancet. 2017; 390:1151-1210.
2. Bruix J, Reig M, Sherman M. Evidence-based diagnosis, staging, and treatment of patients with hepatocellular carcinoma. Gastroenterology. 2016; 150:835-853.
3. Lau WY, Ho SK, Yu SC, Lai EC, Liew CT, Leung TW. Salvage surgery following downstaging of unresectable hepatocellular carcinoma. Ann Surg. 2004; 240:299-305.
4. Gholam PM, Iyer R, Johnson MS. Multidisciplinary management of patients with unresectable hepatocellular carcinoma: A critical appraisal of current evidence. Cancers (Basel). 2019; 11:873.
5. Lau WY, Lai EC. Salvage surgery following downstaging of unresectable hepatocellular carcinoma – A strategy to increase resectability. Ann Surg Oncol. 2007; 14:3301-3309.
6. Zhang J, Zhang X, Mu H, Yu G, Xing W, Wang L, Zhang T. Surgical conversion for initially unresectable locally advanced hepatocellular carcinoma using a triple combination of angiogenesis inhibitors, anti-PD-1 antibodies, and hepatic arterial infusion chemotherapy: A retrospective study. Front Oncol. 2021; 11:729764.
7. He C, Ge N, Wang X, Li H, Chen S, Yang Y. Conversion therapy of large unresectable hepatocellular carcinoma with ipsilateral portal vein tumor thrombus using portal vein embolization plus transcatheter arterial chemoembolization. Front Oncol. 2022; 12:923566.
8. Zeng ZC, Tang ZY, Yang BH, Liu KD, Wu ZQ, Fan J, Qin LX, Sun HC, Zhou J, Jiang GL. Comparison between radioimmunotherapy and external beam radiation therapy for patients with hepatocellular carcinoma. Eur J Nucl Med Mol Imaging. 2002; 29:1657-1668.
9. Wu JY, Yin ZY, Bai YN, Chen YF, Zhou SQ, Wang SJ, Zhou JY, Li YN, Qiu FN, Li B, Yan ML. Lenvatinib combined with anti-PD-1 antibodies plus transcatheter arterial chemoembolization for unresectable hepatocellular carcinoma: A multicenter retrospective study. J Hepatocell Carcinoma. 2021; 8:1233-1240.
10. Zhang X, Zhu X, Liu C, Lu W, Li Q, Chen W, Li Z, Lu Q, Peng W, Li C. The safety and efficacy of transarterial chemoembolization (TACE)+ lenvatinib+ programmed cell death protein 1 (PD-1) antibody of advanced unresectable hepatocellular carcinoma. Amer Soc Clin Oncol, 2022: 453-453.
11. Zhang W, Hu B, Han J, Wang H, Wang Z, Ye H, Ma

G, Chen M, Cai S, Wang X. 174P A real-world study of PD-1 inhibitors combined with TKIs for HCC with major vascular invasion as the conversion therapy: A prospective, non-randomized, open-label cohort study. Annals of Oncology. 2020; 31:S1307.
12. Qu WF, Ding ZB, Qu XD, *et al*. Conversion therapy for initially unresectable hepatocellular carcinoma using a combination of toripalimab, lenvatinib plus TACE: Real-world study. BJS Open. 2022; 6:zrac114.
13. Li B, Qiu J, Zheng Y, Shi Y, Zou R, He W, Yuan Y, Zhang Y, Wang C, Qiu Z, Li K, Zhong C, Yuan Y. Conversion to resectability using transarterial chemoembolization combined with hepatic arterial infusion chemotherapy for initially unresectable hepatocellular carcinoma. Ann Surg Open. 2021; 2:e057.
14. Liu D, Mu H, Liu C, Zhang W, Cui Y, Wu Q, Zhu X, Fang F, Zhang W, Xing W, Li Q, Song T, Lu W, Li H. Hepatic artery infusion chemotherapy (HAIC) combined with sintilimab and bevacizumab biosimilar (IBI305) for initial unresectable hepatocellular carcinoma (HCC): A prospective, single-arm phase II trial. J Clin Oncol. 2022; 40:4073-4073.
15. Gan L, Lang M, Tian X, *et al*. A retrospective analysis of conversion therapy with lenvatinib, Ssintilimab, and arterially-directed therapy in patients with initially unresectable hepatocellular carcinoma. J Hepatocell Carcinoma. 2023; 10:673-686.
16. Wu JY, Zhang ZB, Zhou JY, Ke JP, Bai YN, Chen YF, Wu JY, Zhou SQ, Wang SJ, Zeng ZX, Li YN, Qiu FN, Li B, Yan ML. Outcomes of salvage surgery for initially unresectable hepatocellular carcinoma converted by transcatheter arterial chemoembolization combined with lenvatinib plus anti-PD-1 antibodies: A multicenter retrospective study. Liver Cancer. 2023; 12:229-237.
17. Li X, Chen J, Wang X, Bai T, Lu S, Wei T, Tang Z, Huang C, Zhang B, Liu B, Li L, Wu F. Outcomes and prognostic factors in initially unresectable hepatocellular carcinoma treated using conversion therapy with lenvatinib and TACE plus PD-1 inhibitors. Front Oncol. 2023; 13:1110689.
18. Wang L, Wang H, Cui Y, Liu M, Jin K, Xu D, Wang K, Xing B. Sintilimab plus lenvatinib conversion therapy for intermediate/locally advanced hepatocellular carcinoma: A phase 2 study. Front Oncol. 2023; 13:1115109.
19. Yi Y, Sun BY, Weng JL, Zhou C, Zhou CH, Cai MH, Zhang JY, Gao H, Sun J, Zhou J, Fan J, Ren N, Qiu SJ. Lenvatinib plus anti-PD-1 therapy represents a feasible conversion resection strategy for patients with initially unresectable hepatocellular carcinoma: A retrospective study. Front Oncol. 2022; 12:1046584.
20. Chen S, Wu Z, Shi F, Mai Q, Wang L, Wang F, Zhuang W, Chen X, Chen H, Xu B, Lai J, Guo W. Lenvatinib plus TACE with or without pembrolizumab for the treatment of initially unresectable hepatocellular carcinoma harbouring PD-L1 expression: A retrospective study. J Cancer Res Clin Oncol. 2022; 148:2115-2125.
21. Zhu XD, Huang C, Shen YH, *et al*. Hepatectomy after conversion therapy using tyrosine kinase inhibitors plus anti-PD-1 antibody therapy for patients with unresectable hepatocellular carcinoma. Ann Surg Oncol. 2023; 30:2782-2790.
22. Luo L, Xiao Y, Zhu G, Huang A, Song S, Wang T, Ge X, Xie J, Deng W, Hu Z, Wen W, Mei H, Wan R, Shan R. Hepatic arterial infusion chemotherapy combined with PD-1 inhibitors and tyrosine kinase inhibitors for unresectable hepatocellular carcinoma: A tertiary medical center experience. Front Oncol. 2022; 12:1004652.
23. Sun H-C, Zhu X-D, Huang C, Shen Y-H, Ji Y, Ge N-L, Tan C-J, Zhou J, Fan J. Initially unresectable hepatocellular carcinoma treated by combination therapy of tyrosine kinase inhibitor and anti-PD-1 antibody followed by resection. J Clin Oncol. 2020; 38(15_suppl):e16690-e16690.
24. Leung TW, Patt YZ, Lau WY, Ho SK, Yu SC, Chan AT, Mok TS, Yeo W, Liew CT, Leung NW, Tang AM, Johnson PJ. Complete pathological remission is possible with systemic combination chemotherapy for inoperable hepatocellular carcinoma. Clin Cancer Res. 1999; 5:1676-1681.
25. He MK, Liang RB, Zhao Y, Xu YJ, Chen HW, Zhou YM, Lai ZC, Xu L, Wei W, Zhang YJ, Chen MS, Guo RP, Li QJ, Shi M. Lenvatinib, toripalimab, plus hepatic arterial infusion chemotherapy versus lenvatinib alone for advanced hepatocellular carcinoma. Ther Adv Med Oncol. 2021; 13:17588359211002720.
26. Zhu XD, Huang C, Shen YH, *et al*. Downstaging and resection of initially unresectable hepatocellular carcinoma with tyrosine kinase inhibitor and anti-PD-1 antibody combinations. Liver Cancer. 2021; 10:320-329.
27. He M, Li Q, Zou R, *et al*. Sorafenib plus hepatic arterial infusion of oxaliplatin, fluorouracil, and leucovorin *vs* sorafenib alone for hepatocellular carcinoma with portal vein invasion: A randomized clinical trial. JAMA Oncol. 2019; 5:953-960.
28. Chiang CL, Chiu KWH, Chan KSK, *et al*. Sequential transarterial chemoembolisation and stereotactic body radiotherapy followed by immunotherapy as conversion therapy for patients with locally advanced, unresectable hepatocellular carcinoma (START-FIT): A single-arm, phase 2 trial. Lancet Gastroenterol Hepatol. 2023; 8:169-178.
29. Li J, Kong M, Yu G, Wang S, Shi Z, Han H, Lin Y, Shi J, Song J. Safety and efficacy of transarterial chemoembolization combined with tyrosine kinase inhibitors and camrelizumab in the treatment of patients with advanced unresectable hepatocellular carcinoma. Front Immunol. 2023; 14:1188308.
30. Zhang Y, Huang G, Wang Y, Liang L, Peng B, Fan W, Yang J, Huang Y, Yao W, Li J. Is salvage liver resection necessary for initially unresectable hepatocellular carcinoma patients downstaged by transarterial chemoembolization? Ten years of experience. Oncologist. 2016; 21:1442-1449.
31. Zhang B, Shi X, Cui K, *et al*. Real-world practice of conversion surgery for unresectable hepatocellular carcinoma - A single center data of 26 consecutive patients. BMC Cancer. 2023; 23:465.
32. Kudo M, Aoki T, Ueshima K, *et al*. Achievement of complete response and drug-free status by atezolizumab plus bevacizumab combined with or without curative conversion in patients with transarterial chemoembolization-unsuitable, intermediate-stage hepatocellular carcinoma: A multicenter proof-of-concept study. Liver Cancer. 2023; 12:321-338.
33. Kudo M. Atezolizumab plus bevacizumab followed by curative conversion (ABC conversion) in patients with unresectable, TACE-unsuitable intermediate-stage hepatocellular carcinoma. Liver Cancer. 2022; 11:399-406.
34. Takeyama H, Beppu T, Higashi T, *et al*. Impact of

surgical treatment after sorafenib therapy for advanced hepatocellular carcinoma. Surg Today. 2018; 48:431-438.
35. Shimose S, Iwamoto H, Shirono T, *et al*. The impact of curative conversion therapy aimed at a cancer-free state in patients with hepatocellular carcinoma treated with atezolizumab plus bevacizumab. Cancer Med. 2023; 12:12325-12335.
36. Tomonari T, Tani J, Sato Y, Tanaka H, Tanaka T, Taniguchi T, Kawano Y, Morishita A, Okamoto K, Sogabe M, Miyamoto H, Masaki T, Takayama T. Clinical features and outcomes of conversion therapy in patients with unresectable hepatocellular carcinoma. Cancers (Basel). 2023; 15:5221.
37. Byun HK, Kim HJ, Im YR, Kim DY, Han KH, Seong J. Dose escalation by intensity modulated radiotherapy in liver-directed concurrent chemoradiotherapy for locally advanced BCLC stage C hepatocellular carcinoma. Radiother Oncol. 2019; 133:1-8.
38. Lee HS, Choi GH, Choi JS, Kim KS, Han KH, Seong J, Ahn SH, Kim DY, Park JY, Kim SU, Kim BK. Surgical resection after down-staging of locally advanced hepatocellular carcinoma by localized concurrent chemoradiotherapy. Ann Surg Oncol. 2014; 21:3646-3653.
39. Lee WH, Byun HK, Choi JS, Choi GH, Han DH, Joo DJ, Kim DY, Han KH, Seong J. Liver-directed combined radiotherapy as a bridge to curative surgery in locally advanced hepatocellular carcinoma beyond the Milan criteria. Radiother Oncol. 2020; 152:1-7.
40. Yoon SM, Ryoo BY, Lee SJ, Kim JH, Shin JH, An JH, Lee HC, Lim YS. Efficacy and safety of transarterial chemoembolization plus external beam radiotherapy *vs* sorafenib in hepatocellular carcinoma with macroscopic vascular invasion: A randomized clinical trial. JAMA Oncol. 2018; 4:661-669.
41. Lee IJ, Kim JW, Han KH, Kim JK, Kim KS, Choi JS, Park YN, Seong J. Concurrent chemoradiotherapy shows long-term survival after conversion from locally advanced to resectable hepatocellular carcinoma. Yonsei Med J. 2014; 55:1489-1497.
42. Kaseb AO, Shindoh J, Patt YZ, Roses RE, Zimmitti G, Lozano RD, Hassan MM, Hassabo HM, Curley SA, Aloia TA, Abbruzzese JL, Vauthey JN. Modified cisplatin/interferon alpha-2b/doxorubicin/5-fluorouracil (PIAF) chemotherapy in patients with no hepatitis or cirrhosis is associated with improved response rate, resectability, and survival of initially unresectable hepatocellular carcinoma. Cancer. 2013; 119:3334-3342.
43. Meric F, Patt YZ, Curley SA, Chase J, Roh MS, Vauthey JN, Ellis LM. Surgery after downstaging of unresectable hepatic tumors with intra-arterial chemotherapy. Ann Surg Oncol. 2000; 7:490-495.
44. Labgaa I, Tabrizian P, Titano J, Kim E, Thung SN, Florman S, Schwartz M, Melloul E. Feasibility and safety of liver transplantation or resection after transarterial radioembolization with Yttrium-90 for unresectable hepatocellular carcinoma. HPB (Oxford). 2019; 21:1497-1504.
45. Inarrairaegui M, Pardo F, Bilbao JI, Rotellar F, Benito A, D'Avola D, Herrero JI, Rodriguez M, Marti P, Zozaya G, Dominguez I, Quiroga J, Sangro B. Response to radioembolization with yttrium-90 resin microspheres may allow surgical treatment with curative intent and prolonged survival in previously unresectable hepatocellular carcinoma. Eur J Surg Oncol. 2012; 38:594-601.
46. Tabone M, Calvo A, Russolillo N, Langella S, Carbonatto P, Lo Tesoriere R, Richetta E, Pellerito R, Ferrero A. Downstaging unresectable hepatocellular carcinoma by radioembolization using 90-yttrium resin microspheres: A single center experience. J Gastrointest Oncol. 2020; 11:84-90.
47. El-Khoueiry AB, Sangro B, Yau T, *et al*. Nivolumab in patients with advanced hepatocellular carcinoma (CheckMate 040): An open-label, non-comparative, phase 1/2 dose escalation and expansion trial. Lancet. 2017; 389:2492-2502.
48. Cheng AL, Qin S, Ikeda M, *et al*. Updated efficacy and safety data from IMbrave150: Atezolizumab plus bevacizumab *vs*. sorafenib for unresectable hepatocellular carcinoma. J Hepatol. 2022; 76:862-873.
49. Finn RS, Qin S, Ikeda M, *et al*. Atezolizumab plus bevacizumab in unresectable hepatocellular carcinoma. N Engl J Med. 2020; 382:1894-1905.
50. Abou-Alfa GK, Chan SL, Kudo M, *et al*. Phase 3 randomized, open-label, multicenter study of tremelimumab (T) and durvalumab (D) as first-line therapy in patients (pts) with unresectable hepatocellular carcinoma (uHCC): HIMALAYA. J Clin Oncol. 2022; 40:379-379.
51. Kudo M, Finn RS, Qin S, *et al*. Lenvatinib versus sorafenib in first-line treatment of patients with unresectable hepatocellular carcinoma: A randomised phase 3 non-inferiority trial. Lancet. 2018; 391:1163-1173.
52. Llovet JM, Ricci S, Mazzaferro V, *et al*. Sorafenib in advanced hepatocellular carcinoma. N Engl J Med. 2008; 359:378-390.
53. Zhu AX, Kang YK, Yen CJ, *et al*. Ramucirumab after sorafenib in patients with advanced hepatocellular carcinoma and increased alpha-fetoprotein concentrations (REACH-2): A randomised, double-blind, placebo-controlled, phase 3 trial. Lancet Oncol. 2019; 20:282-296.
54. Bruix J, Qin S, Merle P, *et al*. Regorafenib for patients with hepatocellular carcinoma who progressed on sorafenib treatment (RESORCE): A randomised, double-blind, placebo-controlled, phase 3 trial. Lancet. 2017; 389:56-66.
55. Abou-Alfa GK, Meyer T, Cheng AL, *et al*. Cabozantinib in patients with advanced and progressing hepatocellular carcinoma. N Engl J Med. 2018; 379:54-63.
56. Pei Y, Li W, Wang Z, Liu J. Successful conversion therapy for unresectable hepatocellular carcinoma is getting closer: A systematic review and meta-analysis. Front Oncol. 2022; 12:978823.
57. Kudo M, Han G, Finn RS, *et al*. Brivanib as adjuvant therapy to transarterial chemoembolization in patients with hepatocellular carcinoma: A randomized phase III trial. Hepatology. 2014; 60:1697-1707.
58. Yu SC, Hui JW, Hui EP, Chan SL, Lee KF, Mo F, Wong J, Ma B, Lai P, Mok T, Yeo W. Unresectable hepatocellular carcinoma: Randomized controlled trial of transarterial ethanol ablation versus transcatheter arterial chemoembolization. Radiology. 2014; 270:607-620.
59. Okusaka T, Kasugai H, Shioyama Y, Tanaka K, Kudo M, Saisho H, Osaki Y, Sata M, Fujiyama S, Kumada T, Sato K, Yamamoto S, Hinotsu S, Sato T. Transarterial chemotherapy alone versus transarterial chemoembolization for hepatocellular carcinoma: A randomized phase III trial. J Hepatol. 2009; 51:1030-1036.
60. Lo CM, Ngan H, Tso WK, Liu CL, Lam CM, Poon RT, Fan ST, Wong J. Randomized controlled trial of

transarterial lipiodol chemoembolization for unresectable hepatocellular carcinoma. Hepatology. 2002; 35:1164-1171.
61. Llovet JM, Real MI, Montana X, Planas R, Coll S, Aponte J, Ayuso C, Sala M, Muchart J, Sola R, Rodes J, Bruix J, Barcelona Liver Cancer G. Arterial embolisation or chemoembolisation versus symptomatic treatment in patients with unresectable hepatocellular carcinoma: A randomised controlled trial. Lancet. 2002; 359:1734-1739.
62. Wu JY, Wu JY, Liu DY, Li H, Zhuang SW, Li B, Zhou JY, Huang JY, Zhang ZB, Li SQ, Yan ML, Wang YD. Clinical complete response after conversion therapy for unresectable hepatocellular carcinoma: Is salvage hepatectomy necessary? J Hepatocell Carcinoma. 2023; 10:2161-2171.
63. Gory I, Fink M, Bell S, Gow P, Nicoll A, Knight V, Dev A, Rode A, Bailey M, Cheung W, Kemp W, Roberts SK, Melbourne Liver G. Radiofrequency ablation versus resection for the treatment of early stage hepatocellular carcinoma: A multicenter Australian study. Scand J Gastroenterol. 2015; 50:567-576.
64. Liu PH, Hsu CY, Hsia CY, Lee YH, Huang YH, Chiou YY, Lin HC, Huo TI. Surgical resection versus radiofrequency ablation for single hepatocellular carcinoma </= 2 cm in a propensity score model. Ann Surg. 2016; 263:538-545.
65. Kim GA, Shim JH, Kim MJ, Kim SY, Won HJ, Shin YM, Kim PN, Kim KH, Lee SG, Lee HC. Radiofrequency ablation as an alternative to hepatic resection for single small hepatocellular carcinomas. Br J Surg. 2016; 103:126-135.
66. Park EK, Kim HJ, Kim CY, Hur YH, Koh YS, Kim JC, Kim HJ, Kim JW, Cho CK. A comparison between surgical resection and radiofrequency ablation in the treatment of hepatocellular carcinoma. Ann Surg Treat Res. 2014; 87:72-80.
67. Hoang M, Chow P K H. Downstaging locally advanced hepatocellular carcinoma with selective internal radiation therapy. Amer Soc Clin Oncol, 2023:536-536.
68. Majno PE, Adam R, Bismuth H, Castaing D, Ariche A, Krissat J, Perrin H, Azoulay D. Influence of preoperative transarterial lipiodol chemoembolization on resection and transplantation for hepatocellular carcinoma in patients with cirrhosis. Ann Surg. 1997; 226:688-701; discussion 701-703.
69. Wenwen Z, Bingyang H, Jun H, Hongguang W, Zhanbo W, Mingyi C, Shouwang C, Xun W, Junning C, Jihang S. Preliminary report on the combination of PD-1 inhibitor and multi-target tyrosine kinase inhibitor in conversion therapy of advanced hepatocellular carcinoma Chin J Hepatobiliary Surg. 2020; 26:947-948.
70. Zhang W, Lu S, Hu B, Wan T, Wang H, Han J, Zhang Z, Cao J, Xin X, Pan Y. PD-1 inhibitor combined with lenvatinib for unresectable liver cancer as the conversion therapy: An open-label, non-randomized, phase IV study. Wolters Kluwer Health, 2021: e16173-e16173.
71. Zhang W, Hu B, Han J, *et al*. Surgery after conversion therapy with PD-1 inhibitors plus tyrosine kinase inhibitors are effective and safe for advanced hepatocellular carcinoma: A pilot study of ten patients. Front Oncol. 2021; 11:747950.
72. Singal AG, Kudo M, Bruix J. Breakthroughs in hepatocellular carcinoma therapies. Clin Gastroenterol Hepatol. 2023; 21:2135-2149.
73. Kudo M, Ueshima K, Saeki I, Ishikawa T, Inaba Y, Morimoto N, Aikata H, Tanabe N, Wada Y, Kondo Y. A phase 2, prospective, multicenter, single-arm trial of transarterial chemoembolization therapy in combination strategy with lenvatinib in patients with unresectable intermediate-stage hepatocellular carcinoma: TACTICS-L Trial. 2023.DOI: 10.1159/000531377.
74. Kudo M, Ueshima K, Ikeda M, *et al*. Final results of TACTICS: A randomized, prospective trial comparing transarterial chemoembolization plus sorafenib to transarterial chemoembolization alone in patients with unresectable hepatocellular carcinoma. Liver Cancer. 2022; 11:354-367.
75. Kudo M, Ueshima K, Ikeda M, *et al*. Randomised, multicentre prospective trial of transarterial chemoembolisation (TACE) plus sorafenib as compared with TACE alone in patients with hepatocellular carcinoma: TACTICS trial. Gut. 2020; 69:1492-1501.
76. Haopeng L, Yuhang K, Qingsong L, Chang L, Qiu L, Weixia C, Zhiping L, Zhiping L, Yan L, Qiang L, Wusheng L, Xiaoyun Z, Tianfu W, Liver Cancer MDT Team of West China Hospital. Effect of conversion therapy with lenvatinib + transhepatic arterial chemoembolization + PD-1 monoclonal antibody (LEN-TAP) on residual liver volume in patients with moderately advanced hepatocellular carcinoma. Chin J Bases and Clinics in Gen Surg. 2023; 31:1-7. (in Chinese)
77. Li W, Pei Y, Wang Z, Liu J. Efficacy of transarterial chemoembolization monotherapy or combination conversion therapy in unresectable hepatocellular carcinoma: A systematic review and meta-analysis. Front Oncol. 2022; 12:930868.
78. Yu B, Zhang N, Feng Y, Zhang Y, Zhang T, Wang L. Hepatectomy after conversion therapy with hepatic arterial infusion chemotherapy, tyrosine kinase inhibitors and anti-PD-1 antibodies for initially unresectable hepatocellular carcinoma. J Hepatocell Carcinoma. 2023; 10:1709-1721.
79. Palmer DH, Malagari K, Kulik LM. Role of locoregional therapies in the wake of systemic therapy. J Hepatol. 2020; 72:277-287.
80. Montasser A, Beaufrere A, Cauchy F, Bouattour M, Soubrane O, Albuquerque M, Paradis V. Transarterial chemoembolisation enhances programmed death-1 and programmed death-ligand 1 expression in hepatocellular carcinoma. Histopathology. 2021; 79:36-46.
81. Kim MJ, Jang JW, Oh BS, Kwon JH, Chung KW, Jung HS, Jekarl DW, Lee S. Change in inflammatory cytokine profiles after transarterial chemotherapy in patients with hepatocellular carcinoma. Cytokine. 2013; 64:516-522.
82. Park H, Jung JH, Jung MK, Shin EC, Ro SW, Park JH, Kim DY, Park JY, Han KH. Effects of transarterial chemoembolization on regulatory T cell and its subpopulations in patients with hepatocellular carcinoma. Hepatol Int. 2020; 14:249-258.
83. Kudo M, Han KH, Ye SL, Zhou J, Huang YH, Lin SM, Wang CK, Ikeda M, Chan SL, Choo SP, Miyayama S, Cheng AL. A changing paradigm for the treatment of intermediate-stage hepatocellular carcinoma: Asia-Pacific primary liver cancer expert consensus statements. Liver Cancer. 2020; 9:245-260.
84. Terashima T, Yamashita T, Arai K, Kawaguchi K, Kitamura K, Yamashita T, Sakai Y, Mizukoshi E, Honda M, Kaneko S. Response to chemotherapy improves hepatic reserve for patients with hepatocellular carcinoma and Child-Pugh B cirrhosis. Cancer Sci. 2016; 107:1263-1269.
85. Terashima T, Yamashita T, Arai K, Kawaguchi K,

Kitamura K, Yamashita T, Sakai Y, Mizukoshi E, Honda M, Kaneko S. Beneficial effect of maintaining hepatic reserve during chemotherapy on the outcomes of patients with hepatocellular carcinoma. Liver Cancer. 2017; 6:236-249.
86. D'Avola D, Granito A, Torre-Alaez M, Piscaglia F. The importance of liver functional reserve in the non-surgical treatment of hepatocellular carcinoma. J Hepatol. 2022; 76:1185-1198.
87. Paternostro R, Sieghart W, Trauner M, Pinter M. Cancer and hepatic steatosis. ESMO Open. 2021; 6:100185.
88. Iacovelli R, Palazzo A, Procopio G, Santoni M, Trenta P, De Benedetto A, Mezi S, Cortesi E. Incidence and relative risk of hepatic toxicity in patients treated with anti-angiogenic tyrosine kinase inhibitors for malignancy. Br J Clin Pharmacol. 2014; 77:929-938.
89. Xu Z, Qi G, Liu X, Li Z, Zhang A, Ma J, Li Z. Hepatotoxicity in immune checkpoint inhibitors: A pharmacovigilance study from 2014-2021. PLoS One. 2023; 18:e0281983.
90. Atallah E, Welsh SJ, O'Carrigan B, *et al*. Incidence, risk factors and outcomes of checkpoint inhibitor-induced liver injury: A 10-year real-world retrospective cohort study. JHEP Rep. 2023; 5:100851.
91. Luo L, He Y, Zhu G, Xiao Y, Song S, Ge X, Wang T, Xie J, Deng W, Hu Z, Shan R. Hepatectomy after conversion therapy for initially unresectable HCC: What is the difference? J Hepatocell Carcinoma. 2022; 9:1353-1368.
92. Dubbelman AC, Rosing H, Nijenhuis C, Huitema AD, Mergui-Roelvink M, Gupta A, Verbel D, Thompson G, Shumaker R, Schellens JH, Beijnen JH. Pharmacokinetics and excretion of (14)C-lenvatinib in patients with advanced solid tumors or lymphomas. Invest New Drugs. 2015; 33:233-240.
93. Tomonari T, Sato Y, Tanaka H, Tanaka T, Taniguchi T, Sogabe M, Okamoto K, Miyamoto H, Muguruma N, Saito Y, Imura S, Bando Y, Shimada M, Takayama T. Conversion therapy for unresectable hepatocellular carcinoma after lenvatinib: Three case reports. Medicine (Baltimore). 2020; 99:e22782.
94. Kudo M. A novel treatment strategy for patients with intermediate-stage HCC who are not suitable for TACE: Upfront systemic therapy followed by curative conversion. Liver Cancer. 2021; 10:539-544.
95. Zhang B, Xu D, Wang R, Zhu P, Mei B, Wei G, Xiao H, Zhang B, Chen X. Perioperative antiviral therapy improves safety in patients with hepatitis B related HCC following hepatectomy. Int J Surg. 2015; 15:1-5.
96. Chong CC, Wong GL, Wong VW, Ip PC, Cheung YS, Wong J, Lee KF, Lai PB, Chan HL. Antiviral therapy improves post-hepatectomy survival in patients with hepatitis B virus-related hepatocellular carcinoma: A prospective-retrospective study. Aliment Pharmacol Ther. 2015; 41:199-208.
97. Pan Y, Yuan Z, Wang J, Ngai S, Hu Z, Sun L, Yang Z, Hu D, Chen M, Zhou Z, Zhang Y. Survival benefit and impact of adjuvant therapies following FOLFOX-HAIC-based conversion therapy with unresectable hepatocellular carcinoma: A retrospective cohort study. J Cancer Res Clin Oncol. 2023; 149:14761-14774.
98. Forner A, Reig M, Bruix J. Hepatocellular carcinoma. Lancet. 2018; 391:1301-1314.
99. Park JW, Chen M, Colombo M, Roberts LR, Schwartz M, Chen PJ, Kudo M, Johnson P, Wagner S, Orsini LS, Sherman M. Global patterns of hepatocellular carcinoma management from diagnosis to death: The BRIDGE Study. Liver Int. 2015; 35:2155-2166.

Received November 2, 2023; Revised December 14, 2023; Accepted December 21, 2023.

**Address correspondence to:*
Peipei Song, Center for Clinical Sciences, National Center for Global Health and Medicine, Tokyo, Japan.
E-mail: psong@it.ncgm.go.jp

Released online in J-STAGE as advance publication December 23, 2023.

Review

DOI: 10.5582/bst.2023.01275

The immune response of hepatocellular carcinoma after locoregional and systemic therapies: The available combination option for immunotherapy

Yuxin Duan[1,§], Hua Zhang[1,§], Tao Tan[2,§], Wentao Ye[1], Kunli Yin[1], Yanxi Yu[1], Meiqing Kang[1], Jian Yang[1], Rui Liao[1,*]

[1] Department of Hepatobiliary Surgery, the First Affiliated Hospital of Chongqing Medical University, Chongqing, China;
[2] Chongqing Health Statistics Information Center, Chongqing, China.

SUMMARY Hepatocellular carcinoma (HCC) is associated with a highly heterogeneous immune environment that produces an immune response to various locoregional treatments (LRTs), which in turn affects the effectiveness of immunotherapy. Although LRTs still dominate HCC therapies, 50-60% of patients will ultimately be treated with systemic therapies and might receive those treatments for the rest of their life. TACE, SIRT, and thermal ablation can dramatically increase the immunosuppressive state of HCC, a condition that can be addressed by combination with immunotherapy to restore the activity of lymphocytes and the secretion of cellular immune factors. Immune treatment with locoregional and systemic treatments has dramatically changed the management of HCC. In this review, we examine the research on the changes in the immune microenvironment after locoregional or systemic treatment. We also summarize the regulation of various immune cells and immune factors in the tumor microenvironment and discuss the different infiltration degrees of immune cells and factors on the prognosis of HCC to better compare the efficacy between different treatment methods from the perspective of the tumor microenvironment. This information can be used to help develop treatment options for the upcoming new era of HCC treatment in the future.

Keywords Hepatocellular carcinoma, locoregional treatment, systemic treatment, immune therapy, immune microenvironment

1. Introduction

Hepatocellular carcinoma is one of the most common causes of cancer-related mortality worldwide, and it was also the sixth most common malignancy in 2020 (*1*). The stage, location, and comorbidities of the tumor largely determine the choice of an appropriate treatment including surgical resection, liver transplantation, percutaneous ablation, hepatic arterial infusion chemotherapy (HAIC), transarterial chemoembolization (TACE), and radiation embolization (*2*). Due to the high recurrence and metastasis rates of HCC, there are also certain limitations to regional therapy. Therefore, the advent of effective systemic therapies that have been used as preoperative neoadjuvant and postoperative adjuvant therapies may be beneficial in reducing recurrence (*3*). Nonetheless, in HCC, some specific immunotherapy attempts tended to result in short-term drug resistance and failed to dramatically improve efficacy and clinical outcome in HCC patients due to a strong intrinsic immune microenvironment. Excitedly, several high-level clinical studies have recently confirmed that immune checkpoint inhibitors (ICIs) are an effective and well-tolerated treatment option for patients with HCC (*4-6*). In particular, programmed cell death-1 (PD-1) and its ligand (PD-L1), cytotoxic T lymphocyte-associated antigen-4 (CTLA-4), and others obtained early success in clinical trials of HCC. Recently, with advances in combination of immune therapy and local therapy or targeted systemic therapy, a growing number of patients with HCC have achieved longer survival. Based on the comprehensive guidelines for the management of HCC published worldwide, the main difference between the guidelines is the different staging systems which were used to select the best treatment option for patients with HCC. But the safety and efficacy of various combination immunotherapies requires further confirmation.

2. Immune response induced by locoregional treatments (LRTs)

Locoregional treatment (LRT) is an essential treatment for patients with HCC. Surgical resection, liver transplantation, and ablation techniques might also have a stimulatory effect on oncogenesis, related to the proliferation of HCC tumor cells, microenvironmental changes, and both angiogenetic and metastasis triggers of HCC. LRTs enable de novo immune priming by inducing the release of tumor-associated antigens after cell death. Therefore, LRTs, both thermal and nonthermal, and invasive and noninvasive, applied to HCC as well as to other conditions in the liver have been correlated with a more changeable immune microenvironment (Figure 1).

2.1. Surgical resection

Surgical resection (partial hepatectomy, PH) is one of the main radical treatments for HCC, but recurrence is still the main cause of death. It has been demonstrated that surgical resection may impact the liver regeneration microenvironment through suppression of the immune system, inflammation, and the vascular environment during HCC development (*7*). The immune response after surgical resection is mainly manifested in changes in the degree of infiltration of Tregs and the type and robustness of T-cell responses *via* an increase in the depletion of T cells in peripheral blood. As effector factors of liver innate immunity, liver Kupffer cells, natural killer (NK) cells, and natural killer T (NKT) cells can directly affect liver regeneration. After PH, the number of NKT cells and the proportion of $CD11b^+$ Kupffer cells/macrophages (Mφ) shows an increasing trend, and the consumption of NKT cells and NK cells can promote liver regeneration (*8,9*). Dendritic cells (DCs) and hepatic stellate cells (HSCs) have also been shown to promote liver regeneration and to have immunomodulatory effects in the inflammatory environment of the liver (*10,11*). Moreover, cold hepatic ischemia–reperfusion injury (IRI), an innate immunity-driven inflammatory response induced by hepatic vascular occlusion, is a major complication of liver resection and mainly manifests as damage to hepatic sinusoidal endothelial cells and destruction of the microcirculation (*12*). However, IRI is extremely complex, involving a large number of changes in cellular components, factors, and mediators. IRI can induce YAP/Hippo expression, amplified macrophage/neutrophil sequestration and increased the expression of cytokines and ischemia during PH activates Kupffer cells and adherent neutrophils to create reactive oxygen species (ROS) during the initial reperfusion period and. Which can stimulate the transcription factors NF-κB and activator protein-1 (AP-1) and enhance the expression of genes, such as tumor necrosis factor-α (TNF-α), TNF-α, Interleukin (IL)-1β, and IL-6, inducible nitric oxide (NO) synthase (iNOS), heme oxygenase-1, C-X-C motif ligand (CXC) chemokines, and adhesion molecules to inhibit HSC activation (*13,14*). In a mouse model, IRI triggered macrophage-specific T-cell immunoglobulin mucin-4 (TIM-4) activation by stressed hepatocellular phosphatidylserine (PS) presentation (*15*), which may provide us with an IRI therapeutic target to minimize innate inflammatory responses after liver resection. In patients following hepatectomy, C5L2 expression on monocytes and neutrophils decreases after liver resection, and there is a parallel decrease in the chemotactic response of neutrophils to C5a stimulation. C3a, C4a, and their des-Arg forms also showed significant distinct changes in plasma levels after liver resection (*16*). Therefore, after surgery, rapid and dramatic immune responses occur in the liver microenvironment, and postoperative adjuvant immunotherapy maybe necessary for high-risk recurrent patients with hepatocellular carcinoma (Figure 2).

2.2. Liver transplantation

Due to the special immune environment, HCC has a high recurrence rate after liver transplantation (LT). In numerous animal experiments that have investigated the changes in the immune microenvironment after LT, as a radical treatment method for HCC, the number and infiltration degree of immune cells in the HCC microenvironment had drastically changed after LT. As a predictor of HCC recurrence, the postoperative C-reactive protein (CRP) level is increased to varying degrees before, during, and after LT. However, the specificity and sensitivity of CRP have certain limitations. There are numerous reports suggesting that $CD4^+CD25^+$FoxP3 Tregs are elevated at the graft site at the time of rejection in clinical transplant recipients, which decreased to baseline numbers by day >100 in the population of cells within the liver allografts of long-surviving recipients (*17*). These results indicate that CD4+CD25+FoxP3 Tregs, as the most specific Tregs, are more capable of assessing the prognosis of transplantation than CRP. On the other hand, after liver transplantation, recipient NK cells exhibit tolerant phenotypes, with the downregulation of activating receptors and reduced cytotoxicity and cytokine production (*18*). In addition, the animal model of HCC showed that the levels of intragraft TGF-β in Day 35 liver allografts after LT increased markedly; however, they diminished by Day 100. In contrast, intragraft IL-10 mRNA is increased persistently in liver allografts (*17*). In addition to the changes in immune cells and immune factors, the changes in the infiltration degree of immune factors can also explain the changes in the immune microenvironment of the recipient and donor after LT to a certain extent. The lymphocyte-to-monocyte ratio (LMR) could reflect the immune status of the tumor microenvironment after LT, in particular, for HCC patients undergoing living donor liver transplantation (LDLT). Clear studies have indicated that the LMR values decreased within one month and increased again one year after surgery in almost all patients who received LDLT. The reduction in $CD3^+/CD68^+$ cells was greater in patients with a lower LMR (*19*). In addition, macrophages

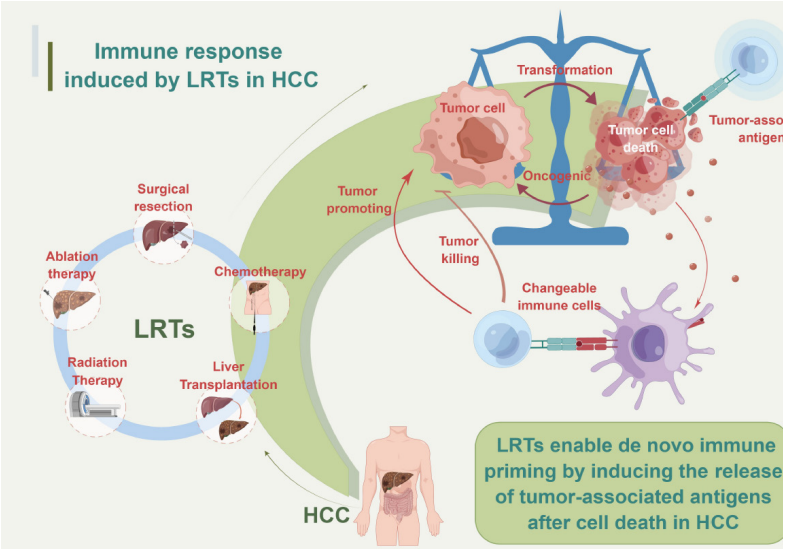

Figure 1. Overview of immune response induced by locoregional treatments via the release of tumor-associates antigens after cell death in hepatocellular carcinoma.

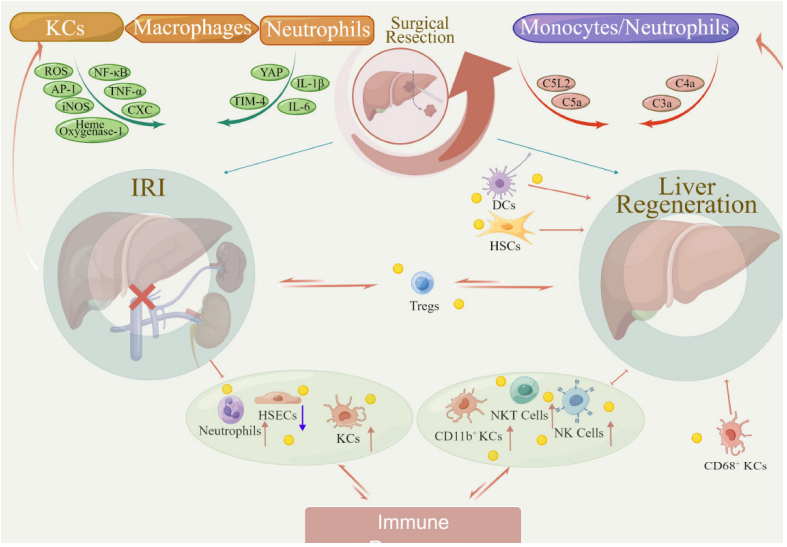

Figure 2. Surgical resection may trigger immune response during the liver regeneration and after ischemia-reperfusion in immune microenvironment of hepatocellular carcinoma.

and Kupffer cells are relevant to immune tolerance due to T-cell apoptosis through the factor-associated suicide/factor-associated suicide ligand (Fas/Fasl) pathway (*20*). In addition to the changes in immune cells, the nonimmune cells in the immune microenvironment after LT were also changed to varying degrees. Based on plasma metabolomics profiling, phosphatidylcholine (PC), nutriacholic acid, and 2-oxo-4-methylthiobutanoic acid were decreased in 122 patients undergoing LT (*21*). Controversially, there is no consensus on the use of postoperative immunosuppressants because the balance between rejection and tumor response is still an unresolved barrier after LT (Figure 3).

2.3. Transarterial chemotherapy

As the standard treatment for patients with intermediate-stage HCC, transarterial chemotherapy (TACE) is generally performed as the treatment for large, unresectable, or multinodular HCC in well-functioning patients. By collecting peripheral blood from liver cancer patients before and one month after TACE treatment, it was discovered that the expression of PD-L1 and PD-1 after TACE treatment was significantly higher in patients with poor TACE response. Moreover, PD-L1 mRNA expression was higher in peripheral blood monocytes, while the ratio of $CD4^+$ to $CD8^+$ cells decreased(*22*). In contrast, in research on tumor pathology in HCC patients, there was no difference in the expression of coinhibitory proteins, including PD-L1, Indoleamine2,3-dioxyge-1(IDO-1), lymphocyte activation gene-3 (LAG-3), TIM-3, or CTLA-4 corepressor proteins, in HCC tissue samples treated with TACE(*23*). On the other hand, using high-throughput sequencing technologies to verify the changes in gene expression within the TME, the results showed evidence of the significant upregulation of a number of proinflammatory genes in TACE-pretreated samples (*23*). Other studies support this conclusion. Cytometric bead immunoassays were used to simultaneously measure cytokines in the sera of patients with HCC after TACE, which revealed that the inflammatory cytokines IL-6 and IL-22 significantly increased early and that Th2

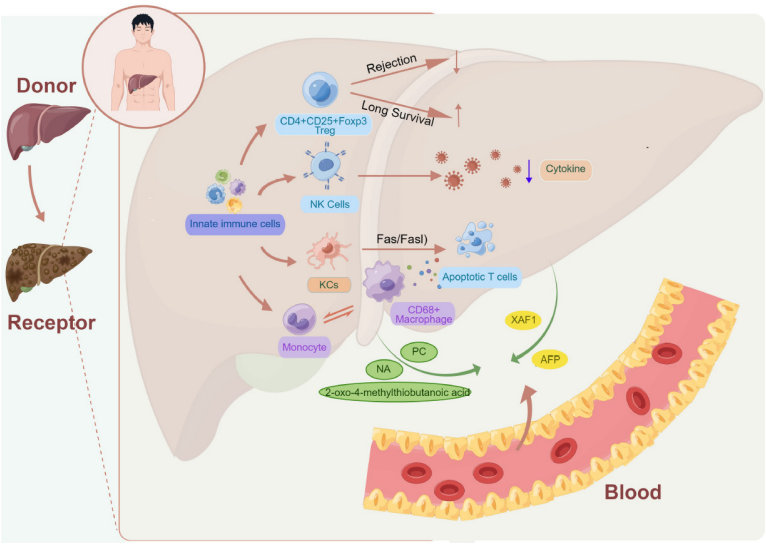

Figure 3. The changes in the immune microenvironment after liver transplantation summarized in this review.

cytokines (IL-4, IL-5, or the suppressive cytokine IL-10) were also increased in the late phase (*24*). In addition, evidence from other studies suggests that the levels of several cytokines, including IL-1β, IL-2R, IL-6, IL-22, and IL-8, were all increased after TACE (*25*). Regarding the changes in the tumor microenvironment of HCC patients caused by TACE, retrospective studies have proven that patients who received TACE were found to experience peritumoral portal lipiodol enhancement (*26*). Additionally, hypoxia regulators such as vascular endothelial growth factor (VEGF), which are induced by HIF-1α, also underwent dynamic changes after TACE in HCC patients (*27,28*). Researchers evaluated the levels of VEGF and tryptase serum concentrations from 71 unresectable HCC patients before and after hepatic TACE and obtained higher serum VEGF levels and lower tryptase levels (*28*). In addition to VEGF, the levels of AST, ALT, and lactate dehydrogenase (LDH) in the sera of patients with HCC who underwent TACE reached peak values within 1 day, while basic fibroblast growth factor (bFGF) and TNF-α levels exhibited mild increases during the 1st week. Conversely, angiogenin, epidermal growth factor (EGF), and TGF-β levels decreased following TACE (*29*).

Whereas hepatic arterial infusion chemotherapy (HAIC) entails infusing chemotherapeutic agents directly into hepatic tumors, which can avoid the first-pass effect and provide a higher intratumoral concentration of chemotherapeutic agents.Theoretically, compared with TACE, HAIC yields less hepatocellular injury and greater treatment efficacy. In a study involving 36 HCC patients treated with HAIC, the frequency of TAA-specific T cells and Tregs and myeloid-derived suppressor cells (MDSCs) was measured by interferon-gamma enzyme-linked immunospot assays and multicolor fluorescence-activated cell sorting analysis (*30*). In 22.2% of patients, after HAIC, the frequency of TAA-specific T cells increased. However, the frequency of Tregs decreased. Patients with a low MDSC frequency were also found to have a longer overall survival time. In addition to the levels of various immune cells, and similar to the changes in cytokines after TACE, for example, the increase in serum cytokine levels, chemokines, and other growth factors in the HCC microenvironment (*31*), the combination of the neutrophil-to-lymphocyte ratio and the ratio of early des-carboxyprothrombin changes (*32*) can also be a useful predictor of HAIC. Among 90 patients from a retrospective study evaluating AFP and des-gamma-carboxyprothrombin (DCP) levels after half a course of HAIC, 8 (8.9%), 19 (21.1%), and 63 (70.0%) had an elevated level of AFP, elevated level of DCP, or elevated level of both of these tumor markers, respectively (*33*). In recent studies, the changes in 20 serum cytokines and growth factors were proven to be associated with prognosis in HCC patients who were treated and underwent HAIC, such as von Willebrand factor (VWF) and VEGF (*34*). The serum level of VEGF was significantly decreased after HAIC, and it is an important predictive factor for therapeutic effect and survival in patients with advanced HCC undergoing HAIC. In addition, the ADAMTS13 activity-VWF levels and serum cell-derived factor 1 levels in HCC patients with stable disease and partial response to HAIC treatment were significantly higher than those in patients with progressive disease and lower serum hepatocyte growth factor (HGF) and IL-4 levels than nonresponders (*34*). Nonetheless, cytokines have limited roles in predicting HCC responses in patients who receive HAIC. Because HAIC mainly targets cancer epithelial cells in HCC, the exposed important biomarkers have greater predictability in advanced HCC patients (Figure 4).

2.4. Radiation therapy

The importance of transarterial radioembolization (TARE) in the treatment of patients with unresectable HCC cannot be ignored. Clinical studies have suggested that higher doses of radiation to the tumor increase the likelihood of

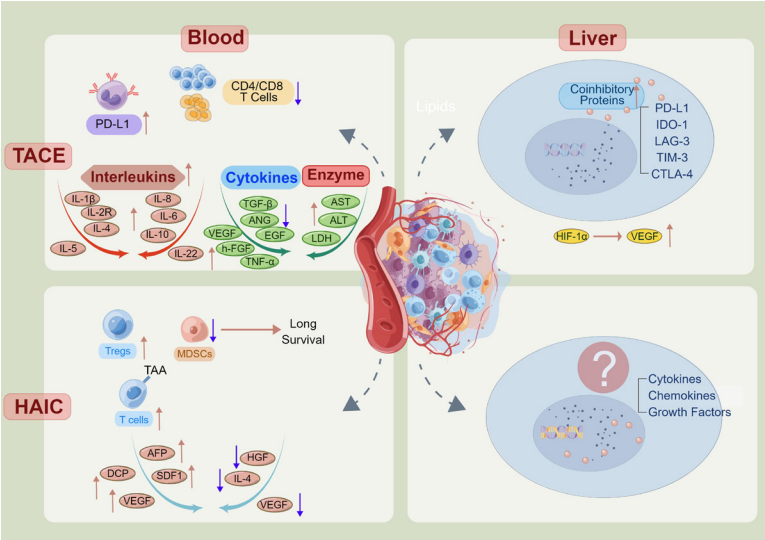

Figure 4. Various immune cells, cytokines, chemokines and growth factors emerging in the blood and liver tissues after trans-arterial chemotherapy and hepatic arterial infusion chemotherapy, respectively.

inducing a positive immune response (*35*). A retrospective assessment of the dynamic changes in lymphocytes following TARE of HCC and its association with normal liver dose (NLD) of TARE found a moderate negative association between the NLD and lymphocyte count at 1 month posttreatment that was most significant at 3 months posttreatment (*36*). In an early prospective clinical study, after TARE, proinflammatory (IL-6 and IL-8) and oxidative stress (malondialdehyde) markers continued to increase, endothelial damage markers (vW factor and PAI-1) and coagulation cascades (factor VIII, PAI-1, and D-dimer) were induced, and a significant increase in factors associated with liver regeneration (FGF-19 and HGF) was observed (*36*).

TARE with yttrium 90 is one kind of palliative lobar therapy for HCC patients with advanced disease or for those in whom other therapies have failed; it delivers local high-dose radiation to tumors through microembolic microspheres, preserving blood flow to promote radiation injury to the tumor. An earlier follow-up trial of the hepatic artery involving (yttrium)-Y-90 microspheres showed that lymphocyte subsets except for NK cells were significantly (> 50% from pretherapy values), promptly (as early as 24 h) and persistently (up to 30 months) depleted post-(90)Yttrium microsphere therapy (*37*), which may lead to increased levels of IL-10 and IP-10 (*38*). ILs isolated after Y90-RE showed signs of local immune activation: elevated granzyme B expression and infiltration of $CD8^+$ T cells, $CD56^+$ NK cells, and $CD8^+$ $CD56^+$ NKT cells.

Stereotactic body radiotherapy (SBRT) is a treatment option for advanced HCC patients who are not candidates for local therapies such as surgery that uses high doses of radiation per fraction in fewer fractions with high precision and accuracy to achieve local tumor control. In preclinical studies, SBRT has been shown to induce tumor cell death by causing tumor-associated endothelial cell death and vascular damage (*39*). SBRT could preserve lymphocytes and increase the expression of various immunostimulatory cytokines within the irradiated tumor microenvironment and the activation of antitumor T cells, thereby eliciting enhanced antitumor immunity. The principle of SBRT in HCC, however, differs partially from that of other radiotherapy methods. The inflammatory environment can be modified to become suitable for HCC after undergoing SBRT. To determine the changes in circulating levels of a panel of soluble cytokine receptors and liver-secreted proteins in HCC patients during SBRT, Sylvia S *et al*. (*40*) assessed the plasma levels of these soluble factors following one to two fractions of SBRT. The researchers found that in patients with HCC after one to two fractions of SBRT, those who developed liver toxicity had significantly higher levels of soluble tumor necrosis factor receptor II and lower levels of soluble CD40 ligand (sCD40L) and chemokine CXCL1 compared to levels in those who did not develop liver toxicity. In addition, plasma sCD40L levels are positively associated with platelet number, and the low platelet and sCD40L levels in HCC patients contribute in part to a decrease in liver immune function (*41*). On the other hand, with the development of immuno-oncology, increasing evidence has suggested that the changes in the neutrophil-to-lymphocyte ratio (NLR), platelet-to-lymphocyte ratio (PLR), and cytokines can respond to antitumor therapies. Several retrospective studies collected peripheral blood cell count, NLR, and PLR data before and after SBRT and found that circulating blood cell, total leukocyte, neutrophil, lymphocyte, and platelet counts decreased significantly after SBRT (*42,43*). While no significant difference was observed for hemoglobin levels, it was found that the NLR and PLR were significantly increased post-SBRT compared with pre-SBRT and were complementary predictors of OS in HCC patients treated with SBRT (*42*) (Figure 5).

2.5. Ablation therapy

2.5.1. Radiofrequency ablation (RFA)

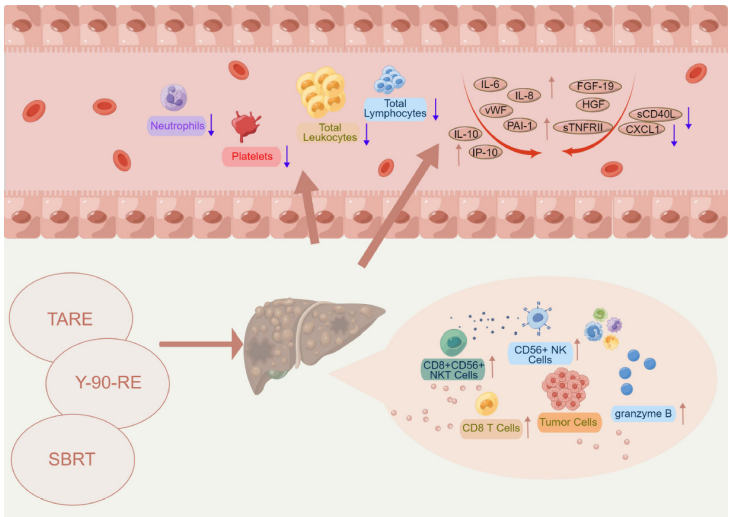

Figure 5. The immune response induced by radiation therapy including trans-arterial radioembolization (TARE), TARE with yttrium 90 (Y-90-RE) and stereotactic body radiotherapy.

RFA is the most validated and widely used technique in the early stages of HCC, and it is the most commonly used technique for local ablation of HCC tumors smaller than 5 cm in diameter. Both local and systemic immune responses induced by RFA have been extensively documented. RFA is performed by using frictional heat generated by the high-frequency alternating current to induce HCC cell death, and the available studies clearly demonstrate that there is a greater release of immunogenic intracellular substrates in areas subjected to heat-induced cell necrosis (*44*).

Thermal ablation induced by RFA can induce a large number of changes in the expression of immune cytokines in HCC tissues, especially in incompletely ablated tissues. One study found that the changes in Th1/Th2 cytokines in HCC patients after RFA exhibit clear upregulation and downregulation trends (*45*). After RFA, the levels of Th1 cytokines, including TNF-α, IFN-γ, and IL-2, were significantly upregulated, and the levels of Th2 cytokines, including IL-4, IL-6, and IL-10, were markedly downregulated, while the serum level of AFP decreased, which indicates that RFA could change the expression of immune cytokines, promoting tumor antigen presentation and activating T lymphocytes. In addition to Th1/Th2 cytokines, after RFA, there is a release of circulating histones, including myeloperoxidase (*46*), and an increase in tumor-specific antibodies, $CD4^+$ T cells (*47*), $CD8^+$ T cells, and NK cells (*48*). Apart from T helper cells, earlier studies have demonstrated that the number of tumor-associated antigen-specific T cells after RFA was inversely correlated with the frequency of $CD14^+$ HLA-DR/low myeloid-derived suppressor cells (MDSCs) (*49*).

On the other hand, RFA can not only effectively kill HCC tumor cells but can also release tumor antigens to induce an immune response or trigger an inflammatory response, resulting in the accumulation of a large number of antigen-presenting cells (APCs). For example, the nuclear proteins high mobility group B1 and heat shock proteins (HSPs) may induce antitumor immune responses by activating dendritic cells (DCs). In particular, the expression levels of HSP70 and HSP90 showed the most pronounced increasing trend after RFA, with 8-fold and 1.2-fold increases, respectively (*50*). In serological studies, three proteins, namely, CLU, Ficolin-3, and RBP4, were also identified as having significantly altered expression, especially Ficolin-3, which showed marked overexpression affected by thermal ablation (*51*). Palliative RFA (pRFA) has also been shown to accelerate residual tumor progression by increasing tumor-infiltrating MDSCs and reducing the T-cell-mediated antitumor immune response (*52*).

Although it is well established that thermal radiation can alter the expression of various immune cells and cytokines in the microenvironment of HCC, the impact of these changes on HCC progression and recurrence remains to be confirmed in further studies. Many available studies have noted that the main actors of RFA immune dynamics are innate immune cells (*e.g.*, NK cells and DCs) and that they are closely linked to HCC recurrence, and the specific mechanisms involved are a hot topic for future studies.

2.5.2. Cryoablation

The safety and feasibility of cryoablation as a new nonthermal locoregional treatment have been verified. Cryoablation is used to promote tumor cell death indirectly or directly through repeated cycles of freezing, and the host immune system can use tumor antigens to trigger the activation of innate and adaptive immunity against tumor antigens. The process of repeated freezing and thawing and cell membrane lysis can promote the release of cellular antigens and trigger a cryoimmunological response.

In a rat liver model, cryoablation induces inflammation and coagulation, and the production by splenocytes of tumor necrosis factor TNF-α, interferon INF-γ, and the interleukins IL-4, IL-6 and IL-10 increased significantly after cryoablation (*53*). In addition, there were increases in WBCs and decreases in platelets

and hemoglobin. Cryoablation also has an effect on angiogenesis, with upregulation of VEGF expression in tumor tissue and a significant increase in angiogenesis in the residual tumor (*54*).

In addition to rat liver models, similar results have been found in clinical studies. A study using flow cytometry to measure the Treg frequency in the peripheral blood of 111 patients with liver cancer showed that the numbers of $CD8^+$ $CD4^+$ and $FoxP3^+$ cells were significantly decreased after cryoablation cycles (*55*). In addition, it has been shown that the PD-1 and PD-L1 receptors on activated T cells and B cells are also altered. The expression of PD-1/PD-L1 decreased after cryoablation but was elevated at the time of tumor recurrence (*56*). The argon-helium cryosurgery system (AHCS) has now been clearly demonstrated to be effective in killing tumor cells and maximizing the protection of normal liver tissue. By monitoring the percentage of $CD4^+$ and $CD8^+$ T cells and NK cells in HCC patients after AHCS, it was found that the percentage of $CD4^+$ T cells and NK cells was significantly higher compared to pretreatment, but the percentage of $CD8^+$ T cells was significantly lower (*57*). These studies can preliminarily demonstrate an excellent synergistic effect between cryoablation and immunotherapy in the treatment of HCC.

2.5.3. Microwave ablation (MWA)

MWA, similar in immune action to RFA, delivers a microwave oscillating electric field through a needle that greatly increases the temperature in the targeted cancer tissue. The effect of MWA on immune cells is well established, with several demonstrations of altered numbers of T cells, B cells and NK cells following MWA. For example, there was a significant increase in Th17 cell levels and a significant increase in $CD3^+$ cells and $CD4^+$ cells 1 month after MWA (*58*). In addition, the percentage of immune cell subsets was also affected by MWA, with the frequency of effector memory T cells decreasing at 7 days after MWA, the percentage of plasmablasts increasing at Day 7 after treatment, and NK cells consistently increasing after MWA treatment. In particular, a significant increase in subsets of activated T and B cells was observed in patients with long survival times (*59*).

As in RFA, in addition to the alteration of immune cells, corresponding immune cytokines were also altered by ablation, such as a significant increase in the frequency of IFN-y and IL-5 responses in patients with long-term remission relative to patients in early relapse and a significant enhancement of IL-12 and a significant decrease in IL-4 and IL-10 1 month after MWA (*59,60*).

2.5.4. High-Intensity focused ultrasound

High-intensity focused ultrasound (HIFU), as a noninvasive medical technique, is safe and well tolerated and has a significant survival advantage compared with other ablation treatments. It is a kind of hyperthermia and ultrasound therapy that can produce mechanical and thermal effects. The mechanical effect is caused by the negative pressure of ultrasound that forms cavitation to destroy the tumor tissue. The thermal effect induced by the ultrasound beam causes coagulative necrosis of the tissue.

As early as a decade ago, studies were conducted to compare the changes in circulating levels of all measured immunosuppressive cytokines in patients with malignant tumors before and after high-intensity focused ultrasound (HIFU) treatment. The results showed that the levels of serum immunosuppressive cytokines decreased after HIFU treatment, especially VEGF, TGF-β1 and TGF-β2, which were all significantly reduced (*61*). Regarding the changes in cellular immune factors in a short period of time after HIFU treatment, an ultrasound-guided HIFU study from Germany showed that tumor ablation with HIFU induced early sterile inflammation and an increase in leukocytes, CRP, and LDH within the first 20 h after HIFU (*62*). However, a major issue with HIFU is that it is difficult to achieve complete tumor ablation. The decrease in the levels of HIFs, including HIF-1α and HIF-2α, are the result of HIFU, and the levels of these factors increased significantly in residual tumor tissue following HIFU treatment. In addition, a high antigen-specific T-cell response was observed after 2 weeks and did not decrease, even after 10 months (*63*).

2.5.5. Laser ablation

Laser ablation (LA) is an efficient and safe novel treatment for HCC. The technology mainly causes photochemical damage to biological tissue with the formation of radicals and inflammation and causes protein denaturation with heat damage (*64*).

In existing animal studies, the moderate heat stress induced by LA could induce the expression of growth factors in HCC cells and hepatocytes, including heparin-binding growth factor, fibroblast growth factor 21, and nerve growth factor (*65*). In addition to immune cytokines, temperature can induce alterations in the tissue constituents and their structural organization, thus resulting in a measurable change in tissue optical properties. Hyperspectral imaging (HSI) has potential for diagnostic purposes such as the detection of cancers, and it can also provide valid support for therapy and surgery guidance. The thermal response in porcine hepatic tissue induced by laser ablation was assessed based on the spectral and spatial information provided by HSI. It was found that methemoglobin (MetHb) and deoxyhemoglobin (Hb) decreased with increasing temperature and then gradually reached a plateau phase with an increase in temperature > 80°C (*66*). However, the effect of LA on the microenvironmental changes and

immune response of HCC prognosis needs to be further studied.

2.5.6. Irreversible Electroporation (IRE)

Irreversible electroporation (IRE), as a new nonthermal ablation technique, is unlikely to damage cancer tissue by thermal effects, which are found with RFA, MWA, HIFU, and LA. Because of this feature, IRE can be used for tumor ablation in special sites such as those adjacent to bile ducts and blood vessels without destroying the adjacent structures (*67*).

IRE can affect many immune factors in the HCC microenvironment to varying degrees. Animal experimental models of IRE in recent years have illustrated the advantages and disadvantages of this ablation method in terms of the postoperative inflammatory response and the degree of immune cell infiltration. On Day 1 after IRE, activated T cells and NK cells increased, and Treg cells and circulating CD4 T-cell subsets (but not CD8) decreased (*68*). Furthermore, a significant increase in the infiltration of cytotoxic CD8 T cells was observed in post-IRE tumors in mice. The serum IFN-γ level was also significantly increased after IRE in rats (*68*). Moreover, the results from the animal model indicated that IRE could induce antitumor adaptive immunity dominated by the infiltration of cytotoxic $CD8^+$ T cells into the tumors, accompanied by reduced Tregs. IRE can evoke $CD8^+$ T-cell immunity by inducing cell necrosis and significant release of risk-related molecular patterns, including ATP, high mobility group box 1, and calreticulin, helping to prevent HCC progression after ablation (*69*). However, studies on the prognostic value of IRE in HCC in clinical patients are limited, and most of the current studies are focused on comparing the survival rate of patients after IRE treatment or on comparing the effects of different ablation modalities in mouse models. Therefore, the changes in the tumor microenvironment when IRE is applied to human HCC need to be further discussed and verified (Figure 6).

3. Immune response induced by systemic therapy

Systemic therapy for HCC has changed drastically since the combination of atezolizumab and bevacizumab was approved by the FDA and shown to improve overall survival relative to sorafenib. Many clinical randomized trials have demonstrated that combined immunotherapy, such as atezolizumab plus bevacizumab and apatinib plus camrelizumab (*70*), can improve prognosis in all aspects compared with sorafenib monotherapy. However, changes in the immune microenvironment of HCC after systemic therapy remain a major cause of resistance and recurrence, and the mechanisms underlying the altered immune response to systemic therapy due to the robust immunosuppression state involve many stromal cells, humoral mediators, and inhibitory checkpoint molecules, which need to be further explored.

3.1. Tyrosine kinase inhibitors (TKI)

Currently, tyrosine kinase inhibitors (TKIs) are used as first-line therapy for HCC. There are clinical shreds of evidence that suggest that the acquisition of somatic mutations can lead to TKI resistance. Since the adaptive immunity of HCC can inhibit tumor recurrence, TKIs can act on multiple tumor-activated signaling pathways, such as KIT, RET, vascular endothelial growth factor receptor (VEGFR), PDGFR, and fibroblast growth factor receptor (FGFR), thus showing the universality and persistence of efficacy.

Sorafenib can facilitate apoptosis, mitigate angiogenesis and inhibit tumor cell proliferation. To explain the effects of RFA alone and in combination with sorafenib, growth factor measurement in a standing tumor in a two-tumor rat model of HCC revealed that sorafenib treatment decreased HGF levels and microvessel density, whereas VEGF, macrophages, T cells and IL-10 levels were increased by sorafenib (*71*). Macrophages serve as an important component of the immune system and are the key for antitumor activity in HCC. In contrast, clinical

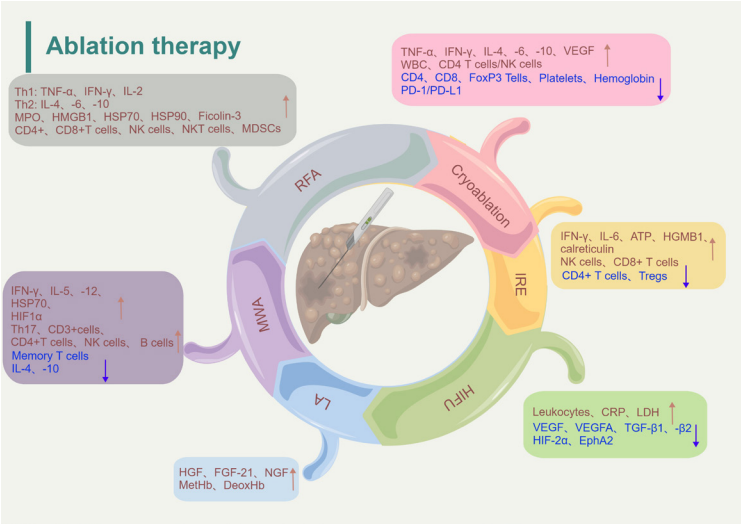

Figure 6. The immune response induced by various ablation therapies summarized in this review.

trials have proven that when dendritic cells are inhibited by sorafenib, macrophages are reduced or activated by altered polarization (*72*).

Lenvatinib has potent antiangiogenic activity, which suppresses VEGFR 1–3, FGFR 1–4, platelet-derived growth factor receptor (PDGFR)-α, and the proto-oncogenes RET and KIT (*73*). Currently, lenvatinib has been approved as a first-line treatment for HCC in Japan, the United States, and China. In addition to the angiogenic effects due to the inhibition of kinases, it also has a regulatory effect on immune function. Lenvatinib reduced tumor PD-L1 levels, Tregs, and the proportion of monocyte and macrophage populations and increased the proportion of CD8 T-cell populations (*74*).

Donafenib is a novel multikinase inhibitor that is similar to sorafenib. As a second-line treatment for patients with HCC, donafenib is superior to sorafenib in terms of improved survival and safety tolerance. Serum cytokines, including IL-6, TNF-α and IFN-γ, were strongly upregulated in a rabbit VX2 liver tumor model after treatment with donafenib (*75*).

Apatinib selectively blocks VEGFR2 by occupying its binding site, thereby preventing the formation of new blood vessels in tumor tissues. In an immunodeficient mouse xenograft model of HCC, apatinib was shown to cause metabolomic changes, with a significant increase in 3-hydroxybutyric acid (3-HB) in serum, tumor tissue, and liver(*76*). In an *in vitro* study on apatinib inhibiting the invasion and metastasis of HCC, the expression of tissue inhibitors of metalloproteinases (TIMPs)-3 and TIMP-4 was upregulated, while the expression of matrix metalloproteinases (MMPs)-1, MMP-2, MMP-3, MMP-7, MMP-9, MMP-10, MMP-11, and MMP-16 was downregulated by apatinib treatment (*77*). However, there is also much evidence that apatinib can cause immune and hematological adverse effects, mainly leukopenia, granulocytopenia and thrombocytopenia (*76*).

As an orally available multitargeted TKI, regorafenib has better efficacy than sorafenib. It can prevent the progression of HCC by reducing cell proliferation, invasion and metastasis; inducing cell death and autophagy; and exerting great antitumor activity. Most importantly, similar to other TKI inhibitors, it can reduce the expression and secretion of the metastasis-related markers MMP-2 and MMP-9. Regorafenib also decreased the levels and secretion of angiogenesis-related proteins, including VEGF, TNF-α, IL-1β and IL-6 (*78*). In addition, regorafenib can regulate tumor-associated macrophages to enhance the body's antitumor immunity, and it can induce T-cell activation and M1 macrophage polarization (*79*).

A growing number of clinical studies have demonstrated that, regardless of the stage of HCC, corresponding TKI therapy can support other treatments for HCC patients, which can help patients achieve better efficacy or improve the prognosis and tumor recurrence to a certain extent.

3.2. Immune checkpoint inhibitor (ICI)

In the application of ICIs in HCC, pembrolizumab and nivolumab, anti-PD-1 humanized antibodies, were approved by the US FDA as a second-line treatment for HCC patients. The main antitumor mechanism of immune checkpoint inhibitors is the reversal of anti-PD-1/anti-PD-L1 CD8 T-cell failure. The major suppressed inhibitory immune checkpoint receptors include PD-1, CTLA4, LAG3 and TIM3, which play an important role in maintaining self-tolerance. Mechanistically, PD-1 binds to T-cell receptors upon binding to its ligand PD-L1, leading to broad dephosphorylation of T-cell-activating kinases and resulting in apoptosis of T cells (*80*). Both in mouse model of primary HCC and in clinical trials, a reduction in PD-L1 and TGF-β expression and Treg infiltration, a significant increase in circulating CD8+ T cell activity, and downregulation of neutrophil-related markers were found during pembrolizumab treatment (*80,81*). More specifically, in a recent study evaluating the efficacy of PD-1 immunotherapy based on single-cell sequencing, patients treated with ICIs were identified as having an increase in B cells and a decrease in dendritic cells, regulatory T cells, and NK cells (especially those overexpressing CD16, CD38, and CD11c)(*82*).

Anti-CTLA-4 is most strongly expressed on Tregs, so the effect of anti-CTLA-4 antibodies may be related to the inhibition of Treg activity. The two most common anti-CTLA-4 antibody drugs are ipilimumab and tremelimumab. A result from survival analyses and an immune monitoring study of tremelimumab therapy showed that $CD3^+$ T-cell infiltration and PD-1 expression increased in the tumor tissue, and $CD4^+$-$HLA\text{-}DR^+$, $CD4^+PD\text{-}1^+$, $CD8^+HLA\text{-}DR^+$, $CD8^+PD\text{-}1^+$, $CD4^+ICOS^+$ and $CD8^+ICOS^+$ T cells in the peripheral blood also increased after tremelimumab therapy (*83*). Similar results were obtained in a study in which CTLA-4 blockade suppressed the progression of tumors in a subcutaneous murine hepatoma model. IHC showed that the expression of CD4+ and CD8+ T cells and the level of IFN-γ were increased in tumor tissues treated with an anti-CTLA-4 antibody alone compared with untreated tumor tissues (*84*). In other words, anti-CTLA-4 antibodies might exert antitumor effects by depleting the Treg cell population in the tumor microenvironment.

According to numerous former studies on the poor prognosis of anti-CTLA-4 antibodies, the adverse effects of CTLA-4 inhibition occur mainly after activation of T cells in lymphoid organs (*85*). These insights may also provide evidence for why anti-CTLA-4 antibodies should be used in combination with other immunotherapies.

In addition to anti-PD-1, anti-PD-L1 and anti-CTLA-4 antibodies that have been widely used in the clinical treatment of HCC, Tim-3, as a newly discovered immune checkpoint molecule, also shows antitumor effects in the targeted treatment of HCC. In contrast to the limited expression of PD-1 on depleted T cells,

Tim-3 is an immune checkpoint molecule that is widely expressed in humans. Previous research has established that there are biointerfacing antagonizing T-cell inhibitory nanoparticles (BAT NPs) for HCC, which were developed by cloaking the platelet membrane on the PLGA microsphere surface to load T-cell immunoglobulin domain and mucin domain-3 antibodies (anti-TIM-3) as well as PD-L1. This therapeutic effect could subsequently activate effector T lymphocytes and the polarization of M1-type macrophages as well as antigen presentation by dendritic cells (*86*). Finally, the relationship between the high expression of Tim-3 and the poor prognosis of HCC has been clearly confirmed, and it can regulate the microenvironment of stem cells and affect the regulation of the biological behavior of HCC. Although the development of anti-TIM-3 antibodies in HCC is still relatively new, it must be a potential strategy for HCC immunotherapy. The immune response of hepatocellular carcinoma induced by systemic therapies is summarized in Table 1.

4. Combination of LRTs and immunotherapy

One of the theoretical bases of combination therapy is that LRTs can induce an immune response and inform the immunosuppressive microenvironment of HCC. The combination of LRTs and immunotherapy has synergistic antitumor effects. Previous studies have shown that LRTs such as TACE, SIRT, and thermal ablation can increase tumor immunogenicity by inducing inflammation and releasing more tumor-associated antigens, thereby increasing tumor invasion cytotoxicity and inducing systemic antitumor immune responses. Immunotherapy can address these immunosuppressive states by modulating the activity of lymphocytes and the secretion of cellular immune factors, helping patients achieve longer survival; for example, the combination of TACE and sorafenib has both efficacy and safety benefits due to the use of either treatment alone (*87*). The combination therapy of RFA and adoptive cell immunotherapy has shown excellent clinical efficacy, and RFA and RetroNectin activated killer cells effectively increase the proportion of $CD3^+/CD8^+$ cells and decrease the ratio of $CD4^+/CD8^+$ cells (*88*). Additionally, a phase I clinical study evaluating the safety of MWA combined with adoptive immunotherapy in HCC patients showed a reduction in the percentage of $CD4^+CD25^{high}$ Treg cells and an increase in $CD8^+CD28^-$ effector cells after 1 month (*89*).

As mentioned earlier, treatment with anti-CTLA-4 antibody alone may produce cytotoxicity and adverse effects, and combination therapy with anti-CTLA-4 antibody with other LRTs is able to achieve a better prognosis. In a clinical trial of tremelimumab in combination with ablation, six-week tumor biopsies following treatment demonstrated a clear increase in CD8 T cells in patients showing clinical benefit (*90*). To demonstrate the efficacy of the combination of RFA and anti-CTLA-4 antibody, Zhang *et al*. divided forty mice with tumors established on their right flanks into four groups: control group (no treatment), RFA group (insufficient RFA alone), anti-CTLA-4 group (anti-CTLA-4 monotherapy), and RFA + anti-CTLA-4 group (insufficient RFA + anti-CTLA-4). The IFN-γ concentration and $CD4^+$ and $CD8^+$ lymphocyte expression in the mice of the RFA + anti-CTLA-4 group were significantly higher than those of the other three groups (*84*).

Nevertheless, there are still clinical findings that run counter to the points mentioned above. As mentioned earlier, sorafenib can affect VEGF and HGF levels in the tumor environment, but sorafenib combined with arterial infusion chemotherapy was more likely to cause adverse events including neutropenia and thrombocytopenia than sorafenib alone. In conclusion, to achieve the best outcome of immunotherapy, the specific implementation of LRTs and immunotherapies needs to be further verified. Table 2 reviews the clinical trials of the combinations of LRTs and immunotherapy in HCC.

5. Combination of systemic therapy and immunotherapy

Although monotherapy for advanced HCC did not show a statistically significant change in efficacy, the combination of immunotherapies has shown an advantage in various survival assessment efficacy values. The combination of an inhibitor of VEGF and PD-1 or its ligand PD-L1 is a standard of care for patients with advanced HCC. Recently, the combination of atezolizumab (anti-PD-L1 antibody) plus bevacizumab (an anti-VEGF monoclonal antibody) demonstrated significantly longer OS and PFS than sorafenib in patients who were not previously treated (*91*). In orthotopic-grafted or induced-murine models of HCC, combination therapy with anti-PD-1 and anti-VEGFR-2 increased cluster $CD8^+$ cytotoxic T-cell infiltration and activation, shifted the M1/M2 ratio of TAMs and reduced Treg and chemokine (C-C motif) receptor 2-positive monocyte infiltration in HCC tissue (*92*). Furthermore, under anti-PD-1 therapy, CD4+ cells promote normalized vessel formation in the face of antiangiogenic therapy with anti-VEGFR-2 antibody (*92*). Compared with PD-1 antibody monotherapy, the combination therapy enhanced T-cell infiltration, improved the efficacy of the PD-1 antibody and prolonged survival. Mechanistically, Peg-IFNα promotes the cytotoxic CD8+ T-cell infiltration microenvironment by inducing the secretion of chemokine CCL4, and the PD-1 antibody was able to restore the cytotoxic capacity of CD8+ T cells by inhibiting the IFNα-IFNAR1-JAK1-STAT3 signaling pathway (*93*).

A series of recent studies involving multiplex IHC, suspension mass cytometry (CyTOF), and Imaging Mass Cytometry™ (*94*) were performed to elucidate both

Table 1. Summary of the immune response of hepatocellular carcinoma induced by systemic therapies

Systemic Therapy	Immune Cell Response		Regulation of Cytokine and Chemokine		Ref
	Increased	Decreased	Up	Down	
TKI	macrophage, T-cells,NK cell		VEGF and IL-10 levels	HGF levels and microvessel density (MVD),growth factor receptor (VEGFR)1–3, fibroblast growth factor receptor (FGFR) 1–4, platelet-derived growth factor receptor (PDGFR)-α	*71,72*
	CD8 T cell				
		Treg, and the proportion of monocyte and macrophage populations		PD-L1	*73*
			serum cytokines including IL-6, TNF-α and IFN-γ, 3-hydroxybutyric acid (3-HB)		*74*
			TIMPs -3 and TIMP-4	MMP-1, MMP-2, MMP-3, MMP-7, MMP-9, MMP-10, MMP-11, and MMP-16	*76*
		leukopenia, granulocytopenia and thrombocytopenia		VEGF, TNF-α, IL-1β and IL-6	
	T cell activation and M1 macrophage				*78*
Immune checkpoint inhibitor (ICI)					
PD-1 PD-L1		T cells		PD-L1	*80*
	cytotoxic T-cell and CD8+ T cells	Tregs		neutrophil-associated markers	*84*
	B cells	DCs, regulatory T cells, and NK cells(over-expressing CD16, CD38, and CD11c)	CXCL9	TGF-β	*81*
CTLA-4	CD3+ T cells (in tumor tissue)		PD-1 expression		
	CD4+-HLA-DR+, CD4+PD-1+, CD8+HLA-DR+, CD8+PD-1+, CD4+ICOS+ and CD8+ICOS+ T cells (in the peripheral blood)				*82*
	CD4+ and CD8+T cell		IFN-γ		*83*
	T cells (in lym-phoid organs)	Tregs			*84*
Tim-3	T lymphocytes and polarization of M1-type macrophages				*86*

Abbreviation: TKI: Tyrosine kinase inhibitors; VEGF: vascular endothelial growth factor; HGF: hepatocyte growth factor; NK: natural killer cell; VEGFR: growth factor receptor; FGFR: fibroblast growth factor receptor; PDGFR: platelet-derived growth factor receptor; PD-L1: Programmed cell death 1 ligand 1; TNF-α: tumor necrosis factor-α; IFN-γ: interferon-γ; 3-HB: 3-hydroxybutyric acid; TIMP: tissue inhibitor of metalloproteinases; MMP: matrix metalloproteinase; CXCL chemokine (C-X-C motif) ligand; TGF-β1: tansforming growth factor-β: CTLA-4: cytotoxic T lymphocyte-associated antigen-4.

systemic and local immune responses to the combination with cabozantinib and nivolumab, and the preliminary findings indicated that cabozantinib and nivolumab promote T-cell-mediated antitumor immunity locally and systemically (*95*). Specifically, the tumor tissue samples from HCC patients with a better response exhibited a greater presence of $CD8^+$ and $CD4^+$ T cells. In addition to the difference in the lymphocyte profile, the combination treatment also promoted the differentiation of macrophage clusters with low CD163 and arginase-1 expression, which was associated with higher plasma levels of CXCL9/10/11, CCL2 and CCL26 (*96*). In conclusion, combination therapy resulted in a sustained twofold increase in response rates, with a complete response rate of ~5% and encouraging survival beyond 18 months (*97*).

Table 2. Clinical trials registered on NIH investigating combinations of LRTs and immunotherapy in HCC

Trials ID	Regimen	Target Population	Status	Phase	Enrollment number	Study Period
	ICI-based Combination therapy					
NCT02851784	Cellular Immunotherapy+Microwave Ablation	HCC	Completed	II/III	40	2021/3/1-2009/12/1
NCT03914352	PD-1 Antiboty + Hepatic Resection	HCC Combined With PVTT After Hepatic Resection	Unknown status	NA	40	2020/1/31-2019/4/1
NCT04521153	Camrelizumab+Apatinib Mesylate	Perioperative of Resectable HCC	Recruiting	NA	290	2026/3/1-2021/3/25
NCT04220944	Immunotherapy +Locoregional Treatment	Unresectable HCC.	Recruiting	I	45	2022/9/30-2020/1/1
NCT05546619	Tislelizumab+Hyperthermic Intraperitoneal Chemotherapy	High-risk HCC After R0 Resection	Active, not recruiting	NA	30	2025/7/31-2022/8/1
NCT05407519	Tislelizumab + Sitravatinib	High Risk of Recurrence After Curative Resection	Recruiting	II	40	2026/6/30-2022/7/25
NCT03867084	Pembrolizumab(MK-3475)+Surgical Resection or Local Ablation	HCC	Active, not recruiting	III	950	2029/8/31-2019/5/28
NCT04682210	Sintilimab Plus Bevacizumab+Curative Resection		Not yet recruiting	III	246	2024/12/1-2020/12/1
NCT03937830	Durvalumab, Bevacizumab, Tremelimumab+TACE	HCC or Biliary Tract Carcinoma	Recruiting	II	39	2023/12/31-2021/3/10
NCT03630640	Nivolumab+Electroporation	HCC	Active, not recruiting	II	43	2023/11/30-2018/10/11
NCT02960594	hTERT Immunotherapy+IL-12 DNA+Electroporation	Adults With Solid Tumors at High Risk of Relapse	Completed	I	93	2018/11/9-2014/12/1
NCT05240404	Toripalimab+Curative-intent Ablation	Recurrent HCC	Recruiting	II	116	2024/7/31-2020/7/1
NCT03753659	Pembrolizumab+IMMULAB - Immunotherapy+Local Ablation	HCC	Active, not recruiting	II	30	2024/6/1-2019/5/9
NCT05027425	Durvalumab (MEDI4736)+Tremelimumab	HCC in Patients Listed for a Liver Transplant	Recruiting	II	30	2030/12/7-2021/12/7
NCT05609695	Immune Checkpoint Inhibitor+Molecular Targeted Drugs / Locoregional	HCC	Not yet recruiting	NA	100	2025/9/1-2023/3/1
	Therapy	HCC	Unknown status	II	40	2022/12/31-2019/2/12
NCT03510871	Nivolumab+Ipilimumab	Advanced Liver Cancer	Active, not recruiting	I/II	659	2024/12/29-2012/10/30
NCT01658878	Nivolumab+Other Agents	Advanced Hepatopancreabiliary Tumors (BLOCKED)	Not yet recruiting	II	62	2028/10/1-2023/3/1
NCT05451043	Durvalumab+Tremelimumab+Propranolol+Chemotherapy	HCC	Suspended	II	150	2028/5/1-2023/5/1
NCT05063565	Durvalumab+Tremelimumab	Hepatocellular Carcinom	Not yet recruiting	II/III	574	2026/4/1-2023/2/1
NCT05665348	Ipilimumab+Atezolizumab+Bevacizumab	Advanced/Metastatic HCC	Recruiting	I	20	2024/3/31-2021/10/30
NCT05031949	Camrelizumab+Hyperbaric Oxygen	HCC	Recruiting	I/II	32	2023/12/1-2019/3/1
NCT03682276	Ipilimumab+Nivolumab+Liver Resection	High-risk HCC	Not yet recruiting	II	27	2028/12/5-2023/3/1
NCT05194293	Regorafenib+Durvalumab (MEDI4736)	Advanced HCC	Completed	NA	124	2023/3/9-2021/5/1
NCT04862949	Atezolizumab+Bevacizumab	Resectable Liver Cancer	Completed	II	30	2022/9/14-2017/9/28
NCT03222076	Nivolumab+Ipilimumab	Advanced Liver Cancer	Unknown status	II	27	2022/8/1-2020/8/30
NCT04523662	Carrelizumab+Apatinib Mesylate+Radiotherapy	Advanced Liver Cancer	Recruiting	II	88	2025/1/31-2022/2/11
NCT05211323	Chemotherapy+Bevazicumab+Atezolizumab	Resectable Liver Cancer	Recruiting	II	30	2027/12/31-2021/2/10
NCT04721132	Atezolizumab+Bevacizumab Before Surgery	Treatment of Liver Cancer After Progression on Prior	Recruiting	II	30	2027/2/28-2022/2/4
NCT04430452	Hypofractionated Radiotherapy+Durvalumab+Tremelimumab	PD-1 Inhibition				
		Unresectable, Locally Advanced, or Metastatic Liver	Recruiting	II	122	2026/12/31-2022/5/27
NCT05168163	Atezolizumab+Multi-Kinase Inhibito	Cancer				
		Advanced Refractory Liver Cancer	Active, not recruiting	II	12	2022/12/31-2016/12/9
NCT02940496	Pembrolizumab+Elbasvir/Grazoprevir+Ribavirin	Advanced Solid Tumors	Recruiting	1	230	2023/12/29-2021/2/3
NCT04580485	INCB106385+Immunotherapy	Advanced HCC	Active, not recruiting	II	433	2023/12/29-2015/10/19
NCT02519348	Durvalumab/Tremelimumab+Durvalumab +Tremelimumab/					
	Bevacizumab	HCC	Recruiting	II	134	2025/3/1-2022/4/12
NCT05359861	Atezolizumab+Bevacizumab+SRF388	Fibrolamellar HCC	Recruiting	I	56	2027/3/1-2020/4/20
NCT04248569	Nivolumab+Ipilimumab+DNAJB1-PRKACA Fusion Kinase Peptide					
	Vaccine	in Advanced HCC Patients Who Have Progressed on	Recruiting	II	40	2027/1/31-2023/1/19
NCT05199285	Nivolumab+Ipilimumab	First Line Atezolizumab + Bevacizumab				

Abbreviations: NIH: National Institutes of Health; LRTs: locoregional treatments; HCC: Hepatocellular Carcinoma; NA: Not Applicable;

Table 2. Clinical trials registered on NIH investigating combinations of LRTs and immunotherapy in HCC (continued)

Trials ID	Regimen	Target Population	Status	Phase	Enrollment number	Study Period
NCT05269381	Pembrolizumab+Personalized Neoantigen Peptide-Based Vaccine	Advanced Solid Tumors	Recruiting	I	36	2025/2/24-2022/3/31
NCT05431270	PD-1 Inhibitor+PT199 (an Anti-CD73 mAb)	HCC	Recruiting	I	41	2024/1/1-2022/6/23
NCT03836352	Low Dose Cyclophosphamide & Pembrolizumab+Immunotherapeutic, DPX-Survivac	Selected Advanced & Recurrent Solid Tumors	Active, not recruiting	II	184	2023/12/31-2018/12/21
NCT03544723	Immune Checkpoint Inhibitors+p53 Gene Therapy	Solid Tumors	Unknown status	II	40	2022/12/31-2018/10/1
NCT03638141	Durvalumab+Tremelimumab+CTLA-4 /PD-L1 Blockade Following Transarterial Chemoembolization (DEB-TACE)	Intermediate Stage of HCC	Recruiting	II	30	2023/11/1-2019/10/2
NCT04785287	Nivolumab+Anti-CTLA4-NF mAb (BMS986218)+Stereotactic Body RadiationTherapy	Metastatic Solid Malignancies	Active, not recruiting	I/II	13	2024/5/27-2021/3/29
NCT02886897	Anti-PD-1+D-CIK Immunotherapy	In Refractory Solid Tumors	Unknown status	I/II	50	2019/10/1-2016/7/1
	TKI-based Combination therapy					
NCT05535998	TKI+TACE-HAIC +Immunotherapy	Hepatocellular Carcinoma With PVTT	Completed	NA	743	2022/6/30-2021/1/1
NCT05135364	TKI+HAIC+Camrelizumab	Unresectable Hepatocellular Carcinoma After TACE Failure	Recruiting	II	48	2024/12/5-2021/11/5
NCT04518852	Sorafenib+TACE+PD-1 Monoclonal Antibody	HCC	Unknown status	II	60	2023/1/31-2020/9/14
NCT04229355	Sorafenib+DEB-TACE+Lenvatinibor PD-1 Inhibitor	Unresectable Hepatocellular Carcinoma	Unknown status	III	90	2022/12/30-2021/2/2
NCT02989870	Sorafenib+Bavituximab+SBRT	Unresectable Hepatocellular Carcinoma	Withdrawn	1	0	2018/10/15-2017/3/27
NCT05286320	Lenvatinib+Pembrolizumab+SBRT	HCC Patients With Portal Vein Thrombosis.	Not yet recruiting	I/II	27	2026/9/30-2023/3/1
NCT03841201	Lenvatinib+Immunotherapy With Nivolumab	Advanced Stage Hepatocellular Carcinoma	Active, not recruiting	II	50	2023/3/1-2019/6/12
NCT02562755	Sorafenib+Vaccinia Virus	HCC	Completed	III	459	2020/7/1-2015/10/1
NCT04273100	Lenvatinib+TACE+PD-1 Monoclonal Antibody	HCC	Unknown status	II	56	2021/6/30-2019/11/14
NCT04627012	Lenvatinib+Anti-PD1 Antibody	Advanced Hepatocellular Carcinoma	Completed		600	2022/7/1-2018/1/1
NCT02988440	Sorafenib+PDR001	Advanced Hepatocellular	Completed	I	20	2020/2/27-2017/4/20
	local treatment-based Immunotherapy					
NCT01749865	CIK+Radical Resection	HCC	Completed	III	200	2014/12/1-2008/10/1
NCT04658147	Nivolumab+Relatlimab	Potentially Resectable Hepatocellular Carcinoma	Recruiting	I	20	2026/6/1-2021/5/28
NCT03755739	Trans-Artery/Intra-Tumor Infusion of ICI+Chemodrug	Advanced Solid Tumors	Recruiting	II/III	200	2033/11/1-2018/11/1
NCT03299946	Cabozantinib+Nivolumab (CaboNivo)+Resection	Patients With Locally Advanced Hepatocellular Carcinoma	Completed	I	15	2021/10/1-2018/5/14
NCT03966209			Unknown status	I	20	2022/10/31-2019/5/1
NCT05411926	PD-1 /PD-L1 Inhibitor Therapy+Liver Transplantation	Acute Rejection After Liver Transplantation in Patients With Hepatocellular Carcinoma	Recruiting	NA	30	2023/9/1-2021/3/17
NCT01828762	Autologous Immune Cell Therapy+Resection+TACE Therapy	Primary Hepatocellular Carcinoma	Completed	NA	8	1900/1/0-2012/12/1
NCT04564313	Camrelizumab+Liver Transplantation	Recurrent HCC After Liver Transplantation	Recruiting	I	20	2023/7/1-2020/9/21
NCT03575806	Autologous Tcm Immunotherapy+TACE	HCC With MVI After Radical Resection	Completed	II	52	2019/10/31-2017/1/9
NCT02638857	Immunotherapy Using Precision T Cells Specific to Multiple Common Tumor-Associated Antigen+Transcatheter Arterial Chemoembolization	Advanced Hepatocellular Carcinoma	Unknown status	I/II	60	2017/9/1-2015/9/1
NCT05475613	HAIC+Targeted Therapy and Immunotherapy	Down-stage Therapy of liver transplantation	Not yet recruiting	II	75	2028/7/30-2022/8/1
NCT04988945	TACE+SBRT+Double Immunotherapy	for Downstaging Hepatocellular Carcinoma	Recruiting	II	33	2026/12/1-2020/12/1
NCT05613478	Camrelizumab+Apatinib Mesylate+TACE	Perioperative Treatment of Hepatocellular Carcinoma	Recruiting	III	130	2027/11/1-2022/11/1
NCT04522544	Durvalumab (MEDI4736)+Tremelimumab +Y-90 SIRT/TACE	Intermediate Stage HCC	Recruiting	II	84	2024/9/30-2020/12/15
NCT05198609	Camrelizumab, Apatinib+HAIC	HCC With Portal Vein Invasion	Recruiting	III	214	2026/1/1-2022/1/17
NCT05313282	Hepatic Arterial Infusion+Apatinib+Camrelizumab	C-staged Hepatocellular Carcinoma in BCLC Classification	Recruiting	III	140	2025/6/1-2022/6/15

Abbreviations: NIH: National Institutes of Health; LRTs: locoregional treatments; HCC: Hepatocellular Carcinoma; NA: Not Applicable;

Table 2. Clinical trials registered on NIH investigating combinations of LRTs and immunotherapy in HCC (continued)

Trials ID	Regimen	Target Population	Status	Phase	Enrollment number	Study Period
NCT03817736	TACE+SBRT+Immuno Therapy	Downstaging HCC for Hepatectomy	Active, not recruiting	II	33	2023/1/31-2019/3/1
NCT04945720	Durvalumab +HAIC	Advanced Hepatocellular Carcinoma	Recruiting	II	30	2023/12/30-2022/4/11
NCT04981665	TACE+Tislelizumab	HCC at High Risk of Recurrence After Curative Resection	Recruiting	II	50	2024/12/1-2021/11/8
NCT04796025	Sintilimab+Bevacizumab Biosimilar+TACE	Hepatocellular Carcinoma (BCLC-C Stage)	Recruiting	II	34	2024/8/31-2021/9/23
NCT05701488	SIRT+Tremelimumab+Durvalumab	Resectable HCC	Not yet recruiting	I	20	2025/10/1-2023/5/1
NCT02487017	DC-CIK+TACE	Hepatocellular Carcinoma	Unknown status	II	60	2018/12/1-2015/5/1
NCT04268888	Nivolumab+TACE/TAE	Intermediate Stage HCC	Recruiting	II/III	522	2026/6/1-2019/5/8
NCT04547452	Sintilimab+Stereotactic Body Radiotherapy	Advanced Metastatic HCC	Recruiting	II	84	2023/7/1-2020/7/1
NCT03086564	Hepatitis B Virus (HBV)-Specific Antigen Peptides+HepG2 Cell Lysate Co-activated Dendritic Cells+TACE	HBV-related HCC Treatment	Completed	I/II	70	2020/10/29-2017/5/1
NCT01853618	Tremelimumab+Chemoembolization/Ablation	Liver Cancer	Completed	I/II	61	2017/6/7-2013/5/2
NCT04191889	Hepatic Arterial Infusion+Apatinib+Camrelizumab	C-staged Hepatocellular Carcinoma in BCLC	Recruiting	II	47	2025/12/31-2020/4/13
NCT04167293	Sintilimab+Stereotactic Body Radiotherapy	Hepatocellular Carcinoma	Unknown status	II/III	116	2022/10/31-2019/11/16
NCT03864211	Thermal Ablation+Immunotherapy	HCC	Active, not recruiting	I/II	145	2023/5/30-2019/6/15
NCT05809869	Immunotherapy+Radioembolisation	Metastatic Hepatocellular Carcinoma	Recruiting	II	25	2026/6/30-2023/2/15
NCT02678013	RFA+Highly-purified CTL	Recurrent HCC	Unknown status	III	210	2022/1/1-2016/2/1
NCT03067493	RFA/Surgical Resection+Neo-MASCT	Primary HCC	Recruiting	II	98	2023/3/31-2017/7/25
NCT03939975	Anti-PD-1therapy+Thermal Ablation	Advanced HCC	Completed	II	50	2019/7/31-2019/6/1
NCT04724226	Camrelizumab and Apatinib+Cryoablation	Advanced Hepatocellular Carcinoma	Recruiting	II	34	2024/8/31-2021/9/1
NCT03812562	Nivolumab+Yttrium-90	Patients With Liver Cancer Undergoing Surgical Resection	Unknown status	I	2	2022/12/1-2019/2/7
NCT05327738	Atezolizumab+ Cabozantinib+Yttrium Y 90 Glass Microspheres	Unresectable or Locally Advanced Hepatocellular Carcinoma	Withdrawn	II	0	2027/12/4-2022/12/10
NCT03008343	Irreversible Electroporation+NK Immunotherapy	Recurrent Liver Cancer	Completed	I/II	20	2019/7/1-2016/12/1

Abbreviations: NIH: National Institutes of Health; LRTs: locoregional treatments; HCC: Hepatocellular Carcinoma; NA: Not Applicable;

6. Conclusion and prospect

The immune microenvironment of HCC is a system composed of hepatocytes, immune cell subsets, immune receptors and ligands, cytokines and chemokines, extracellular matrix, and other elements (*98,99*). From the above studies, we know that local therapy, systemic therapy, or immunotherapy can affect the immune microenvironment of HCC. Immunotherapy is an increasingly recognized and used method in clinical practice, and its combination with LRTs and systemic therapy is also increasingly used in the clinical treatment of HCC. However, there is great individual variability in combination therapy, which is affected by the tumor size, location, sequence and duration of treatment, and frequency of treatment. More clinical trials are needed to explore the specific time and regimen of immune combination therapy and to continue to optimize the development of the most accurate treatment.

Acknowledgements

Thanks 'HOME for Researchers' and 'Figdraw' for the graphic assistance.

Funding: This research was supported by the Natural Science Foundation of Chongqing (No. CSTB2022NSCQ-MSX0112); Science and Health Joint Research Project of Chongqing Municipality (2020GDRC013); Program for Youth Innovation in Future Medicine, Chongqing Medical University (W0087).

Conflict of Interest: The authors have no conflicts of interest to disclose.

Availability of data and materials: The datasets generated during the current study are available in the *https://clinicaltrials.gov/repository*

References

1. Vogel A, Meyer T, Sapisochin G, Salem R, Saborowski A. Hepatocellular carcinoma. Lancet. 2022; 400:1345-1362.
2. Wang H, Li W. Recent update on comprehensive therapy for advanced hepatocellular carcinoma. World Journal of Gastrointestinal Oncology. 2021; 13:845-855.
3. Horrow MM, Huynh MHL, Callaghan MM, Rodgers SK. Complications after Liver Trans-plant Related to Preexisting Conditions: Diagnosis , Treatment, and Prevention. Radiographics. 2020; 40:895-909.
4. Bai J, Liang P, Li Q, Feng R, Liu J. Cancer Immunotherapy - Immune Checkpoint Inhibitors in Hepatocellular Carcinoma. Recent Pat Anticancer Drug Discov. 2021; 16:239-248.
5. Feng GS, Hanley KL, Liang Y, Lin X. Improving the Efficacy of Liver Cancer Immunotherapy: The Power of Combined Preclinical and Clinical Studies. Hepatology. 2021; 73 Suppl 1:104-114.
6. Sharma R, Motedayen Aval L. Beyond First-Line Immune Checkpoint Inhibitor Therapy in Patients With Hepatocellular Carcinoma. Front Immunol. 2021; 12:652007.
7. Li H, Zhang L. Liver regeneration microenvironment of hepatocellular carcinoma for prevention and therapy. Oncotarget. 2017; 8:1805-1813.
8. Yin S, Wang H, Bertola A, Feng D, Xu MJ, Wang Y, Gao B. Activation of invariant natural killer T cells impedes liver regeneration by way of both IFN-γ- and IL-4-dependent mechanisms. Hepatology. 2014; 60:1356-1366.
9. Nishiyama K, Nakashima H, Ikarashi M, Kinoshita M, Nakashima M, Aosasa S, Seki S, Yamamoto J. Mouse CD11b+Kupffer Cells Recruited from Bone Marrow Accelerate Liver Regeneration after Partial Hepatectomy. PloS one. 2015; 10:e0136774-e0136774.
10. Almeda-Valdes P, Aguilar Olivos NE, Barranco-Fragoso B, Uribe M, Méndez-Sánchez N. The Role of Dendritic Cells in Fibrosis Progression in Nonalcoholic Fatty Liver Disease. Biomed Res Int. 2015; 2015:768071.
11. Schon HT, Bartneck M, Borkham-Kamphorst E, Nattermann J, Lammers T, Tacke F, Weiskirchen R. Pharmacological Intervention in Hepatic Stellate Cell Activation and Hepatic Fibrosis. Front Pharmacol. 2016; 7:33.
12. Wang H, Xi Z, Deng L, Pan Y, He K, Xia Q. Macrophage Polarization and Liver Ischemia-Reperfusion Injury. International journal of medical sciences. 2021; 18:1104-1113.
13. Wang H, Xi Z, Deng L, Pan Y, He K, Xia Q. Macrophage Polarization and Liver Ischemia-Reperfusion Injury. Int J Med Sci. 2021; 18:1104-1113.
14. Liu Y, Lu T, Zhang C, Xue Z, Busuttil R, Kupiec-Weglinski J, Ji H. Activation of YAP Attenuates Hepatic Damage and Fibrosis in Liver Ischemia-Reperfusion Injury: From Bench to Bedside. American Journal of Transplantation. 2020; 20:735-735.
15. Ji H, Liu Y, Zhang Y, Shen XD, Gao F, Busuttil RW, Kuchroo VK, Kupiec-Weglinski JW. T-cell immunoglobulin and mucin domain 4 (TIM-4) signaling in innate immune-mediated liver ischemia-reperfusion injury. Hepatology. 2014; 60:2052-2064.
16. Strey CW, Siegmund B, Rosenblum S, Marquez-Pinilla RM, Oppermann E, Huber-Lang M, Lambris JD, Bechstein WO. Complement and neutrophil function changes after liver resection in humans. World J Surg. 2009; 33:2635-2643.
17. Fujiki M, Esquivel CO, Martinez OM, Strober S, Uemoto S, Krams SM. Induced tolerance to rat liver allografts involves the apoptosis of intragraft T cells and the generation of CD4(+)CD25(+)FoxP3(+) T regulatory cells. Liver Transpl. 2010; 16:147-154.
18. Jamil KM, Hydes TJ, Cheent KS, Cassidy SA, Traherne JA, Jayaraman J, Trowsdale J, Alexander GJ, Little AM, McFarlane H, Heneghan MA, Purbhoo MA, Khakoo SI. STAT4-associated natural killer cell tolerance following liver transplantation. Gut. 2017; 66:352-361.
19. Mano Y, Yoshizumi T, Yugawa K, Ohira M, Motomura T, Toshima T, Itoh S, Harada N, Ikegami T, Soejima Y, Maehara Y. Lymphocyte-to-Monocyte Ratio Is a Predictor of Survival After Liver Transplantation for Hepatocellular Carcinoma. Liver Transpl. 2018; 24:1603-1611.
20. Chen G-S, Qi H-Z. Effect of Kupffer cells on immune tolerance in liver transplantation. Asian Pacific Journal of Tropical Medicine. 2012; 5:970-972.

21. Lu D, Yang F, Lin Z, Zhuo J, Liu P, Cen B, Lian Z, Xie H, Zheng S, Xu X. A prognostic fingerprint in liver transplantation for hepatocellular carcinoma based on plasma metabolomics profiling. European Journal of Surgical Oncology. 2019; 45:2347-2352.
22. Guo JJ, Wang SX, Han YJ, Jia ZY, Wang RC. Effects of transarterial chemoembolization on the immunological function of patients with hepatocellular carcinoma. Oncology Letters. 2021; 22.
23. Pinato DJ, Murray SM, Forner A, *et al*. Trans-arterial chemoembolization as a loco-regional inducer of immunogenic cell death in hepatocellular carcinoma: implications for immunotherapy. J Immunother Cancer. 2021; 9.
24. Kim MJ, Jang JW, Oh BS, Kwon JH, Chung KW, Jung HS, Jekarl DW, Lee S. Change in inflammatory cytokine profiles after transarterial chemotherapy in patients with hepatocellular carcinoma. Cytokine. 2013; 64:516-522.
25. Lin W, Wang H, Zhong M, Yu S, Zhao S, Liang S, Du J, Cheng B, Gu W, Ling C. Effect and Molecular Mechanisms of Jiedu Recipe on Hypoxia-Induced Angiogenesis after Transcatheter Arterial Chemoembolization in Hepatocellular Carcinoma. Evid Based Complement Alternat Med. 2021; 2021:6529376-6529376.
26. Nyman SS, Creusen AD, Johnsson U, Rorsman F, Vessby J, Barbier CE. Peritumoral portal enhancement during transarterial chemoembolization: a potential prognostic factor for patients with hepatocellular carcinoma. Acta Radiol. 2021;2841851211041832.
27. Liu K, Min XL, Peng J, Yang K, Yang L, Zhang XM. The Changes of HIF-1α and VEGF Expression After TACE in Patients With Hepatocellular Carcinoma. J Clin Med Res. 2016; 8:297-302.
28. Ranieri G, Ammendola M, Marech I, Laterza A, Abbate I, Oakley C, Vacca A, Sacco R, Gadaleta CD. Vascular endothelial growth factor and tryptase changes after chemoembolization in hepatocarcinoma patients. World J Gastroenterol. 2015; 21:6018-6025.
29. Raoul JL, Forner A, Bolondi L, Cheung TT, Kloeckner R, de Baere T. Updated use of TACE for hepatocellular carcinoma treatment: How and when to use it based on clinical evidence. Cancer Treat Rev. 2019; 72:28-36.
30. Mizukoshi E, Yamashita T, Arai K, Terashima T, Kitahara M, Nakagawa H, Iida N, Fushimi K, Kaneko S. Myeloid-derived suppressor cells correlate with patient outcomes in hepatic arterial infusion chemotherapy for hepatocellular carcinoma. Cancer Immunology, Immunotherapy. 2016; 65:715-725.
31. Matsui D, Nagai H, Mukozu T, Ogino YU, Sumino Y. VEGF in patients with advanced hepatocellular carcinoma receiving intra-arterial chemotherapy. Anticancer Res. 2015; 35:2205-2210.
32. Tsunematsu S, Suda G, Yamasaki K, *et al*. Combination of neutrophil-to-lymphocyte ratio and early des--carboxyprothrombin change ratio as a useful predictor of treatment response for hepatic arterial infusion chemotherapy against advanced hepatocellular carcinoma. Hepatology Research. 2017; 47:533-541.
33. Saeki I, Yamasaki T, Tanabe N, Iwamoto T, Matsumoto T, Urata Y, Hidaka I, Ishikawa T, Takami T, Yamamoto N, Uchida K, Terai S, Sakaida I. A new therapeutic assessment score for advanced hepatocellular carcinoma patients receiving hepatic arterial infusion chemotherapy. PloS one. 2015; 10:e0126649-e0126649.
34. Takaya H, Namisaki T, Moriya K, *et al*. Association between ADAMTS13 activity-VWF antigen imbalance and the therapeutic effect of HAIC in patients with hepatocellular carcinoma. World J Gastroenterol. 2020; 26:7232-7241.
35. Filatenkov A, Baker J, Mueller AM, Kenkel J, Ahn GO, Dutt S, Zhang N, Kohrt H, Jensen K, Dejbakhsh-Jones S, Shizuru JA, Negrin RN, Engleman EG, Strober S. Ablative Tumor Radiation Can Change the Tumor Immune Cell Microenvironment to Induce Durable Complete Remissions. Clin Cancer Res. 2015; 21:3727-3739.
36. Young S, Ragulojan R, Chen T, Owen J, D'Souza D, Sanghvi T, Golzarian J, Flanagan S. Dynamic Lymphocyte Changes Following Transarterial Radioembolization: Association with Normal Liver Dose and Effect on Overall Survival. J Hepatocell Carcinoma. 2022; 9:29-39.
37. Carr BI, Metes DM. PERIPHERAL BLOOD LYMPHOCYTE DEPLETION AFTER HEPATIC ARTERIAL (YTTRIUM)-Y-90 MICROSPHERE THERAPY FOR HEPATOCELLULAR CARCINOMA. International Journal of Radiation Oncology Biology Physics. 2012; 82:1179-1184.
38. Liu CA, Lee IC, Lee RC, Chen JL, Chao YE, Hou MC, Huang YH. Prediction of survival according to kinetic changes of cytokines and hepatitis status following radioembolization with yttrium-90 microspheres. Journal of the Formosan Medical Association. 2021; 120:1127-1136.
39. Song CW, Kim MS, Cho LC, Dusenbery K, Sperduto PW. Radiobiological basis of SBRT and SRS. Int J Clin Oncol. 2014; 19:570-578.
40. Ng SSW, Zhang H, Wang L, Citrin D, Dawson LA. Association of pro-inflammatory soluble cytokine receptors early during hepatocellular carcinoma stereotactic radiotherapy with liver toxicity. NPJ Precis Oncol. 2020; 4:17.
41. Cuneo KC, Devasia T, Sun Y, Schipper MJ, Karnak D, Davis MA, Owen D, Feng M, El Naqa I, Bazzi L, Ten Haken R, Lawrence TS. Serum Levels of Hepatocyte Growth Factor and CD40 Ligand Predict Radiation-Induced Liver Injury. Transl Oncol. 2019; 12:889-894.
42. Hsiang CW, Huang WY, Yang JF, Shen PC, Dai YH, Wang YF, Lin CS, Chang WC, Lo CH. Dynamic Changes in Neutrophil-to-Lymphocyte Ratio are Associated with Survival and Liver Toxicity Following Stereotactic Body Radiotherapy for Hepatocellular Carcinoma. Journal of Hepatocellular Carcinoma. 2021; 8:1299-1309.
43. Zhuang Y, Yuan BY, Hu Y, Chen GW, Zhang L, Zhao XM, Chen YX, Zeng ZC. Pre/Post-Treatment Dynamic of Inflammatory Markers Has Prognostic Value in Patients with Small Hepatocellular Carcinoma Managed by Stereotactic Body Radiation Therapy. Cancer Management and Research. 2019; 11:10929-10937.
44. Kang TW, Rhim H. Recent Advances in Tumor Ablation for Hepatocellular Carcinoma. Liver Cancer. 2015; 4:176-187.
45. Ji L, Gu J, Chen L, Miao D. Changes of Th1/Th2 cytokines in patients with primary hepatocellular carcinoma after ultrasound-guided ablation. Int J Clin Exp Pathol. 2017; 10:8715-8720.
46. Duan XH, Li H, Han XW, Ren JZ, Li FY, Ju SG, Chen PF, Kuang DL. Upregulation of IL-6 is involved in moderate hyperthermia induced proliferation and invasion of hepatocellular carcinoma cells. European Journal of Pharmacology. 2018; 833:230-236.
47. Yu ZS, Li GW, Yu H, Asakawa T. Changes of immune cells in patients with hepatocellular carcinoma treated by

radiofrequency ablation and hepatectomy, a pilot study. Open Life Sciences. 2021; 16:1002-1009.
48. Rochigneux P, Nault JC, Mallet F, *et al*. Dynamic of systemic immunity and its impact on tumor recurrence after radiofrequency ablation of hepatocellular carcinoma. Oncoimmunology. 2019; 8.
49. Mizukoshi E, Yamashita T, Arai K, Sunagozaka H, Ueda T, Arihara F, Kagaya T, Yamashita T, Fushimi K, Kaneko S. Enhancement of tumor-associated antigen-specific T cell responses by radiofrequency ablation of hepatocellular carcinoma. Hepatology. 2013; 57:1448-1457.
50. Schueller G, Kettenbach J, Sedivy R, Stift A, Friedl J, Gnant M, Lammer J. Heat shock protein expression induced by percutaneous radiofrequency ablation of hepatocellular carcinoma *in vivo*. Int J Oncol. 2004; 24:609-613.
51. Shen S, Peng H, Wang Y, Xu M, Lin M, Xie X, Peng B, Kuang M. Screening for immune-potentiating antigens from hepatocellular carcinoma patients after radiofrequency ablation by serum proteomic analysis. BMC Cancer. 2018; 18:117.
52. Wu H, Li SS, Zhou MJ, Jiang AN, He YN, Wang S, Yang W, Liu HM. Palliative Radiofrequency Ablation Accelerates the Residual Tumor Progression Through Increasing Tumor-Infiltrating MDSCs and Reducing T-Cell-Mediated Anti-Tumor Immune Responses in Animal Model. Frontiers in Oncology. 2020; 10.
53. Urano M, Tanaka C, Sugiyama Y, Miya K, Saji S. Antitumor effects of residual tumor after cryoablation: the combined effect of residual tumor and a protein-bound polysaccharide on multiple liver metastases in a murine model. Cryobiology. 2003; 46:238-245.
54. Pimentel CB, Moraes AM, Cintra ML. Angiogenic effects of cryosurgery with liquid nitrogen on the normal skin of rats, through morphometric study. An Bras Dermatol. 2014; 89:410-413.
55. Zhou L, Fu JL, Lu YY, Fu BY, Wang CP, An LJ, Wang XZ, Zeng Z, Zhou CB, Yang YP, Wang FS. Regulatory T cells are associated with post-cryoablation prognosis in patients with hepatitis B virus-related hepatocellular carcinoma. Journal of Gastroenterology. 2010; 45:968-978.
56. Zeng Z, Shi F, Zhou L, *et al*. Upregulation of circulating PD-L1/PD-1 is associated with poor post-cryoablation prognosis in patients with HBV-related hepatocellular carcinoma. PLoS One. 2011; 6:e23621.
57. Huang M, Wang X, Bin H. Effect of Transcatheter Arterial Chemoembolization Combined with Argon–Helium Cryosurgery System on the Changes of NK Cells and T Cell Subsets in Peripheral Blood of Hepatocellular Carcinoma Patients. Cell Biochemistry and Biophysics. 2015; 73:787-792.
58. Zhou Y, Xu X, Ding J, Jing X, Wang F, Wang Y, Wang P. Dynamic changes of T-cell subsets and their relation with tumor recurrence after microwave ablation in patients with hepatocellular carcinoma. J Cancer Res Ther. 2018; 14:40-45.
59. Leuchte K, Staib E, Thelen M, *et al*. Microwave ablation enhances tumor-specific immune response in patients with hepatocellular carcinoma. Cancer Immunol Immunother. 2021; 70:893-907.
60. Zhang H, Hou X, Cai H, Zhuang X. Effects of microwave ablation on T-cell subsets and cytokines of patients with hepatocellular carcinoma. Minim Invasive Ther Allied Technol. 2017; 26:207-211.
61. Zhou Q, Zhu XQ, Zhang J, Xu ZL, Lu P, Wu F. Changes in circulating immunosuppressive cytokine levels of cancer patients after high intensity focused ultrasound treatment. Ultrasound Med Biol. 2008; 34:81-87.
62. Tonguc T, Strunk H, Gonzalez-Carmona MA, *et al*. US-guided high-intensity focused ultrasound (HIFU) of abdominal tumors: outcome, early ablation-related laboratory changes and inflammatory reaction. A single-center experience from Germany. International Journal of Hyperthermia. 2021; 38:65-74.
63. Yi Y, Han J, Fang Y, Liu D, Wu Z, Wang L, Zhao L, Wei Q. Sorafenib and a novel immune therapy in lung metastasis from hepatocellular carcinoma following hepatectomy: A case report. Molecular and clinical oncology. 2016; 5:337-341.
64. Vogl TJ, Mack MG, Balzer JO, Engelmann K, Straub R, Eichler K, Woitaschek D, Zangos S. Liver metastases: neoadjuvant downsizing with transarterial chemoembolization before laser-induced thermotherapy. Radiology. 2003; 229:457-464.
65. Jondal DE, Thompson SM, Butters KA, Knudsen BE, Anderson JL, Carter RE, Roberts LR, Callstrom MR, Woodrum DA. Heat Stress and Hepatic Laser Thermal Ablation Induce Hepatocellular Carcinoma Growth: Role of PI3K/mTOR/AKT Signaling. Radiology. 2018; 288:730-738.
66. De Landro M, Espíritu García-Molina I, Barberio M, Felli E, Agnus V, Pizzicannella M, Diana M, Zappa E, Saccomandi P. Hyperspectral Imagery for Assessing Laser-Induced Thermal State Change in Liver. Sensors (Basel). 2021; 21.
67. Lu DS, Kee ST, Lee EW. Irreversible electroporation: ready for prime time? Tech Vasc Interv Radiol. 2013; 16:277-286.
68. Guo X, Du F, Liu Q, Guo Y, Wang Q, Huang W, Wang Z, Ding X, Wu Z. Immunological effect of irreversible electroporation on hepatocellular carcinoma. BMC Cancer. 2021; 21:443.
69. Dai ZH, Wang ZR, Lei K, Liao JB, Peng ZW, Lin MX, Liang P, Yu J, Peng S, Chen SL, Kuang M. Irreversible electroporation induces CD8(+) T cell immune response against post-ablation hepatocellular carcinoma growth. Cancer Letters. 2021; 503:1-10.
70. Ju S, Zhou C, Yang C, Wang C, Liu J, Wang Y, Huang S, Li T, Chen Y, Bai Y, Yao W, Xiong B. Apatinib Plus Camrelizumab With/Without Chemoembolization for Hepatocellular Carcinoma: A Real-World Experience of a Single Center. Front Oncol. 2021; 11:835889.
71. Erös de Bethlenfalva-Hora C, Mertens Joachim C, Piguet A-C, Kettenbach J, Schmitt J, Terracciano L, Weimann R, Dufour J-F, Geier A. Radiofrequency ablation suppresses distant tumour growth in a novel rat model of multifocal hepatocellular carcinoma. Clinical Science. 2013; 126:243-252.
72. Deng YR, Liu WB, Lian ZX, Li XS, Hou X. Sorafenib inhibits macrophage-mediated epithelial-mesenchymal transition in hepatocellular carcinoma. Oncotarget. 2016; 7:38292-38305.
73. Tohyama O, Matsui J, Kodama K, Hata-Sugi N, Kimura T, Okamoto K, Minoshima Y, Iwata M, Funahashi Y. Antitumor activity of lenvatinib (e7080): an angiogenesis inhibitor that targets multiple receptor tyrosine kinases in preclinical human thyroid cancer models. J Thyroid Res. 2014; 2014:638747.
74. Torrens L, Montironi C, Puigvehí M, *et al*. Immunomodulatory Effects of Lenvatinib Plus Anti-Programmed Cell Death Protein 1 in Mice and Rationale for Patient Enrichment in Hepatocellular Carcinoma. Hepatology. 2021; 74:2652-2669.

75. Shi Q, Li T, Huang S, Bai Y, Wang Y, Liu J, Zhou C, Chen Y, Xiong B. Transcatheter Arterial Embolization Containing Donafenib Induces Anti-Angiogenesis and Tumoricidal CD8(+) T-Cell Infiltration in Rabbit VX2 Liver Tumor. Cancer Manag Res. 2021; 13:6943-6952.
76. Feng S, Wang H, Wang Y, Sun R, Xie Y, Zhou Z, Wang H, Aa J, Zhou F, Wang G. Apatinib induces 3-hydroxybutyric acid production in the liver of mice by peroxisome proliferator-activated receptor α activation to aid its antitumor effect. Cancer Sci. 2019; 110:3328-3339.
77. He X, Huang Z, Liu P, Li Q, Wang M, Qiu M, Xiong Z, Yang S. Apatinib Inhibits the Invasion and Metastasis of Liver Cancer Cells by Downregulating MMP-Related Proteins *via* Regulation of the NF-κB Signaling Pathway. Biomed Res Int. 2020; 2020:3126182.
78. Liu YC, Wu RH, Wang WS. Regorafenib diminishes the expression and secretion of angiogenesis and metastasis associated proteins and inhibits cell invasion *via* NF-κB inactivation in SK-Hep1 cells. Oncol Lett. 2017; 14:461-467.
79. Ou DL, Chen CW, Hsu CL, Chung CH, Feng ZR, Lee BS, Cheng AL, Yang MH, Hsu C. Regorafenib enhances antitumor immunity *via* inhibition of p38 kinase/Creb1/Klf4 axis in tumor-associated macrophages. J Immunother Cancer. 2021; 9.
80. Yokosuka T, Takamatsu M, Kobayashi-Imanishi W, Hashimoto-Tane A, Azuma M, Saito T. Programmed cell death 1 forms negative costimulatory microclusters that directly inhibit T cell receptor signaling by recruiting phosphatase SHP2. J Exp Med. 2012; 209:1201-1217.
81. Feun LG, Li YY, Wu C, Wangpaichitr M, Jones PD, Richman SP, Madrazo B, Kwon D, Garcia-Buitrago M, Martin P, Hosein PJ, Savaraj N. Phase 2 study of pembrolizumab and circulating biomarkers to predict anticancer response in advanced, unresectable hepatocellular carcinoma. Cancer. 2019; 125:3603-3614.
82. Shi J, Liu J, Tu X, Li B, Tong Z, Wang T, Zheng Y, Shi H, Zeng X, Chen W, Yin W, Fang W. Single-cell immune signature for detecting early-stage HCC and early assessing anti-PD-1 immunotherapy efficacy. J Immunother Cancer. 2022; 10.
83. Agdashian D, ElGindi M, Xie C, *et al*. The effect of anti-CTLA4 treatment on peripheral and intra-tumoral T cells in patients with hepatocellular carcinoma. Cancer Immunol Immunother. 2019; 68:599-608.
84. Zhang L, Wang J, Jiang J, Zhang M, Shen J. CTLA-4 Blockade Suppresses Progression of Residual Tumors and Improves Survival After Insufficient Radiofrequency Ablation in a Subcutaneous Murine Hepatoma Model. Cardiovasc Intervent Radiol. 2020; 43:1353-1361.
85. Selby MJ, Engelhardt JJ, Quigley M, Henning KA, Chen T, Srinivasan M, Korman AJ. Anti-CTLA-4 antibodies of IgG2a isotype enhance antitumor activity through reduction of intratumoral regulatory T cells. Cancer Immunol Res. 2013; 1:32-42.
86. Wu H, Zhu JQ, Xu XF, Xing H, Wang MD, Liang L, Li C, Jia HD, Shen F, Huang DS, Yang T. Biointerfacing Antagonizing T-Cell Inhibitory Nanoparticles Potentiate Hepatocellular Carcinoma Checkpoint Blockade Therapy. Small. 2021; 17:e2105237.
87. Kudo M, Ueshima K, Ikeda M, *et al*. Randomised, multicentre prospective trial of transarterial chemoembolisation (TACE) plus sorafenib as compared with TACE alone in patients with hepatocellular carcinoma: TACTICS trial. Gut. 2020; 69:1492-1501.
88. Ma H, Zhang Y, Wang Q, Li Y, He J, Wang H, Sun J, Pan K, Chen M, Xia J. Therapeutic safety and effects of adjuvant autologous RetroNectin activated killer cell immunotherapy for patients with primary hepatocellular carcinoma after radiofrequency ablation. Cancer Biol Ther. 2010; 9:903-907.
89. Zhou P, Liang P, Dong B, Yu X, Han Z, Xu Y. Phase I clinical study of combination therapy with microwave ablation and cellular immunotherapy in hepatocellular carcinoma. Cancer Biol Ther. 2011; 11:450-456.
90. Duffy AG, Ulahannan SV, Makorova-Rusher O, *et al*. Tremelimumab in combination with ablation in patients with advanced hepatocellular carcinoma. J Hepatol. 2017; 66:545-551.
91. Catalano M, Casadei-Gardini A, Vannini G, Campani C, Marra F, Mini E, Roviello G. Lenvatinib: established and promising drug for the treatment of advanced hepatocellular carcinoma. Expert Review of Clinical Pharmacology. 2021; 14:1353-1365.
92. Shigeta K, Datta M, Hato T, *et al*. Dual Programmed Death Receptor-1 and Vascular Endothelial Growth Factor Receptor-2 Blockade Promotes Vascular Normalization and Enhances Antitumor Immune Responses in Hepatocellular Carcinoma. Hepatology. 2020; 71:1247-1261.
93. Zhu Y, Chen M, Xu D, Li TE, Zhang Z, Li JH, Wang XY, Yang X, Lu L, Jia HL, Dong QZ, Qin LX. The combination of PD-1 blockade with interferon-α has a synergistic effect on hepatocellular carcinoma. Cell Mol Immunol. 2022; 19:726-737.
94. Qi X, Yang M, Ma L, Sauer M, Avella D, Kaifi JT, Bryan J, Cheng K, Staveley-O'Carroll KF, Kimchi ET, Li G. Synergizing sunitinib and radiofrequency ablation to treat hepatocellular cancer by triggering the antitumor immune response. Journal for immunotherapy of cancer. 2020; 8.
95. Mi H, Ho WJ, Yarchoan M, Popel AS. Multi-Scale Spatial Analysis of the Tumor Microenvironment Reveals Features of Cabozantinib and Nivolumab Efficacy in Hepatocellular Carcinoma. Front Immunol. 2022; 13:892250.
96. Ho WJ, Zhu Q, Durham J, *et al*. Neoadjuvant Cabozantinib and Nivolumab Converts Locally Advanced HCC into Resectable Disease with Enhanced Antitumor Immunity. Nat Cancer. 2021; 2:891-903.
97. Sangro B, Sarobe P, Hervas-Stubbs S, Melero I. Advances in immunotherapy for hepatocellular carcinoma. Nat Rev Gastroenterol Hepatol. 2021; 18:525-543.
98. Fu Y, Liu S, Zeng S, Shen H. From bench to bed: the tumor immune microenvironment and current immunotherapeutic strategies for hepatocellular carcinoma. J Exp Clin Cancer Res. 2019; 38:396.
99. Lawal G, Xiao Y, Rahnemai-Azar AA, Tsilimigras DI, Kuang M, Bakopoulos A, Pawlik TM. The Immunology of Hepatocellular Carcinoma. Vaccines (Basel). 2021; 9:1184.

Received October 20, 2023; Revised November 11, 2023; Accepted November 16, 2023.

[§]These authors contributed equally to this work.
**Address correspondence to:*
Rui Liao, Department of Hepatobiliary Surgery, the First Affiliated Hospital of Chongqing Medical University, Chongqing 400016, China.
E-mail: liaorui99@163.com

Released online in J-STAGE as advance publication November 19, 2023.

Review

DOI: 10.5582/bst.2023.01311

An update on diagnosis and treatment of hepatoblastoma

Yinbiao Cao[1,2,§], Shurui Wu[2,§], Haowen Tang[1,2,*]

[1] Faculty of Hepato-Pancreato-Biliary Surgery, Chinese PLA General Hospital, Beijing, China;
[2] The First Medical Center of the Chinese PLA General Hospital, Beijing, China.

SUMMARY Hepatoblastoma (HB) remains the most common paediatric liver tumour and survival in children with hepatoblastoma has improved considerably since the advent of sequential surgical regimens of chemotherapy based on platinum-based chemotherapeutic agents in the 1980s. With the advent of modern diagnostic imaging and pathology techniques, new preoperative chemotherapy regimens and the maturation of surgical techniques, new diagnostic and treatment options for patients with hepatoblastoma have emerged and international collaborations are investigating the latest diagnostic approaches, chemotherapy drug combinations and surgical strategies. Diagnosis of hepatoblastoma relies on imaging studies (such as ultrasound, computed tomography, and magnetic resonance imaging), alpha-fetoprotein (AFP) levels, and histological confirmation through biopsy. The standard treatment approach involves a multimodal strategy with neoadjuvant chemotherapy followed by surgical resection. In cases where complete resection is not feasible or tumors exhibit invasive characteristics, liver transplantation is considered. The management of metastatic and recurrent hepatoblastoma poses significant challenges, and ongoing research focuses on developing targeted therapies and exploring the potential of immunotherapy. Further studies are necessary to gain a better understanding of the etiology of hepatoblastoma, develop prevention strategies, and personalize treatment approaches. We aim to review the current status of diagnosis and treatment of hepatoblastoma.

Keywords PRETEXT staging, neoadjuvant chemotherapy, hepatectomy, recurrent hepatoblastoma

1. Introduction

Hepatoblastoma (HB) has been the most common primary pediatric liver malignancy in young children who developed liver cancer, accounting for 90% of malignant liver tumors in children younger than 5 years, and it is especially prevalent in children under the age of 3(*1,2*). With the development of imagining examination, the diagnostic method has been common and more precise staging can be applied through imaging tools (*3,4*). In the treatment of hepatoblastoma, since the application of platinum-based chemotherapy regimens and advances in surgical techniques and surgical tools, which facilitated precision hepatectomies and resection of focal metastasis, survival has greatly improved (*5*). After the International Childhood Liver Tumor Strategy Group (SIOPEL)-I study in the 1980s, which found that platinum-based chemotherapy regimens were quite effective in children with hepatoblastoma, more international collaborative organizations became involved in the trend of studying preoperative chemotherapy regimens in combination with sequential surgical treatment (*6-9*). Among these, the Children's Oncology Group (COG), Japanese study group for Pediatric Liver Tumor (JPLT), German Paediatric Oncology and Haematology Society (GPOH) and SIOPEL cohorts are the most authoritative and systematic. In subsequent studies, even though the basic chemotherapeutic drug combinations are relatively fixed, an increasing number of chemotherapy regimens have emerged, and the pursuit of better tumor remission, adjusting the dose of chemotherapy drugs within a reasonable range, and combining the use of other drugs to reduce the damage of chemotherapy side effects have become the goals of new chemotherapy regimens (*7,9-11*). At the same time, surgical resection of liver tumors has advanced dramatically over the past few decades (*12*). The use of more sophisticated surgical techniques has further increased the resection rate of patients with hepatoblastoma after chemotherapy. The identification of lesions, the removal of metastatic lesions and the implementation of extreme hepatectomy have increased the surgical benefit for patients(*5,13*). We aim to present the progression and current situation of diagnoses and treatments in hepatoblastoma.

2. Progress and current situation in diagnosis of hepatoblastoma

2.1. Symbols of hepatoblastoma

The most common presentation of hepatoblastoma is asymptomatic celiac mass, the accompanying symbol includes ascites, febrile, jaundice, feeding intolerance and weight loss, caused by the mass effect upon the stomach or intestine (*14,15*). Some symbols containing pseudo precocious puberty and thrombocytosis could help to make a clinical diagnosis (*16*). The serum alpha-feto protein (AFP) level is also an element in diagnosis of hepatoblastoma. The sensitivity and specificity of the abnormal increase of serum AFP in the diagnosis of hepatoblastoma were 98.0% (95%CI: 0.89-1.00) and 100% (95%CI: 0.88-1.00). The clinical diagnosis was consistent with the pathological diagnosis of hepatoblastoma (Kappa = 0.97, $P < 0.001$) (*17*). However, low-AFP level was highly associated with poor prognosis (*18*).

2.2. Imaging diagnosis of hepatoblastoma

2.2.1. Ultrasound

Ultrasound remains the first imaging study performed for screening and diagnosis of pediatric abdominal mass. By assessment the echo signal and significant mass effect on adjacent organs, ultrasound can confirm the hepatic mass origin (*19*). Hepatoblastoma can appear as a solitary mass, a dominant mass with satellite lesions, as multiple nodules throughout the liver or, rarely, a diffusely infiltrative mass involving the entire liver on sonography. Most tumors are hyperechoic relative to normal liver but are often nonhomogenous due to mesenchymal components. Calcifications may be present and appear as punctate or linear hyperechoic foci with posterior shadowing. Areas of internal hemorrhage and necrosis are not uncommon and will appear anechoic (*19*). Also, doppler ultrasound is sensitive to evaluate the invasion of hepatic and portal venous, which contributed to high-risk stratification in several studies conducted by international conjunction groups (*20*).

2.2.2. Computed Tomography (CT)

The CT presentation of hepatoblastoma depends on the histologic composition of the tumor and is highly variable. Calcification may be present in the epithelial pathological subtype and are usually small and fine, whereas in mixed mesenchymal-epithelial tumors the calcifications are coarse and extensive (*19*). After contrast injection, hepatoblastoma generally shows heterogeneous enhancement and is less enhanced than the surrounding normal liver. If imaging is performed in the arterial phase, there may be an enhanced peripheral margin. The tumor may involve one, two, three or all four hepatic segments. Although coronal and sagittal reconstructed CT images help to define the tumor margins, sometimes it is difficult to define the margins on CT. In such cases, MRI can provide additional information.

Since approximately 20% of portions of hepatoblastoma patients were diagnosed with lung metastasis initially, pulmonary CT was required and can be used to scan abdomen at the same time (*3*).

2.2.3. Magnetic Resonance Imaging (MRI)

MRI is more widely used in the diagnosis of hepatoblastoma due to its ability to reflect more accurately the location of the tumor in relation to the vital tissue vessels and to determine roughly the pathological type of the tumor by the presentation of many different sequences (*21*). Epithelial tumors are generally homogeneous, appearing as hypodense on T1-weighted images and dense on T2-weighted. Mixed epithelial-mesenchymal tumors are usually heterogeneous due to varying amounts of internal haemorrhage, necrosis, fibrosis, calcification, cartilage and septa (*19*). However, MRI takes longer to perform and therefore sedation is usually required for paediatric patients.

2.3. Biopsy of hepatoblastoma

Though imaging tools played a vital role in diagnosis in hepatoblastoma, only biopsy can confirm it. It's obliged in children under 6 months old and over 3 years of age undergoing tumor biopsy, because various tumors could present at the former group and a high-AFP level may be attributed to the age of the child, and to tell if hepatoblastoma and hepatocellular carcinoma occurs in older children. To children between 6 months and 3 years old, diagnostic biopsy is controversial (*16*). Biopsy tissue can be obtained through percutaneous core, laparoscopic core or wedge, or open biopsies, which depend on the balance between the risk of bleeding and acquiring enough of target tissue. It's recommended to obtain five cores of tumor and one core of normal liver or at least three cores for pathological examination (*6*).

Since the forge of staging systems (PRETEXT, COG *et al*) and risk stratification were mature in recent years, histological subtype is raising great importance in formulating treatment protocols (*8,9,18,22*). Not only histological subtype, but also the results of immunohistochemical testing could guide the chemotherapy algorithms. The clinical meaning revealed by immunohistochemistry differs a lot. Integrase interactor 1(INI 1) negative epithelial hepatoblastoma with low serum AFP level may suggest a rhabdoid originated tumor and receive a compromised chemotherapy regimen. Comparison between PRETEXT stage I/II and stage III/IV have shown that CD44 is higher expressed in the latter (*23*). Abnormal expression

of CD 90, CD133 and CD44 were associated with disease progression and decreased survival in hepatoblastoma (*24*). Studies concentrated on new immunohistochemical markers are conducted globally. A report from AHEP 0731 has shown that pretreatment percutaneous biopsy of pediatric liver tumors yielded the lowest frequency of clinically significant hemorrhaging requiring transfusion, without evidence of sacrificing diagnostic accuracy (*10*).

2.4. Hepatoblastoma risk stratifying staging system

The first risk stratifying system was pre-treatment extent of tumor system (PRETEXT system), reported by SIOPEL in 1992. Evan's risk stratification was adopted by Children's Oncology Group (COG), and the stratification was based on initial surgery. Since the advances applied in imagine techniques, PRETEXT system has been a hybrid to apply serial trails conducted by international cooperative groups. In 2017, four international cooperative groups (SIOPEL, COG, JPLT, GPOH) have collaborated to write a new staging system- CHIC-HS. CHIC-HS is a stratification based on PRETEXT system, and was used by ongoing hepatoblastoma trials.

2.4.1. PRETEXT staging system

The Société Internationaled' Oncologie Pédiatrique Epithelial Liver Tumor Study Group (SIOPEL) first described the pre-treatment extent of tumor system (PRETEXT system) in 1992 to stratify the risk stage for children diagnosed with hepatoblastoma prior to neoadjuvant chemotherapy (Figure 1). The PRETEXT system contains content concerning standardized imaging evaluation at the same time (*25*). A consequence of SIOPEL trials reported PRETEXT system stratified risk patients distinctly, and easily to be reproduced in clinical practice (*13,22,26-29*). The PRETEXT system was contributed by two components: the PRETEXT group and annotation factors. The former depicted the intrahepatic extent of hepatoblastoma and the latter was used to reveal characters like vascular invasion (including portal vein or hepatic vein/ inferior vena cava), extrahepatic disease, multifocality, tumor rupture and metastatic disease (to both the lungs and lymph nodes).

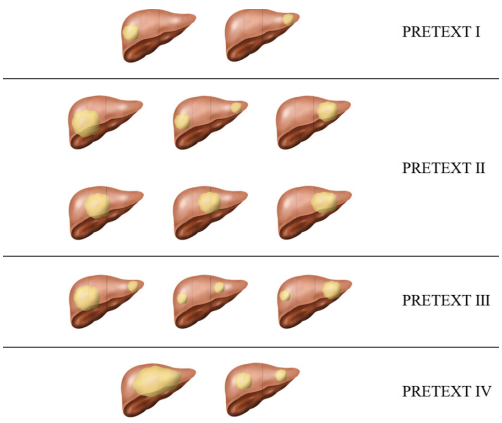

Figure 1. PRETEXT staging. (I = one section involved, three sections tumour free; II= one or two sections involved, two sections tumour free; III = two or three sections involved, one section tumour free; IV = four sections involved).

PRETEXT system was revised several times since the first publication in 1992, and several trails conducted by Children's Oncology Group (COG), the International Childhood Liver Tumors Strategy Group (SIOPEL), and the Japanese Study Group for Pediatric Liver Tumor (JPLT, now part of the Japan Children's Cancer Group) have some differences in definitions of annotation factors.

In 2017, these organization wrote a common set of definitions to be used in future trials together (*3*). The modified PRETEXT annotation contains **V:** Hepatic or vena cava involvement, **P:** Portal vein involvement, **E:** Extrahepatic adjacent tissue involvement, **M**: Distal tissue involvement, **C:** Caudate lobe involvement, **F**: Intrahepatic multiple tumor nodules, **R**: Pre-diagnostic tumor rupture. These definitions will be used in the forthcoming Trial to Pediatric Hepatic International Tumor Trial (PHITT) (*3*).

2.4.2. Evan's surgical stage

In trial INT-0098, which was conducted by Children's Oncology Group (COG), presented Evan's surgical stage based on initial surgical intervention prior to neoadjuvant chemotherapy. With the development of imaging techniques, COG has used a staging system mixed with PRETEXT and Evan's system (Table 1).

2.4.3. PRETEXT: pre-treatment extent of tumor system

In order to create a standard staging system, SIOPEL, COG, JPLT and GPOH cooperated to summarize their clinical trial data. The Children's Hepatic Tumors International Collaboration (CHIC)has reviewed these data and formed CHIC-HS risk stratification (Table 2). The new system uses PRETEXT groups and PRETEXT annotation factors, as well as age and alpha-fetoprotein (AFP) levels, to determine treatment cohorts on the new Trial to Pediatric Hepatic International Tumor Trial (PHITT).

Table 1. Evan's surgical stage

Stage	Specifics
I	Complete gross resection with clear margins
II	Gross total resection with microscopic residual disease at margin of resection
III	Gross total resection with nodal involvement or tumor spill or incomplete resection with gross residual intrahepatic disease
IV	Metastatic disease with either complete or incomplete resection

3. Treatments of hepatoblastoma

3.1. Pre/Post-operative chemotherapy

Since the apparent reduction of tumor volume caused by cisplatin-based chemotherapy was reported in the 1980s, neoadjuvant chemotherapy with sequential surgery became a paradigm of treatment of hepatoblastoma gradually (*30,31*). In consecutive trials conducted by SIOPEL, the children were treated with chemotherapy prior to surgery (*29*). The COG believes that very low risk, low risk patients should have surgery first; medium to high-risk patients should have neoadjuvant chemotherapy in combination with surgery and adjuvant chemotherapy (*32*). GPOH and JPLT preferred to apply surgery to relatively early-stage patients and administer post-operative chemotherapy(*9,33*). Both GPOH and JPLT are now increasingly advocating the use of pre-operative chemotherapy. However, patients suitable for surgery at initial diagnosis and undergoing surgery were recommended for postoperative chemotherapy by COG, GPOH and JPLT (*7,9*). The summarization of these collaborations is shown in Table 3.

Table 2. Risk stratification of CHIC-HS

Risk Stratification	Specifics
Very low	PRETEXT I, M(-), VEGFR(-), resectable at diagnosis PRETEXT II, M(-),< 8 years, VEGFR(-), AFP > 1,000 ng/mL, resectable at diagnosis
Low	PRETEXT I, M(-),VEGFR(-), non-resectable at diagnosis PRETEXT II, M(-),< 8 years, VEGFR(-), AFP > 1,000 ng/mL, non-resectable at diagnosis PRETEXT III, M(-), < 8 years, VEGFR(-), AFP>1,000 ng/mL
Intermediate	PRETEXT I, M(-), < 8 years, VEGFR(+) PRETEXT II, M(-), < 8 years, VEGFR(+), AFP > 1,000 ng/mL PRETEXT III, M(-),< 8 years, VEGFR(+)/ AFP 100-1,000 ng/mL PRETEXT IV, M(-), < 3 years, AFP>100ng/mL
High	Any PRETEXT, M(+) PRETEXT I, M(-), > 8 years, VEGFR(+) PRETEXT II/III, M(-), <8 years, AFP ≤ 100 ng/mL PRETEXT II/III, M(-), > 8 years PRETEXT IV, M(-), < 3 years, AFP ≤ 100 ng/mL PRETEXT IV, M(-), > 3 years

3.1.1. SIOPEL

The SIOPEL initiative of cisplatin-based neoadjuvant chemotherapy in combination with surgery and postoperative chemotherapy has shown a significant improvement in patient prognosis (*22*). The first HB prospective clinical trial (SIOPEL-1) used a cisplatin + adriamycin regimen (PLADO) with a 5-year event-free survival (EFS) and overall survival (OS) of 66% and 75%, respectively, for the entire group (*29*). In subsequent trials, SIOPEL-2 has stratified patients into standard-risk group and high-risk group depending on the PRETEXT system and lung metastasis. Cisplatin alone (CDDP 80 mg/m^2) was shown to be comparable to cisplatin combined with adriamycin for the standard-risk group (3-year EFS (83% *vs.* 85%) and OS (95% *vs.* 93%) and relapse rate (15% *vs.* 12%) (*29*). For the treatment of patients in the high-risk group, the SIOPEL-4 study increased the preoperative cisplatin dose density from

Table 3. Summarization of chemotherapy of international collaborations

International collaborations	Risk stratification	PRETEXT staging and disease manifestations	Preoperative chemotherapy	Postoperative chemotherapy
SIOPEL-4	Standardize risk	PRETEXT I/II/III and AFP > 100 ng/mL	CDDP*4	C5V-DOXO*2
	High risk	PRETEXT IV or M,H,P,E,R, AFP < 100 ng/mL	CDDP*4 alternate CARBO/DOXO*3	C5V-DOXO alternate CARBO/DOXO*2
AHEP0731 (COG)	Very low risk	PRETEXT I with pure fetal histology hepatoblastoma	N	N
	Low risk	PRETEXT I/II, non-small-cell undifferentiated disease	N	C5V*2
	Intermediate risk	PRETEXT I/II with small-cell undifferentiated histology or PRETEXT III hepatoblastoma	C5V and DOXO*4-6	C5V-DOXO
	High risk	PRETEXT IV and Any stage disease with AFP <100 ng/mL	Vincristine (V) and Irinotecan (I)*2 and C5V-DOXO*6	-
HB99 (GPOH)	Standardize risk	Potentially resectable after chemotherapy	IPA*2-3	IPA
	High risk	Non-resectable Multifocal Vessel involvement Positive lymph nodes	Carboplatin + etoposide * 2	CDDP*1 alternate CARBO/ DOXO * 2
JPLT-2		PRETEXT I/II	N	CITA (50% dose)
		PRETEXT II	CITA*2	CITA (50% dose)
		PRETEXT III/IV OR PRETEXT I/II with annotation	CITA+ITEC (high dose)	CITA*2

CDDP: cisplatin; C5V: vincristine; DOXO: doxorubicin; CARBO: carboplatin; IPA: ifosfamide+cisplatin+doxorubicin, cisplatin and doxorubicin CITA: CDDP + 4'-O-tetrahydropyranyladriamycin ITEC: cisplatin, pirarubicin or pirarubicin, ifosfamide/carboplatin.

22. 9 mg/(m^2 -week) to 47. 5 mg/(m^2 -week), and after high-dose cisplatin + adriamycin preoperative chemotherapy and carboplatin + adjuvant chemotherapy, patients had an increase in complete remission rates of approximately 20% compared to SIOPEL3, with 3-year EFS and OS of 76% and 83%, respectively (*22,34*). The prognosis of patients in the high-risk group was significantly better than before, with 77% and 73% 3-year OS in patients with metastases or PRETEXT stage IV, respectively, suggesting that weekly application of cisplatin may improve patient survival (*22*). In SIOPEL IV, postoperative chemotherapy was applied to patients who underwent sequential surgery after neoadjuvant chemotherapy. The postoperative chemotherapy protocols were doxorubicin (20 mg/m²) and carboplatin6 mg/mL per min per day) (*22*).

3.1.2. COG

The COG initially favored a post-operative chemotherapy regimen based on Evans classification criteria. In COG-INT0098, a postoperative chemotherapy protocol based on cisplatin, fluorouracil and vincristine (C5V) regimen were applied to avoid adriamycin cardiotoxicity with improved prognosis (*35*). In 1993, the COG first demonstrated the efficacy of the C5V regimen, with a 5-year EFS of 90% in Evan's stage I and II patients and a poorer prognosis in later stage patients (*36*). Subsequent studies comparing C5V and cisplatin + adriamycin regimens found similar overall survival rates (5-year OS 69% *vs.* 72%), with the former having a slightly higher recurrence rate (5-year EFS 57% *vs.* 69%) but less toxic side effects (*36*). AHEP0731 further optimized the chemotherapy regimen for the low-risk group, suggesting that in children with completely resectable tumors, reducing the C5V regimen by 2 courses postoperatively would reduce drug accumulation and ensure efficacy, and reduce the total cisplatin dose by 1/2 (*8*). Also, the AHEP0731 study used vincristine/irinotecan for the pre-treatment of high-risk HB. The 3-year EFS and OS were 49% and 62%, respectively (*37*). In 2021, the COG suggested that the C5V regimen combined with adriamycin (C5VD regimen) could further improve outcomes in children with HB, with a 5-year EFS and OS of 88% and 95%, respectively, in children with unresectable disease at diagnosis (*11*).

3.1.3. GPOH

GPOH has led three clinical trials, HB89, HB94 and HB99, in which the indications for initial surgical procedures have become increasingly stringent (*38-40*). In GPOH 99, the protocol allowed the primary resection only in very small tumors confined to one liver segment on the liver margin, which was equal to PRETEXT I, and PRETEXT system used to stratify parallel patients (*40*). The German GPOH prospective studies of HB89, HB94 and HB99 using IPA (isocyclophosphamide + cisplatin + adriamycin), PA-cont (cisplatin + adriamycin continuous therapy) and Carbo/VP16 (carboplatin + etoposide) had 3-year OS of 75%, 77% and 89%, respectively, but the GPOH regimen did not outperform the SIOPEL and COG regimens over the same period. HB94 had a slightly improved prognosis (29% *vs.* 36%) in advanced, relapsed refractory HB with IPA and Carbo/VP16 (*33*). High-dose Carbo/VP16 chemotherapy combined with autologous HSCT had limited efficacy in the high-risk group, with a 5-year OS of only 58% (*7*).

3.1.4. JPLT

The first clinical trial of JPLT (JPLT-1) used a cisplatin + adriamycin regimen with 3-year and 6-year OS of 77. 8% and 73. 4%, and a 3-year EFS of < 50% after doubling the cisplatin dose in patients with advanced disease (stages IIIB and IV) (*9,41*). In JPLT-2, patients staged PRETEXT I/II were recommended to undergo surgery first, and remaining patients received cisplatin + pirarubicin (CITA) used as the first-line regimen; isocyclophosphamide, pirarubicin. VP-16 and carboplatin (ITEC) were used as the second-line regimen, with a 5-year EFS of 71. 6-84. 8%. However, ITEC second-line regimen and autologous stem cell transplantation has limited efficacy (*9*). The effectiveness and safety of the SIOPEL-4 regimen was confirmed by JPLT3-H (*42*).

3.2. Common chemotherapy adverse reactions and management

3.2.1. Cisplatin

Cisplatin is indispensable for HB treatment, but can cause irreversible Ototoxicity in children and reduce quality of life. In SR patients treated with cisplatin monotherapy, SIOPEL-6 found a significantly lower incidence of grade 1+ hearing loss in the sodium thiosulfate group compared to the control group (33% *vs.* 63%), with no difference in 3-year EFS and OS between the two groups, confirming that sodium thiosulfate significantly reduced cisplatin ototoxicity without compromising efficacy (*43*). This was corroborated by the results of the COG's ACCL0431 trial, which showed a 27. 8% reduction in hearing loss in children with cancer in the sodium thiosulfate group (28.6% *vs.* 56.4%). However, the prognosis was worse in the sodium thiosulfate group in patients with metastases, suggesting that sodium thiosulfate may diminish the effect of cisplatin and may not be used in the high-risk group (*44*). Amifostine has a hearing protective effect but unfortunately does not work in HB (*45*).

3.2.2. Anthracyclines

The main side effects of chemotherapy with anthracyclines are cardiotoxicity, including acute

myocardial injury and chronic impairment of cardiac function. The former is transient and reversible myocardial localised ischaemia, which may manifest as panic, shortness of breath, chest tightness and precordial discomfort; the latter is irreversible congestive heart failure, which is related to the cumulative dose of the drug (*46*). Once cardiac function tests suggest an ejection fraction < 55% or an axis shortening fraction < 28%, anthracycline antibiotics may be continued if abnormal left heart function can be demonstrated to be related to bacterial infection, otherwise they should be suspended until the ejection fraction is ≥ 55% or the axis shortening fraction is ≥ 28% (*47*). Dexrazoxane and levocarnitine are chosen according to the dose of anthracycline used or the degree of myocardial damage (*15*).

3.3. Surgical treatment of hepatoblastoma

Surgery remains the most vital intergradient in the cure of hepatoblastoma even though chemotherapy has become sophisticated through these decades. The timing and extent of hepatectomy or liver transplantation contingent on the POSTTEXT classification (staged in the same way as PRETEXT but used to describe status after receiving neoadjuvant chemotherapy), response to neoadjuvant and tumor biology (*3*). The advent of many new techniques has also broadened the scope of resectable hepatoblastoma, making surgery safer and more effective.

3.3.1. Hepatectomy

On the timing of surgical resection of hepatoblastoma, this varies between collaborative groups. The International Childhood Liver Tumors Strategy Group (SIOPEL) recommends preoperative neoadjuvant chemotherapy for all staged children to reduce the extent of hepatic resection, avoid aggressive surgery and reduce surgical trauma (*13*). In the COG, GPOH and JPLT studies, an upfront resection strategy was adopted for patients with PRETEXT I/II and, according to the COG study, pure fetal hepatoblastoma with PRETEXT I can be cured with radical surgery (*48,49*). The COG surgical guidelines recommend: segmental or lobectomy for children with PRETEXT stages I and II; lobectomy or trilobectomy for children with POST-TEXT stages II and III without involvement of large vessels; and complex hepatectomy or liver transplantation for children with POST-TEXT stages III and IV with involvement of large vessels, which should be assessed by an experienced team with competence in liver transplantation (*50-52*). Although the protocols used by the various collaborative groups differed, the final outcomes were generally similar according to the Children's Hepatic tumors International Collaboration (CHIC) (*18*).

In the Chinese guidelines for the diagnosis and management of hepatoblastoma, the indications for primary surgical resection are: (1) American Society of Anesthesiologists grade 1 to 2; (2) residual liver tissue greater than 35% of the original volume and functionally capable of meeting metabolic needs as assessed by imaging; (3) a single tumor lesion in PRETEXT stage I or II with adequate clearance (≥ 1 cm) from important vessels; (4) an anticipated microscopic single tumor lesion in PRETEXT stage I and II with sufficient clearance from important vessels (≥ 1 cm); (5) expected microscopic residual (COG stage II) without secondary surgery. (6) For children with PRETEXT stage III or IV, deferred surgery should be performed after neoadjuvant chemotherapy with a clear diagnosis on biopsy; (7) For children with POSTTEXT stage I or II or POST-TEXT stage III without significant vascular involvement (portal vein or inferior vena cava) after chemotherapy, lobectomy or segmental resection of the liver is feasible; (8) For children with PRETEXT stage I or II, lobectomy or segmental resection of the liver is feasible. (9) Children with PRETEXT stage IV and POSTTEXT stage III with inferior vena cava (V+) or portal vein (P+) involvement after chemotherapy should be transferred to a hospital with complex hepatic segmental resection or liver transplantation capability as soon as possible; (10) Children with single metastatic lesions in the lung or brain remaining after chemotherapy should be surgically resected for residual lesions.

The use of surgical adjuvant techniques also provides a guarantee of safety and effectiveness in hepatoblastoma surgery. Along with the development of laparoscopic techniques, laparoscopic liver tumor resection is becoming increasingly sophisticated. With the assurance of less trauma, less bleeding and faster postoperative recovery, laparoscopic surgery offers adequate safety and efficacy. In the JPLT-2 study, non-anatomical partial hepatectomy and incomplete tumor resection were suggested as risk factors associated with a high risk of recurrence. Combined with the use of intraoperative ultrasound, laparoscopic liver resection can accomplish precise resection of liver segments and complete removal of the lesion. However, due to the small abdominal space in paediatric patients, patient selection for surgery should be considered in relation to the location, size and response to chemotherapy of the paediatric tumor.

Indocyanine green (ICG) fluorescence imaging has been widely used in laparoscopic surgery and paediatric liver resection, and there are international reports of ICG being used in hepatoblastoma resection (*53-55*). Since healthy liver tissue rapidly clears ICG, while tumor tissue retains ICG, preoperative injection of ICG facilitates intraoperative determination of the resection line and identification of residual tumor (*56*). ICG (0.5-1 mg/kg) is currently administered intravenously 48-72 hours prior to surgery to ensure hepatic clearance (*55*). In addition, indocyanine green staining can be applied to indicate resection of distant metastases from hepatoblastoma. See 3.4 of this chapter for details. However, the following

deficiencies remain when using indocyanine green for staining indication of hepatoblastoma. First, for hepatoblastoma with good differentiation, indocyanine green can maintain a good fluorescence image, while for special hepatoblastoma, indocyanine green does not maintain well. Second, most patients with hepatoblastoma received preoperative chemotherapy, and the activity of the tumor is significantly reduced, which also affects the absorption and excretion of indocyanine green by the tumor tissue (*57*).

With regard to the prognostic impact of positive postoperative pathological examination margins, although residual tumor was found to be a high-risk factor for recurrence in the JPLT-2 study, in the SIOPEL study, positive microscopically seen margins did not affect outcome with a median follow-up of 67 months, with local recurrence occurring in 3/58 (5%) patients with microscopically positive resection margins and 23/371 (6%) patients with complete resection. The 5-year overall and event-free survival rates were 91% and 86%, respectively (*58,59*). The more widely shared view is that in patients with hepatoblastoma treated with platinum-based protocols, even if a positive microscopic margin is found after surgery, there is no significant impact on patient survival. The results of some studies suggest that there is no significant difference in the prognosis of patients with positive margins even when compared to patients in complete remission after platinum-based therapy (*59,60*). The reasons for this phenomenon may be as follows: first, the positive margins of the patient's resected liver specimen may not mean that tumor cells remain in the patient's liver body because liver sections are routinely cauterized during liver surgery; second, even small amounts of residual tumor tissue are still more easily controlled or even in complete remission under the control of platinum-based chemotherapy regimens (*59*). In some cases of postoperative recurrence of non-R0 resection, this may also be due to the presence of potential metastases at the time of diagnosis. The survival was not significantly different even after postoperative distant metastases due to good control of distant metastases with platinum-based agents (*60*). This provides some theoretical basis for the acceptance of hepatectomy in patients with POSTTEXT stage III/IV. Indeed, studies by Joerg Fuchs *et al*. and El-Gendi A *et al*. have suggested a survival benefit for patients undergoing hepatectomy in POSTTEXT stage III, with 3-year overall survival rates of 86.6% for the former and 5-year overall survival rates of 80.7% for the latter (*13,61*). Although such clinical practice may be beneficial in diverting the need for allogeneic liver transplantation in advanced patients, the possibility of liver transplantation should always be considered. In addition, a surgical strategy of ex vivo liver resection and autotransplantation (ELRA) may be attempted for those who still have invasion of important tissue structures after chemotherapy treatment and whose growth location is difficult to be directly resected. According to Kang *et al*, an autologous liver transplantation with ex vivo hepatectomy was performed in a 1.5-year-old female child. The patient's AFP level returned to normal rapidly after surgery and the perioperative period was uneventful, providing preliminary evidence of the potential feasibility of the ex vivo hepatectomy combined with the autologous liver transplantation technique for patients who are not suitable for conventional hepatectomy (*62*).

3.3.2. Liver transplantation

There is no unified indication for liver transplantation for hepatoblastoma in international collaborations, but liver transplantation should still be considered first for patients with PRETEXT stage III/IV, or with large vessel or bile duct invasion. Liver transplantation is a more complete eradication of the lesion than hepatectomy, but is limited by the adverse effects of immunosuppressive therapy and an insufficient number of donors, and has been commonly used as a salvage treatment for end-stage HB. So, liver transplantation for hepatoblastoma can be divided into two options: primary liver transplantation and salvage liver transplantation. Salvage liver transplantation may be considered for remaining intrahepatic recurrences that occur after initial liver resection. Based on previous literature, the postoperative survival benefit of salvage liver transplantation is similar to that of initial liver transplantation (*63*). Also, the pathological type of hepatoblastoma, waitlist time, log-fold decrease in AFP and number of adjuvant chemotherapy cycles had a significant effect on the time to EFS after liver transplantation in patients with hepatoblastoma (*63*). Thanks to the use of preoperative chemotherapy and the maturation of surgical techniques, the survival prognosis of liver transplantation in patients with unresectable hepatoblastoma has been significantly improved and the number of liver transplants performed on patients with hepatoblastoma has increased more than 20-fold (*64*). Due to preoperative chemotherapy regimens and improved surgical techniques, liver transplantation for hepatoblastoma now has a 5-year survival rate of 60-80% (*65*). A restorative clinical study based on the Surveillance, Epidemiology, and End Results Program (SEER) database suggests that children with hepatoblastoma who undergo liver transplantation have a 5-year survival rate of 86.5% (*66*). In recent years, studies have confirmed that postoperative survival rates are significantly higher in children who have undergone first-stage liver transplantation than in children who have undergone recurrent remedial liver transplantation after hepatectomy. Therefore, a more positive attitude towards liver transplantation is required in clinical practice.

3.3.3. Assistive technology

Trans-catheter arterial chemo-embolization (TACE) may

be indicated for patients who have had a poor response to chemotherapy and are not candidates for liver resection or liver transplantation (*67,68*). Jiang *et al*. treated 17 patients with PRETEXT stage III-IV with the A combined with B approach, and 14 of them achieved good results. Tumor markers were reduced to normal (*69*). The results of another randomized controlled trial suggested that 110 patients with unresectable hepatoblastoma treated with High Intensity Focused Ultrasound (HIFU) combined with TACE regimen had higher survival rates of 100%, 84%, and 16% at 1, 3, and 5 years, respectively (*70*). The above results support that TACE and various treatment options in combination with TACE may have some efficacy in difficult-to-resect hepatoblastoma, leading to longer survival times. In addition, portal vein embolisation (PVE) or associating liver partition and portal vein ligation for staged hepatectomy (ALPPS) has the potential to promote normal liver volume gain and safeguard liver function in the perioperative period in patients who have insufficient future liver remnant (FLR) but still require liver resection. The world's first patient with hepatoblastoma treated surgically with ALPPS was reported in 2014 by Chan *et al* (*71*). The use of ALPPS in paediatric liver tumors is still in its infancy and has only been carried out in a small number of experienced paediatric hospitals, and is mostly reported as a case study (*72,73*). However, some studies now show that rapid tumor recurrence and metastasis may occur after ALPPS, which may be related to changes in the immune microenvironment within the liver (*74*).

3.4. Treatment of metastatic lesions

The most common distant metastatic organ for hepatoblastoma is the lung, with 20% of children having lung metastases at diagnosis. In patients with hepatoblastoma found at initial diagnosis and with pulmonary metastases, surgical resection of the still present pulmonary metastases after chemotherapy helps to prolong overall survival (*13,75,76*). According to the JPLT-2 and SIOPEL-3 studies, more than half of patients who received intensive neoadjuvant chemotherapy experienced complete remission of their lung lesions (*13,77*). For patients with complete remission of lung lesions who undergo resection of the primary lesion, the overall survival rate at 3 years can exceed 80% (*78*). Whereas in patients with residual lung lesions despite chemotherapy, residual lung lesions are a significant risk factor for reduced EFS and OS and undergoing lung nodule resection is a viable means of doing so. Wanaguru *et al*. reported on the resection of eight patients with hepatoblastoma with long-term curative results (*76*). Intraoperative identification and resection of lung metastases can now also be achieved with the aid of ICG fluorescent labelling. Kitagawa *et al* reported that ICG can detect lung lesions as small as 0.062 mm. In a study of 10 patients, all pathologically positive lesions were significantly fluorescence positive (*79*). In contrast, survival data for pulmonary recurrence after surgery vary widely, but the basic treatment idea is also based on surgical options after chemotherapy or relying on chemotherapy alone for disease control, but in general, the prognosis for patients with this condition is relatively poorer than for patients with lung metastases at the time of initial diagnosis, perhaps due to the development of resistance to chemotherapy in postoperative recurrent tumors (*80*). The difference in survival of patients with recurrent lung disease, however, may be due to differences in patient metastasis, with shorter survival for patients who also have extra-pulmonary recurrent lesions compared to those with limited intrapulmonary recurrence (*81,82*). Currently, the common surgical approach for resection of lung lesions is irregular resection or wedge resection of the lung, rather than resection of the complete lung lobes or segments. Also, simultaneous and heterochronic resection is controversial in patients with metastatic lesions in both lungs (*83*). Although heterochronic surgery is less invasive, the interval between surgical procedures may affect the development and implementation of the patient's postoperative chemotherapy regimen. The procedure is also more invasive and more likely to affect the patient's respiratory function, requiring more careful assessment of the patient's surgical and respiratory tolerances. In addition, radiofrequency ablation can be used for the treatment of pulmonary metastatic lesions (*84*).

3.5. Treatment of recurrent hepatoblastoma

The most common sites of recurrence of hepatoblastoma are intrahepatic recurrence and pulmonary metastases. Recurrence of hepatoblastoma is relatively common in patients who are not sensitive to first-line therapy, with less than 12% of patients in complete remission to first-line therapy experiencing recurrence, according to the SIOPEL study and combined treatment with chemotherapy and surgical removal of the tumor is essential for long-term survival (*85*). Chemotherapy as well as surgery is still recommended for the treatment of recurrent hepatoblastoma. In the aforementioned SIOPEL study, 31 of 59 patients with recurrence achieved a secondary complete remission and 15 of 21 patients with local recurrence in the liver were treated with radical surgery (*85*). Salvage liver transplantation may also be considered for those with complex localised recurrent lesions in the liver that make reoperation difficult. However, the long-term survival of salvage liver transplantation is currently poor, with a 5-year survival rate of only about 30%-40% compared to the 5-year overall survival rate of over 80% for primary liver transplantation (*86,87*). Management of metastatic lung lesions with the same chemotherapeutic and aggressive surgical approach does not achieve similar results as in intrahepatic recurrences. In the SIOPEL series, a

second remission could be achieved by resection in 15 of 27 patients with pulmonary recurrence (*85*). Shi *et al* reported the surgical experience of 10 patients with pulmonary recurrence, one of whom had bilateral pulmonary metastases. eight were effectively treated by pulmonary metastasectomy for long-term survival (*81*). Multiple thoracotomies can be repeated as needed to remove pulmonary recurrences to prolong disease-free interval. However, its value in prolonging long-term overall survival remains to be demonstrated. For patients with recurrent hepatoblastoma after initial liver transplantation, re-hepatectomy is still an effective treatment. Liu *et al* reported that 18 patients with recurrent hepatoblastoma after liver transplantation underwent hepatic resection and significant prolonged survival time was observed (*88*).

4. Outlook

The efforts of international collaborations have led to significant advances in the treatment of hepatoblastoma, with significant increases in cure rates and long-term survival for children. However, there are still issues to be addressed.

As hepatoblastoma is a relatively rare type of tumor, the etiology of hepatoblastoma still needs to be further investigated. Although several studies have suggested that low birth weight and tobacco intake during pregnancy are risk factors for the development of hepatoblastoma (*89*). However, no epidemiological models have been successfully constructed to guide the primary prevention of hepatoblastoma. With unprecedented close collaboration and information sharing among international clinical research groups on hepatoblastoma, it is expected that future research on the etiological mechanisms of hepatoblastoma will be deepened and a preventive mechanism for the disease will be constructed from an etiological perspective.

In addition, despite promising improvements in survival rates for children with hepatoblastoma due to advances in chemotherapy and surgical techniques, there are still some children who are not sensitive to conventional chemotherapy regimens or whose tumors have recurred and metastasized after surgery. In the treatment of hepatocellular carcinoma, targeted combination immunotherapy regimens have shown significant efficacy and may also be useful in subsequent clinical trials for the treatment of recurrent or refractory hepatoblastoma (*90*). Small clinical trials have found that sorafenib (SFN) and irinotecan (CPT-11) resulted in remission in approximately 80% of patients with relapsed/refractory HB, and the combination of the two drugs still holds promise for partial response (PR) in patients with single agent resistance (*91*). Some phase I studies by the COG have shown the effectiveness of Aurora kinase inhibitors and the multi-receptor tyrosine kinase inhibitor pazopanib in HB (*92*). In immunotherapy, case reports have shown that immunotherapy with pabolizumab controlled HB disease progression for up to 22 months (*93*). Studies on the efficacy of GPC3, CAR-T cells for AFP or the humanized antibody codrituzumab in HB are ongoing (*92*). The limited inhibitory effect of anti-PD-1 monoclonal antibodies on HB may be related to the low mutational load of the tumor, and further studies are needed to determine whether the prognosis of HB can be improved by mutation screening or in combination with conventional chemotherapy (*93*).

5. Conclusion

Advances in diagnostic techniques and treatment options have led to survival benefits for children with hepatoblastoma. In light of the advancements in imaging technology, the diagnosis, preoperative assessment, and staging of hepatoblastoma have become more accessible, thus facilitating treatment modalities and surgical strategizing. New chemotherapy regimens are increasingly looking at ways to reduce the side effects of chemotherapy in addition to seeking higher rates of disease remission. Meanwhile, advances in surgical techniques have expanded surgical indications to further achieve a better survival benefit.

Funding: This work was supported by the Young Elite Scientists Sponsorship Program by CAST, No. 2022QNRC001.

Conflict of Interest: The authors have no conflicts of interest to disclose.

References

1. Aronson DC, Meyers RL. Malignant tumors of the liver in children. Semin Pediatr Surg. 2016; 25:265-275.
2. Feng J, Polychronidis G, Heger U, Frongia G, Mehrabi A, Hoffmann K. Incidence trends and survival prediction of hepatoblastoma in children: a population-based study. Cancer Commun (Lond). 2019; 39:62.
3. Towbin AJ, Meyers RL, Woodley H, Miyazaki O, Weldon CB, Morland B, Hiyama E, Czauderna P, Roebuck DJ, Tiao GM. 2017 PRETEXT: radiologic staging system for primary hepatic malignancies of childhood revised for the Paediatric Hepatic International Tumour Trial (PHITT). Pediatr Radiol. 2018; 48:536-554.
4. Schooler GR, Squires JH, Alazraki A, Chavhan GB, Chernyak V, Davis JT, Khanna G, Krishnamurthy R, Lungren MP, Masand PM, Podberesky DJ, Sirlin CB, Towbin AJ. Pediatric Hepatoblastoma, Hepatocellular Carcinoma, and Other Hepatic Neoplasms: Consensus Imaging Recommendations from American College of Radiology Pediatric Liver Reporting and Data System (LI-RADS) Working Group. Radiology. 2020; 296:493-497.
5. Yang T, Whitlock RS, Vasudevan SA. Surgical Management of Hepatoblastoma and Recent Advances. Cancers (Basel). 2019; 11:1944.
6. Lim IIP, Bondoc AJ, Geller JI, Tiao GM. Hepatoblastoma-

The Evolution of Biology, Surgery, and Transplantation. Children (Basel). 2018; 6:1.
7. Haberle B, Maxwell R, Schweinitz DV, Schmid I. High Dose Chemotherapy with Autologous Stem Cell Transplantation in Hepatoblastoma does not Improve Outcome. Results of the GPOH Study HB99. Klin Padiatr. 2019; 231:283-290.
8. Katzenstein HM, Langham MR, Malogolowkin MH, *et al*. Minimal adjuvant chemotherapy for children with hepatoblastoma resected at diagnosis (AHEP0731): a Children's Oncology Group, multicentre, phase 3 trial. Lancet Oncol. 2019; 20:719-727.
9. Hiyama E, Hishiki T, Watanabe K, *et al*. Outcome and Late Complications of Hepatoblastomas Treated Using the Japanese Study Group for Pediatric Liver Tumor 2 Protocol. J Clin Oncol. 2020; 38:2488-2498.
10. Weldon CB, Madenci AL, Tiao GM, *et al*. Evaluation of the diagnostic biopsy approach for children with hepatoblastoma: A report from the children's oncology group AHEP 0731 liver tumor committee. J Pediatr Surg. 2020; 55:655-659.
11. Katzenstein HM, Malogolowkin MH, Krailo MD, *et al*. Doxorubicin in combination with cisplatin, 5-flourouracil, and vincristine is feasible and effective in unresectable hepatoblastoma: A Children's Oncology Group study. Cancer. 2022; 128:1057-1065.
12. Maki H, Hasegawa K. Advances in the surgical treatment of liver cancer. Biosci Trends. 2022; 16:178-188.
13. Zsiros J, Maibach R, Shafford E, *et al*. Successful treatment of childhood high-risk hepatoblastoma with dose-intensive multiagent chemotherapy and surgery: final results of the SIOPEL-3HR study. J Clin Oncol. 2010; 28:2584-2590.
14. Czauderna P, Lopez-Terrada D, Hiyama E, Haberle B, Malogolowkin MH, Meyers RL. Hepatoblastoma state of the art: pathology, genetics, risk stratification, and chemotherapy. Curr Opin Pediatr. 2014; 26:19-28.
15. hepatoblastoma. CaEEGfGftdato. Guidelines for the diagnosis and treatment of hepatoblastoma. J Clin Hepatol. 2019; 35:2431-2434.
16. Perilongo G, Shafford E, Plaschkes J, Liver Tumour Study Group of the International Society of Paediatric O. SIOPEL trials using preoperative chemotherapy in hepatoblastoma. Lancet Oncol. 2000; 1:94-100.
17. Liao X, Jiang S, Yang J. Feasibility of the neoadjuvant chemotherapy for children with hepatoblastoma diagnosed by serum alpha-fetoprotein. Lin Chuang Er Ke Za Zhi. 2021; 39:596-599.
18. Meyers RL, Maibach R, Hiyama E, *et al*. Risk-stratified staging in paediatric hepatoblastoma: a unified analysis from the Children's Hepatic tumors International Collaboration. Lancet Oncol. 2017; 18:122-131.
19. McCarville MB, Roebuck DJ. Diagnosis and staging of hepatoblastoma: imaging aspects. Pediatr Blood Cancer. 2012; 59:793-799.
20. Ohtsuka Y, Takahashi H, Ohnuma N, Tanabe M, Yoshida H, Iwai J. Detection of tumor thrombus in children using color Doppler ultrasonography. J Pediatr Surg. 1997; 32:1507-1510.
21. Baheti AD, Chapman T, Rudzinski E, Albert CM, Stanescu AL. Diagnosis, histopathologic correlation and management of hepatoblastoma: What the radiologist needs to know. Clin Imaging. 2018; 52:273-279.
22. Zsiros J, Brugieres L, Brock P, *et al*. Dose-dense cisplatin-based chemotherapy and surgery for children with high-risk hepatoblastoma (SIOPEL-4): A prospective, single-arm, feasibility study. Lancet Oncol. 2013; 14:834-842.
23. Cai HY, Yu B, Feng ZC, Qi X, Wei XJ. Clinical significance of CD44 expression in children with hepatoblastoma. Genet Mol Res. 2015; 14:13203-13207.
24. Bahnassy AA, Fawzy M, El-Wakil M, Zekri AR, Abdel-Sayed A, Sheta M. Aberrant expression of cancer stem cell markers (CD44, CD90, and CD133) contributes to disease progression and reduced survival in hepatoblastoma patients: 4-year survival data. Transl Res. 2015; 165:396-406.
25. Grant CN, Rhee D, Tracy ET, Aldrink JH, Baertschiger RM, Lautz TB, Glick RD, Rodeberg DA, Ehrlich PF, Christison-Lagay E. Pediatric solid tumors and associated cancer predisposition syndromes: Workup, management, and surveillance. A summary from the APSA Cancer Committee. J Pediatr Surg. 2022; 57:430-442.
26. Aronson DC, Schnater JM, Staalman CR, Weverling GJ, Plaschkes J, Perilongo G, Brown J, Phillips A, Otte JB, Czauderna P, MacKinlay G, Vos A. Predictive value of the pretreatment extent of disease system in hepatoblastoma: results from the International Society of Pediatric Oncology Liver Tumor Study Group SIOPEL-1 study. J Clin Oncol. 2005; 23:1245-1252.
27. Brown J, Perilongo G, Shafford E, Keeling J, Pritchard J, Brock P, Dicks-Mireaux C, Phillips A, Vos A, Plaschkes J. Pretreatment prognostic factors for children with hepatoblastoma-- results from the International Society of Paediatric Oncology (SIOP) study SIOPEL 1. Eur J Cancer. 2000; 36:1418-1425.
28. Perilongo G, Shafford E, Maibach R, *et al*. Risk-adapted treatment for childhood hepatoblastoma. final report of the second study of the International Society of Paediatric Oncology--SIOPEL 2. Eur J Cancer. 2004; 40:411-421.
29. Pritchard J, Brown J, Shafford E, Perilongo G, Brock P, Dicks-Mireaux C, Keeling J, Phillips A, Vos A, Plaschkes J. Cisplatin, doxorubicin, and delayed surgery for childhood hepatoblastoma: a successful approach--results of the first prospective study of the International Society of Pediatric Oncology. J Clin Oncol. 2000; 18:3819-3828.
30. Douglass EC, Green AA, Wrenn E, Champion J, Shipp M, Pratt CB. Effective cisplatin (DDP) based chemotherapy in the treatment of hepatoblastoma. Med Pediatr Oncol. 1985; 13:187-190.
31. Quinn JJ, Altman AJ, Robinson HT, Cooke RW, Hight DW, Foster JH. Adriamycin and cisplatin for hepatoblastoma. Cancer. 1985; 56:1926-1929.
32. Malogolowkin MH, Katzenstein H, Krailo MD, Chen Z, Bowman L, Reynolds M, Finegold M, Greffe B, Rowland J, Newman K, Womer RB, London WB, Castleberry RP. Intensified platinum therapy is an ineffective strategy for improving outcome in pediatric patients with advanced hepatoblastoma. J Clin Oncol. 2006; 24:2879-2884.
33. Fuchs J, Rydzynski J, Von Schweinitz D, Bode U, Hecker H, Weinel P, Burger D, Harms D, Erttmann R, Oldhafer K, Mildenberger H, Study Committee of the Cooperative Pediatric Liver Tumor Study Hb 94 for the German Society for Pediatric O, Hematology. Pretreatment prognostic factors and treatment results in children with hepatoblastoma: a report from the German Cooperative Pediatric Liver Tumor Study HB 94. Cancer. 2002; 95:172-182.
34. Perilongo G, Maibach R, Shafford E, *et al*. Cisplatin versus cisplatin plus doxorubicin for standard-risk hepatoblastoma. N Engl J Med. 2009; 361:1662-1670.

35. Ortega JA, Douglass EC, Feusner JH, Reynolds M, Quinn JJ, Finegold MJ, Haas JE, King DR, Liu-Mares W, Sensel MG, Krailo MD. Randomized comparison of cisplatin/vincristine/fluorouracil and cisplatin/continuous infusion doxorubicin for treatment of pediatric hepatoblastoma: A report from the Children's Cancer Group and the Pediatric Oncology Group. J Clin Oncol. 2000; 18:2665-2675.
36. Douglass EC, Reynolds M, Finegold M, Cantor AB, Glicksman A. Cisplatin, vincristine, and fluorouracil therapy for hepatoblastoma: A Pediatric Oncology Group study. J Clin Oncol. 1993; 11:96-99.
37. Katzenstein HM, Furman WL, Malogolowkin MH, Krailo MD, McCarville MB, Towbin AJ, Tiao GM, Finegold MJ, Ranganathan S, Dunn SP, Langham MR, McGahren ED, Rodriguez-Galindo C, Meyers RL. Upfront window vincristine/irinotecan treatment of high-risk hepatoblastoma: A report from the Children's Oncology Group AHEP0731 study committee. Cancer. 2017; 123:2360-2367.
38. von Schweinitz D, Burger D, Bode U, Weinel P, Erttmann R, Hecker H, Mildenberger H. Results of the HB-89 Study in treatment of malignant epithelial liver tumors in childhood and concept of a new HB-94 protocol. Klin Padiatr. 1994; 206:282-288. (in German)
39. von Schweinitz D, Burger D, Mildenberger H. Is laparatomy the first step in treatment of childhood liver tumors?--The experience from the German Cooperative Pediatric Liver Tumor Study HB-89. Eur J Pediatr Surg. 1994; 4:82-86.
40. Haberle B, Bode U, von Schweinitz D. [Differentiated treatment protocols for high- and standard-risk hepatoblastoma--an interim report of the German Liver Tumor Study HB99]. Klin Padiatr. 2003; 215:159-165.
41. Sasaki F, Matsunaga T, Iwafuchi M, *et al*. Outcome of hepatoblastoma treated with the JPLT-1 (Japanese Study Group for Pediatric Liver Tumor) Protocol-1: A report from the Japanese Study Group for Pediatric Liver Tumor. J Pediatr Surg. 2002; 37:851-856.
42. Watanabe K, Mori M, Hishiki T, *et al*. Feasibility of dose-dense cisplatin-based chemotherapy in Japanese children with high-risk hepatoblastoma: Analysis of the JPLT3-H pilot study. Pediatr Blood Cancer. 2022; 69:e29389.
43. Brock PR, Maibach R, Childs M, *et al*. Sodium Thiosulfate for Protection from Cisplatin-Induced Hearing Loss. N Engl J Med. 2018; 378:2376-2385.
44. Freyer DR, Chen L, Krailo MD, Knight K, Villaluna D, Bliss B, Pollock BH, Ramdas J, Lange B, Van Hoff D, VanSoelen ML, Wiernikowski J, Neuwelt EA, Sung L. Effects of sodium thiosulfate versus observation on development of cisplatin-induced hearing loss in children with cancer (ACCL0431): A multicentre, randomised, controlled, open-label, phase 3 trial. Lancet Oncol. 2017; 18:63-74.
45. Tang Q, Wang X, Jin H, Mi Y, Liu L, Dong M, Chen Y, Zou Z. Cisplatin-induced ototoxicity: Updates on molecular mechanisms and otoprotective strategies. Eur J Pharm Biopharm. 2021; 163:60-71.
46. Sawicki KT, Sala V, Prever L, Hirsch E, Ardehali H, Ghigo A. Preventing and Treating Anthracycline Cardiotoxicity: New Insights. Annu Rev Pharmacol Toxicol. 2021; 61:309-332.
47. Stoddard MF, Seeger J, Liddell NE, Hadley TJ, Sullivan DM, Kupersmith J. Prolongation of isovolumetric relaxation time as assessed by Doppler echocardiography predicts doxorubicin-induced systolic dysfunction in humans. J Am Coll Cardiol. 1992; 20:62-69.
48. Malogolowkin MH, Katzenstein HM, Meyers RL, Krailo MD, Rowland JM, Haas J, Finegold MJ. Complete surgical resection is curative for children with hepatoblastoma with pure fetal histology: a report from the Children's Oncology Group. J Clin Oncol. 2011; 29:3301-3306.
49. Hafberg E, Borinstein SC, Alexopoulos SP. Contemporary management of hepatoblastoma. Curr Opin Organ Transplant. 2019; 24:113-117.
50. Molmenti EP, Wilkinson K, Molmenti H, *et al*. Treatment of unresectable hepatoblastoma with liver transplantation in the pediatric population. Am J Transplant. 2002; 2:535-538.
51. Guerin F, Gauthier F, Martelli H, Fabre M, Baujard C, Franchi S, Branchereau S. Outcome of central hepatectomy for hepatoblastomas. J Pediatr Surg. 2010; 45:555-563.
52. Kim EF, Shatalov KV, Filin AV, Arnautova IV, Galyan TN, Tarba NS, Kachanov DY, Varfolomeyeva SR. [Surgical treatment of hepatoblastoma PRETEXT/POST-TEXT III and IV]. Khirurgiia (Mosk). 2017;70-74.
53. Ishizawa T, Saiura A, Kokudo N. Clinical application of indocyanine green-fluorescence imaging during hepatectomy. Hepatobiliary Surg Nutr. 2016; 5:322-328.
54. Souzaki R, Kawakubo N, Matsuura T, Yoshimaru K, Koga Y, Takemoto J, Shibui Y, Kohashi K, Hayashida M, Oda Y, Ohga S, Taguchi T. Navigation surgery using indocyanine green fluorescent imaging for hepatoblastoma patients. Pediatr Surg Int. 2019; 35:551-557.
55. Yamamichi T, Oue T, Yonekura T, Owari M, Nakahata K, Umeda S, Nara K, Ueno T, Uehara S, Usui N. Clinical application of indocyanine green (ICG) fluorescent imaging of hepatoblastoma. J Pediatr Surg. 2015; 50:833-836.
56. Nakaseko Y, Ishizawa T, Saiura A. Fluorescence-guided surgery for liver tumors. J Surg Oncol. 2018; 118:324-331.
57. Yamada Y, Ohno M, Fujino A, *et al*. Fluorescence-Guided Surgery for Hepatoblastoma with Indocyanine Green. Cancers (Basel). 2019; 11(8):1215.
58. Hiyama E, Hishiki T, Watanabe K, Ida K, Yano M, Oue T, Iehara T, Hoshino K, Koh K, Tanaka Y, Kurihara S, Ueda Y, Onitake Y. Resectability and tumor response after preoperative chemotherapy in hepatoblastoma treated by the Japanese Study Group for Pediatric Liver Tumor (JPLT)-2 protocol. J Pediatr Surg. 2016; 51:2053-2057.
59. Aronson DC, Weeda VB, Maibach R, *et al*. Microscopically positive resection margin after hepatoblastoma resection: what is the impact on prognosis? A Childhood Liver Tumours Strategy Group (SIOPEL) report. Eur J Cancer. 2019; 106:126-132.
60. Ren X, Li H, Diao M, Xu H, Li L. Impact of microscopically margin-positive resection on survival in children with hepatoblastoma after hepatectomy: a retrospective cohort study. Int J Clin Oncol. 2020; 25:765-773.
61. El-Gendi A, Fadel S, El-Shafei M, Shawky A. Avoiding liver transplantation in post-treatment extent of disease III and IV hepatoblastoma. Pediatr Int. 2018; 60:862-868.
62. Shi SJ, Wang DL, Hu W, Peng F, Kang Q. Ex vivo liver resection and autotransplantation with cardiopulmonary bypass for hepatoblastoma in children: A case report. Pediatr Transplant. 2018; 22:e13268.
63. Boster JM, Superina R, Mazariegos GV, *et al*. Predictors

of survival following liver transplantation for pediatric hepatoblastoma and hepatocellular carcinoma: Experience from the Society of Pediatric Liver Transplantation (SPLIT). Am J Transplant. 2022; 22:1396-1408.
64. Moosburner S, Schmelzle M, Schoning W, Kastner A, Seika P, Globke B, Dziodzio T, Pratschke J, Ollinger R, Gul-Klein S. Liver Transplantation Is Highly Effective in Children with Irresectable Hepatoblastoma. Medicina (Kaunas). 2021; 57 (8):819.
65. Hibi T, Rela M, Eason JD, Line PD, Fung J, Sakamoto S, Selzner N, Man K, Ghobrial RM, Sapisochin G. Liver Transplantation for Colorectal and Neuroendocrine Liver Metastases and Hepatoblastoma. Working Group Report From the ILTS Transplant Oncology Consensus Conference. Transplantation. 2020; 104:1131-1135.
66. McAteer JP, Goldin AB, Healey PJ, Gow KW. Surgical treatment of primary liver tumors in children: outcomes analysis of resection and transplantation in the SEER database. Pediatr Transplant. 2013; 17:744-750.
67. Wang S, Yang C, Zhang J, Kong XR, Zhu H, Wu F, Wang Z. First experience of high-intensity focused ultrasound combined with transcatheter arterial embolization as local control for hepatoblastoma. Hepatology. 2014; 59:170-177.
68. Hirakawa M, Nishie A, Asayama Y, Fujita N, Ishigami K, Tajiri T, Taguchi T, Honda H. Efficacy of preoperative transcatheter arterial chemoembolization combined with systemic chemotherapy for treatment of unresectable hepatoblastoma in children. Jpn J Radiol. 2014; 32:529-536.
69. Jiang Y, Zhou S, Shen G, Jiang H, Zhang J. Microwave ablation combined with transcatheter arterial chemoembolization is effective for treating unresectable hepatoblastoma in infants and children. Medicine (Baltimore). 2018; 97:e12607.
70. Tang X, He X, Jiang H. Efficacy and safety of HIFU in combination with TACE in unresectable pediatric HB: A randomized, controlled, single-center clinical trial. Medicine (Baltimore). 2022; 101:e32022.
71. Chan A, Chung PH, Poon RT. Little girl who conquered the "ALPPS". World J Gastroenterol. 2014; 20:10208-10211.
72. Hong JC, Kim J, Browning M, Wagner A, Lerret S, Segura AD, Zimmerman MA. Modified Associating Liver Partition and Portal Vein Ligation for Staged Hepatectomy for Hepatoblastoma in a Small Infant: How Far Can We Push the Envelope? Ann Surg. 2017; 266:e16-e17.
73. Wiederkehr JC, Avilla SG, Mattos E, Coelho IM, Ledesma JA, Conceicao AF, Wiederkehr HA, Wiederkehr BA. Associating liver partition with portal vein ligation and staged hepatectomy (ALPPS) for the treatment of liver tumors in children. J Pediatr Surg. 2015; 50:1227-1231.
74. Qazi AQ, Syed AA, Khan AW, Hanif F. Early multifocal recurrence of hepatoblastoma in the residual liver after R0 liver resection with ALPPS procedure: a case report. Ann Transl Med. 2016; 4:375.
75. Meyers RL, Katzenstein HM, Krailo M, McGahren ED, 3rd, Malogolowkin MH. Surgical resection of pulmonary metastatic lesions in children with hepatoblastoma. J Pediatr Surg. 2007; 42:2050-2056.
76. Wanaguru D, Shun A, Price N, Karpelowsky J. Outcomes of pulmonary metastases in hepatoblastoma--is the prognosis always poor? J Pediatr Surg. 2013; 48:2474-2478.
77. Hishiki T, Watanabe K, Ida K, *et al*. The role of pulmonary metastasectomy for hepatoblastoma in children with metastasis at diagnosis: Results from the JPLT-2 study. J Pediatr Surg. 2017; 52:2051-2055.
78. Angelico R, Grimaldi C, Gazia C, Saffioti MC, Manzia TM, Castellano A, Spada M. How Do Synchronous Lung Metastases Influence the Surgical Management of Children with Hepatoblastoma? An Update and Systematic Review of the Literature. Cancers (Basel). 2019; 11:1693.
79. Kitagawa N, Shinkai M, Mochizuki K, Usui H, Miyagi H, Nakamura K, Tanaka M, Tanaka Y, Kusano M, Ohtsubo S. Navigation using indocyanine green fluorescence imaging for hepatoblastoma pulmonary metastases surgery. Pediatr Surg Int. 2015; 31:407-411.
80. Matsunaga T, Sasaki F, Ohira M, Hashizume K, Hayashi A, Hayashi Y, Mugishima H, Ohnuma N, Japanese Study Group for Pediatric Liver T. Analysis of treatment outcome for children with recurrent or metastatic hepatoblastoma. Pediatr Surg Int. 2003; 19:142-146.
81. Shi Y, Geller JI, Ma IT, Chavan RS, Masand PM, Towbin AJ, Chintagumpala M, Nuchtern JG, Tiao GM, Thompson PA, Vasudevan SA. Relapsed hepatoblastoma confined to the lung is effectively treated with pulmonary metastasectomy. J Pediatr Surg. 2016; 51:525-529.
82. Hacker FM, von Schweinitz D, Gambazzi F. The relevance of surgical therapy for bilateral and/or multiple pulmonary metastases in children. Eur J Pediatr Surg. 2007; 17:84-89.
83. Fuchs J, Seitz G, Handgretinger R, Schafer J, Warmann SW. Surgical treatment of lung metastases in patients with embryonal pediatric solid tumors: an update. Semin Pediatr Surg. 2012; 21:79-87.
84. Dunn CL, Lucas JT, Jr., Clark H, McLean TW. Successful Radiofrequency Ablation for Recurrent Pulmonary Hepatoblastoma. Pediatr Blood Cancer. 2015; 62:2242.
85. Semeraro M, Branchereau S, Maibach R, *et al*. Relapses in hepatoblastoma patients: clinical characteristics and outcome--experience of the International Childhood Liver Tumour Strategy Group (SIOPEL). Eur J Cancer. 2013; 49:915-922.
86. Otte JB, Pritchard J, Aronson DC, Brown J, Czauderna P, Maibach R, Perilongo G, Shafford E, Plaschkes J, International Society of Pediatric O. Liver transplantation for hepatoblastoma: results from the International Society of Pediatric Oncology (SIOP) study SIOPEL-1 and review of the world experience. Pediatr Blood Cancer. 2004; 42:74-83.
87. Trobaugh-Lotrario AD, Meyers RL, Tiao GM, Feusner JH. Pediatric liver transplantation for hepatoblastoma. Transl Gastroenterol Hepatol. 2016; 1:44.
88. Li X, Wang Z, Zhang D, Zhao D, Ye J, Duan W, Duan L, Liu Q. Repeat hepatectomy for pediatric recurrent chemotherapy-resistant hepatoblastoma: a report of 18 cases. J Cancer Res Clin Oncol. 2022; 149(7):4015-4023.
89. Spector LG, Birch J. The epidemiology of hepatoblastoma. Pediatr Blood Cancer. 2012; 59:776-779.
90. Tang H, Cao Y, Jian Y, Li X, Li J, Zhang W, Wan T, Liu Z, Tang W, Lu S. Conversion therapy with an immune checkpoint inhibitor and an antiangiogenic drug for advanced hepatocellular carcinoma: A review. Biosci Trends. 2022; 16:130-141.
91. Keino D, Yokosuka T, Hirose A, *et al*. Pilot study of the combination of sorafenib and fractionated irinotecan in pediatric relapse/refractory hepatic cancer (FINEX pilot study). Pediatr Blood Cancer. 2020; 67:e28655.

92. Wu PV, Rangaswami A. Current Approaches in Hepatoblastoma-New Biological Insights to Inform Therapy. Curr Oncol Rep. 2022; 24:1209-1218.
93. Tsai HL, Yeh YC, Yu TY, Lee CY, Hung GY, Yeh YT, Liu CS, Yen HJ. Complete and durable response to immune checkpoint inhibitor in a patient with refractory and metastatic hepatoblastoma. Pediatr Hematol Oncol. 2021; 38:385-390.

Received December 6, 2023; Revised December 20, 2023; Accepted December 21, 2023.

[§]These authors contributed equally to this work.
**Address correspondence to:*
Haowen Tang, Faculty of Hepato-Pancreato-Biliary Surgery, Chinese PLA General Hospital, Beijing, China.
E-mail: haowen_tang@163.com

Released online in J-STAGE as advance publication December 23, 2023.

Review

DOI: 10.5582/bst.2023.01133

The effect of the female genital tract and gut microbiome on reproductive dysfunction

Wenli Cao[1,§], Xiayan Fu[1,§], Jing Zhou[2,3,4], Qing Qi[2,3,4], Feijun Ye[1], Lisha Li[2,3,4,*], Ling Wang[2,3,4,*]

[1] Reproductive Medicine Center, Zhoushan Maternal and Child Health Care Hospital, Zhoushan, Zhejiang, China;
[2] Laboratory for Reproductive Immunology, Obstetrics and Gynecology Hospital of Fudan University, Shanghai, China;
[3] The Academy of Integrative Medicine, Fudan University, Shanghai, China;
[4] Shanghai Key Laboratory of Female Reproductive Endocrine-related Diseases, Shanghai, China.

SUMMARY Microorganisms are ubiquitous in the human body; they are present in various areas including the gut, mouth, skin, respiratory tract, and reproductive tract. The interaction between the microbiome and reproductive health has become an increasingly compelling area of study. Disruption of the female genital tract microbiome can significantly impact the metabolism of amino acids, carbohydrates, and lipids, increasing susceptibility to reproductive tract diseases such as vaginitis, chronic endometritis, endometrial polyps, endometriosis, and polycystic ovary syndrome. The gut microbiome, considered an endocrine organ, plays a crucial role in the reproductive endocrine system by interacting with hormones like estrogen and androgens. Imbalances in the gut microbiome composition can lead to various diseases and conditions, including polycystic ovary syndrome, endometriosis, and cancer, although research on their mechanisms remains limited. This review highlights the latest advancements in understanding the female genital tract and gut microbiomes in gynecological diseases. It also explores the potential of microbial communities in the treatment of reproductive diseases. Future research should focus on identifying the molecular mechanisms underlying the association between the microbiome and reproductive diseases to develop new and effective strategies for disease prevention, diagnosis, and treatment related to female reproductive organs.

Keywords microbiome, female genital tract, gut, reproductive disease, dysbiosis

1. Introduction

In recent decades, a focus of research in public health and translational medicine has been the human microbiome. Billions of microorganisms, including bacteria, archaea, fungi, and viruses, colonize the human body, affecting various aspects of human health such as growth, digestion, nutrient absorption, immune regulation, and metabolism (*1,2*). Imbalances in human microorganisms have been linked to diseases including dental caries, malnutrition, gastrointestinal ulcers, diabetes, cancer, depression, allergic asthma, and autoimmune diseases (*3*). Over the past two decades, the human microbiome has become a focus of research in public health and translational medicine. With advances in next-generation sequencing technology and related bioinformatic tools, the US and Europe conducted the Human Microbiome Project (HMP) and the Human Intestinal Tract (MetaHIT). These two large-scale human microbiome-related studies have brought about major advances in the entire field.

The intestinal and female genital tract (FGT) harbor stable microbial communities. The FGT, encompassing the vagina, cervix, endometrium, fallopian tubes, and ovaries, possesses a distinct microbiome, constituting around 9% of the total bacterial count in women (*4*). However, the FGT is not static, but rather a dynamically balanced ecosystem affected by factors including age, lifestyle, hormone levels, and environmental influences (*5*). The human symbiotic microbiota, exemplified by the gut microbiota, is often referred to as the "second genome" of the human body and is closely connected to female reproductive diseases. The gut microbiome is considered an extended endocrine organ, crucial in the reproductive endocrine system, interacting with hormones like estrogen and androgens throughout a woman's life (*6*). Disruptions to this microbiome, such as through epigenetic modifications, nervous system changes, and metabolic imbalances, can interfere with zygote formation, hinder embryo implantation and development, and increase susceptibility to diseases (*7*), significantly impairing reproductive capacity and pregnancy. Imbalances in the FGT and gut microbiome

composition can lead to the onset of reproductive-related diseases, including vaginitis, polycystic ovary syndrome (PCOS), endometriosis (EMs), chronic endometritis (CE), and endometrial polyps (EPs) (*8,9*).

This review delves into the interaction between the FGT and gut microbiome. It also examines the link between microbiome imbalance and reproductive diseases, emphasizing potential pathogenesis and therapeutic applications.

2. Characteristics of female microbiome

2.1. Female reproductive tract microbiome

The FGT consists of the upper genital tract (UGT), consisting of the fallopian tubes, ovaries, uterus, and endocervix, and the lower genital tract (LGT), consisting of the ectocervix and vagina. The use of high-throughput sequencing technology has provided deeper insights into the distribution of the FGT microbiome. In comparison to the LGT, the UGT exhibits lower bacterial density but higher diversity. Both domestic and international studies have indicated that the colonization of bacterial communities in the lower third of the vagina, posterior fornix, cervix, uterine cavity, fallopian tubes, and peritoneum in women of childbearing age undergoes continuous changes. Samples taken from various parts of the vagina and cervix have shown low species diversity, with *Lactobacillus* dominating (*10*). However, the FGT is highly dynamic and influenced by factors such as age, lifestyle, hormone levels, and the menstrual cycle (Figure 1).

2.1.1. Vaginal-cervical microbiome

The composition of the vaginal microbiome is closely related to reproductive health. In 2011, Ravel *et al.* (*11*) used 16srRNA sequencing technology to classify the community status types (CST) in the vagina of healthy women into five types based on the dominant species and pH level of *Lactobacillus*. CST-I, CST-II, CST-III, and CST-V involve the dominant species *Lactobacillus crispatus* (26.2%), *L. gasseri* (6.3%), *L. iners* (34.1%) and *L. jensenii* (5.3%), respectively. The abundance of *Lactobacillus* in CST-IV is low, while the abundance of specific anaerobic bacteria (*Dialister, Prevotella, Atopobium, Gardnerella,* and *Sneathia*) is high. A recent study based on a large sample dataset subsequently subdivided CST-IV into 7 subtypes, dominated by different non-lactobacilli species (*12*). This indicated that Streptococcus vaginalis may produce other end products of fermentation in the vagina and not just lactic acid as traditionally thought, and it may be related to elevated vaginal PH. Some studies have shown that CST-I tends to be the most stable, while CST-IV is prone to change. The vaginal microbiota dominated by *L. crispatus* is more likely to first transform into the vaginal microbiome dominated by *L. iners* or mixed Lactobacillus, rather than directly transitioning to complete dysregulation of the microbiome (*13,14*). Vaginal microorganisms interact with each other and are regulated by the host organism, which in turn regulates the host's local immune function. Some microorganisms interact with the host genome to maintain a relatively independent ecological environment (*15*). The female vaginal microbiome is dynamically changing due to multiple factors. At present, menstruation is generally believed to lead to changes in certain CST types, but the change in individual microbial community types does not necessarily accompany an increase in bacterial diversity (*16*). Srinivasan *et al.* (*17*) reported that during menstruation, the abundance of *Gardnerella* and *L. iners* in the vagina increased in 81%

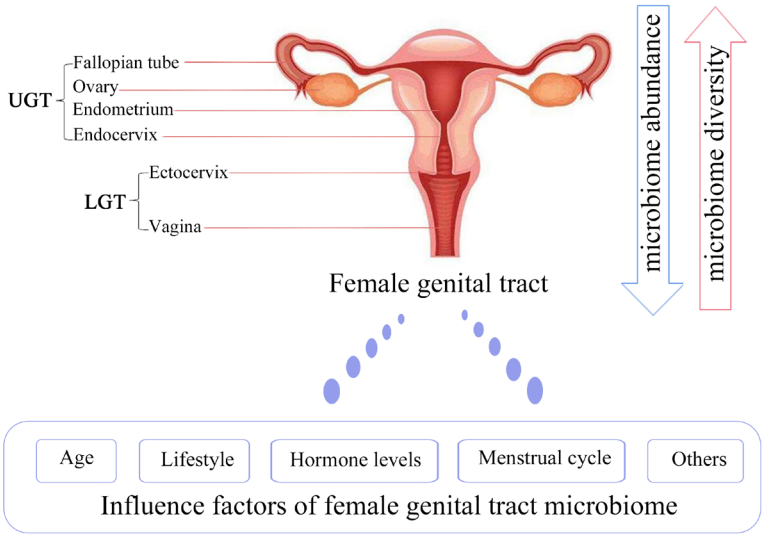

Figure 1. Female reproductive tract microbiome. The upper genital tract (UGT) consists of the fallopian tubes, ovaries, uterus, and endocervix, while the lower genital tract (LGT) consists of the ectocervix and vagina. Compared to the LGT, the UGT exhibits less bacterial density but higher diversity. The FGT can be influenced by various factors, including age, lifestyle, hormone levels, and the menstrual cycle.

of subjects, but the abundance of other *Lactobacillus* spp. decreased, and the microbiome gradually returned to a stable state before menstruation. Although the altered CST pattern has been described during menstruation, its relationship to reproductive health has not been fully determined. Gajer *et al*. (*18*) monitored the dynamic changes in the vaginal microbiome in 32 healthy women and they found that CST-I and CST-II are relatively stable and that the transformation of these two types is usually related to menstruation - the transition to CST-III dominated by *L. iners* during menstruation, which quickly returns to its original state after menstruation. The normal vaginal microbiome can prevent urogenital tract diseases (such as vaginitis, pelvic inflammatory disease, sexually transmitted diseases, and urinary tract infections) by sticking to the vaginal epithelium, preventing the invasion of pathogenic microorganisms, producing H_2O_2, bacteriocin and biosurfactants to maintain the acidic environment in the vagina and other mechanisms (Table 1).

In women of childbearing age, the composition of the cervical microbiome is usually similar to that of the vaginal microbiome (*25*). Punzón-Jiménez *et al.* (*9*) found that *Lactobacilli* accounted for 97.56% of cervical mucus according to qPCR detection, with *L. iners* and *L. crispatus* being the most abundant species. Pelzer *et al*. (*26*) reported that the highest content detected in cervical specimens is *Lactobacillus* spp., followed by *Gardnerella* spp., *Veillonella* spp., *Prevotella* spp., *Sneathia* spp., or *Fusobacterium* spp. In recent years, research on the cervical microbiome has mainly focused on its relationship to cervical cancer. The high diversity of species in the cervical microbiome and specific genera (such as *Gardnerella* spp.) are associated with the risk of human papilloma virus (HPV) infection in women (*27*). Persistent high-risk HPV infection increases the risk of cervical intraepithelial neoplasia (CIN) and even cervical cancer. Some taxa are associated with a vaginal microbiome imbalance, such as *Gardnerella*, *L. iners*, *Mycoplasma*, *Sneathia*, and *Fusobacterium*. These are reported to be risk factors for CIN and cervical cancer, inducing Toll like receptor 4 signaling, NF-κB activation and upregulation of pro-inflammatory cytokines (such as γ-interferon and IL-1), promoting the progression of cervical lesions by promoting inflammation and disrupting the cervical mucus barrier (*28-30*).

2.1.2. Endometrial microbiome

The endometrium plays a crucial role in female reproductive function. Despite the conventional belief that the uterus is a sterile environment, the endometrium has a unique microbial community (*31*). The bacterial load in the uterus is estimated to be 100 to 10,000 times less than that in the vaginal microbiome (*32*). Given the inertia but differences in the composition of endometrial and vaginal microbiota, the source of the endometrial microbiota is still controversial. Some researchers believe that microorganisms colonize the uterus through the vagina and cervix, but the vaginal microbiota is not a persistent source of endometrial microbiota and may be influenced by multiple factors (*33*). Another hypothesis suggests that uterine microbiota colonization involves multiple pathways such as gastrointestinal microbiota migration and blood transmission of respiratory and oral bacteria (*34*).

Thus far, most studies have reported that the uterine microbiota mainly consists of *Lactobacilli* (*35,36*). However, results of different studies in terms of the composition of the uterine microbiota are not consistent. Moreno *et al*. (*36*) found that *Lactobacillus* still accounts for the highest proportion (30.6%) in the endometrial microbiota and that there are also bacterial genera such as *Bifidobacterium*, *Gardnerella*, *Macrosporidium*, *Prevotella*, and *Streptococcus*. This is similar to the conclusions of Mitchell *et al*. (*37*), which found that the most common bacteria species in the uterine cavity were *L. iners*, and that *Gardnerella*, *Bacillus mirabilis*, and *L. plantarum* were detected in more than 40% of subjects. In contrast, Chen *et al*. (*38*) contends that the biomass of lactic acid bacteria is 1,000 times lower than that of the vagina and no longer dominates the endometrial environment, with *Pseudomonas* spp., *Acinetobacter* spp., *Vaginococcus* spp., and *Sphingobium* spp. being important components. Numerous studies have also shown that differences in the uterine microbiome may be related to different physiological or pathological states of the body. In 25 uterine samples from patients

Table 1. Types of vaginal microbiomes and the possible mechanisms by which they prevent reproductive and urinary diseases

CST	Vaginal PH	Dominant species	Role in reproductive diseases	References
I	4.0 ± 0.3	*L. crispatus*	Possible mechanisms for preventing reproductive and urinary diseases:	(*11,12,17*)
II	5.0	*L. gasseri*	Adhere to vaginal epithelium to prevent the invasion of pathogenic	(*12,17*)
III	4.4	*L. iners*	microorganisms	(*17-19*)
IV A	5.3 ± 0.6	*Gardnerella Atopotella*	Produce H_2O_2, bacteriocins, and biosurfactants to maintain an acidic environment in the vagina	(*20-22*)
		Campylobacter	Activates the NF- κB cascade	
IV B		*Atopobium Bifidobacteria*	Adhesins that promote epithelial colonization	
		Prevotella	Produce hemolysin to promote cytotoxicity	
V	4.4	*L. jensenii*		(*23,24*)

undergoing a hysterectomy for uterine fibroids, Winters *et al*. (*39*) found that the endometrial microbiome mainly consisted of *Acinetobacter*, *Clostridium*, *Pleuromonas*, and *Pseudomonas*.

2.1.3. Ovarian and fallopian tubal microbiome

The human ovaries and fallopian tubes are not always sterile and can be colonized by microorganisms (*30*). A study reported that 34.4% of women have microbial colonization in the follicular fluid (FF) (*40*). Previous studies have also reported that in infertile women, FF colonization rates range from 24% to 37%, with colonization rates of 40% and 32% in the left and right ovaries, respectively (*41*). Pelzer *et al*. (*42*) conducted a microbial culture of the FF obtained from 71 women undergoing sssisted reproductive technology (ART) during embryo retrieval and found microbial colonization in the FF, including *L. iners*, *Actinomyces* spp., *Corynebacterium aurimucosum*, *Fusobacterium* spp., *Peptoniphilus accharolyticus*, *Peptostreptococcus* spp., *Propionibacterium* spp., *Puccinia*, *Staphylococcus*, and *Candida parapsilosis*.

Pelzer *et al*. used a microbial culture and NGS technology to analyze 16 female fallopian tube samples and confirmed that there was microbial colonization in the female fallopian tubes mainly consisting of *Staphylococcus* spp., *Enterococcus* spp., and *Lactobacillus* (*43*). Other common bacteria include *Pseudomonas*, *Burkholderia* spp., and *Propionibacterium* spp.. The right fallopian tube mainly has *Staphylococcus*, and the left fallopian tube mainly has *Lactobacillus*, *Enterococcus*, and *Pasteurella* (*43*). In analyzing the microbial community of fallopian tubes in patients with chronic salpingitis, Wang *et al*. (*44*) found that samples with salpingitis fluid contained a more abundant microbial composition, while samples with salpingitis pus were more likely to exhibit a single dominant bacterium. A study on laparoscopic examinations of 26 patients with acute salpingitis showed that gonococci were isolated from the fallopian tubes of 19% of patients, and 38% of patients had aerobic and/or anaerobic bacteria present in the fallopian tubes (*45*). Understanding the composition of these microbial communities may help propose alternative treatment options for patients undergoing salpingectomy due to certain pathological conditions.

2.1.4. FGT microbiome throughout the entire lifecycle

The reproductive tract microbiome of an individual undergoes changes throughout its lifetime, and especially during infancy, and then changes again in old age. Due to the presence of microbial colonization in the uterine cavity, the maternal microbiome has been assumed to be the main contributor to provide microbial strains to newborns through vertical transmission (*46*). The vaginal microbiome of newborns born naturally is similar to that of the mother, but colonies of microorganisms are only temporary, and the infant continues to obtain microorganisms from different maternal sources after birth (*47*). Many studies on the transmission of maternal microbiota have focused on the gut, skin, or oral microbiota of newborns (*47,48*). Because the pH level of the infant's vagina is neutral or alkaline and there is a lack of *Lactobacilli*, any microorganisms that are transferred at birth cannot survive (*49*). Only in early adolescence do common species in the vaginal microbiome of women of childbearing age (such as *L. crispatus*, *L. iners*, and *Gardnerella*) dominate the vaginal microbiome (*50*). Throughout a woman's life, the vaginal microbiota is not always dominated by *Lactobacilli*. During childhood, anaerobic bacteria and *Escherichia coli* dominate. After puberty, the increase in estrogen leads to the production and accumulation of glycogen, allowing *Lactobacillus* to maintain a dominant position in women of reproductive age. During the perimenopausal period, the proportion of *Lactobacilli* decreases again due to the decrease in endogenous estrogen. The vaginal microbiome in the premenopausal and perimenopausal stages consists of *Firmicutes*, while the postmenopausal stage is dominated by *Aspergillus*, *Anaplasma*, and *Actinobacteria* (*51*). A cross-sectional study (*52*) involving 70 patients showed that in the vaginal microbiome of premenopausal women, *Lactobacilli* accounted for 71.98%, and non-optimal microbiome accounted for 16.87%, while in postmenopausal women those proportions were 10.08% and 26.78%, respectively. The proportion of lactic acid bacteria in postmenopausal women is significantly low, while microbial diversity and vaginal pH are significantly high. A study has shown that *Lactobacillus* levels and lower vaginal pH levels can be maintained in women who receive hormone replacement therapy during perimenopause (*4*). In addition to age and hormone levels, the composition of the vaginal microbiome is also influenced by various factors, such as race, gestational age, sexual activity, stress, and dietary factors. An epidemiological study has shown that the abundance of *Lactobacillus* is related to race; compared to African/Hispanic women, Caucasian/Asian women have higher levels of *Lactobacillus* (*19*). A cohort study showed that as the gestational age increased, the relative abundance of the thick-walled portal increased. In addition, a new microbiome (*Atopobium*, *Aerococcus*, *Gemella*, *Sneathia*, *Parvimonas*, *Gardnerella*, and *Megasphaera*) was observed in the vaginal microenvironment during early pregnancy. By mid-pregnancy, the number of this new vaginal microbiota has sharply decreased, replaced by abundant *Lactobacilli* (*53*).

Due to the limited availability of upper reproductive tract specimens from children and adolescent women, the microbial sources and differences between them and adult women are still unclear. There are differences in the microbiome colonizing the fallopian tubes of premenopausal women and postmenopausal women (*54*),

indicating that sex hormones may play a regulatory role in the microbiome colonization of the female UGT.

2.2. Gut microbiome

2.2.1. Overview of the gut microbiome

There are approximately 10^{14} bacterial colonies in the human gut, including over 1,000 species of bacteria, that can provide various benefits to the host, such as enhancing the immune system and supporting intestinal function (*55*). In addition, the gut microbiome regulates host metabolism through various pathways and it participates in the regulation of the female reproductive endocrine system. The gut microbiome is dominated by five bacterial phyla: *Firmicutes*, *Bacteroidetes*, *Proteobacteria*, *Actinobacteria*, and *Verrucomicrobia*, accounting for approximately 90% of the total gut microbiome (*56*). Approximately 200 genera of Firmicutes in the human gut are dominated by Clostridium (95%). The Bacteroidetes phylum mainly consists of the genera *Bacteroides* and *Prevotella*, while there is relatively small number of the Actinobacteria phylum, which mainly manifests as the genus *Bifidobacterium* (*57*). The relationship between the human microbiome and host is a mutual one. The composition and functional changes or destruction of gut microbiome caused by various factors are related to the development and progression of various diseases (*58*).

2.2.2. Gut microbiome-The foundation of an endocrine organ

The gut microbiome is a complex microbial community that not only plays a crucial role in gut microecology but also has significant impacts on external organs. These impacts extend to areas such as the host's mental state and neurological function, *via* the brain-gut axis, as well as insulin secretion and resistance, and participation in processes such as depression, autoimmune diseases, and cardiovascular diseases (*59*). The decrease in the abundance of the gut microbiome leads to a significant increase in lipopolysaccharides, thereby increasing intestinal permeability and activating the NF-κB signaling pathway, stimulating the release of pro-inflammatory factor tumor necrosis factor (TNF)-α, interleukin (IL)-8, and IL-6. Activated c-Jun amino terminal kinase and IκB kinase regulate serine phosphorylation of insulin receptor substrates, thereby inhibiting insulin signaling and leading to insulin resistance (IR) (*60*). The gut microbiome and its metabolites can act on TLRs and NLRs in the intestinal wall, inducing the production of TNF-α, IL-1, and IL-6, as well as locally resident and migrating antigen-presenting cells and circulating adaptive immune cells, causing a systemic immune response and trigger systemic autoimmune diseases (*61*). The gut microbiome can be viewed as a substantial endocrine organ based on a variety of key findings. Evidence of their direct effects comes from the ability of their produced and metabolized metabolites to reach the circulatory system and impact numerous organ and system functions throughout the host's body (*62*). Unlike other endocrine systems or organs that typically produce only a small number of hormone molecules, the gut microbiome has the potential to synthesize hundreds of functional metabolites (*63*). In fact, the complexity of the gut microbiome colonizing mammals actually exceeds that of the brain. Moreover, many hormones that microorganisms synthesize also function as neurotransmitters within the host's central nervous system. For example, several *Lactobacilli* synthesize γ-Aminobutyric acid, the most important inhibitory transmitter in the brain, while specific bacterial strains produce monoamines such as norepinephrine, dopamine, and serotonin (*64,65*). In the reproductive endocrine system, the gut microbiome plays an important physiological role by complex interaction with insulin, estrogen, androgen and other hormones.

2.2.3. Gut microbiome and estrogen regulation

Reproductive hormones play a direct role in regulating the reproductive activities of female animals. In recent years, many researchers have contended that further research on the regulation of reproductive microorganisms and sex hormones is needed, while the gut microbiome has been proven to have direct or indirect regulatory effects on sex hormones. Estrogen, a steroid reproductive hormone, undergoes metabolism *via* enterohepatic circulation. As a result, numerous studies have focused on its interaction with the gut microbiome, which was first identified over three decades ago by Adlercreutz *et al.* (*66*). The study in question found that supplementation with antibiotics led to a reduction in estrogen levels in women. Estrogen undergoes metabolism in the liver, which includes hydroxylation and coupling. Following this, some conjugated estrogen is excreted *via* urine, while some also enters the intestines and is eliminated through feces (*67*). The gut microbiome plays a critical role in regulating estrogen levels *via* the secretion of β-glucuronidase (GUS), which transforms conjugated estrogen into deconjugated estrogen (*68*) (Figure 2). The enterohepatic circulation of estrogens and their reabsorption are also regulated by the gut microbiome. Estrogen binds to the ligand binding region of receptors (ERα and ERβ) in the nucleus, causing conformational changes and promoting cell growth, apoptosis, proliferation, adhesion, and signal transduction through pathways such as MAPK, PI3K, and Src kinase (*69*). However, the imbalance of the gut microbiome may lead to decreased GUS activity, resulting in lower circulating estrogen levels, and ultimately lead to the development of obesity and cardiovascular disease. In addition, estrogen increases

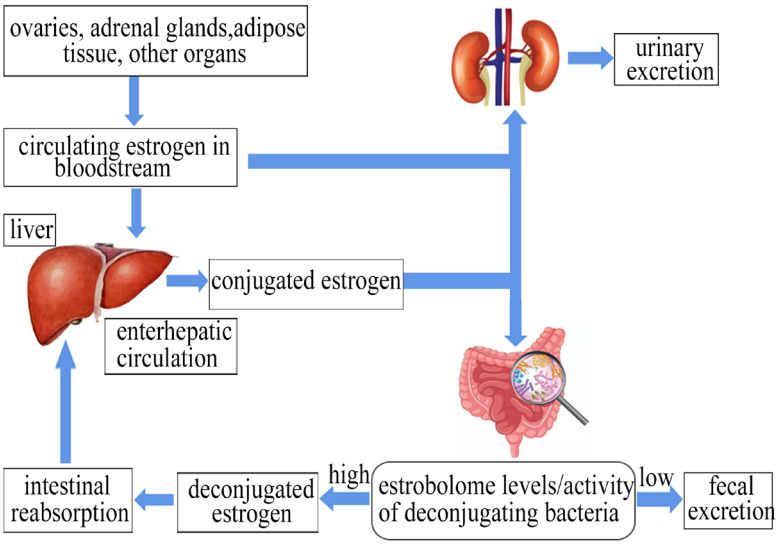

Figure 2. Gut microbiome and estrogen. Estrogen migrates in the blood, reaches the liver, and is inactivated by metabolism into conjugated estrogen. Some is excreted through urine and some is excreted through feces. The gut microbiome mainly secretes β-glucuronidase, which converts conjugated estrogen into deconjugated estrogen that enters the hepatic circulation through intestinal reabsorption.

circulating estrogen levels by reducing the abundance of bacteria producing glucuronidase, *i.e.* increasing the proportion of *Firmicutes*/*Bacteroidetes*, thereby increasing the interaction with ERα and ERβ, leading to endometrial cancer (EC), cancer breast cancer, EMs, and other diseases (*70*). Therefore, optimal GUS activity is essential for maintaining estrogen levels in women.

The gut microbiome may affect female sex steroid hormone levels through the production of short-chain fatty acids (SCFAs), such as abundant acetate, propionate, and butyrate. According to Lu *et al.* (*71*), the synthesis of progesterone and estradiol in pig granulosa cells can be regulated by butyrate through the cAMP signaling pathway. Recent research has shown that enteric-derived butyrate can cause non-alcoholic fatty liver disease due to an estrogen deficiency in premenopausal women (*72*). While a correlation between the gut microbiome and the endocrine system has been reported, the mechanisms of interaction, and particularly those relating to progesterone, remain poorly understood.

3. Role of female dysbiosis in reproductive and gynecological diseases

3.1. FGT dysbiosis in reproductive and gynecological diseases

Lactobacillus is dominant in the normal FGT microbiome. It produces active compounds, facilitates coaggregation based on cell wall molecules, promotes the integrity of the epithelium, and regulates immune responses. The disruption of the FGT microbiome significantly affects the metabolism of amino acids, carbohydrates, and lipids, thereby increasing disease susceptibility. Therefore, the interaction between the microbiome, metabolites, and host in the reproductive tract microenvironment is crucial for maintaining the balance of the reproductive tract. Dysbiosis in the FGT microbiome has been linked to a variety of gynecological disorders, including vaginitis, CE, EPs, EMs, and PCOS (Figure 3).

3.1.1 FGT dysbiosis and vaginitis

Vaginitis is characterized by inflammation of the vaginal mucosa and submucosal connective tissue, and the condition can manifest in several different forms. The most prevalent types of vaginitis include bacterial vaginosis (BV), vulvovaginal candidiasis (VVC), and trichomoniasis vaginitis. BV is the most commonly observed vaginal infectious disease affecting women of childbearing age. This condition is marked by the overgrowth of anaerobic bacteria, primarily *Xenobacteria*, *Gardnerella*, and human *Mycoplasma*. A longitudinal study conducted by Vodstrcil *et al.* (*73*) on 52 young Australian women found that *Gardnerella* was more likely to be detected in sexually active women, implicating sexual activity as an important risk factor for BV. Moreover, sexual activity increased the diversity of vaginal microbiome evolution in women both with and without BV, which could increase the pathogenic potential of the microbiome. Unfortunately, current treatments have a high rate of recurrence (> 50% rate of recurrence within 6 - 12 months) due to potential factors such as reinfection from sexual partners or endogenous sources, biofilm formation, or the failure for appropriate *Lactobacillus* bacteria to take hold (*74*). BV is closely linked to the metabolites present in the reproductive tract. In fact, researchers have found that alterations in specific metabolites (such as maltose, nicotinate, malonate,

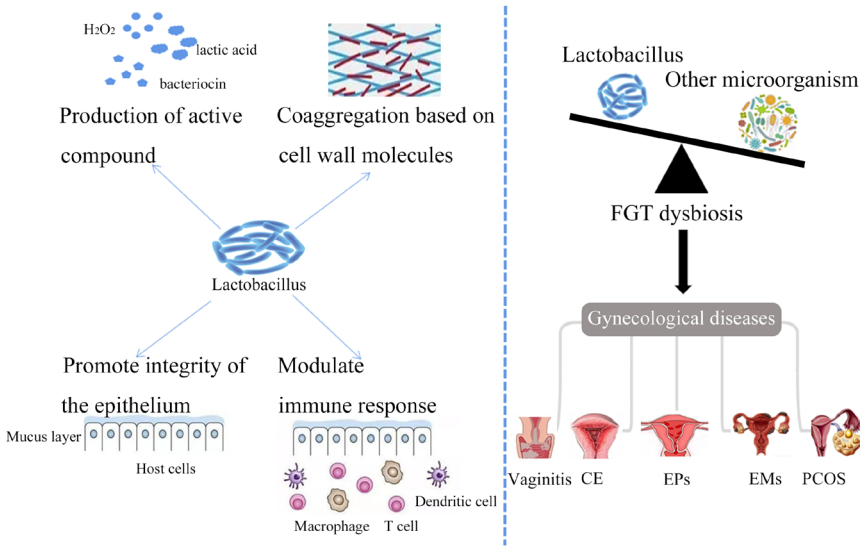

Figure 3. The relationship between FGT dysbiosis and diseases. *Lactobacillus* is dominant in the normal FGT microbiome. It produces active compounds, facilitates coaggregation based on cell wall molecules, promotes the integrity of the epithelium, and regulates immune responses. FGT dysbiosis increase the risk of diseases such as vaginitis, CE, EPs, EMs, and PCOS.

acetate, and nicotinamide adenine dinucleotide) can serve as metabolic markers, distinguishing individuals with BV from healthy individuals (*75*). Following successful treatment, these BV-associated metabolites decrease significantly. Given this, metabolic analysis of the reproductive tract is considered crucial to the identification and diagnosis of BV. According to a study conducted by McMillan *et al.* (*76*), an increase in 2-hydroxyisovalerate and γ-hydroxybutyrate in the vagina, as well as a decrease in lactate and tyrosine, are the most reliable indicators of BV. Nevertheless, further research is necessary to fully understand the effects of metabolites on both the microbiome and host immunity. The vaginal mucosa is an important line of defense for local immunity that can resist pathogen invasion by rapidly shedding epithelial cells and secreting cytotoxic cytokines. The imbalance of the gut microbiome activates the NF-κB pathway through Toll-like receptors, leading to increased release of pro-inflammatory cytokines and epithelial cell damage (*77*). *Lactobacillus* is able to inhibit HeLa cell apoptosis caused by pathogens, thus protecting epithelial cells (*78*).

VVC is the second most frequently occurring vaginitis following BV. Studies have estimated that around 10% to 15% of asymptomatic women carry *C. albicans* in their vaginas, and approximately 70% to 75% of women experience VVC at some point in their lives, impacting millions of women every year (*79*). A recent *in vivo* study indicated that colonization by *Lactobacillus* may not necessarily lower the risk of VVC, while colonization by *L. crispatus* can even lead to an increased risk of *C. albicans* colonization (*80,81*). Despite the association between VVC and the vaginal microbiome, whether specific *Lactobacillus* species are associated with this condition is still unknown. Further research is necessary to identify any potential links. *Chlamydia trachomatis* (CT) is a widespread sexually transmitted infection among women age 15-49, with global rates of infection ranging from 1.5% to 7% (*82*). Lactic acid present in the genital tract acts as a critical inhibitor of CT infection. Nevertheless, the *L. iners* species produces far less lactic acid than other *Lactobacillus* spp., making women with *L. iners* as the dominant flora particularly susceptible to CT infection (*83*). In addition, certain individuals with CT infections may have an abundance of anaerobic bacteria in their genital tract, such as *Gardnenella*, *Prevotella*, *Megalococcus*, and *Rosella*. In comparison to healthy controls, reproductive tract metabolites from individuals infected with CT demonstrated only a slight decline in several amino acids and biogenic amines (*18*). Upon experiencing CT reinfection or chronic infection, activated helper T cell (Th) - 1, Th2, and Th17 cells can stimulate tissue destruction, fibrosis, and scarring, ultimately contributing to pelvic inflammation (*84*).

3.1.2. FGT dysbiosis and CE and EPs

CE is a distinct alteration in the population of endometrial microorganisms present in the uterine cavity, predominantly caused by bacterial pathogens such as *Streptococcus*, *Escherichia coli*, *Enterococcus faecalis*, *Mycoplasma*, and other bacteria like tuberculosis bacilli and viruses (*85*). A study conducted by Liu *et al.* (*85*) found that CE is linked to a significant increase in the prevalence of 18 groups of bacteria within the endometrial cavity. Moreover, the relative abundance of *Lactobacillus* was notably higher in individuals with CE in comparison to those without CE (80.7% *vs.* 1.89%), while there was a lower prevalence of *L. crispatus* in

the CE microbiome. Antibiotic therapy administered to patients with CE has demonstrated an ability to markedly enhance reproductive outcomes, indicating a crucial correlation between the host and colonizing bacteria (*86*). In cases of CE, microbial infections, including those caused by Gram-negative bacteria, can trigger potent immune responses that may trigger B-cell entry into the endometrial stroma, subsequently leading to the aberrant expression of various pro-inflammatory molecules. Other studies have also found that *Streptococcus pyogenes* infects the human endometrium by limiting innate immune responses (*87*). Concurrently, endometrial microvascular endothelial cells express adhesion molecules and chemokines associated with B-cells in CE, resulting in alterations to the uterus's receptivity and unfavorable pregnancy outcomes (*88*). In addition, Chen *et al*. (*89*) found that endometrial microorganisms can interfere with glucose and lipid metabolism processes through the PWY-7347 and SUCSYN-PWY metabolic pathways to regulate immune cells, thereby affecting endometrial receptivity.

EPs are likely triggered by several factors, including genetics, endocrine imbalances, immune inflammation, irregular cell proliferation/apoptosis, angiogenesis, oxidative stress, and an imbalanced FGT microbiome. The composition of the LGT microbiome can markedly heighten the likelihood of developing EPs. A study conducted by Marchenco *et al*. (*90*) indicated that women with vaginal microbiome disorders are 3.5 times more susceptible to BV than healthy people. In addition, Kovalenko *et al*. (*91*) suggested that vaginal *Gardnerella*, commonly associated with BV, may fuel the emergence of EPs. Similarly, Horban *et al*. (*92*) found that 93.6% of individuals living with recurring BV had endometrial lesions, comprising 42% of all pathology results diagnosed as EPs. Fang *et al*. (*93*) examined the differences in the composition of the endometrial microbiome between patients experiencing EPs and healthy women, and they found that the bacterial diversity of the endometrial microbiome was higher in EPs patients than in their healthy counterparts. EPs patients exhibited higher ratios of endometrial *Lactobacillus*, *Bifidobacteria*, *Gardnerella*, *Streptococcus*, *Alternaria*, and *Prevotella* but lower proportions of *Pseudomonas*, *Enterobacteriaceae*, and *Sphingosine*. In specific terms, the proportion of *Lactobacillus* was significantly elevated in EP patients (38.64% *vs.* 6.17%), indicating that vaginal bacteria in individuals with EPs may also proliferate in the uterine cavity (*93*). When an intrauterine infection or changes in the microbiome of intrauterine colonization occur, immune cells can interact with microorganisms through pattern recognition receptors, recruiting circulating B cells to the endometrial stroma and stroma regions, reducing the antiviral and fungal infection function of natural killer cells, and severely reducing the abnormal immune microenvironment inside the uterine cavity, affecting sperm fertilization and embryo implantation (*94*). Nonetheless, there is still a need for further research concerning specific alterations in the microbial composition and pathogenic microbial species associated with EPs.

3.1.3. FGT dysbiosis and EMs

Despite the incidence of EMs increasing yearly to 5% - 15% (*95*), the pathogenesis of this condition remains unclear. In a cohort study conducted by Lin *et al*. (*96*) involving 79,512 patients with reproductive tract infections, the incidence of EMs was significantly higher compared to that in the control group. In addition, reproductive tract infections were identified as an independent risk factor for EMs, markedly increasing the likelihood of patients with a reproductive tract infection developing endometriosis (*96*). Moreover, Akiyama *et al*. (*97*) performed NGS analysis on the cervical mucus in women with and without EMs, and they found that the quantity of *Enterobacteriaceae* and *Streptococcus* in the cervical mucus of the EMs group was substantially higher than that of the control group, irrespective of the various phases of the menstrual cycle, except for the primary *Lactobacillus* species. Yang *et al*. (*98*) observed accumulation of several less abundant genera in the vaginal and cervical microbiome of EM patients, such as *Fannyhessea*, *Prevotella*, *Streptococcus*, *Bifidobacterium*, *Veillonella*, *Megasphaera*, and *Sneathia*. The microbial imbalance of EMs can promote disease progression through immune activation, impaired intestinal function of cytokines, changes in estrogen metabolism and signal transduction, and abnormalities in the homeostasis of progenitor cells and stem cells (*99*). Despite these findings, further research is required to clarify the mechanistic aspects that link these bacteria to the pathophysiology of endometriosis. Endometrial microbial infections may harm the contractility of the uterus and facilitate the implantation of retrograde endometrial cells (*100*), thus promoting the progression of this disease.

3.1.4. FGT dysbiosis and PCOS

The pathological and physiological mechanisms underlying PCOS are relatively intricate, encompassing multifaceted interactions within multiple mechanisms and pathways. Several studies have shown that the level of the *Lactobacillus* genus, and specifically *L. curlicus*, in the reproductive tract of PCOS patients is lower compared to that in the control group (*101*). In addition, PCOS patients also exhibit an increased abundance of species such as *Gardnerella*, *Chlamydia*, and *Prevotella* in the cervical canal, whereas the vaginal microbiome is enriched in species such as *Prevotella*, *Ageophilia*, and *Mycoplasma*, unlike in the control group (*101*). A Kyoto Encyclopedia of Genes and Genomes analysis showed

that oxidative phosphorylation, amino acid metabolism, and N-glucan biosynthesis were upregulated in the LGT of PCOS patients (*102*). These changes are beneficial to the colonization of several pathogenic bacteria (such as Gardnerella) but not to the growth of *Lactobacillus* (*103*).

Currently, the treatment for PCOS primarily involves Diane-35 (ethinylestradiol cyproterone). Reviews of the relevant literature have indicated that using hormonal contraception can decrease the risk of BV (*103*). The use of hormonal contraceptives can regulate the local inflammatory response of BV, which is significantly associated with high levels of IL, TNF, INF-r, IL-2, and IL-4 in contrast to the normal vaginal microbiome (*103*). These findings suggest that the use of hormone contraceptives may impact the immune system of the reproductive tract.

3.2.Gut dysbiosis in reproductive and gynecological diseases

The gut mucosal layer provides a vital protective barrier against microbial invasion. However, gut dysbiosis can disrupt the normal mucosal layer, leading to the increased incidence of various gynecological diseases, including PCOS, EMs, cancer, and obesity (Figure 4).

3.2.1. Gut dysbiosis and PCOS

PCOS is a multifactorial endocrine and metabolic disorder, and the gut microbiome is implicated in various metabolic activities in the human body. Indeed, exploring alterations in the gut microbiome of PCOS patients has become a focus of research in recent years. Notably, Torres *et al*. (*104*) found that both the α diversity (overall species richness) and β diversity (microbial community composition) of the gut microbiome in PCOS patients decreased compared to those in healthy women. In addition, they identified an increased abundance of specific gut microbiome in PCOS patients such as *Streptomyces* and *Candella* (*104*). Interestingly, these changes in the gut microbiome appear to be correlated with increased serum androgen levels in PCOS patients (*104*). In a mouse model of PCOS induced with dihydrotestosterone, the relative abundance of anaerobic bacteria in animals with a high dose of androgens increased (*105*). Multiple components of the gut microbiome can assist in the synthesis and transformation of androgens by synthesizing enzymes for androgen metabolism. *Actinobacteria* and *Proteobacteria* can degrade androgens (*106*). Due to its genome encoding 20α- hydroxysteroid dehydrogenase, Clostridium subtilis is involved in the conversion of glucocorticoids into androgens (*107*). However, the limitation of these studies lies in the lack of in-depth evaluation of the mechanism underlying the interaction between the gut microbiome and androgens. The observed decrease in gut microbiome diversity may contribute to decreased activity of the GUS, resulting in reduced circulating estrogen levels, and therefore a decrease in active estrogen receptors. As a result, this decrease in estrogen receptor activity may increase the risk of a variety of metabolic diseases including obesity, metabolic syndrome, and cardiovascular diseases, as well as a decrease in cognitive ability (*108*). Regarding the changes in microbiome composition observed in PCOS patients, several studies have reported an increase in the genus *Bacteroides*, which is consistent with findings from rodent models of PCOS. In contrast, the abundance of *Bifidobacterium* and *Faecalibacterium* apparently decreased in PCOS patients (*109,110*).

IR is common in women with PCOS, and the incidence of IR varies from 25% to 70% (*111*). Zhang *et*

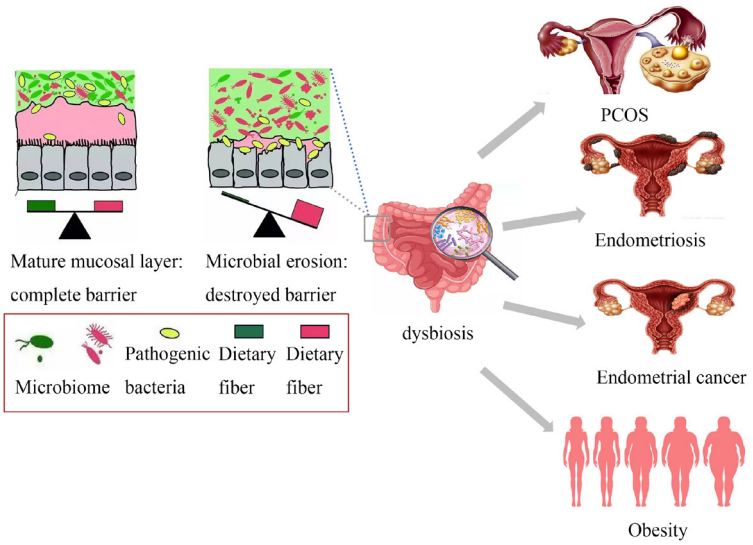

Figure 4. The relationship between gut dysbiosis and diseases. The gut mucosal layer is a protective barrier. When the gut is invaded by microorganisms, the normal mucosal layer is destroyed. Gut dysbiosis increases the risk of diseases such as PCOS, EMs, cancer, and obesity.

al. (*110*) also noted that the levels of acetate, propionate, and butyrate in the gut of PCOS patients decreased significantly compared to that in healthy women. Specifically, reductions of around 30% to 66% were observed. However, following probiotic treatment, the abundance of *Lactobacillus* in the gut of PCOS patients increased significantly, and SCFA levels in the intestines also increased. Overall, insulin secretion also increased (*110*). The gut microbiome has been found to impact insulin sensitivity *via* branched-chain amino acids such as leucine, isoleucine, and valine (*112*). This illustrates the complex and intimate relationship between PCOS and the gut microbiome. Further research is required to explore the potential mechanisms underlying the pathogenesis of PCOS in relation to the gut microbiome.

3.2.2. Gut dysbiosis and EMs

Endometriosis, an estrogen-dependent chronic inflammatory disease, has garnered significant attention due to its potential correlations with the gut microbiome. Mounting evidence suggests a link between the gut microbiome and the incidence of endometriosis. Svensson *et al.* (*113*) performed 16S rRNA sequencing on the gut microbiome of patients with EMs and healthy controls, and their results showed that compared to the healthy control group, the gut microbiome of patients with endometriosis showed lower levels of α and β diversity. Moreover, Svensson *et al*. (*113*) found significant variations in the abundance of twelve bacteria across the classes *Bacilli*, *Bacteroidia*, *Clostridia*, *Coriobacteriia*, and *Gammaproteobacteria* in the feces of patients with endometriosis. Similarly, Ata *et al*. (*114*) noted an increase in the number of Escherichia coli and Shigella, both belonging to the *Enterobacteriaceae* family, in the gut microbiome of patients with stage III-IV endometriosis.

Gut dysbiosis could potentially result in immune disorders, inflammatory reactions, and abnormal estrogen metabolism, and these factors may play significant roles in the emergence of endometriosis (*115*). Wei *et al.* (*116*) showed that Gram-negative bacteria can increase the number and volume of lesions and the number of macrophages in a mouse model of EMs by producing GUS. Other researchers have shown that there are significant differences in the gut microbiome in EMs patients compared to normal individuals, and the levels of expression of inflammatory factors, nuclear factors-κB p65, and cyclooxygenase-2 increased in EM patients (*117*). This suggests that an imbalance of the gut microbiome activates the inflammatory pathway of the gut-brain axis and participates in the progression of EMs. Moreover, disruption of the gut microbiome may lead to increases in the levels of specific neuroactive metabolites, including glutamate and aminobutyric acid. As a result, these metabolites can activate brain neurons (such as GnRH neurons) and increase estrogen production in the ovaries *via* the hypothalamic-pituitary-ovarian axis (*118*). Consequently, increased exposure to estrogen - caused by gut microbiome imbalances - may represent a significant risk factor for the development and progression of endometriosis.

3.2.3. Gut dysbiosis and EC

Over the past 20 years, the incidence of EC has continued to increase and affect younger women (*119*). Studies have shown that changes in the ratio of *Firmicutes*/*Bacteroidetes* can increase GUS active bacteria, increase estrogen levels, and enhance estrogen receptor binding, thereby promoting endometrial hyperplasia and the development of EC (*72*). In EC, estrogen upregulates the production of pro-inflammatory mediators such as IL-6 and TNF-α, which in turn synergistically upregulate the expression of enzymes involved in ovarian steroid production (17β-hydroxysteroid dehydrogenase, aromatase, and estrone sulfate esterase), thereby forming a feedback loop (*120*). An *in vitro* study showed that *Atopobium vaginae* and *Porphyromonas somerae* promote EC development by inducing the expression of inflammatory cytokines and chemokines (TNF-α, IL-1α, IL-1β, and IL-17α) in endometrial cells (*121*). The specific mechanisms underlying the disruption of normal homeostasis by gut microbiota leading to EC, as well as the competition between microorganisms for nutrition, signal transduction between microorganisms and hosts, and the impact of microbial metabolites, all require further research.

4. Use of microbial therapy

4.1. Dietary interventions

In recent years, interventions involving the FGT and gut microbiome as a treatment for female reproductive tract diseases has become a focus of research. More recently, nutrition has been recognized as another factor affecting women's reproductive health. Neggers *et al*. (*122*) and Tohill *et al*. (*123*) first demonstrated the role of malnutrition in BV and other gynecological infections in women of childbearing age. In 2007, Neggers *et al*. (*122*) described the subclinical deficiency of iron and vitamin D during pregnancy as associated with an increased risk of BV. A large cross-sectional study (*123*) subsequently confirmed that lower serum concentrations of vitamins A, C, E, and β-carotenoids were associated with BV, while lower iron levels were associated with increased *Candida* plaque measurement.

Although there is little understanding of the mechanisms by which nutrition affects female reproductive tract homeostasis, studies on gut microbiome in other parts of the body have revealed the impact of diet on bacterial community composition and function, with profound impacts on diseases such as obesity, metabolic

disorders, immune diseases, and cancer (*124*). In addition, the intestine is known to serve as the ultimate host of BV-related lactic acid bacteria and bacteria (*125*). Eating fiber-rich foods is important for the immune system by boosting the diversity of the microbiome, which boosts anti-inflammatory abilities. A high-fat diet is linked to a decrease in *Bacteroides* and *Coprobacillus* levels, while a low-fat diet promotes α diversity of the gut microbiome. Moreover, the concentration of SCFAs in the high-fat diet group is notably lower than that of the low-fat diet group. High-fat diets are also associated with an enrichment of arachidonic acid in feces and an increase in plasma proinflammatory factors (*126*).

An important parameter in the pathogenesis of PCOS is the presence of advanced glycosylation end products (AGEs). Research has confirmed that an unhealthy diet in PCOS patients can lead to an inflammatory state, inducing oxidative stress and stimulating androgen synthesis in ovarian tissue, leading to an increased inflammatory response and ultimately forming a vicious cycle (*127*). In contrast, a high-fiber diet based on polyunsaturated fatty acids can increase insulin sensitivity and thus alleviate hyperandrogenism (*128*). The impact of vitamin D on the diversity of the gut microbiome has been validated in multiple studies. Supplementing vitamin D increases the overall diversity of the gut microbiota and increases the proportion of *Firmicutes/Bacteroidetes*, thereby maintaining intestinal homeostasis (*129*). *In vitro* and animal studies have shown that dietary vitamin D supplementation contributes to the regression of endometriosis lesions with reduced invasion and proliferation (*130*).

4.2. Probiotics

The efficacy of probiotics in the treatment of microbial disorders has been reported in several studies (*131-133*). Currently, the available probiotics can be classified into three categories: *Lactobacillus*, *Bifidobacteria*, and Gram-positive cocci, such as *Streptococcus* and *Lactococcus.* Studies have revealed that probiotics help regulate gut microbiome, treat metabolic disorders, and restore gut microbiome damaged by a high-fat diet to a healthy state (*131*). Chenoll *et al.* (*132*) isolated *Lactobacillus rhamnosus* BPL005 from vaginal samples and co-cultured it with a primary endometrial epithelial cell model with the colonization of *Atopobium vaginae*, *Propionibacterium acnes*, *Gardnerella vaginalis*, and *Streptococcus agalactiae*. They noted a significant reduction in *Propionibacterium acnes* and *Streptococcus agalactiae*, suggesting that microbial agents have the potential to facilitate improved reproductive health. Studies have demonstrated that the combination of a vaginal lactobacillus preparation is more effective in curing vaginal infectious diseases and decreasing the rate of recurrence compared to antibiotic treatment alone (*133*).

Probiotics have been proven to treat other reproductive diseases, including those not transmitted by microbial pathogens. A study in human subjects revealed that, compared to the control group, PCOS patients who received probiotic supplements for 12 weeks experienced an increase in sex hormone binding protein, a decrease in their hirsutism score and extremely low density lipoprotein levels, and improvement in insulin sensitivity (*134*). Zhang *et al.* (*110*) found that oral administration of *Bifidobacterium lactis* V9 can alleviate PCOS by increasing the release of gastrin and peptide YY, thereby restoring sexual hormones at the brain level in a manner similar to normal hormone levels. In addition, probiotic therapy is also quite effective in the treatment of endometriosis. Animal experiments have shown that oral *Lactobacilli* can reduce the growth of mouse EM lesions by increasing IL-12 and NK cell activity (*135*). Itoh *et al*. (*136*) also found that oral probiotics can activate NK cells in the body and inhibit the development of EM lesions. A randomized controlled trial found that oral *Lactobacilli* can alleviate pain related to EMs in women (*137*). In addition, probiotics have been found to improve the fertilization rate, pregnancy success rate, and offspring survival rate of several animals by altering the activity of the microbiota, promoting nutrient absorption and digestion, and improving the immune system (*138,139*).

4.3. Fecal microbial transplantation(FMT)

Fecal microbiota transplantation (FMT) is a rapidly evolving therapy that aims to reconstruct a patient's dysbiotic microbiota with the beneficial fecal microbiota of a healthy individual. In recent years, FMT has displayed great potential for the treatment of female reproductive tract diseases. A study in a rat model of induced PCOS confirmed that after FMT treatment, the estrus cycle of PCOS rats improved, androgen biosynthesis decreased, ovarian morphology returned to normal, and the intestinal microbiota composition was characterized by an increase in *Lactobacilli* and *Clostridium* and a decrease in *Prevotella* (*140*). Preclinical mouse models suggest that short-chain fatty acids derived from the gut microbiota can prevent the progression of endometriosis, thereby reducing EM-related pain (*141*). Despite the lack of clinical data, FMT is a potential treatment option for endometriosis due to its beneficial effect in reducing EM-related pain. In breeders, FMT can regulate increased hormone secretion, intestinal health, and ovarian function through SIRT1-related cell apoptosis and cytokine signaling pathways (*142*). In addition to animal models, prospective data should be obtained from laboratory studies for further research in humans.

5. Methods of studying the microbiome

Early microbiology research relied on optical microscopy

and microbial culture techniques, but microbial culture took a long time and the results obtained were incomplete and unrepresentative, posing numerous obstacles to microbiology research (*143*). In recent years, molecular biology theory and techniques have greatly promoted the innovation of microbial classification and identification and expanded our understanding of microbial structure and function. From the perspective of genetic evolution, people classify and identify microorganisms at the molecular level, making the classification of microorganisms increasingly refined and precise. The main techniques used are: denaturing gradient gel electrophoresis, temperature gradient gel electrophoresis, terminal-restriction fragment length polymorphism, temporal temperature gradient gel electrophoresis, single-strand conformation polymorphism, western blot hybridization, quantitative PCR, and 16S rRNA library detection (*144*). However, the above methods all have the drawbacks of low throughput (fewer samples can be analyzed and fewer data can be obtained) and high cost, precluding their widespread use by ordinary laboratories.

Sequencing is the most commonly used technique in modern molecular biology research. With the completion of the Human Genome Project, research has entered the era of functional genomics. Conventional Sanger sequencing can no longer meet the requirements of large-scale gene sequencing. After more than 30 years of development, next generation sequencing (NGS) has arrived. At present, NGS has become the mainstream method for classifying and identifying bacteria by detecting the sequence of 16S rRNA genes in bacteria. 16S rRNA widely exists in prokaryotic cells. In the process of bacterial evolution, the evolution of rRNA genes is relatively conserved. A large amount of information is retained, facilitating amplification and sequencing, and is considered to be the most ideal yardstick to measure the evolutionary history of life. The unique advantages of 16S rRNA enable bioinformatic analysis of the generated sequences within a relatively short sequencing range (V1-V9), effectively distinguishing bacterial communities (*145*). Understanding the composition and function of microorganisms helps to understand the potential ecological adverse states represented by microbial species or community types. Future research on metabolome composition may reveal complex interactions between species and host microorganisms.

6. Conclusion

A balanced and healthy microbiome is crucial for maintaining reproductive health as it assists in protecting the host from pathogens, enhancing reproductive potential, and reducing the likelihood of adverse pregnancy outcomes. Implementing effective measures, such as addressing dysbiosis, monitoring dynamic changes in the microbiome, and bolstering levels of beneficial bacteria, can significantly improve reproductive health. To gain a comprehensive understanding of all microbial species undergoing modifications in reproductive pathology, an essential task is to conduct large-scale longitudinal studies encompassing bacteria, fungi, and viruses. As further research on the FGT and gut microbiome unfolds, microbial therapy has the potential to serve as a prospective approach to enhance female reproductive health.

Funding: This work was supported by grants from a project under the Scientific and Technological Innovation Action Plan of the Shanghai Natural Science Fund (grant no. 20ZR1409100 to L Wang), a project of the Chinese Association of Integration of Traditional and Western Medicine special foundation for Obstetrics and Gynecology-PuZheng Pharmaceutical Foundation (grant no. FCK-PZ-08 to L Wang), a project for hospital management of the Shanghai Hospital Association (grant no. X2021046 to L Wang), a clinical trial project of the Special Foundation for Healthcare Research of the Shanghai Municipal Health Commission (grant no. 202150042 to L Wang), a grant from Science and Technology Plan of Zhoushan City, Zhejiang Province (grant no. 2021C31055 to WL Cao) and a project from Zhejiang Province Traditional Chinese Medicine Technology (grant no. 2023ZL769 to WL Cao).

Conflict of Interest: The authors have no conflicts of interest to disclose.

References

1. Wan X, Yang Q, Wang X, Bai Y, Liu Z. Isolation and cultivation of human gut microorganisms: A review. Microorganisms. 2023; 11:1080.
2. Lozupone CA, Stombaugh JI, Gordon JI, Jansson JK, Knight R. Diversity, stability and resilience of the human gut microbiota. Nature. 2012; 489:220-230.
3. Tian C. The role of microorganisms in the human body. World's Latest Medical Information Abstracts (Continuous Electronic Journal). 2019; 19:41.
4. Moreno I, Simon C. Deciphering the effect of reproductive tract microbiome on human reproduction. Reprod Med Biol. 2018; 18:40-50.
5. Shen J, Song N, Williams CJ, Brown CJ, Yan Z, Xu C, Forney LJ. Effects of low dose estrogen therapy on the vaginal microbiomes of women with atrophic vaginitis. Sci Rep. 2016; 6:24380.
6. Chadchan SB, Singh V, Kommagani R. Female reproductive dysfunctions and the gut microbiota. J Mol Endocrinol. 2022; 69:R81-R94.
7. Simon C. Introduction: Do microbes in the female reproductive function matter? Fertil Steril. 2018; 110:325-326.
8. Salliss ME, Farland LV, Mahnert ND, Herbst-Kralovetz MM. The role of gut and genital microbiome and the estrobolome in endometriosis, infertility and chronic pelvic pain. Hum Reprod Update. 2021; 28:92-131.

9. Punzón-Jiménez P, Labarta E. The impact of the female genital tract microbiome in women health and reproduction: A review. J Assist Reprod Genet. 2021; 38:2519-2541.
10. Ding T, Schloss PD. Dynamics and associations of microbial community types across the human body. Nature. 2014; 509:357-360.
11. Ravel J, Gajer P, Abdo Z, Schneider GM, Koenig SS, McCulle SL, Karlebach S, Gorle R, Russell J, Tacket CO, Brotman RM, Davis CC, Ault K, Peralta L, Forney LJ. Vaginal microbiome of reproductive-age women. Proc Natl Acad Sci U S A. 2011; 108:4680-4687.
12. France MT, Ma B, Gajer P, Brown S, Humphrys MS, Holm JB, Waetjen LE, Brotman RM, Ravel J. VALENCIA: A nearest centroid classification method for vaginal microbial communities based on composition. Microbiome. 2020; 8:166.
13. Aldunate M, Srbinovski D, Hearps AC, Latham CF, Ramsland PA, Gugasyan R, Cone RA, Tachedjian G. Antimicrobial and immune modulatory effects of lactic acid and short chain fatty acids produced by vaginal microbiota associated with eubiosis and bacterial vaginosis. Front Physiol. 2015; 6:164.
14. van de Wijgert JH, Borgdorff H, Verhelst R, Crucitti T, Francis S, Verstraelen H, Jespers V. The vaginal microbiota: What have we learned after a decade of molecular characterization? PLoS One. 2014; 9:e105998.
15. Williams VM, Filippova M, Filippov V, Payne KJ, Duerksen-Hughes P. Human papillomavirus type 16 E6* induces oxidative stress and DNA damage. J Virol. 2014; 88:6751-6761.
16. Kroon SJ, Ravel J, Huston WM. Cervicovaginal microbiota, women's health, and reproductive outcomes. Fertil Steril. 2018; 110:327-336.
17. Srinivasan S, Liu C, Mitchell CM, Fiedler TL, Thomas KK, Agnew KJ, Marrazzo JM, Fredricks DN. Temporal variability of human vaginal bacteria and relationship with bacterial vaginosis. PLoS One. 2010; 5:e10197.
18. Gajer P, Brotman RM, Bai G, *et al*. Temporal dynamics of the human vaginal microbiota. Sci Transl Med. 2012; 4:132ra52.
19. Mitra A, MacIntyre DA, Marchesi JR, Lee YS, Bennett PR, Kyrgiou M. The vaginal microbiota, human papillomavirus infection and cervical intraepithelial neoplasia: What do we know and where are we going next? Microbiome. 2016; 4:58.
20. Miko E, Barakonyi A. The role of hydrogen-peroxide (H2O2) produced by vaginal microbiota in female reproductive health. Antioxidants (Basel). 2023; 12:1055.
21. Abdelmaksoud AA, Girerd PH, Garcia EM, Brooks JP, Leftwich LM, Sheth NU, Bradley SP, Serrano MG, Fettweis JM, Huang B, Strauss JF 3rd, Buck GA, Jefferson KK. Association between statin use, the vaginal microbiome, and Gardnerella vaginalis vaginolysin-mediated cytotoxicity. PLoS One. 2017; 12:e0183765.
22. Dong B, Huang Y, Cai H, *et al*. Prevotella as the hub of the cervicovaginal microbiota affects the occurrence of persistent human papillomavirus infection and cervical lesions in women of childbearing age *via* host NF-κB/C-myc. J Med Virol. 2022; 94:5519-5534.
23. Jang SJ, Lee K, Kwon B, You HJ, Ko G. Vaginal lactobacilli inhibit growth and hyphae formation of Candida albicans. Sci Rep. 2019; 9:8121.
24. Ding C, Yu Y, Zhou Q. Bacterial vaginosis: Effects on reproduction and its therapeutics. J Gynecol Obstet Hum Reprod. 2021; 50:102174.
25. Jacobson JC, Turok DK, Dermish AI, Nygaard IE, Settles ML. Vaginal microbiome changes with levonorgestrel intrauterine system placement. Contraception. 2014; 90:130-135.
26. Pelzer ES, Willner D, Buttini M, Huygens F. A role for the endometrial microbiome in dysfunctional menstrual bleeding. Antonie Van Leeuwenhoek. 2018; 111:933-943.
27. Chen Y, Qiu X, Wang W, Li D, Wu A, Hong Z, Di W, Qiu L. Human papillomavirus infection and cervical intraepithelial neoplasia progression are associated with increased vaginal microbiome diversity in a Chinese cohort. BMC Infect Dis. 2020; 20:629.
28. Klein C, Gonzalez D, Samwel K, Kahesa C, Mwaiselage J, Aluthge N, Fernando S, West JT, Wood C, Angeletti PC. Relationship between the cervical microbiome, HIV status, and precancerous lesions. mBio. 2019; 10:e02785-18.
29. Audirac-Chalifour A, Torres-Poveda K, Bahena-Román M, Téllez-Sosa J, Martínez-Barnetche J, Cortina-Ceballos B, López-Estrada G, Delgado-Romero K, Burguete-García AI, Cantú D, García-Carrancá A, Madrid-Marina V. Cervical microbiome and cytokine profile at various stages of cervical cancer: A pilot study. PLoS One. 2016; 11:e0153274.
30. Curty G, Costa RL, Siqueira JD, Meyrelles AI, Machado ES, Soares EA, Soares MA. Analysis of the cervical microbiome and potential biomarkers from postpartum HIV-positive women displaying cervical intraepithelial lesions. Sci Rep. 2017; 7:17364.
31. Chu DM, Valentine GC, Seferovic MD, Aagaard KM. The development of the human microbiome: Why moms matter. Gastroenterol Clin North Am. 2019; 48:357-375.
32. Baker JM, Chase DM, Herbst-Kralovetz MM. Uterine microbiota: Residents, tourists, or invaders? Front Immunol. 2018; 9:208.
33. Winters AD, Romero R, Gervasi MT, Gomez-Lopez N, Tran MR, Garcia-Flores V, Pacora P, Jung E, Hassan SS, Hsu CD, Theis KR. Does the endometrial cavity have a molecular microbial signature? Sci Rep. 2019; 9:9905.
34. Solt I. The human microbiome and the great obstetrical syndromes: A new frontier in maternal-fetal medicine. Best Pract Res Clin Obstet Gynaecol. 2015; 29:165-175.
35. Koedooder R, Mackens S, Budding A, Fares D, Blockeel C, Laven J, Schoenmakers S. Identification and evaluation of the microbiome in the female and male reproductive tracts. Hum Reprod Update. 2019; 25:298-325.
36. Moreno I, Codoñer FM, Vilella F, Valbuena D, Martinez-Blanch JF, Jimenez-Almazán J, Alonso R, Alamá P, Remohí J, Pellicer A, Ramon D, Simon C. Evidence that the endometrial microbiota has an effect on implantation success or failure. Am J Obstet Gynecol. 2016; 215:684-703.
37. Mitchell CM, Haick A, Nkwopara E, Garcia R, Rendi M, Agnew K, Fredricks DN, Eschenbach D. Colonization of the upper genital tract by vaginal bacterial species in nonpregnant women. Am J Obstet Gynecol. 2015; 212:611.e1-9.
38. Chen C, Song X, Wei W, *et al*. The microbiota continuum along the female reproductive tract and its relation to uterine-related diseases. Nat Commun. 2017; 8:875.
39. Winters AD, Romero R, Gervasi MT, Gomez-Lopez N, Tran MR, Garcia-Flores V, Pacora P, Jung E, Hassan SS, Hsu CD, Theis KR. Does the endometrial cavity have a molecular microbial signature? Sci Rep. 2019; 9:9905.

40. Usman SF, Shuaibu IR, Durojaiye K, Medugu N, Iregbu KC. The presence of microorganisms in follicular fluid and its effect on the outcome of *in vitro* fertilization-embryo transfer (IVF-ET) treatment cycles. PLoS One. 2021; 16:e0246644.
41. Hamad TA, Ahmed AT, Sadeq MS, *et al*. Microbial colonization of human follicular fluid and adverse outcome on *in vitro* fertilization cases in Kamal al-Samarrai's Hospital for fertility and *in vitro* fertilization treatment in Baghdad, Iraq 2016. IOSR J Dent Med Sci e-ISSN. 2018; 17: 80-87.
42. Pelzer ES, Allan JA, Cunningham K, Mengersen K, Allan JM, Launchbury T, Beagley K, Knox CL. Microbial colonization of follicular fluid: Alterations in cytokine expression and adverse assisted reproduction technology outcomes. Hum Reprod. 2011; 26:1799-1812.
43. Pelzer ES, Willner D, Buttini M, Hafner LM, Theodoropoulos C, Huygens F. The fallopian tube microbiome: Implications for reproductive health. Oncotarget. 2018; 9:21541-21551.
44. Wang Y, Zhang Y, Zhang Q, Chen H, Feng Y. Characterization of pelvic and cervical microbiotas from patients with pelvic inflammatory disease. J Med Microbiol. 2018; 67:1519-1526.
45. Sweet RL, Mills J, Hadley KW, Blumenstock E, Schachter J, Robbie MO, Draper DL. Use of laparoscopy to determine the microbiologic etiology of acute salpingitis. Am J Obstet Gynecol. 1979; 134:68-74.
46. Mueller NT, Bakacs E, Combellick J, Grigoryan Z, Dominguez-Bello MG. The infant microbiome development: mom matters. Trends Mol Med. 2015; 21:109-117.
47. Ferretti P, Pasolli E, Tett A, *et al*. Mother-to-infant microbial transmission from different body sites shapes the developing infant gut microbiome. Cell Host Microbe. 2018; 24:133-145.e5.
48. Yassour M, Jason E, Hogstrom LJ, *et al*. Strain-level analysis of mother-to-child bacterial transmission during the first few months of life. Cell Host Microbe. 2018; 24:146-154.e4.
49. Hammerschlag MR, Alpert S, Onderdonk AB, Thurston P, Drude E, McCormack WM, Bartlett JG. Anaerobic microflora of the vagina in children. Am J Obstet Gynecol. 1978; 131:853-856.
50. Hickey RJ, Zhou X, Settles ML, Erb J, Malone K, Hansmann MA, Shew ML, Van Der Pol B, Fortenberry JD, Forney LJ. Vaginal microbiota of adolescent girls prior to the onset of menarche resemble those of reproductive-age women. mBio. 2015; 6:e00097-15.
51. Shen L, Zhang W, Yuan Y, Zhu W, Shang A. Vaginal microecological characteristics of women in different physiological and pathological period. Front Cell Infect Microbiol. 2022; 12:959793.
52. Yoshikata R, Yamaguchi M, Mase Y, Tatsuzuki A, Myint KZY, Ohta H. Age-related changes, influencing factors, and crosstalk between vaginal and gut microbiota: A cross-sectional comparative study of pre- and postmenopausal women. J Womens Health (Larchmt). 2022; 31:1763-1772.
53. Ceccarani C, Foschi C, Parolin C, D'Antuono A, Gaspari V, Consolandi C, Laghi L, Camboni T, Vitali B, Severgnini M, Marangoni A. Diversity of vaginal microbiome and metabolome during genital infections. Sci Rep. 2019; 9:14095.
54. Trifanescu OG, Trifanescu RA, Mitrica RI, Bran DM, Serbanescu GL, Valcauan L, Marinescu SA, Gales LN, Tanase BC, Anghel RM. The female reproductive tract microbiome and cancerogenesis: A review story of bacteria, hormones, and disease. Diagnostics (Basel). 2023; 13:877.
55. Tian Y, Mai XD, Ma K, *et al*. Gut microbiota regulates the occurrence and development of metabolic diseases. Chin Sci Bull. 2021; 66:1602-1613.
56. Doaa M, Dalia M, Ahmed FS. Gut bacterial microbiota in psoriasis: A case control study. Afr J Microbiol Res. 2016; 10:1337-1343.
57. Rinninella E, Raoul P, Cintoni M, Franceschi F, Miggiano GAD, Gasbarrini A, Mele MC. What is the healthy gut microbiota composition? A changing ecosystem across age, environment, diet, and diseases. Microorganisms. 2019; 7:14.
58. Rodgers RJ, Avery JC, Moore VM, Davies MJ, Azziz R, Stener-Victorin E, Moran LJ, Robertson SA, Stepto NK, Norman RJ, Teede HJ. Complex diseases and co-morbidities: Polycystic ovary syndrome and type 2 diabetes mellitus. Endocr Connect. 2019; 8:R71-R75.
59. Ahlawat S, Asha, Sharma KK. Gut-organ axis: A microbial outreach and networking. Lett Appl Microbiol. 2021; 72:636-668.
60. Zhai L, Wu J, Lam YY, Kwan HY, Bian ZX, Wong HLX. Gut-microbial metabolites, probiotics and their roles in type 2 diabetes. Int J Mol Sci. 2021; 22:12846.
61. Chénard T, Prévost K, Dubé J, Massé E. Immune system modulations by products of the gut microbiota. Vaccines (Basel). 2020; 8:461.
62. Evans JM, Morris LS, Marchesi JR. The gut microbiome: The role of a virtual organ in the endocrinology of the host. J Endocrinol. 2013; 218:R37-R47.
63. Boulangé CL, Neves AL, Chilloux J, Nicholson JK, Dumas ME. Impact of the gut microbiota on inflammation, obesity, and metabolic disease. Genome Med. 2016; 8:42.
64. Barrett E, Ross RP, O'Toole PW, Fitzgerald GF, Stanton C. γ-Aminobutyric acid production by culturable bacteria from the human intestine. J Appl Microbiol. 2012; 113:411-417.
65. Lyte M. Probiotics function mechanistically as delivery vehicles for neuroactive compounds: Microbial endocrinology in the design and use of probiotics. Bioessays. 2011; 33:574-581.
66. Adlercreutz H, Pulkkinen MO, Hämäläinen EK, Korpela JT. Studies on the role of intestinal bacteria in metabolism of synthetic and natural steroid hormones. J Steroid Biochem. 1984; 20:217-229.
67. Raftogianis R, Creveling C, Weinshilboum R, Weisz J. Estrogen metabolism by conjugation. J Natl Cancer Inst Monogr. 2000; 27:113-124.
68. Kwa M, Plottel CS, Blaser MJ, Adams S. The intestinal microbiome and estrogen receptor-positive female breast cancer. J Natl Cancer Inst. 2016; 108:djw029.
69. Yoon K, Kim N. Roles of sex hormones and gender in the gut microbiota. J Neurogastroenterol Motil. 2021; 27:314-325.
70. Baker JM, Al-Nakkash L, Herbst-Kralovetz MM. Estrogen-gut microbiome axis: Physiological and clinical implications. Maturitas. 2017; 103:45-53.
71. Lu N, Li M, Lei H, Jiang X, Tu W, Lu Y, Xia D. Butyric acid regulates progesterone and estradiol secretion *via* cAMP signaling pathway in porcine granulosa cells. J Steroid Biochem Mol Biol. 2017; 172:89-97.
72. Liu L, Fu Q, Li T, Shao K, Zhu X, Cong Y, Zhao X. Gut

microbiota and butyrate contribute to nonalcoholic fatty liver disease in premenopause due to estrogen deficiency. PLoS One. 2022; 17:e0262855.
73. Vodstrcil LA, Twin J, Garland SM, Fairley CK, Hocking JS, Law MG, Plummer EL, Fethers KA, Chow EP, Tabrizi SN, Bradshaw CS. The influence of sexual activity on the vaginal microbiota and Gardnerella vaginalis clade diversity in young women. PLoS One. 2017; 12:e0171856.
74. Lee CY, Cheu RK, Lemke MM, Gustin AT, France MT, Hampel B, Thurman AR, Doncel GF, Ravel J, Klatt NR, Arnold KB. Quantitative modeling predicts mechanistic links between pre-treatment microbiome composition and metronidazole efficacy in bacterial vaginosis. Nat Commun. 2020; 11:6147.
75. Vitali B, Cruciani F, Picone G, Parolin C, Donders G, Laghi L. Vaginal microbiome and metabolome highlight specific signatures of bacterial vaginosis. Eur J Clin Microbiol Infect Dis. 2015; 34:2367-2376.
76. McMillan A, Rulisa S, Sumarah M, Macklaim JM, Renaud J, Bisanz JE, Gloor GB, Reid G. A multi-platform metabolomics approach identifies highly specific biomarkers of bacterial diversity in the vagina of pregnant and non-pregnant women. Sci Rep. 2015; 5:14174.
77. Wullaert A, Bonnet MC, Pasparakis M. NF-κB in the regulation of epithelial homeostasis and inflammation. Cell Res. 2011; 21:146-158.
78. Shen L, Zhang W, Yuan Y, Zhu W, Shang A. Vaginal microecological characteristics of women in different physiological and pathological period. Front Cell Infect Microbiol. 2022; 12:959793.
79. Gonçalves B, Ferreira C, Alves CT, Henriques M, Azeredo J, Silva S. Vulvovaginal candidiasis: Epidemiology, microbiology and risk factors. Crit Rev Microbiol. 2016; 42:905-927.
80. McClelland RS, Richardson BA, Hassan WM, Graham SM, Kiarie J, Baeten JM, Mandaliya K, Jaoko W, Ndinya-Achola JO, Holmes KK. Prospective study of vaginal bacterial flora and other risk factors for vulvovaginal candidiasis. J Infect Dis. 2009; 199:1883-1890.
81. Brown SE, Schwartz JA, Robinson CK, O'Hanlon DE, Bradford LL, He X, Mark KS, Bruno VM, Ravel J, Brotman RM. The vaginal microbiota and behavioral factors associated with genital Candida albicans detection in reproductive-age women. Sex Transm Dis. 2019; 46:753-758.
82. Idahl A, Le Cornet C, González Maldonado S, *et al*. Serologic markers of Chlamydia trachomatis and other sexually transmitted infections and subsequent ovarian cancer risk: Results from the EPIC cohort. Int J Cancer. 2020; 147:2042-2052.
83. Shipitsyna E, Khusnutdinova T, Budilovskaya O, Krysanova A, Shalepo K, Savicheva A, Unemo M. Bacterial vaginosis-associated vaginal microbiota is an age-independent risk factor for Chlamydia trachomatis, Mycoplasma genitalium and Trichomonas vaginalis infections in low-risk women, St. Petersburg, Russia. Eur J Clin Microbiol Infect Dis. 2020; 39:1221-1230.
84. Molenaar MC, Singer M, Ouburg S. The two-sided role of the vaginal microbiome in Chlamydia trachomatis and Mycoplasma genitalium pathogenesis. J Reprod Immunol. 2018; 130:11-17.
85. Liu Y, Ko EY, Wong KK, Chen X, Cheung WC, Law TS, Chung JP, Tsui SK, Li TC, Chim SS. Endometrial microbiome in infertile women with and without chronic endometritis as diagnosed using a quantitative and reference range-based method. Fertil Steril. 2019; 112:707-717.
86. Cicinelli E, Matteo M, Tinelli R, Lepera A, Alfonso R, Indraccolo U, Marrocchella S, Greco P, Resta L. Prevalence of chronic endometritis in repeated unexplained implantation failure and the IVF success rate after antibiotic therapy. Hum Reprod. 2015; 30:323-330.
87. Weckel A, Guilbert T, Lambert C, Plainvert C, Goffinet F, Poyart C, Méhats C, Fouet A. Streptococcus pyogenes infects human endometrium by limiting the innate immune response. J Clin Invest. 2021; 131:e130746.
88. Kitaya K, Matsubayashi H, Yamaguchi K, Nishiyama R, Takaya Y, Ishikawa T, Yasuo T, Yamada H. Chronic endometritis: Potential cause of infertility and obstetric and neonatal complications. Am J Reprod Immunol. 2016; 75:13-22.
89. Chen P, Chen P, Guo Y, Fang C, Li T. Interaction between chronic endometritis caused endometrial microbiota disorder and endometrial immune environment change in recurrent implantation failure. Front Immunol. 2021; 12:748447.
90. Marchenko LA, Chernukha GE, Yakushevskaya OV, Gombolevskaya NA, Muravieva VV, Priputnevich TV, Ankirskaya AS. Clinical and microbiological aspects of chronic endometritis in women of reproductive age. Antibiot Khimioter. 2016; 61:44-51.
91. Kovalenko VL, Voropaeva EE, Kozachkov EL, Kozachkova EA. Endometrial pathomorphology in bacterial vaginosis associated with chronic endometritis. Arkh Patol. 2008; 70:6-8.
92. Horban NY, Vovk IB, Lysiana TO, Ponomariova IH, Zhulkevych IV. Peculiarities of uterine cavity biocenosis in patients with different types of endometrial hyperproliferative pathology. J Med Life. 2019; 12:266-270.
93. Fang RL, Chen LX, Shu WS, Yao SZ, Wang SW, Chen YQ. Barcoded sequencing reveals diverse intrauterine microbiomes in patients suffering with endometrial polyps. Am J Transl Res. 2016; 8:1581-1592.
94. Liang J, Li M, Zhang L, Yang Y, Jin X, Zhang Q, Lv T, Huang Z, Liao Q, Tong X. Analysis of the microbiota composition in the genital tract of infertile patients with chronic endometritis or endometrial polyps. Front Cell Infect Microbiol. 2023; 13:1125640.
95. Ahn SH, Monsanto SP, Miller C, Singh SS, Thomas R, Tayade C. Pathophysiology and immune dysfunction in endometriosis. Biomed Res Int. 2015; 2015:795976.
96. Lin WC, Chang CY, Hsu YA, Chiang JH, Wan L. Increased risk of endometriosis in patients with lower genital tract infection: A nationwide cohort study. Medicine (Baltimore). 2016; 95:e2773.
97. Akiyama K, Nishioka K, Khan KN, Tanaka Y, Mori T, Nakaya T, Kitawaki J. Molecular detection of microbial colonization in cervical mucus of women with and without endometriosis. Am J Reprod Immunol. 2019; 82:e13147.
98. Yang Q, Wang Y, Cai H, Zhou Q, Zeng L, Li S, Du H, Wei W, Zhang W, Dai W, Wu R. Translocation of vaginal and cervical low-abundance non-Lactobacillus bacteria notably associate with endometriosis: A pilot study. Microb Pathog. 2023; 183:106309.
99. Jiang I, Yong PJ, Allaire C, Bedaiwy MA. Intricate Connections between the microbiota and endometriosis. Int J Mol Sci. 2021; 22:5644.
100. Moreno I, Simon C. Relevance of assessing the uterine

microbiota in infertility. Fertil Steril. 2018; 110:337-343.
101. Tu Y, Zheng G, Ding G, Wu Y, Xi J, Ge Y, Gu H, Wang Y, Sheng J, Liu X, Jin L, Huang H. Comparative analysis of lower genital tract microbiome between PCOS and healthy women. Front Physiol. 2020; 11:1108.
102. Zhou F, Xing Y, Cheng T, Yang L, Ma H. Exploration of hub genes involved in PCOS using biological informatics methods. Medicine (Baltimore). 2022; 101:e30905.
103. Wei J, Wang R, Li CX, Luo XY, Liang ZW, Yao L. Expression of steroid hormone receptors and integrins in the endometrium during the window period of untreated polycystic ovary syndrome. Journal of Practical Medicine. 2009; 25:3979-3982.
104. Torres PJ, Siakowska M, Banaszewska B, Pawelczyk L, Duleba AJ, Kelley ST, Thackray VG. Gut microbial diversity in women with polycystic ovary syndrome correlates with hyperandrogenism. J Clin Endocrinol Metab. 2018; 103:1502-1511.
105. Zheng Y, Yu J, Liang C, Li S, Wen X, Li Y. Characterization on gut microbiome of PCOS rats and its further design by shifts in high-fat diet and dihydrotestosterone induction in PCOS rats. Bioprocess Biosyst Eng. 2021; 44:953-964.
106. Yang YY, Pereyra LP, Young RB, Reardon KF, Borch T. Testosterone-mineralizing culture enriched from swine manure: Characterization of degradation pathways and microbial community composition. Environ Sci Technol. 2011; 45:6879-6886.
107. Ridlon JM, Ikegawa S, Alves JM, *et al*. Clostridium scindens: A human gut microbe with a high potential to convert glucocorticoids into androgens. J Lipid Res. 2013; 54:2437-2449.
108. Zeibich L, Koebele SV, Bernaud VE, Ilhan ZE, Dirks B, Northup-Smith SN, Neeley R, Maldonado J, Nirmalkar K, Files JA, Mayer AP, Bimonte-Nelson HA, Krajmalnik-Brown R. Surgical menopause and estrogen therapy modulate the gut microbiota, obesity markers, and spatial memory in rats. Front Cell Infect Microbiol. 2021; 11:702628.
109. Qi X, Yun C, Sun L, Xia J, *et al*. Gut microbiota-bile acid-interleukin-22 axis orchestrates polycystic ovary syndrome. Nat Med. 2019; 25:1225-1233.
110. Zhang J, Sun Z, Jiang S, Bai X, Ma C, Peng Q, Chen K, Chang H, Fang T, Zhang H. Probiotic bifidobacterium lactis V9 regulates the secretion of sex hormones in polycystic ovary syndrome patients through the gut-brain axis. mSystems. 2019; 4:e00017-19.
111. Aversa A, La Vignera S, Rago R, Gambineri A, Nappi RE, Calogero AE, Ferlin A. Fundamental concepts and novel aspects of polycystic ovarian syndrome: Expert consensus resolutions. Front Endocrinol (Lausanne). 2020; 11:516.
112. Cunningham AL, Stephens JW, Harris DA. Intestinal microbiota and their metabolic contribution to type 2 diabetes and obesity. J Diabetes Metab Disord. 2021; 20:1855-1870.
113. Svensson A, Brunkwall L, Roth B, Orho-Melander M, Ohlsson B. Associations between endometriosis and gut microbiota. Reprod Sci. 2021; 28:2367-2377.
114. Ata B, Yildiz S, Turkgeldi E, Brocal VP, Dinleyici EC, Moya A, Urman B. The endobiota study: Comparison of vaginal, cervical and gut microbiota between women with stage 3/4 endometriosis and healthy controls. Sci Rep. 2019; 9:2204.
115. Leonardi M, Hicks C, El-Assaad F, El-Omar E, Condous G. Endometriosis and the microbiome: A systematic review. BJOG. 2020; 127:239-249.
116. Wei Y, Tan H, Yang R, Yang F, Liu D, Huang B, OuYang L, Lei S, Wang Z, Jiang S, Cai H, Xie X, Yao S, Liang Y. Gut dysbiosis-derived β-glucuronidase promotes the development of endometriosis. Fertil Steril. 2023; 120:682-694.
117. Uzuner C, Mak J, El-Assaad F, Condous G. The bidirectional relationship between endometriosis and microbiome. Front Endocrinol (Lausanne). 2023; 14:1110824.
118. Baj A, Moro E, Bistoletti M, Orlandi V, Crema F, Giaroni C. Glutamatergic signaling along the microbiota-gut-brain axis. Int J Mol Sci. 2019; 20:1482.
119. Brooks RA, Fleming GF, Lastra RR, Lee NK, Moroney JW, Son CH, Tatebe K, Veneris JL. Current recommendations and recent progress in endometrial cancer. CA Cancer J Clin. 2019; 69:258-279.
120. Borella F, Carosso AR, Cosma S, Preti M, Collemi G, Cassoni P, Bertero L, Benedetto C. Gut microbiota and gynecological cancers: A summary of pathogenetic mechanisms and future directions. ACS Infect Dis. 2021; 7:987-1009.
121. Caselli E, Soffritti I, D'Accolti M, Piva I, Greco P, Bonaccorsi G. Atopobium vaginae and Porphyromonas somerae induce proinflammatory cytokines expression in endometrial cells: A possible implication for endometrial cancer? Cancer Manag Res. 2019; 11:8571-8575.
122. Neggers YH, Nansel TR, Andrews WW, Schwebke JR, Yu KF, Goldenberg RL, Klebanoff MA. Dietary intake of selected nutrients affects bacterial vaginosis in women. J Nutr. 2007; 137:2128-2133.
123. Tohill BC, Heilig CM, Klein RS, Rompalo A, Cu-Uvin S, Piwoz EG, Jamieson DJ, Duerr A. Nutritional biomarkers associated with gynecological conditions among US women with or at risk of HIV infection. Am J Clin Nutr. 2007; 85:1327-1334.
124. Marchesi JR, Adams DH, Fava F, *et al*. The gut microbiota and host health: A new clinical frontier. Gut. 2016; 65:330-339.
125. Chen X, Lu Y, Chen T, Li R. The female vaginal microbiome in health and bacterial vaginosis. Front Cell Infect Microbiol. 2021; 11:631972.
126. Wan Y, Wang F, Yuan J, Li J, Jiang D, Zhang J, Li H, Wang R, Tang J, Huang T, Zheng J, Sinclair AJ, Mann J, Li D. Effects of dietary fat on gut microbiota and faecal metabolites, and their relationship with cardiometabolic risk factors: A 6-month randomised controlled-feeding trial. Gut. 2019; 68:1417-1429.
127. Barrea L, Arnone A, Annunziata G, Muscogiuri G, Laudisio D, Salzano C, Pugliese G, Colao A, Savastano S. Adherence to the Mediterranean diet, dietary patterns and body composition in women with polycystic ovary syndrome (PCOS). Nutrients. 2019; 11:2278.
128. Barrea L, Marzullo P, Muscogiuri G, Di Somma C, Scacchi M, Orio F, Aimaretti G, Colao A, Savastano S. Source and amount of carbohydrate in the diet and inflammation in women with polycystic ovary syndrome. Nutr Res Rev. 2018; 31:291-301.
129. Singh P, Rawat A, Alwakeel M, Sharif E, Al Khodor S. The potential role of vitamin D supplementation as a gut microbiota modifier in healthy individuals. Sci Rep. 2020; 10:21641.
130. Kalaitzopoulos DR, Samartzis N, Daniilidis A, Leeners B, Makieva S, Nirgianakis K, Dedes I, Metzler JM, Imesch P, Lempesis IG. Effects of vitamin D supplementation

in endometriosis: A systematic review. Reprod Biol Endocrinol. 2022; 20:176.
131. Shamasbi SG, Ghanbari-Homayi S, Mirghafourvand M. The effect of probiotics, prebiotics, and synbiotics on hormonal and inflammatory indices in women with polycystic ovary syndrome: A systematic review and meta-analysis. Eur J Nutr. 2020; 59:433-450.
132. Chenoll E, Moreno I, Sánchez M, Garcia-Grau I, Silva Á, González-Monfort M, Genovés S, Vilella F, Seco-Durban C, Simón C, Ramón D. Selection of new probiotics for endometrial health. Front Cell Infect Microbiol. 2019; 9:114.
133. Heczko PB, Tomusiak A, Adamski P, Jakimiuk AJ, Stefański G, Mikołajczyk-Cichońska A, Suda-Szczurek M, Strus M. Supplementation of standard antibiotic therapy with oral probiotics for bacterial vaginosis and aerobic vaginitis: A randomised, double-blind, placebo-controlled trial. BMC Womens Health. 2015; 15:115.
134. Nasri K, Jamilian M, Rahmani E, Bahmani F, Tajabadi-Ebrahimi M, Asemi Z. The effects of synbiotic supplementation on hormonal status, biomarkers of inflammation and oxidative stress in subjects with polycystic ovary syndrome: A randomized, double-blind, placebo-controlled trial. BMC Endocr Disord. 2018; 18:21.
135. Molina NM, Sola-Leyva A, Saez-Lara MJ, Plaza-Diaz J, Tubić-Pavlović A, Romero B, Clavero A, Mozas-Moreno J, Fontes J, Altmäe S. New opportunities for endometrial health by modifying uterine microbial composition: Present or future? Biomolecules. 2020; 10:593.
136. Itoh H, Sashihara T, Hosono A, Kaminogawa S, Uchida M. Lactobacillus gasseri OLL2809 inhibits development of ectopic endometrial cell in peritoneal cavity *via* activation of NK cells in a murine endometriosis model. Cytotechnology. 2011; 63:205-210.
137. Khodaverdi S, Mohammadbeigi R, Khaledi M, Mesdaghinia L, Sharifzadeh F, Nasiripour S, Gorginzadeh M. Beneficial effects of oral Lactobacillus on pain severity in women suffering from endometriosis: A pilot placebo-controlled randomized clinical trial. Int J Fertil Steril. 2019; 13:178-183.
138. Antwis RE, Edwards KL, Unwin B, Walker SL, Shultz S. Rare gut microbiota associated with breeding success, hormone metabolites and ovarian cycle phase in the critically endangered eastern black rhino. Microbiome. 2019; 7:27.
139. Salam MA, Islam MA, Paul SI, Rahman MM, Rahman ML, Islam F, Rahman A, Shaha DC, Alam MS, Islam T. Gut probiotic bacteria of Barbonymus gonionotus improve growth, hematological parameters and reproductive performances of the host. Sci Rep. 2021; 11:10692.
140. Guo Y, Qi Y, Yang X, Zhao L, Wen S, Liu Y, Tang L. Association between polycystic ovary syndrome and gut microbiota. PLoS One. 2016; 11:e0153196.
141. Chadchan SB, Popli P, Ambati CR, Tycksen E, Han SJ, Bulun SE, Putluri N, Biest SW, Kommagani R. Gut microbiota-derived short-chain fatty acids protect against the progression of endometriosis. Life Sci Alliance. 2021; 4:e202101224.
142. Cao S, Guo D, Yin H, Ding X, Bai S, Zeng Q, Liu J, Zhang K, Mao X, Wang J. Improvement in ovarian function following fecal microbiota transplantation from high-laying rate breeders. Poult Sci. 2023; 102:102467.
143. Moreno I, Simon C. Deciphering the effect of reproductive tract microbiota on human reproduction. Reprod Med Biol. 2018; 18:40-50.
144. Koedooder R, Mackens S, Budding A, Fares D, Blockeel C, Laven J, Schoenmakers S. Identification and evaluation of the microbiome in the female and male reproductive tracts. Hum Reprod Update. 2019; 25:298-325.
145. Shahi SK, Zarei K, Guseva NV, Mangalam AK. Microbiota analysis using two-step PCR and next-generation 16S rRNA gene sequencing. J Vis Exp. 2019; 152:10.3791/59980.

Received June 11, 2023; Revised December 6, 2023; Accepted December 13, 2023.

[§]These authors contributed equally to this work.
**Address correspondence to:*
Ling Wang and Lisha Li, Laboratory for Reproductive Immunology, Obstetrics and Gynecology Hospital of Fudan University, 419 Fangxie Road, Shanghai 200011, China.
E-mail: dr.wangling@fudan.edu.cn (WL); lishasmv@163.com (LL)

Released online in J-STAGE as advance publication December 17, 2023.

Original Article

DOI: 10.5582/bst.2023.01294

Risk factors for postoperative recurrence of pT2-3N0M0 esophageal squamous cell carcinoma and patterns of its recurrence

Li Niu[1,§], Bo Hu[2,§], Li Zhang[1], Mei Kang[1,*]

[1] Department of Radiation Oncology, The First Affiliated Hospital of Anhui Medical University, Hefei, Anhui, China.
[2] Department of Orthopedics, The First Affiliated Hospital of Anhui Medical University, Hefei, Anhui, China.

SUMMARY This study aimed to explore the patterns of postoperative recurrence in patients with pT2-3N0M0 esophageal squamous cell carcinoma (ESCC) and to identify the risk factors for the recurrence. Patients with pT2-3N0M0 ESCC who were treated at our hospital from January 2010 to August 2019 were divided into three categories: those with anastomotic recurrence, those with lymph node recurrence, and those with hematogenous metastasis. The sites of initial recurrence and metastasis were counted and potential risk factors were analyzed using univariate and multivariate Cox proportional hazard regression. Four hundred and eighty-five patients with pT2-3N0M0 ESCC were ultimately included, 176 (36.29%) of whom experienced tumor recurrence or metastasis. Cox multivariate analysis revealed that the postoperative T-stage, procedure, tumor location, and degree of differentiation were independent risk factors for postoperative recurrence ($P < 0.05$). The median time of recurrence was 38 months, and the most common site of recurrence was the lymph nodes in 126 patients (71.59%), followed by hematogenous metastasis in 73 patients (41.47%), and anastomotic recurrence in 21 patients (11.93%). 119 patients (67.61%) experienced recurrence within 36 months, with a probability of recurrence of 84.09% within 5 years, and recurrence remained relatively unchanged after 5 years. The proportion of postoperative lymph node recurrence and hematogenous metastasis in patients with pT3N0M0 ESCC was significantly higher than that in patients with pT2N0M0 ESCC ($P < 0.05$). At higher tumor locations in the body, the proportion of lymph node recurrence increased ($P < 0.05$). In conclusion, postoperative T-stage, procedure, tumor location, and degree of differentiation were independent risk factors for postoperative recurrence in pT2-3N0M0 ESCC, with regional lymph node recurrence being the most common pattern, emphasizing the importance of regional lymph nodes in this context.

Keywords pT2-3N0M0 esophageal squamous cell carcinoma (ESCC), postoperative recurrence, risk factor, regional lymph node

1. Introduction

Esophageal cancer (EC) is a common malignant tumor of the digestive system in China. Fifty percent of patients have confirmed EC each year, and more than 90% of EC is squamous cell carcinoma, which has been a major public health problem (*1*). Radical resection combined with systemic lymph node dissection was the standard treatment for ESCC, and regional recurrence and distant metastasis were largely responsible for postoperative treatment failure (*2*). A study has reported that positive lymph nodes were the key factor affecting postoperative recurrence and survival status in patients with ESCC, but patients with ESCC and negative lymph nodes also exhibited a high probability of postoperative recurrence (approximately 30%) (*3*). Therefore, the indicators that may affect postoperative recurrence and prognosis in patients with ESCC and negative lymph nodes, and pT2-3N0M0 in particular, need to be studied further.

Currently, studies on risk factors for recurrence in patients with ESCC and negative lymph nodes after radical esophagectomy are conflicting. Several studies have found that the prognosis for patients with ESCC with negative lymph nodes was influenced by the T-stage and the degree of tumor histological differentiation (*4,5*). A crucial task has been to determine the risk factors for postoperative recurrence of EC. Patients with high-risk factors need to be screened for recurrence, postoperative adjuvant treatment needs to be actively provided, and regular monitoring needs to be enhanced.

To investigate the risk factors affecting postoperative recurrence of pT2-3N0M0 ESCC, we conducted a

study at the First Affiliated Hospital of Anhui Medical University. We analyzed demographic and pathological data from patients with pT2-3N0M0 ESCC who underwent radical surgery. This study also analyzed the patterns of postoperative recurrence in order to provide a reference for postoperative monitoring and treatment of patients with ESCC.

2. Patients and Methods

2.1. Patient selection

Information on patients who underwent radical surgery at this Hospital from January 2010 to December 2020 was screened. To allow for a sufficient frequency of follow-up, we ultimately included 485 patients with pT2-3N0M0 ESCC and summarized all patient data. All patients provided informed consent at the time of surgery, including consent to publish and report their data.

The inclusion criteria were as follows: 1) Received radical surgery (R0 resection); 2) The postoperative pathological diagnosis was squamous cell carcinoma; 3) The postoperative pathological staging was pT2-3N0M0 (according to the 8th edition of the AJCC TNM staging system); 4) Having complete postoperative pathological data; 5) Did not undergo any anti-tumor treatment before surgery, including chemotherapy, radiotherapy, immunotherapy, tumor intervention therapy, or laser therapy; and 6) Information on recurrence is available.

The exclusion criteria were as follows: 1) Age under 18 and over 85; 2) Lack of complete postoperative clinical and pathological data; 3) Lack of specific information on postoperative recurrence; 4) Have a history of malignant tumors in the past, or have been found to have primary malignant tumors in other locations during follow-up; 5) Cervical esophageal cancer or gastroesophageal junction tumor; and 6) Progression-free survival (PFS) of less than 3 months.

2.2. Diagnosis of recurrence

The diagnostic criteria for lymph node recurrence included: 1) Enhanced computed tomography (CT) or magnetic resonance (MR) imaging indicating a short axis of ≥ 10 mm or the presence of ≥ 3 affected lymph nodes in the same area, or necrosis or capsule invasion of lymph nodes; 2) Affected lymph nodes found in the tracheoesophageal sulcus, regardless of size, accompanied by hoarseness or vocal cord paralysis; 3) Dynamic imaging revealed changes in lymph nodes, such as a significant increase in lymph node volume, number, or the appearance of new lymph nodes; 4) There is a clear diagnosis of cancer metastasis based on puncture cytology or pathological biopsy; 5) Positron emission tomography (PET) revealed a standardized uptake value (SUV) of ≥ 2.4.

Diagnosis criteria for anastomotic recurrence: 1) Clear diagnosis based on gastroscopy and pathology; 2) Results of PET were positive and indicative of recurrence based on the patient's symptoms.

Hematological metastasis occurred in the lungs, liver, bone, and other areas, mainly due to new lesions discovered through imaging studies, such as CT, ultrasound, MR, or PET.

We only counted the sites that were first identified as recurrence or metastasis. If there were 2 or more sites with recurrence or metastasis and the interval was within 1 month, those were all recorded. If different sites of recurrence or metastasis were found in an interval longer than 1 month, only the first recurrence or metastasis was recorded.

2.3. Regional lymph nodes

Based on the Japan Esophagus Society (JES) standard lymph node anatomy and the range of lymph node drainage areas in the abdominal cavity of patients with gastric cancer, the sites where lymph node recurrence first occurred were statistically classified as cervical lymph node area recurrence, mediastinal lymph node area recurrence, or abdominal lymph node area recurrence (*6,7*).

The specific scope was as follows: 1) Neck lymph nodes: 100-104 groups of lymph nodes; 2) Mediastinal lymph nodes: Uniformly including the upper, middle, and lower mediastinal lymph nodes, this is a group of 105-112 lymph nodes; 3) Abdominal lymph nodes: 1-16 groups of lymph nodes.

2.4. Follow-up

All patients were followed up immediately after surgery, and the deadline was December 2021. The follow-up methodology mainly involved retrieving information from the outpatient or inpatient system. Several patients were contacted by telephone to obtain more detailed and accurate information on diagnosis, treatment, and recurrence. The frequency of follow-up was once every 2-4 months within 2 years after surgery, once every 6 months within 2-5 years after surgery, and once every 1 year after 5 years after surgery. The postoperative follow-up included an esophageal barium swallow or radioactive iodine uptake study, imaging studies of the neck, chest, and abdomen, and CT and MR. Ultrasound of the neck or abdomen could also be performed. If abnormalities were found, further examination was required. Based on the patient's specific circumstances and symptoms, a bone scan, PET, gastroscopy, endoscopic ultrasound, puncture cytology, or biopsy pathology examination could be performed as necessary to assist in diagnosis.

2.5. Statistical analysis

The software IBM SPSS Statistics (version 27.0;

IBM Crop, Armonk, NY, USA) and R Foundation for Statistical Computing, Vienna, Australia (version 4.2.2) were used for statistical analysis. Counts used a chi square test or Fisher's exact probability test. The relevant pathological factors that affect postoperative recurrence were first analyzed using univariate and multivariate Cox regression. Disease-free survival (DFS) was defined as the period from the date of esophageal cancer surgery to the date of tumor recurrence or death at any location, or until the last follow-up date. Overall survival (OS) was defined as the time from when radical surgery for esophageal cancer was undergone to the time of death or last follow-up for any reason. All time events were estimated using Kaplan-Meier analysis and were compared using the log-rank test. $P < 0.05$ was considered statistically significant.

3. Results

3.1. Characteristics of patients

We ultimately enrolled 485 patients with pT2-3N0M0 ESCC, and measured 13 relevant variables, including patient age, sex, T-stage, procedure, the degree of differentiation, the location of the primary tumor, the diameter (long and short axes) of the tumor, the number of lymph nodes dissected, postoperative adjuvant treatment, vessel invasion, perineural invasion, and carcinoma nodules. Up to the last follow-up, 309 of 485 patients with ESCC (63.71%) did not experience tumor recurrence or metastasis, while 176 patients (36.29%) experienced tumor recurrence or metastasis. The median time of recurrence was 38 months (ranging from 3 to 141 months), and 119 patients (67.61%) experienced recurrence within 36 months.

Considering the patient's recurrence status, patients were divided into two groups and a statistical analysis of the included factors was performed. Except for the procedure, T-stage, location of the esophageal tumor, degree of differentiation, and postoperative adjuvant treatment plan, there were no significant differences in the research factors between the groups ($P < 0.05$). The baseline data of all patients are shown in Table 1.

Until the last follow-up, the median duration of follow-up was 56 months (range: 3-144 months). Of the 485 enrolled patients, 286 survived, 199 experienced tumor recurrence or death. The median OS of all patients was 57 months (range 5-141 months), and the median OS of patients in the recurrence group was 49 months (range 5-140 months). The survival curves of the two groups are shown in Figure 1.

3.2. Cox regression analysis

Cox univariate analysis indicated that the T-stage, procedure, the degree of differentiation, tumor diameter, and postoperative adjuvant treatment were risk factors for postoperative recurrence ($P < 0.05$), while other factors did not impact recurrence significantly.

Multivariate Cox analysis revealed that the T-stage, procedure, tumor location, and degree of differentiation were independent risk factors for postoperative recurrence ($P < 0.05$). As can be seen in Table 2, the risk of postoperative recurrence in patients with pT3N0M0 ESCC was significantly higher than in patients with pT2N0M0 ESCCs (HR = 5.21, 95% CI 2.70-7.33, $P < 0.01$). In terms of procedure selection, the risk of postoperative recurrence caused by open esophagectomy (OE) was 1.48 times higher than that of minimally invasive esophagectomy (MIE) (HR = 1.48, 95% CI 1.07-2.03, $P = 0.02$), and the combination of MIE and OE did not impact postoperative recurrence. Compared to ESCC in the upper thoracic region, the risk of recurrence in the middle and lower thoracic regions decreased by 42% ($P = 0.03$) and 54% ($P = 0.01$), respectively. Compared to poorly differentiated ESCC, the risk of recurrence decreased by 46% ($P = 0.04$).

3.3. Patterns of postoperative recurrence

The results of this study depict that the time of recurrence ranged from 3 months to 141 months (median time of recurrence: 24 months), and 176 patients with pT2-3N0M0 ESCC experienced recurrence or metastasis. The rate of recurrence was 36.29%. There were 126 patients with lymph node recurrence (71.59%), 73 with hematogenous metastasis (41.47%), and 21 with anastomotic recurrence (11.93%). Several patients also experienced concurrent recurrence and metastasis. The majority of patients experienced recurrence within 3 years (67.61%), with a probability of recurrence of 84.09% within 5 years. After that, recurrence was basically unchanged.

Among lymph node recurrence, mediastinal lymph nodes were most often affected (13.20%), followed by the cervical lymph nodes (10.31%) and abdominal lymph nodes (5.98%). In hematogenous metastases, lung metastasis was the most common (5.36%), followed by bone metastasis (4.54%), liver metastasis (3.51%), and other metastases such as brain metastasis, pleural metastasis, and malignant serous effusion (3.92%). Some patients also experienced multiple organ metastases at the same time. The specific distribution is detailed in Table 3 and Figure 2.

3.4. Analysis of recurrence patterns

Multivariate analysis shows that both the T-stage and tumor location were independent risk factors for PFS. The two indicators' impact on OS was further analyzed. Results indicated that the T-stage was a high-risk factor affecting OS ($P < 0.01$), while the location of tumor did not impact OS significantly (Figure 3).

As shown in Table 4, compared to patients with

Table 1. Baseline characteristics of included patients

Characteristics	Total (n = 485)	Group with recurrence (n = 176)	Group without recurrence (n = 309)	P value
Sex				0.23
Male	367 (75.67%)	139 (78.98%)	228 (73.79%)	
Female	118 (24.33%)	37 (21.02%)	81 (26.21%)	
Age				0.72
≤ 55 years	66 (13.61%)	21 (11.93%)	45 (14.56%)	
56-66 years	248 (51.13%)	92 (52.27%)	156 (50.49%)	
> 66 years	171 (35.26%)	63 (35.80%)	108 (34.95%)	
T-stage				< 0.01
T2N0	386 (75.59%)	98 (55.68%)	288 (93.20%)	
T3N0	99 (20.41%)	78 (44.32%)	21 (6.8%)	
Procedures				0.04
MIE	240 (49.48%)	76 (43.18%)	164 (53.07%)	
OE	198 (40.82%)	85 (48.30%)	113 (36.57%)	
MIE and OE	47 (9.69%)	15 (8.25%)	32 (10.36%)	
Location				0.01
Upper thoracic region	40 (8.25%)	20 (11.36%)	20 (6.47%)	
Middle thoracic region	326 (67.22%)	125 (71.02%)	201 (65.05%)	
Lower thoracic region	119 (24.54%)	31 (17.61%)	88 (28.48%)	
Differentiation				0.04
Poorly differentiated	106 (21.86%)	43 (24.43%)	63 (20.39%)	
Moderately differentiated	326 (67.22%)	122 (69.32%)	204 (66.02%)	
Well-differentiated	53 (10.93%)	11 (6.25%)	42 (13.59%)	
Tumor diameter (long axis)				0.05
≤ 3 cm	234 (48.25%)	74 (42.05%)	160 (51.78%)	
> 3 cm	251 (51.75%)	102 (57.95%)	149 (48.22%)	
Tumor diameter (short axis)				0.89
≤ 3 cm	417 (85.98%)	152 (86.36%)	265 (85.76%)	
> 3 cm	68 (14.02%)	24 (13.64%)	44 (14.24%)	
Vessel invasion				0.19
Yes	33 (6.80%)	8 (4.55%)	25 (8.09%)	
No	452 (93.20%)	168 (95.45%)	284 (91.19%)	
Perineural invasion				0.33
Yes	19 (3.92%)	9 (5.11%)	10 (3.24%)	
No	466 (96.08%)	167 (94.89%)	299 (96.76%)	
Carcinoma nodules				0.90
Yes	16 (3.30%)	6 (3.41%)	10 (3.24%)	
No	468 (96.49%)	169 (96.02%)	299 (96.76%)	
Resected lymph nodes				0.29
< 15	325 (67.01%)	112 (63.64%)	213 (68.93%)	
≥ 15	160 (32.99%)	64 (36.36%)	96 (31.07%)	
Postoperative treatment				< 0.01
Surgery only	268 (55.26%)	80 (45.45%)	188 (60.84%)	
Radiotherapy	49 (10.10%)	18 (10.23%)	31 (10.03%)	
Chemotherapy	137 (28.25%)	69 (39.20%)	68 (22.01%)	
Radiochemotherapy	31 (6.39%)	9 (5.11%)	22 (7.12%)	

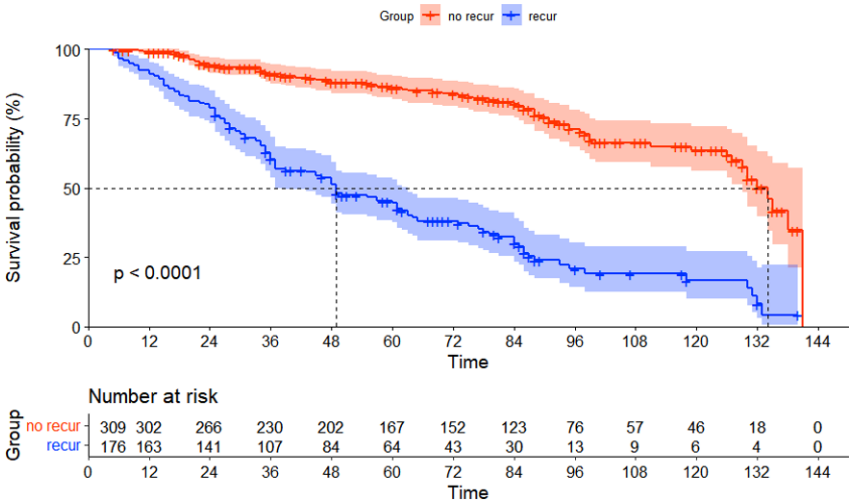

Figure 1. OS curves for patients in the group with recurrence and the group without recurrence.

Table 2. Univariate and multivariate Cox analysis of variables affecting the postoperative recurrence of pT2-3N0M0 ESCC

Characteristics	Univariate analysis			Multivariate analysis		
	HR	95%CI	*P* value	HR	95%CI	*P* value
Sex						
Male	1.00					
Female	0.79	0.55-1.13	0.20			
Age						
≤ 55 years	1.00					
56-66 years	1.13	0.70-1.82	0.61			
> 66 years	1.33	0.81-2.19	0.26			
T-stage						
T2N0	1.00			1.00		
T3N0	5.88	4.30-8.03	< 0.01	5.21	2.70-7.33	< 0.01
Procedures						
MIE	1.00			1.00		
OE	1.49	1.09-2.03	0.01	1.48	1.07-2.03	0.02
MIE and OE	0.96	0.55-1.67	0.88	1.15	0.66-2.07	0.63
Location						
Upper thoracic region	1.00			1.00		
Middle thoracic region	0.69	0.43-1.12	0.13	0.58	0.35-0.95	0.03
Lower thoracic region	0.45	0.26-0.79	< 0.01	0.46	0.25-0.83	0.01
Differentiation						
Poorly differentiated	1.00			1.00		
Moderately differentiated	0.94	0.66-1.33	0.71	0.86	0.61-1.24	0.43
Well-differentiated	0.44	0.22-0.86	0.02	0.54	0.27-1.07	0.04
Tumor diameter (long axis)						
≤ 3 cm	1.00			1.00		
> 3 cm	1.35	1.00-1.82	0.04	1.12	0.82-1.54	0.47
Tumor diameter (short axis)						
≤ 3 cm	1.00					
> 3 cm	1.07	0.69-1.64	0.78			
Vessel invasion						
Yes	1.00					
No	0.62	0.31-1.274	0.19			
Perineural invasion						
Yes	1.00					
No	0.83	0.68-1.61	0.40			
Carcinoma nodules						
Yes	1.00					
No	0.90	0.44-2.24	0.98			
Resected lymph nodes						
< 15	1.00					
≥ 15	0.98	0.68-1.41	0.91			
Postoperative treatment						
Surgery only	1.00			1.00		
Radiotherapy	1.96	1.42-2.71	0.01	1.31	0.93-1.84	0.12
Chemotherapy	1.31	0.78-2.18	0.30	1.03	0.60-1.76	0.91
Radiochemotherapy	1.09	0.54-2.16	0.82	0.85	0.42-1.72	0.65

T2 ESCC, the rate of recurrence in patients with T3 ESCC was significantly high ($P < 0.01$). In terms of hematogenous metastasis, the total probability of postoperative hematogenous metastasis in T3 ESCC was higher than that in T2 ESCC. Patients with ESCC in the T3 stage exhibited a higher proportion of bone metastasis and other metastasis, but there were no significant differences in the proportion of liver metastasis and lung metastasis. The probability of anastomotic recurrence in ESCC in the T3 stage was slightly higher than that in the T2 stage, but the difference was not statistically significant ($P = 0.05$).

Similarly, the patterns of recurrence were analyzed at different locations (Table 5). The results indicated that the proportion of mediastinal lymph node recurrence varied depending on the location of the tumor. As the location moved up, the proportion of lymph node recurrence increased ($P < 0.05$). However, there were no statistical differences in different regional lymph nodes. Pulmonary and bone metastases were the most common types of hematogenous metastasis, but statistical analysis revealed that there were no significant differences in the proportion of hematogenous metastasis and anastomotic recurrence after surgery in different locations ($P < 0.05$).

4. Discussion

The current study found that the postoperative T-stage, procedure, location, and degree of differentiation were

independent risk factors for postoperative recurrence in patients with pT2-3N0M0 ESCC. The T-stage was an important basis for defining pathological staging of EC, revealing the depth of longitudinal infiltration of the tumor. Multiple studies have shown that the T-stage was a risk factor for postoperative recurrence and poor prognosis of ESCC (*4,8*). The current study indicated that patients with pT3N0M0 ESCC had a significantly higher rate of recurrence than patients with pT2N0M0 ESCC, which was consistent with other studies. Considering the continued advancement of endoscopic surgery technology, MIE surgery had gradually become more accepted, but OE surgery was still the main procedure. There is continuous debate about the clinical safety and effectiveness of the two surgeries, as their pros and cons are still not entirely clear (*9*). Some studies have shown that MIE was able to clear a wider range of lymph nodes than OE and was safer. Postoperative pulmonary complications and perioperative mortality rates were also lower (*10,11*), which is supported by the current study.

Table 3. Number and proportion of patients with different forms of recurrence

Recurrence	Patients.	Proportion
Anastomotic recurrence	21	4.33%
Lymph node recurrence	126	25.98%
Cervical lymph nodes	50	10.31%
Mediastinal lymph nodes	64	13.20%
Abdominal lymph nodes	29	5.98%
Hematogenous metastases	73	15.05%
Liver metastasis	17	3.51%
Lung metastasis	26	5.36%
Bone metastasis	22	4.54%
Other metastases	19	3.92%
Lymph node recurrence and anastomotic recurrence	10	2.06%
Lymph node recurrence and hematogenous metastases	41	8.45%
Anastomotic recurrence and hematogenous metastases	5	1.03%
Anastomotic recurrence, hematogenous metastases, and lymph node recurrence	4	0.82%

A study has reported that the further down the legion is located, the greater the incidence of postoperative lymph node recurrence and hematogenous metastasis (*12*). The results of this study indicate that, compared to the upper thoracic region, the prognosis for a tumor in the upper thoracic region decreased by 42% and 54% ($P < 0.05$) in the middle and lower thoracic regions. Complete resection of a tumor located in the upper thoracic region is more difficult to achieve due to the limitations of the complex anatomical structure of the neck. Other studies have pointed out the difficulty of thoroughly clearing lymph nodes during surgery in patients with upper thoracic ESCC due to postoperative complications such as aspiration, chylothorax, and recurrent laryngeal nerve injury caused by neck lymph node dissection (*13,14*). The poorer the degree of differentiation, the higher the risk of postoperative recurrence or metastasis (*15,16*). In this study, postoperative pathology revealed a lower risk of recurrence in well-differentiated than poorly differentiated ESCC (HR = 0.54, $P < .05$), while there was no significant difference in moderately differentiated ESCC.

Vessel invasion was a histopathological feature associated with invasiveness and was closely associated with the increased risk of tumor metastasis. A study (*17*) found that in patients with negative lymph nodes, vessel invasion and the T-stage were independent predictors for survival and DFS ($P < 0.001$), but it was not the same for patients with positive lymph nodes. Carcinoma nodules are often reported in gastrointestinal cancer, and especially in colorectal cancer or gastric cancer, and they are believed to be closely related to prognosis (*18*). There are few studies on cancer nodules in EC. The current study indicated that the aforementioned factors did not impact recurrence in patients with pT2-3N0M0 ESCC ($P < 0.05$). Given the sample size of patients with pT3N0M0 ESCC was relatively small in this study, further confirmation in a larger sample is still required in the future.

The current results revealed that age, sex, the tumor diameter, and the number of lymph nodes dissected

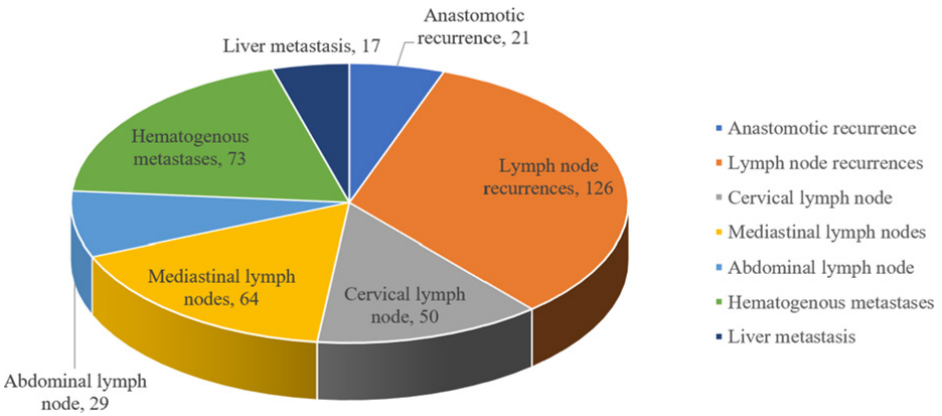

Figure 2. Pie chart of the distribution of different types of recurrence.

Table 4. Distribution of the postoperative recurrence of ESCC in different T-stages

Recurrence	Total (n = 485)	T2 stage (n = 386)	T3 stage (n = 99)	P value
Lymph node recurrence	126 (25.98%)	69 (17.88%)	57 (57.58%)	< 0.01
Cervical lymph nodes	50 (10.31%)	25 (6.48%)	25 (25.25%)	< 0.01
Mediastinal lymph nodes	64 (13.20%)	36 (9.33%)	28 (28.28%)	< 0.01
Abdominal lymph nodes	29 (5.98%)	18 (4.66%)	11 (11.11%)	0.03
Hematogenous metastases	73 (15.05%)	44 (11.40%)	29 (29.29%)	< 0.01
Liver metastasis	17 (3.51%)	12 (3.11%)	5 (5.05%)	0.36
Lung metastasis	26 (5.36%)	19 (4.92%)	7 (7.07%)	0.45
Bone metastasis	22 (4.54%)	11 (2.85%)	11 (11.11%)	< 0.01
Other metastases	19 (3.92%)	10 (2.59%)	9 (9.09%)	0.01
Anastomotic recurrence	21 (4.33%)	13 (3.37%)	8 (8.08%)	0.05

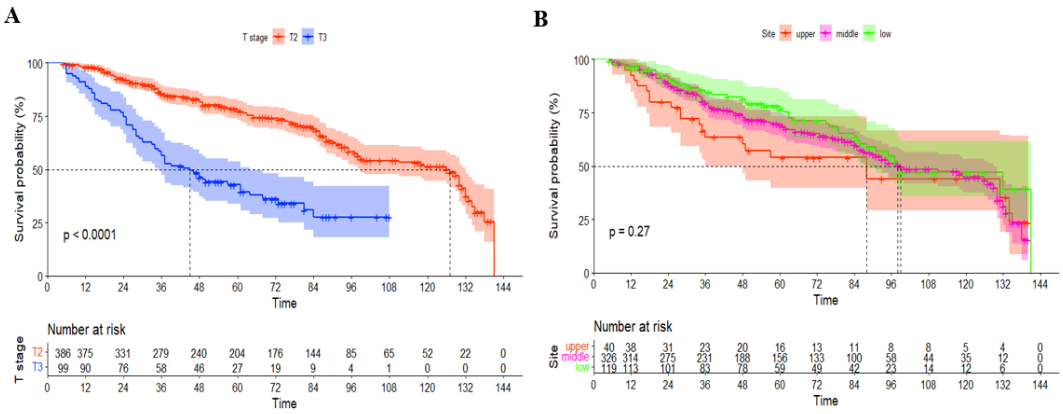

Figure 3. Kaplan-Meier curves for independent risk factors affecting OS. A, T-stage; **B**, Site.

Table 5. Distribution of the postoperative recurrence of ESCC in different locations

Recurrence	Upper thoracic region (n = 40)	Middle thoracic region (n = 326)	Lower thoracic region (n = 119)	P value
Lymph node recurrence	15 (37.50%)	89 (27.30%)	22 (18.49%)	0.04
Cervical lymph nodes	6 (15.00%)	33 (10.12%)	11 (9.24%)	0.57
Mediastinal lymph nodes	8 (20.00%)	46 (14.11%)	10 (8.40%)	0.12
Abdominal lymph nodes	3 (7.50%)	18 (5.52%)	8 (6.72%)	0.82
Hematogenous metastases	6 (15.00%)	52 (15.95%)	15 (12.61%)	0.68
Liver metastasis	1 (2.50%)	11 (3.37%)	5 (4.20%)	0.86
Lung metastasis	3 (7.50%)	17 (5.21%)	6 (5.04%)	0.82
Bone metastasis	2 (5.00%)	16 (4.91%)	4 (3.36%)	0.78
Other metastases	1 (2.50%)	15 (4.60%)	3 (2.52%)	0.54
Anastomotic recurrence	3 (7.50%)	15 (4.60%)	3 (2.52%)	0.34

were not risk factors for postoperative recurrence of pT2-3N0M0 ESCC. These findings differed with the results of previous studies (*19,20*). This may be due to the high heterogeneity of patients enrolled from different hospitals, thus resulting in inconsistent results. Previous studies have reported that EC postoperative adjuvant therapy, as a necessary treatment to prevent local recurrence and improve prognosis, was especially recommended for stage III-IV ESCC or patients with positive lymph nodes (*21*). According to the NCCN guidelines, providing postoperative adjuvant treatment is not recommended for patients with pT2-3N0M0 ESCC. However, clinicians may choose to provide postoperative adjuvant treatment based on the individual characteristics of patients. A study has shown that, compared to simple surgery during the same period, postoperative adjuvant radiotherapy reduced the rate of metastasis and local recurrence of pT3N0M0 ESCC (P = 0.001) and improved 5-year DFS and OS (*22*). In the current study, some patients received adjuvant treatment after surgery. Univariate analysis indicated that postoperative adjuvant chemotherapy reduced the risk of postoperative recurrence, but such impact did not reach statistical significance in multivariate analysis, which perhaps was due to the small sample size.

This study has several strengths. First, this study explored the pattern of postoperative recurrence in patients with pT2-3N0M0 ESCC and identified the risk factors for the recurrence as previous studies have reported mixed results in this field. Second, a prospective cohort study design was used as it is the strongest research design in observational studies. Finally, patients

enrolled in this study were relatively homogeneous because they were from the same hospital.

However, this study also has some limitations. First, this is a single center study, with limited generalizability. Second, comprehensive and systematic evaluation of factors that affect recurrence or metastasis in patients with pT2-3N0M0 ESCC was difficult as only a small set of risk factors were considered in this study. In a future study, imaging parameters and highly sensitive and specific biomarkers will be linked to further explore the risk factors for postoperative recurrence in EC, which may provide practical diagnostic and treatment strategies for patients with pT2-3N0M0 ESCC.

In conclusion, the current results indicated that the postoperative T-stage, procedure, tumor location, and degree of differentiation were independent risk factors affecting postoperative recurrence in patients with pT2-3N0M0 ESCC. Results also revealed that regional lymph node recurrence was the most common recurrence in EC patients, which often occurred within 3 years. These results indicate that the clinical monitoring of EC patients with the high-risk factors mentioned above, and especially those involving regional lymph nodes, should be enhanced.

Acknowledgements

The authors wish to thank everyone who helped with this project.

Funding: This work was supported by the Key Scientific Research Foundation of the Education Department of Province Anhui in 2023 (No. 2023AH053314).

Conflict of Interest: The authors have no conflicts of interest to disclose.

References

1. Chen W, Zheng R, Baade PD, Zhang S, Zeng H, Bray F, Jemal A, Yu XQ, He J. Cancer statistics in China, 2015. CA Cancer J Clin. 2016; 66:115-132.
2. Mariette C, Balon JM, Piessen G, Fabre S, Van Seuningen I, Triboulet JP. Pattern of recurrence following complete resection of esophageal carcinoma and factors predictive of recurrent disease. Cancer. 2003; 97:1616-1623.
3. Guo XF, Mao T, Gu ZT, Ji CY, Fang WT, Chen WH. Clinical study on postoperative recurrence in patients with pN0 esophageal squamous cell carcinoma. J Cardiothorac Surg. 2014; 9:150.
4. Deng W, Yang J, Ni W, *et al*. Postoperative radiotherapy in pathological T2-3N0M0 thoracic esophageal squamous cell carcinoma: Interim report of a prospective, phase III, randomized controlled study. Oncologist. 2020; 25:e701-e708.
5. Liu Q, Cai XW, Wu B, Zhu ZF, Chen HQ, Fu XL. Patterns of failure after radical surgery among patients with thoracic esophageal squamous cell carcinoma: Implications for the clinical target volume design of postoperative radiotherapy. PLoS One. 2014; 9:e97225.
6. Japanese Classification of Esophageal Cancer, 11th Edition: Part II and III. Esophagus. 2017; 14:37-65.
7. Xu S, Feng L, Chen Y, Sun Y, Lu Y, Huang S, Fu Y, Zheng R, Zhang Y, Zhang R. Consistency mapping of 16 lymph node stations in gastric cancer by CT-based vessel-guided delineation of 255 patients. Oncotarget. 2017; 8:41465-41473.
8. Zhu ZJ, Hu Y, Zhao YF, Chen XZ, Chen LQ, Chen YT. Early recurrence and death after esophagectomy in patients with esophageal squamous cell carcinoma. Ann Thorac Surg. 2011; 91:1502-1508.
9. Anderegg MC, Gisbertz SS, van Berge Henegouwen MI. Minimally invasive surgery for oesophageal cancer. Best Pract Res Clin Gastroenterol. 2014; 28:41-52.
10. Lee JM, Cheng JW, Lin MT, Huang PM, Chen JS, Lee YC. Is there any benefit to incorporating a laparoscopic procedure into minimally invasive esophagectomy? The impact on perioperative results in patients with esophageal cancer. World J Surg. 2011; 35:790-797.
11. Gao Y, Wang Y, Chen L, Zhao Y. Comparison of open three-field and minimally-invasive esophagectomy for esophageal cancer. Interact Cardiovasc Thorac Surg. 2011; 12:366-369.
12. Wang Y, Ye D, Kang M, Zhu L, Pan S, Wang F. Risk factors and patterns of abdominal lymph node recurrence after radical surgery for locally advanced thoracic esophageal squamous cell cancer. Cancer Manag Res. 2020; 12:3959-3969.
13. Shim YM, Kim HK, Kim K. Comparison of survival and recurrence pattern between two-field and three-field lymph node dissections for upper thoracic esophageal squamous cell carcinoma. J Thorac Oncol. 2010; 5:707-712.
14. Nozoe T, Kakeji Y, Baba H, Maehara Y. Two-field lymph-node dissection may be enough to treat patients with submucosal squamous cell carcinoma of the thoracic esophagus. Dis Esophagus. 2005; 18:226-229.
15. Hulscher JB, van Sandick JW, Tijssen JG, Obertop H, van Lanschot JJ. The recurrence pattern of esophageal carcinoma after transhiatal resection. J Am Coll Surg. 2000; 191:143-148.
16. Gertler R, Stein HJ, Schuster T, Rondak IC, Höfler H, Feith M. Prevalence and topography of lymph node metastases in early esophageal and gastric cancer. Ann Surg. 2014; 259:96-101.
17. Huang Q, Luo K, Chen C, *et al*. Identification and validation of lymphovascular invasion as a prognostic and staging factor in node-negative esophageal squamous cell carcinoma. J Thorac Oncol. 2016; 11:583-592.
18. Gu L, Chen P, Su H, Li X, Zhu H, Wang X, Khadaroo PA, Mao D, Chen M. Clinical significance of tumor deposits in gastric cancer: A retrospective and propensity score-matched study at two institutions. J Gastrointest Surg. 2020; 24:2482-2490.
19. Chen J, Zhu J, Pan J, Zhu K, Zheng X, Chen M, Wang J, Liao Z. Postoperative radiotherapy improved survival of poor prognostic squamous cell carcinoma esophagus. Ann Thorac Surg. 2010; 90:435-442.
20. Lin G, Liu H, Li J. Pattern of recurrence and prognostic factors in patients with pT1-3N0 esophageal squamous cell carcinoma after surgery: Analysis of a single center experience. J Cardiothorac Surg. 2019; 14:58.
21. Worni M, Martin J, Gloor B, Pietrobon R, D'Amico TA, Akushevich I, Berry MF. Does surgery improve

outcomes for esophageal squamous cell carcinoma? An analysis using the surveillance epidemiology and end results registry from 1998 to 2008. J Am Coll Surg. 2012; 215:643-651.
22. Yang J, Zhang W, Xiao Z, *et al*. The impact of postoperative conformal radiotherapy after radical surgery on survival and recurrence in pathologic T3N0M0 esophageal carcinoma: A propensity score-matched analysis. J Thorac Oncol. 2017; 12:1143-1151.

Received November 19, 2023; Revised December 15, 2023; Accepted December 18, 2023.

[§]These authors contributed equally to this work.
**Address correspondence to:*
Mei Kang, Department of Radiation Oncology, The First Affiliated Hospital of Anhui Medical University, No. 218, Jixi Road, Hefei, Anhui 230022, China.
E-mail: km1187825367@126.com

Released online in J-STAGE as advance publication December 20, 2023.

Original Article

DOI: 10.5582/bst.2023.01265

Feasibility of novel intraoperative navigation for anatomical liver resection using real-time virtual sonography combined with indocyanine green fluorescent imaging technology

Changsheng Pu[1,2], Tiantian Wu[2], Qiang Wang[2], Yinmo Yang[1,*], Keming Zhang[2,*]

[1] Department of General Surgery, Peking University First Hospital, Beijing, China;
[2] Department of Hepatobiliary Surgery, Peking University International Hospital, Beijing, China.

SUMMARY To analyze the feasibility and clinical effect of novel intraoperative navigation of real-time virtual sonography (RVS) combined with indocyanine green (ICG) fluorescent imaging technology in anatomical liver resection (ALR) for hepatocellular carcinoma. The clinical data of 41 patients who underwent ALR using RVS intraoperative navigation combined with ICG fluorescent imaging technology in the Department of Hepatobiliary Surgery of Peking University International Hospital from January 2020 to May 2022 were retrospectively analyzed. RVS was applied to guide the surgical plane through fusing real-time intraoperative ultrasound images with corresponding preoperative CT or MRI images. Operation methods, operation time, intraoperative blood loss, operative margin, hospital stay and postoperative complications were analyzed. The 1-year overall survival rate and tumor-free survival rate of patients were followed up by outpatient review or telephone calls. ALR surgery was performed on each of 41 patients. There were no deaths during perioperative period and postoperative complications occurred in 7 cases (17.1%). The postoperative pathological examinations demonstrated all cases of hepatocellular carcinoma and negative operative margins. The 41 patients were followed up for 12 to 20 months, with a median follow-up time of 14 months. The overall survival rate 1 year after surgery was 100.0% (41/41), 3 patients (7.3%) experienced tumor recurrence, and the tumor-free survival rate of 1 year after surgery was 92.7% (38/41). In conclusion, novel intraoperative navigation of RVS combined with ICG fluorescent imaging technology is safe and feasible in anatomical segmental hepatectomy of hepatocellular carcinoma.

Keywords hepatocellular carcinoma, hepatectomy, real-time virtual sonography, Indocyanine green

1. Introduction

Hepatocellular carcinoma (HCC) is one of the most common malignant tumors in the world, and liver resection is still one of the most effective radical treatments for HCC (*1*). However, the overall prognosis of patients with HCC after surgery is poor, and the rate of 5-year recurrence exceeds 60% (*2*). Due to the characteristics of biological behavior of HCC metastasizing through the portal vein, *Makuuchi* proposed the concept of anatomical liver resection (ALR), which refers to the complete resection of the tumor lesion and the invaded portal vein branches, including the resection of hepatic segment, hepatic subsegment or combined hepatic subsegment with scattered micro-metastasis (*1,3*). Theoretically, ALR is considered to be the most ideal surgical method for the treatment of HCC in terms of tumor eradication, which may reduce the risk of tumor recurrence and improve the overall survival. ALR intends to maximize the benefits with minimal trauma through the surgical operation procedure as well as the perioperative management, and precise intraoperative navigation of the surgical plane is one of the most critical and difficult points while performing the surgery.

The working principle of Indocyanine green (ICG) fluorescent imaging technology is that ICG would bind to the liver parenchymal cells in the body, then the positive staining method which punctures the portal vein of the target liver segment under guidance of intraoperative ultrasound (IOUS) or the negative staining method which ligates the portal vein of the target liver segment and injects it into the peripheral vein are applied, so ALR is able to be performed based

on the fluorescent imaging boundary of the area where the portal vein is located (*4*). However, ICG, with its limitations, is applicable only to superficial lesions since it cannot penetrate the deep layer of the liver with its only 5-10mm in depth. Meanwhile it may stain non-target liver segments through communicating blood vessels over time, and lead to the surgical resection plane deviating from the intended plane. Real-time virtual sonography (RVS) technology could simultaneously display real-time IOUS images and corresponding fusion images of real-time IOUS and preoperative CT/MRI side by side on the monitor. Three-dimensional reconstruction software is used to color-mark the target blood vessels and the planned liver resection lines before the surgery, and the RVS system then uses the ultrasound image and the synchronized color CT/MRI fusion image as navigation (*5*). Now RVS has been applied to radiofrequency ablation treatment of liver tumors (*6*) according to a number of literature reviews while currently RVS plus ICG fluorescent imaging technology for ALR have not been reported yet. This study focuses on the application of RVS intraoperative navigation combined with ICG fluorescent imaging technology in ALR, and intends to describe it in detail and to clarify its feasibility and safety.

2. Materials and Methods

2.1. Research subjects

We retrospectively analyzed the clinical data of 41 patients who underwent ALR using RVS intraoperative navigation combined with ICG fluorescent imaging technology at the Department of Hepatobiliary Surgery, Peking University International Hospital from January 2020 to May 2022. Among them, there were 26 males and 15 females, aged (59.8 ± 11.6) years old. The inclusion criteria included: (i) Patients with HCC from a single tumor adopted surgical treatment for the first time; (ii) Upper abdominal contrast-enhanced CT or MRI were performed before the surgery, and RVS intraoperative navigation combined with ICG fluorescent imaging was performed for ALR; (iii) Preoperative assessment of liver function Child-Pugh was in grade A. The exclusion criteria included: (i) Radiotherapy, chemotherapy, interventional therapy and other treatments applied for hepatocellular carcinoma within 4 weeks before the surgery; (ii) Allergy to ICG or iodine; (iii) Preoperative imaging examinations indicating tumor embolus in the main portal vein, common hepatic duct, hepatic vein, or inferior vena cava; (iv) Extrahepatic invasion or metastasis found in the surgery; (v) Organic disease of important organs occurring in heart, lung, kidney, brain, *etc*. This study was approved by the Ethics Committee of Peking University International Hospital and conforms to the provisions of the Declaration of Helsinki (as revised in 2013). Written informed consent was obtained from each patient before the surgery.

2.2. RVS system

The RVS intraoperative navigation system is a combination of intraoperative ultrasound and electromagnetic tracking technology (*5,7*), which includes an ultrasound examination system (HI VISION Ascendus, Hitachi, Tokyo, Japan), a convex-type intraoperative ultrasound probe (EUP-O732T, 4.0~10.0 MHz; Hitachi, Tokyo, Japan), an electromagnetic tracker (trakSTAR, Ascension, USA), an electromagnetic generator (Ascension, USA) and electromagnetic sensor (Ascension, USA). An electromagnetic generator was installed on the right front of the patient, and the spatial position of the ultrasound probe was detected using a sterile electromagnetic sensor (Figure 1). A dynamic contrast-enhanced CT or MRI scanning, with a thickness of 1.0 mm, was performed for all patients before the surgery, then CT or MRI images were converted into the format

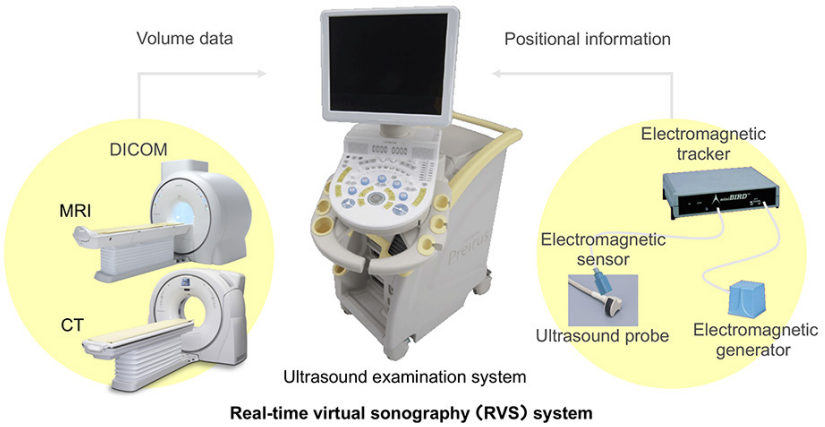

Figure 1. Real-time virtual sonography (RVS) system, including ultrasound examination system, ultrasound probe, electromagnetic tracker, electromagnetic generator and electromagnetic sensor.

of digital imaging and communications in medicine (DICOM), and three-dimensional reconstruction was done through 3D simulation software (Toshiba, Tokyo, Japan) while the data of liver parenchyma, liver vessels and tumors were extracted. The DICOM data were then input into the RVS system.

2.3. Procedure

The round ligament and the falciform ligament of liver are incised after performing an exploratory laparotomy. RVS system then is started and adjusted according to the following procedure: (i) selecting the CT image of the sagittal part of the portal vein, display and fix it on the left side of the RVS screen; (ii) selecting the IOUS image about the same location as the left image, and display it on the right side of the RVS screen, pressing the start button to synchronize the left and right images. At this point, the synchronization of images is a rough match only, and the complete matching requires another two intrahepatic anatomical points to conduct image synchronization; (iii) selecting the hepatic vein or portal vein branches near the tumor and the tumor center as anatomical points to conduct image synchronizations as specified above until the hepatic vein or portal vein branches near the tumor are matched accurately (Figure 2).

2.4. Surgical operation

After the accurate spatial position registration, the liver is kept in a relatively stable position, RVS intraoperative navigation combined with ICG fluorescent imaging technology is then applied to determine the boundaries of surgical resection of liver segments or subsegments, and the resection line is marked with electrotome. The liver parenchyma is dissected by Pringle and clamp technique. During the process of liver segments resection, the resection plane is observed intermittently by RVS to verify its correctness and to confirm the adequate surgical margins and preservation of key vessels (Figure 3).

2.5. Observation indicators

Observation indicators include the operation method, operation time, intraoperative blood loss, location of tumor, pathological results, surgical margins, hospital stay, postoperative complications, and application of RVS intraoperative navigation combined with ICG fluorescent imaging technology during the operation. Postoperative complications were graded by the Clavien-Dindo system (*8*). The one-year overall survival rate and tumor-free survival rate of the patients were followed up by outpatient review or telephone calls with the follow-up deadline as of May 2023.

2.6. Statistical analysis

SPSS 22.0 (SPSS, Chicago, IL) was used for data processing. The measurement data conforming to the normal distribution is represented as the mean ± standard error and the measurement data conforming to the non-normal distribution is represented as median with range.

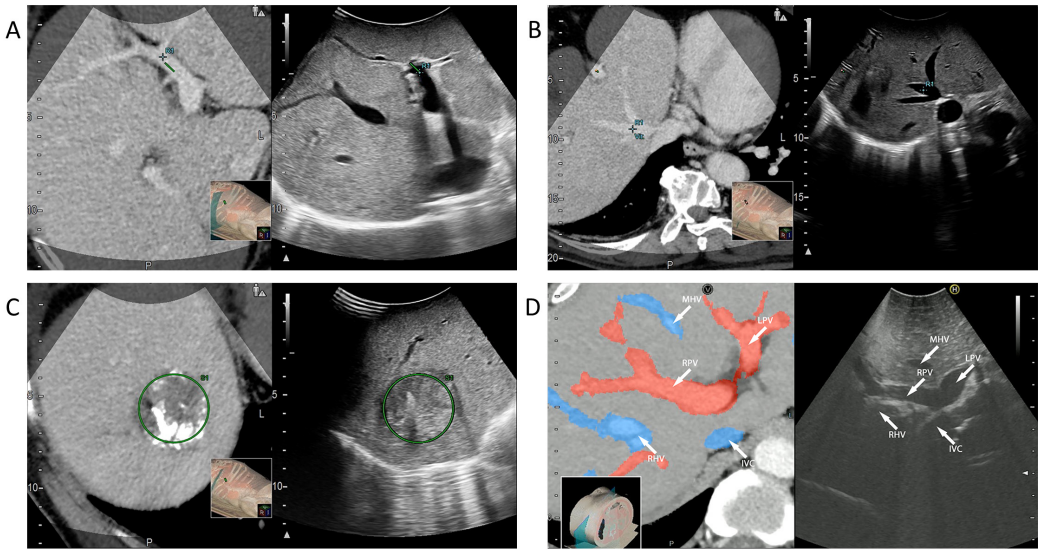

Figure 2. The adjusting procedure of real-time virtual sonography (RVS) system. (A) Adjust and match the CT image of the sagittal part of the portal vein (R1 in left image) and the intraoperative ultrasound image (R1 in right image). **(B)** Adjust and match the CT image of the middle hepatic vein (R1 in left image) and the intraoperative ultrasound image (R1 in right image). **(C)** Adjust and match the CT image of the tumor (S1 in left image) and the intraoperative ultrasound image (S1 in right image). **(D)** The fusion image (left image) and the intraoperative ultrasound image (right image) were observed after adjusting and matching procedure. Right hepatic vein (RHV), middle hepatic vein (MHV), left hepatic vein (LHV), right portal vein (RPV), left portal vein (LPV) and inferior vena cava (IVC) were marked with white arrows.

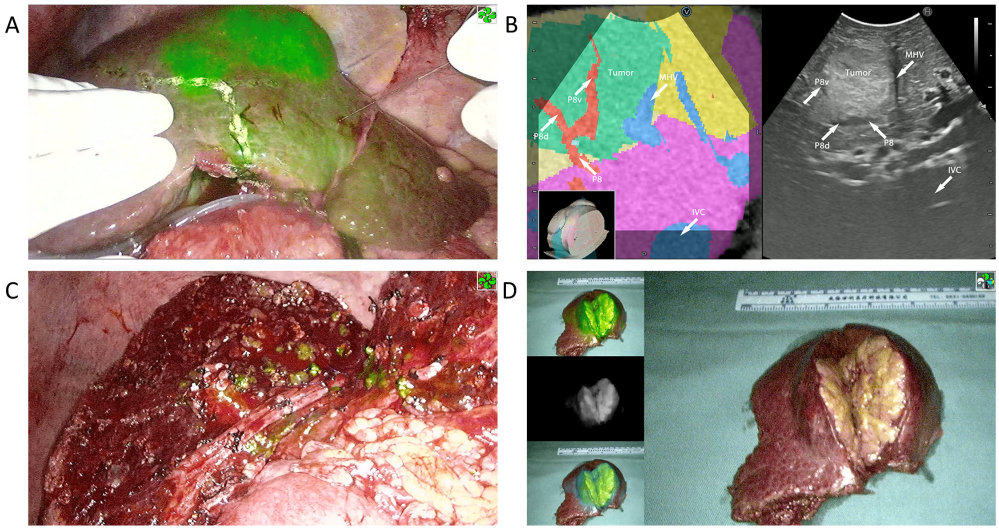

Figure 3. Anatomical liver resection (ALR) of segments 8 and 4b was performed by real-time virtual sonography (RVS) combined with indocyanine green (ICG) fluorescent imaging technology. (A) Fluorescent staining of segment 8 and segment 4b of liver. **(B)** The fusion image (left image) and the intraoperative ultrasound image (right image) were observed in RVS system. Tumor was marked with green in the left image. Middle hepatic vein (MHV), portal vein of segment 8 (P8), dorsal branch of portal vein of segment 8 (P8d), ventral branch of portal vein of segment 8 (P8v), and inferior vena cava (IVC) were marked with white arrows. **(C)** The resection plane of liver. **(D)** Frontal view of the specimen.

3. Results

3.1. Clinical characteristics of included patients

The clinical characteristics of included patients are summarized in Table 1. According to ECOG (Eastern Cooperative Oncology Group) performance status, 39 patients (95.1%) scored 0 and 2 patients (4.9%) scored 1 out of 41 patients. The 15-minute retention rate of ICG for each patient was less than 10% and all patients were classified as stage I in accordance with China liver cancer staging (CNLC). All 41 patients had open surgery of ALR.

3.2. Information of anatomic hepatic segmentectomy

The surgical procedures of patients are summarized in Table 2. Among them, there was 1 case of segment II resection (2.4%), 1 case of segment III resection (2.4%), 4 cases of segment IV resection (9.8%), 5 cases of segment V resection (12.2%), 10 cases of segment VI resection (24.4%), 7 cases of segment VII resection (17.1%), 6 cases of segment VIII resection (14.6%), 1 case of segments IVb+VIII resection (2.4%), and 1 case of segments V+VIII resection (2.4%). The perioperative outcomes of patients are shown in Table 3. The operation time of 41 patients was (417.3 ±123.1) min, the intraoperative blood loss was 390.0 (250.0, 500.0) ml, and 5 cases (12.2%) received intraoperative blood transfusions. The hospital stay of 41 patients was (15.1 ± 2.9) days. No perioperative deaths occurred. Postoperative complications occurred in 7 cases (17.1%), of which 4 cases (9.8%) were ascites, 1 case (2.4%) was incision infection in Clavien-Dindo grade I, 1 case (2.4%) was postoperative bleeding, and 1 case (2.4%) was pulmonary infection in Clavien-Dindo grade II. Postoperative pathological examinations indicated hepatocellular carcinoma, including 6 cases (14.6%) of Edmondson-Steiner grade I, 24 cases (58.5%) of grade II, and 11 cases (26.8%) of grade III, and the surgical

Table 1. Patients' baseline and clinical characteristics

Parameters	Total (n = 41)
Age, years (median, IQR)	61 (50–66)
< 60	18 (43.9%)
≥ 60	23 (56.1%)
Sex, n (%)	
Female	15 (36.6)
Male	26 (63.4)
ECOG performance, n (%)	
0	39 (95.1)
1	2 (4.9)
Child-Pugh score, n (%)	
A	40 (97.6)
B	1 (2.4)
ICGR-15, % (median, IQR)	5.6 (4.0–7.0)
HBV infection, n (%)	
Positive	38 (92.7)
Negative	3 (7.3)
AFP, ng/mL (median, IQR)	73.5 (2.9–755.2)
< 20	19 (46.3)
≥ 20	22 (53.7)
CNLC stage, n (%)	
Ia	32 (78.0)
Ib	9 (22.0)
Tumor diameter, cm (median, IQR)	4.0 (2.4–5.0)

Abbreviation: AFP, alpha fetal protein; CNLC, China liver cancer staging; ECOG, Eastern Cooperative Oncology Group; ICGR, indocyanine green rate; IQR, inter quartile range.

Table 2. The operative procedures of patients

Operative procedure	Total (n = 41)
Segmentectomy, n (%)	
S2	1 (2.4)
S3	1 (2.4)
S4	4 (9.8)
S5	5 (12.2)
S6	10 (24.4)
S7	7 (17.1)
S8	6 (14.6)
Multisegmentectomy, n (%)	
S4b+8	1 (2.4)
S5+8	1 (2.4)
Hemihepatectomy, n (%)	
S2+3+4	3 (7.3)
S5+6+7+8	2 (4.9)

Abbreviation: S, segment, defined by Couinaud's nomenclature.

Table 3. The perioperative outcomes of patients

Perioperative outcomes	Patients (n = 41)
Intraoperative outcomes	
Operation time, min (median, IQR)	400.0 (345.0–450.0)
Pringle time, min (median, IQR)	30.0 (25.0–45.0)
Operative blood loss, mL (median, IQR)	390.0 (250.0–500.0)
Intraoperative blood transfusion, n (%)	5 (12.2)
Negative resection margin, n (%)	41 (100.0)
Postoperative results	
Postoperative hospital stay, days (median, IQR)	14.0 (10.0–19.0)
90-day mortality, n (%)	0
R0 resection, n (%)	41 (100.0)
Hepatocellular carcinoma, n (%)	41 (100.0)
Microvascular invasion, n (%)	22 (53.7)
Edmondson-Steiner grade, n (%)	
I	6 (14.6)
II	24 (58.5)
III	11 (26.8)
IV	0
Cases of recurrence, n (%)	3 (7.3)
The 1-year overall survival, n (%)	41 (100.0)
The 1-year disease-free survival, n (%)	38 (92.7)
Type of complications	
Postoperative hemorrhage, n (%)	1 (2.4)
Incision infection, n (%)	1 (2.4)
Seroperitoneum, n (%)	4 (9.8)
Lung infection, n (%)	1 (2.4)
Clavien-Dindo Classification, n (%)	
I	5 (12.2)
II	2 (4.9)
III	0
IV	0

Abbreviation: IQR, inter quartile range.

margins of all patients were negative. 41 patients were followed up for 14 to 22 months, with a median follow-up time of 14 months. The overall survival rate of 1 year after surgery was 100.0% (41/41). There were 3 patients (7.3%) with tumor recurrence after the surgery, and the tumor-free survival rate of 1 year after surgery was 92.7% (38/41).

3.3. Safety and feasibility

(i) *Intraoperative situation*: RVS intraoperative navigation combined with ICG fluorescent imaging technology does not interfere with the surrounding environment, and is able to guide the puncture of portal vein of liver segment and the operation plane of segmental hepatectomy accurately. The resection plane under RVS navigation was consistent with that of the preoperative plan in each case. (ii) *Postoperative situation*: there were 7 patients (17.1%) with postoperative complications. According to the Clavien-Dindo system classification, 5 cases (12.2%) were in grade I, 2 cases (4.9%) were in grade II and no perioperative death occurred. It is safe and feasible to apply RVS intraoperative navigation combined with ICG fluorescent imaging technology in ALR.

4. Discussion

In 1985, Makuuchi *et al*. (*9-11*) proposed the concept of ALR including anatomic segmental and subsegmental liver resections based on the theory of Couinaud's liver segment. Makuuchi is the first to put forward the IOUS for surgery of ALR, and also to practice liver segmental staining, dissection of glisson's sheath (extrathecal dissection and intrathecal dissection) and other surgical methods, which then created an era of precise liver resection.

HCC tends to metastasize along the portal vein in the liver segments where the tumor is located (*12*). ALR not only removes the tumor but also removes the liver segment of the portal vein branch where the tumor is located, which can reduce the risk of metastasis (*13*). The theory of tumor blood flow drainage proposed by Sakon *et al*. (*14*) also demonstrated that the recurrence of liver cancer is the direct spread of tumor through portal vein blood flow. Retrospective studies have also been reported that anatomic hepatectomy reduces the risk of recurrence of local tumor and has a better prognosis than non-anatomic hepatectomy (*2,15*).

In anatomic hepatectomy, it is crucial to determine the surgical resection plane. Traditional ALR mainly relies on blocking the portal vein of the target liver segment to display the ischemic line on the liver surface, and exposing the hepatic veins throughout the entire operation under IOUS to determine the surgical resection plane. However, due to the irregular boundaries between the liver segments and the variation of intrahepatic vessels, the plane of hepatectomy and the extent of resection are often not accurate enough during the liver resection. Staining with ethylene blue can be used to assist in judging the plane of hepatectomy, but with shortcomings including short imaging time, unclear field of view, and rapid clearance. ICG has been widely used in cholangiography and tests of reserved liver function, and has been gradually applied in anatomic hepatectomy (*16*). ICG fluorescent imaging technology can display

the resection range of liver segments and tumor boundaries, which allows for a more accurate anatomic hepatectomy (*17*). Nevertheless, ICG fluorescent imaging technology also has certain limitations: (i) Fluorescent signal interference: ICG can diffuse through the rami communicantes between liver segments, thus affects the judgment of the surgical resection plane; (ii) Poor imaging of deep tumors: since the fluorescent signal of ICG can only penetrate 5-10 mm of liver tissue, ICG usually does not provide enough image for deep tumors (*18*).

RVS fuses the images of ultrasound and CT/MRI, and thus is able to combine the good spatial resolution of CT/MRI with the advantages of real-time dynamic observation of ultrasound (*19*). Adopting the method of spatial magnetic positioning, RVS is able to achieve real-time correspondence between ultrasound images and CT/MRI images through image position registration, and then the IOUS and fusion images are simultaneously displayed on the RVS operation interface (*20*). On the basis of image fusion, the RVS system uses the electromagnetic sensor fixed on the ultrasound probe and the electromagnetic generator of the navigation system to precisely match the image of ultrasound with CT/MRI to realize free tracking of spatial positioning. It can make any section displayed on the same screen or fused in real time, simulate the scope and plane of liver resection, identify the location of the tumor and its surrounding duct structure during the surgery to guide the plane of liver resection in real time for performing ALR.

Studies have shown that RVS's ability to distinguish liver cancer from surrounding normal tissues is better than IOUS, with a better detection rate for small lesions (*21*). RVS can use different colors to mark the simulated images of liver tumors, portal veins, hepatic veins, and normal liver tissues, and determine the tumor boundary which cannot be clearly distinguished by IOUS, to guide the resection plane in real time through the fusion images (*22*). Real-time navigation of RVS during the surgery makes up for limitations of ICG fluorescent imaging, and most importantly, it is a bridge between preoperative CT/MRI and IOUS which helps the surgeons in planning and adjusting the optimal surgical plan during the surgery.

There are two main issues concerned when using the RVS systems: (i) whether the initial position markers remained accurate; and (ii) whether the position registration procedure is too complex and time-consuming. The accuracy of position registration is the foundation of the RVS system, without it, RVS cannot perform accurate surgical navigation. Surgical operations easily lead to changes in the position and shape of the liver, which makes it more difficult for RVS to match the scanning planes of CT/MRI and IOUS during surgery, and it is almost impossible to intraoperatively register the position of the entire liver. Nevertheless, the target area for ALR is usually limited to within the liver segments or to an area around the tumor, so it is not necessary to record the entire liver but only the location near the target area with acceptable accuracy. According to our experience, we suggest the following points that are helpful in position registration: (i) The electromagnetic generator should be placed as close as possible to the operating bed (20–70 cm), otherwise the registration accuracy may be affected; (ii) Appropriate intraoperative detection points of IOUS need to be selected. The detection point of ultrasound must be set on the liver surface when conducting the intraoperative scanning. We prefer to choose the round ligament of the liver, which is easy to be identified and of which the position is fixed; (iii) Portal vein branches or hepatic veins near the tumor are recommended as important landmarks; (iv) For more precise adjustment, it is recommended to select the tumor center as the marking point and accurately match the direction and angle of the hepatic vein or portal vein near the tumor. The accuracy of position matching can be maximized through the above practices, thereby obtaining accuracy of image matching. It is noted that accurate image matching is not a simple process, and the time for spatial position registration could be significantly reduced with improvement of operating proficiency and skills, to achieve satisfactory accuracy.

However, the RVS system also has some limitations. First, the magnetic field is susceptible to bending by magnetic materials during the surgery. Therefore, magnetic materials should not be placed between the electromagnetic sensor and the electromagnetic generator, medical tweezers, scissors, metal tractors and other magnetic materials should be placed 5~10 cm away from the electromagnetic sensor. Second, with the development of laparoscopic technology, liver surgery tends to gradually become minimally invasive, RVS has yet to be used in laparoscopy, and it is expected that an update of equipment or devices will enable RVS to be used in laparoscopic anatomic hepatectomy in the future.

For this study, there are some limitations because it is an exploratory study without a control group, and may affect the credibility of the conclusion. Thus, prospective randomized controlled trials may need to be carried out for the sake of a high grade of evidence.

We evaluated the safety and feasibility of RVS intraoperative navigation combined with ICG fluorescent imaging technology for hepatectomy in our study. This novel intraoperative navigation uses ICG fluorescence imaging to determine the surface boundary of hepatectomy while the plane of liver resection can be modified in real time through RVS to make up for the shortcomings of ICG fluorescence imaging, thus helping to determine a clear route of hepatectomy, reducing intraoperative bleeding and preserving the normal liver parenchyma to the greatest extent, so as to achieve the goal of anatomic segments or subsegments hepatectomy.

Funding: This work was supported by Peking University International Hospital Research Funds (YN2021QN01),

Capital's Funds for Health Improvement and Research (2020-2-8021)

Conflict of Interest: The authors have no conflicts of interest to disclose.

References

1. Wakabayashi G, Cherqui D, Geller DA, *et al*. The Tokyo 2020 terminology of liver anatomy and resections: Updates of the Brisbane 2000 system. J Hepatobiliary Pancreat Sci. 2022; 29:16-15.
2. Kaibori M, Kon M, Kitawaki T, *et al*. Comparison of anatomic and non-anatomic hepatic resection for hepatocellular carcinoma. J Hepatobiliary Pancreat Sci. 2017; 24:616-626.
3. Forner A, Reig M, Bruix J. Hepatocellular carcinoma. Lancet. 2018; 391:1301-1314.
4. Berardi G, Igarashi K, Li CJ, Mishima K, Nakajima K, Honda M, Wakabayashi G. Parenchymal sparing anatomical liver resections with full laparoscopic approach: Description of technique and short-term results. Ann Surg. 2021; 273:785-791.
5. Satou S, Aoki T, Kaneko J, Sakamoto Y, Hasegawa K, Sugawara Y, Arai O, Mitake T, Miura K, Kokudo N. Initial experience of intraoperative three-dimensional navigation for liver resection using real-time virtual sonography. Surgery. 2014; 155:255-262.
6. Nakai M, Sato M, Sahara S, Takasaka I, Kawai N, Minamiguchi H, Tanihata H, Kimura M, Takeuchi N. Radiofrequency ablation assisted by real-time virtual sonography and CT for hepatocellular carcinoma undetectable by conventional sonography. Cardiovasc Intervent Radiol. 2009; 32:62-69.
7. Sofuni A, Itoi T, Itokawa F, Tsuchiya T, Kurihara T, Ishii K, Tsuji S, Ikeuchi N, Tanaka R, Umeda J, Tonozuka R, Honjo M, Mukai S, Moriyasu F. Real-time virtual sonography visualization and its clinical application in biliopancreatic disease. World J Gastroenterol. 2013; 19:7419-7425.
8. Clavien PA, Barkun J, de Oliveira ML, Vauthey NJ, Dindo D, Schulick RD, Santibañes ED, Pekolj J, Slankamenac K, Bassi C, Graf R, Vonlanthen R, Padbury R, Cameron JL, Makuuchi M. The Clavien-Dindo classification of surgical complications: Five-year experience. Ann Surg. 2009; 250:187-196.
9. Makuuchi M. Surgical treatment for HCC - special reference to anatomical resection. Int J Surg. 2013; 11:S47-S49.
10. Takasaki K. Glissonean pedicle transection method for hepatic resection: A new concept of liver segmentation. J Hepatobiliary Pancreat Surg. 1998; 5:286-291.
11. Makuuchi M, Hasegawa H, Yamazaki S. Ultrasonically guided subsegmentectomy. Surg Gynecol Obstet. 1985; 161:346-350.
12. Makuuchi M, Imamura H, Sugawara Y, Takayama T. Progress in surgical treatment of hepatocellular carcinoma. Oncology. 2002; 62:74-81.
13. Moris D, Tsilimigras DI, Kostakis ID, Ntanasis-Stathopoulos I, Shah KN, Felekouras E, Pawlik TM. Anatomic versus non-anatomic resection for hepatocellular carcinoma: A systematic review and meta-analysis. Eur J Surg Oncol. 2018; 44:927-938.
14. Sakon M, Ogawa H, Fujita M, Nagano H. Hepatic resection for hepatocellular carcinoma based on tumor hemodynamics. Hepatol Res. 2013; 43:155-164.
15. Shindoh J, Kobayashi Y, Umino R, Kojima K, Okubo S, Hashimoto M. Successful anatomic resection of tumor-bearing portal territory delays long-term stage progression of hepatocellular carcinoma. Ann Surg Oncol. 2021; 28:844-853.
16. Marino MV, Ramirez SB, Ruiz MG. The application of indocyanine green (ICG) staining technique during robotic-assisted right hepatectomy: With video. J Gastrointest Surg. 2019; 23:2312-2313.
17. Ishizawa T, Zuker NB, Kokudo N, Gayet B. Positive and negative staining of hepatic segments by use of fluorescent imaging techniques during laparoscopic hepatectomy. Arch Surg. 2012; 147:393-394.
18. Ishizawa T, Fukushima N, Shibahara J, Masuda K, Tamura S, Aoki T, Hasegawa K, Beck Y, Fukayama M, Kokudo N. Real-time identification of liver cancers by using indocyanine green fluorescent imaging. Cancer. 2009; 115:2491-504.
19. Takamoto T, Mise Y, Satou S, Kobayashi Y, Miura K, Saiura A, Hasegawa K, Kokudo N, Makuuchi M. Feasibility of intraoperative navigation for liver resection using real-time virtual sonography with novel automatic registration system. World J Surg. 2018; 42:841-848.
20. Sakata K, Kijima T, Arai O. Initial Report: A novel intraoperative navigation system for laparoscopic liver resection using real-time virtual sonography. Sci Rep. 2020; 10:6174.
21. Miyata A, Arita J, Shirata C, Abe S, Akamatsu N, Kaneko J, Kokudo N, Hasegawa K. Quantitative Assessment of the Accuracy of Real-Time Virtual Sonography for Liver Surgery. Surg Innov. 2020; 27:60-67.
22. Lv A, Li Y, Qian HG, Qiu H, Hao CY. Precise Navigation of the Surgical Plane with Intraoperative Real-time Virtual Sonography and 3D Simulation in Liver Resection. J Gastrointest Surg. 2018; 22:1814-1818.

Received October 10, 2023; Revised December 6, 2023; Accepted December 9, 2023.

**Address correspondence to:*
Yinmo Yang, Department of General Surgery, Peking University First Hospital, Beijing 100034, China.
E-mail: yangyinmo@263.net

Keming Zhang, Department of Hepatobiliary Surgery, Peking University International Hospital, Beijing 102206, China.
E-mail: zhangkeming@pkuih.edu.cn

Released online in J-STAGE as advance publication December 13, 2023.

Brief Report

DOI: 10.5582/bst.2023.01278

Pal power: Demonstration of the functional association of the *Helicobacter pylori* flagellar motor with peptidoglycan-associated lipoprotein (Pal) and its preliminary crystallographic analysis

Xiaotian Zhou[1], Mohammad M. Rahman[1], Sharmin Q. Bonny[1], Yue Xin[1], Nikki Liddelow[2], Mohammad F. Khan[1], Alexandra Tikhomirova[1], Jihane Homman-Ludiye[3], Anna Roujeinikova[1,2,*]

[1] Department of Microbiology, Infection and Immunity Program, Monash Biomedicine Discovery Institute, Monash University, Melbourne, Victoria, Australia;
[2] Department of Biochemistry and Molecular Biology, Monash University, Melbourne, Victoria, Australia;
[3] Monash Micro Imaging, Biomedicine Discovery Institute, Monash University, Melbourne, Victoria, Australia.

SUMMARY The bacterial flagellar motor is a molecular nanomachine, the assembly and regulation of which requires many accessory proteins. Their identity, structure and function are often discovered through characterisation of mutants with impaired motility. Here, we demonstrate the functional association of the *Helicobacter pylori* peptidoglycan-associated lipoprotein (*Hp*Pal) with the flagellar motor by analysing the motility phenotype of the Δ*pal* mutant, and present the results of the preliminary X-ray crystallographic analysis of its globular C-terminal domain *Hp*Pal-C. Purified *Hp*Pal-C behaved as a dimer in solution. Crystals of *Hp*Pal-C were grown by the hanging drop vapour diffusion method using medium molecular weight polyethylene glycol (PEG) Smear as the precipitating agent. The crystals belong to the primitive orthorhombic space group P1 with unit cell parameters a = 50.7, b = 63.0, c = 75.1 Å. X-ray diffraction data were collected to 1.8 Å resolution on the Australian Synchrotron beamline MX2. Calculation of the Matthews coefficient (V_M=2.24 Å^3/Da) and molecular replacement showed that the asymmetric unit contains two protein subunits. This study is an important step towards elucidation of the non-canonical role of *H. pylori* Pal in the regulation, or function of, the flagellar motor.

Keywords peptidoglycan-associated lipoprotein, bacterial flagellar motor, motility, *Helicobacter pylori*, crystals

1. Introduction

More than 50% of the world's population carry Gram-negative pathogenic bacteria *Helicobacter pylori* in their stomach (*1*). The presence of *H. pylori* has been causatively linked to chronic gastritis and gastric and duodenal ulcers; furthermore, untreated *H. pylori* infections can lead to the development of gastric cancer (*2-4*). In fact, *H. pylori* infections are the main cause of cancer ascribed to infectious agents, accounting for 0.8 million cancer cases in 2018 alone (*5*). In terms of cancer-related deaths, gastric cancer holds the fourth position (*6*).

The pathogenesis of *H. pylori* infection is partly attributed to the secretion of bacterial toxins, cytotoxin-associated gene product A (CagA) and vacuolating cytotoxin A (VacA), which induce a pathological transformation of the epithelial layer (*7-9*). It is not fully understood why the host's immune system is unable to eradicate *H. pylori* and how it manages to persist in the highly acidic stomach lining. What is known is that *H. pylori* produces enzymes that facilitate adaptation to the very low pH of the stomach (*10*), protect against the host's immune system by digesting innate immune peptides (*11*), eliminate reactive oxygen species produced by white blood cells (*12*), or mask outer surface bacterial proteins with sugars (*13*).

It is also well understood that *H. pylori* requires motility in order to colonize the host and to attain full infection level (*14*). *H. pylori* swims through the dense mucous layer in the stomach by means of its flagella and it uses chemotaxis to move into nutrient-rich areas and towards small molecules that its can use to defend itself from elimination by host complement (*14-16*). Cryo-electron tomography studies showed that the molecular nanomachine at the base of the flagellum, the bacterial flagellar motor, is wider and significantly more complex in *H. pylori* compared to

the motors in *Escherichia coli* and *Salmonella* (*17*). The *H. pylori* motor structure appears to be reinforced by a periplasmic scaffold made of proteins (*17*). The exact function of the scaffold is not yet known, but it has been proposed that it may stabilize the force-generating MotA/MotB stator units and support the wider stator ring to produce a larger turning force (*18*). It is also possible that it serves to regulate the stator function, or, perhaps, forms an extension of the stator itself. The flagellar motor is an example of a biological nanomachine that self-assembles from many different proteins; it was hypothesized that the binding energy released upon incorporation of the MotA/MotB complexes into the periplasmic scaffold drives their activation through conformational changes (*19,20*) that open the stator's proton channel.

Recent advances in the field of cryo-electron tomography led to the discoveries of a similarly complex architecture of polar flagellar motors in many other bacteria (*18*). However, progress in establishing the molecular make-up of the discovered periplasmic scaffolds has been slow, partly because identification of additional motor components through bioinformatic analyses alone may be challenging due to gene recombination events. New putative motor components are often discovered by investigating the underlying molecular mechanisms responsible for impaired motility in strains produced by random or targeted mutagenesis. It was recently reported that deletion of the gene encoding peptidoglycan-associated lipoprotein (Pal) in uropathogenic or enterohemorrhagic *E. coli* produced mutants with lower motility as judged by the migration diameter on 0.3% agar plates (*21,22*). Since Pal has never been directly implicated in the function or regulation of the flagella motor, we wished to examine the motility phenotype of the respective *H. pylori* mutant. We assessed the effect of inactivation the *pal* gene in *H. pylori* strain SS1 on migration in semi-solid agar and on linear swimming speed in liquid medium. Having established that mutants swim slower than wild-type (WT) cells, we performed cloning, purification, crystallization and the preliminary X-ray crystallographic analysis of the C-terminal outer membrane protein A (OmpA)-like globular domain of *H. pylori* Pal (*Hp*Pal-C). This is an important step towards elucidation of its role in the regulation, or function of, the flagellar motor.

2. Materials and Methods

2.1. Insertional inactivation of pal in H. pylori strain SS1

SS1 Δ*pal::kan* mutant strain was created by replacing the middle part of the *pal* gene (locus tag HPYLSS1_01070) with the *Campylobacter coli* kanamycin resistance gene *aphA3* (encoding aminoglycoside 3'-phosphotransferase, Genbank ID HG515011.2). A DNA fragment containing *aphA3* (795 bp), flanked by *H. pylori* chromosomal DNA sequences corresponding to 200 bp upstream plus the first 100 bp of the *pal* gene at the 5' end, and the last 100 bp plus 200 bp downstream of the *pal* gene at the 3' end, was synthesized and ligated into the pUC18 vector by GenScript (USA). The SS1 Δ*pal::kan* mutant was generated by natural transformation method and selection on Columbia blood agar (Oxoid) plates supplemented with 5%(v/v) defibrinated horse blood and an antibiotic mixture comprising 10 µg/mL kanamycin, 10 µg/mL vancomycin, 2.5 U/mL polymyxin B, 5 µg/mL trimethroprim (all antibiotics from Sigma-Aldrich). The mutation was verified by Sanger sequencing.

2.2. Semisolid agar motility assay

Brucella broth plates were prepared with 0.4%(w/v) bacteriological agar (Oxoid), 7%(v/v) fetal bovine serum (Gibco), 40 µg/mL triphenyl tetrazolium chloride (Sigma, UK), and *H. pylori*-selective antibiotics (10 µg/mL vancomycin, 2.5 U/mL polymyxin B, 5 µg/mL trimethroprim, plus 10 µg/mL kanamycin for the Δ*pal::kan* mutant). *H. pylori* SS1 WT or mutant strains were cultured overnight in BB10 (Brucella broth (Becton Dickinson) supplemented with 10 µg/mL vancomycin and 10%(v/v) foetal bovine serum (plus 10 µg/mL kanamycin for the mutant) under microaerobic conditions generated using the CampyGen (Oxoid) system. Five µL of the overnight culture adjusted to an OD_{600} nm of 0.74 was inoculated into agar, and the plates were incubated under microaerobic conditions at 37°C for 7 days. The diameter of the migration halos was measured, and the values averaged over 7 biological repeats.

2.3. Measurement of swimming speeds

For optical microscopy filming of bacteria swimming in liquid media, strains were cultured overnight in BB10, inoculated into fresh pre-warmed BB10 to an optical density at 600 nm (OD600) of 0.05 and grown for a further 2–3 hrs. To observe the cells swimming behaviour, 10 µL of the cell suspension was placed in a EVE cell counting slide (EVS-050) and imaged using a Leica DMi8 microscope (Leica Microsystems, Germany) fitted with a Scientific CMOS K8 camera in bright-field mode at 20× magnification. Five 30-sec time-lapse videos (16 frames per second; fields of view picked randomly) were captured for both wild type (WT) and Δ*pal* cultures, in three independent biological replicates for WT and 2 replicates for Δ*pal*. The time-lapse videos were analysed using ImageJ v. 1.53. A total of 66 cells (WT) and 60 cells (Δ*pal*) that swam in linear fashion for at least 0.5 sec were tracked manually using

the MTrack plug-in to allow calculation of the mean straight swimming speed. A two-sample Student's *t*-test was performed to determine statistical significance of the observed swimming speed differences between the WT and Δ*pal::kan* mutant.

2.4. Gene cloning and overexpression

The amino acid sequence of *H. pylori* Pal (Uniprot ID A0A1U9IUR5) was analysed for the presence of signal peptides and disordered regions using the servers SignalP 6.0 (*https://services.healthtech.dtu.dk/services/SignalP-6.0/#6.0*) (*23*) and DISOPRED3 (*http://bioinf.cs.ucl.ac.uk/disopred*) (*24*), respectively. The codon-optimized coding sequence for the C-terminal outer membrane protein A (OmpA)-like globular domain of *H. pylori* Pal (*Hp*Pal-C, amino-acid residues 66-179) was synthesized and ligated into the pET151/D-TOPO vector (Invitrogen) by GenScript (Piscataway, USA) to produce an *Escherichia coli* expression vector that adds an N-terminal His_6 tag, V5-epitope and a tobacco etch virus (TEV) protease cleavage site. *E. coli* BL21(DE3) cells were transformed with the expression vector and grown at 37°C in LB medium supplemented with 50 mg/L ampicillin. Overexpression of *Hp*Pal-C was induced with 1 mM isopropyl-*D*-1-thiogalactopyranoside at an OD_{600} of 0.6-0.8, the cells were grown for a further 4 hrs and then harvested by centrifugation at 6,000 g for 15 min.

2.5. Purification and oligomeric state analysis

Recombinant *Hp*Pal-C was purified by following the procedure modified from that described in (*25*). The cell lysate was loaded onto a 5-mL Ni-NTA affinity column (Cytiva) pre-equilibrated with 20 mM Tris-HCl pH 8.0, 500 mM NaCl and 15 mM imidazole. The column was washed with 100 mL of 20 mM Tris-HCl pH 8.0, 500 mM NaCl, 40 mM imidazole and the protein was eluted with the buffer containing 20 mM Tris-HCl pH 8.0, 500 mM NaCl and 500 mM imidazole. TEV was added (Invitrogen), and the sample was dialyzed overnight at 4°C against the buffer containing 20 mM Tris-HCl pH 8.0, 150 mM NaCl, 2 mM DTT, 1% (v/v) glycerol to cleave the tag off, producing the *Hp*Pal-C protein comprising residues 66–179 (the C-terminal domain) of *Hp*Pal plus six additional residues from the TEV cleavage site (GIDPFT). The protease, tag and uncleaved protein were removed by passing the sample through the Ni-NTA column, and the protein was further purified using a HiLoad 16/600 Superdex 75 prep grade gel filtration column (Cytiva) equilibrated with 10 mM Tris-HCl pH 8.0, 150 mM NaCl. Protein concentration was determined using the Bradford assay (*26*), and SDS-PAGE was used to ascertain the degree of protein purity.

The calibration curve for the gel filtration column was established by fitting the retention volumes (V_R) and molecular weights (MW) of calibration standards listed in the manufacturer's manual (*https://cdn.cytivalifesciences.com/api/public/content/digi-11217-pdf*) to the equation $MW = A \times \exp(-B \times V_R)$ (*27*). The resulting standard curve $MW = 957.6 \times \exp(-0.048 \times V_R)$ was used to determine the oligomeric state of *Hp*Pal-C in solution.

2.6. Crystallisation

*Hp*Pal-C was concentrated to 15 mg/mL and subjected to 20-min centrifugation at 17,000 g to remove insoluble particles and aggregates. The crystallization screening was carried out by the sitting-drop vapour-diffusion method using an automated Phoenix crystallization robot (Art Robbins Instruments) and commercial screens LFS, LMB, BCS, MIDAS (Molecular Dimensions), Crystal Screen HT, and PEG/Ion HT (Hampton Research). 100 nL protein solution was combined with an equal volume of reservoir solution and equilibrated against 50 µL reservoir solution in a 96-well Art Robbins CrystalMation Intelli-Plate (Hampton Research). Rod-like crystals appeared after one day in condition B6 of the BCS screen, which contained 25%(w/v) PEG Smear Medium and 100 mM Bicine pH 9.3. Following optimization, larger crystals were produced using drops containing 1 µL protein solution (13.2 mg/mL) mixed with 2 µL reservoir solution (25%(w/v) PEG Smear Medium, 100 mM Bicine pH 8.7) and equilibrated against 500 µL reservoir solution at 293 K.

2.7. X-ray diffraction data collection and processing

For data collection, crystals of *Hp*Pal-C were briefly soaked in a cryoprotectant solution, prepared as the reservoir solution supplemented with 15%(v/v) glycerol, and flash-frozen by plunging in liquid nitrogen. X-ray diffraction data from a cryocooled crystal were collected to 1.8 Å on the MX2 beamline of the Australian Synchrotron. The data were processed and scaled using *XDS* (*28*) and *AIMLESS* (*29*) from the Collaborative Computational Project, Number 4 (*CCP4*) suite (*30*). Data collection and processing statistics are summarized in Table 1.

2.8. Molecular replacement

To identify an appropriate model for molecular replacement, we conducted a sequence-similarity search against the crystal structures deposited in the RCSB Protein Data Bank. The three most similar sequences were those of Pals from *Burkholderia cenocepacia* (PDB ID 5n2c (*31*)), *Burkholderia pseudomallei* (PDB ID 4b5c (*32*)) and *Acinetobacter baumannii* (PDB ID 4g4x). Molecular replacement with these structures

Table 1. Data collection and processing. Values in parentheses correspond to the highest resolution shell

Diffraction source	MX2 beamline, Australian Synchrotron
Wavelength (Å)	0.95
Temperature (K)	100
Detector	Dectris EIGER 16M
Total rotation range (º)	80
Space group	$P2_12_12_1$
a, b, c (Å)	50.7, 63.0, 75.1
α, β, γ (º)	90, 90, 90
Mosaicity (º)	0.05
Resolution range (Å)	48.26-1.79 (1.83–1.79)
Total No. of reflections	69,134 (4.093)
No. of unique reflections	22,855 (1,348)
Completeness (%)	98.6 (98.7)
Multiplicity	3.0
$<I/\sigma(I)>$	8.4 (1.8)
$CC_{1/2}$ (%)	99.7 (80.7)
R_{merge}	0.054 (0.425)

as search models and preliminary refinement were performed using Phaser (*33*) and Phenix (*34*).

3. Results and Discussion

3.1. *H. pylori* SS1 Δ*pal* mutant shows a significant motility defect in semisolid agar

To examine whether *H. pylori* Pal is required for motility, we generated an isogenic Δ*pal* mutant strain lacking functional Pal by replacing the middle part of the gene with the kanamycin resistance gene *aphA3*. We first compared motility of the WT and mutant cells using the semisolid agar plates assay, where a small, set amount of the strain to be tested is stabbed into the thickness of the agar and the diameter of the bacterial migration halo is measured after several days. The ability of *H. pylori* mutants lacking Pal to migrate through semisolid (0.4%) agar was drastically reduced compared to wild type (WT) strain (Figure 1A). We concluded that Pal promotes migration of bacteria on a semisolid agar surface.

3.2. *H. pylori* SS1 Δ*pal* mutants are unable to achieve WT linear swimming speeds in liquid media

We recognise that although the diameter of the halos in soft agar plate assays strongly correlates with migration ability, it is also influenced by the growth rate and chemotaxis artefacts. Therefore, to further characterize the motility phenotype of the *H. pylori* Δ*pal* strain, we filmed bacteria swimming in liquid media (BB10) using bright-field optical microscopy and measured their linear swimming speeds. The mean straight swimming speeds for the WT cells and Δ*pal* mutants were 97 ± 16 μm/sec and 88 ± 13 μm/sec, respectively (Figure 1b). The reduction in the linear swimming speed caused by elimination of Pal was small (9%) but statistically significant ($p < 0.01$). The flagella in *H. pylori* Δ*pal* mutants have normal morphology (*35*). The observed linear speed reduction is therefore likely caused by the reduction in the rotational speed of the flagellar motor. Our observation thus indicates that the loss of the cellular function of *H. pylori* Pal impacts on the generation of force in the flagellar motor.

3.3. Cloning, overexpression, purification and biochemical characterisation of the C-terminal globular domain of *H. pylori* Pal (*Hp*Pal-C)

Bioinformatic analysis of *H. pylori* Pal revealed that is contains a signal peptide and a lipobox recognisable by the signal peptidase II (Figure 2A), identifying it as a lipoprotein. Secondary structure prediction and homology searches suggested that *Hp*Pal contains a C-terminal OmpA-like globular domain (*Hp*Pal-C, residues 66–179) connected to the lipid anchor by a flexible, unstructured tether (19–65). The globular domain *Hp*Pal-C was over-expressed in BL21(DE3) cells from the pET151/D-TOPO vector and purified using Ni-NTA affinity and size exclusion chromatography to > 98% electrophoretic homogeneity based on Coomassie Blue staining of the SDS-PAGE gel (Figure 2B).

It migrated on SDS–PAGE with an apparent molecular weight of ~13.5 kDa, which is close to the value calculated from the amino-acid sequence (13.0 kDa). When subjected to size exclusion chromatography, *Hp*Pal-C eluted as a single symmetrical peak with the retention volume of 72.6 mL (data not shown). Estimation of the particle weight based on the calibration of the size exclusion column using globular proteins of a known mass gave the value of approximately 29.4 kDa, which suggested that *Hp*Pal-C is a dimer in solution under the tested conditions.

3.4. Crystallisation and preliminary crystallographic analysis

Crystals of *Hp*Pal-C (Figure 2C) were obtained using screening by sparse matrix sampling. An X-ray diffraction data set was collected from a single cryo-cooled crystal on beamline MX2 at the Australian Synchrotron (AS) to a resolution of 1.8 Å. Autoindexing of the diffraction data using *XDS* and analysis of axial systematic absences indicated that the crystal belonged to the primitive orthorhombic space group $P2_12_12_1$, with unit-cell parameters a = 50.7, b = 63.0, c = 75.1 Å, α = β = γ = 90°. The average $I/\sigma(I)$ value was 8.4 for all reflections (resolution range 48.3–1.8 Å) and 1.8 in the highest resolution shell (1.83–1.79 Å). The *R*merge value for intensities was 0.054 (0.425 in the highest resolution shell), and these data were 99% complete (99% completeness in the outer shell as well).

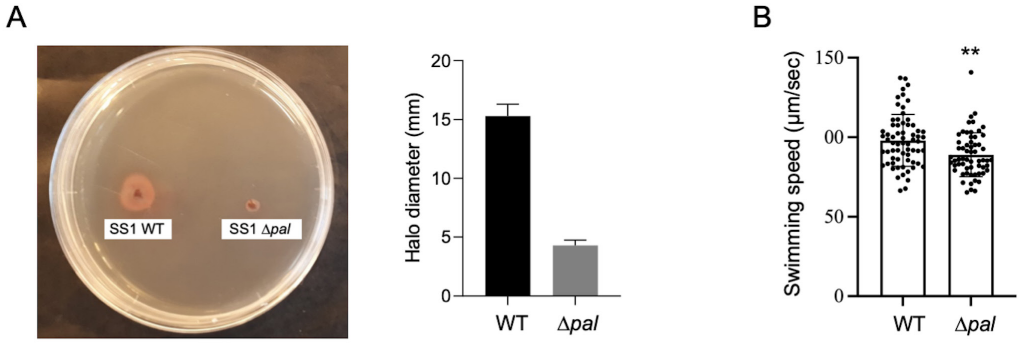

Figure 1. *H. pylori* SS1 Δ*pal* mutant shows motility defects both in semi-solid and liquid media. (A) Soft agar motility assay of *H. pylori* SS1 WT and Δ*pal::kan* mutant with visualisation aided by a colorimetric metabolic activity indicator triphenyl tetrazolium chloride. Brucella broth plates were prepared with 0.4%(w/v) bacteriological agar, 7%(v/v) fetal bovine serum, 40 μg/mL triphenyl tetrazolium chloride, and *H. pylori*-selective antibiotics (10 μg/mL vancomycin, 2.5 U/mL polymyxin B, 5 μg/mL trimethroprim). **(B)** Swimming speeds of *H. pylori* SS1 WT and Δ*pal* in liquid media BB10. For each strain, the speeds of individual cells, the mean value (97 ± 16 μm/sec for WT, 88 ± 13 μm/sec for the mutant) and the standard deviation are shown. $^{**}p < 0.01$.

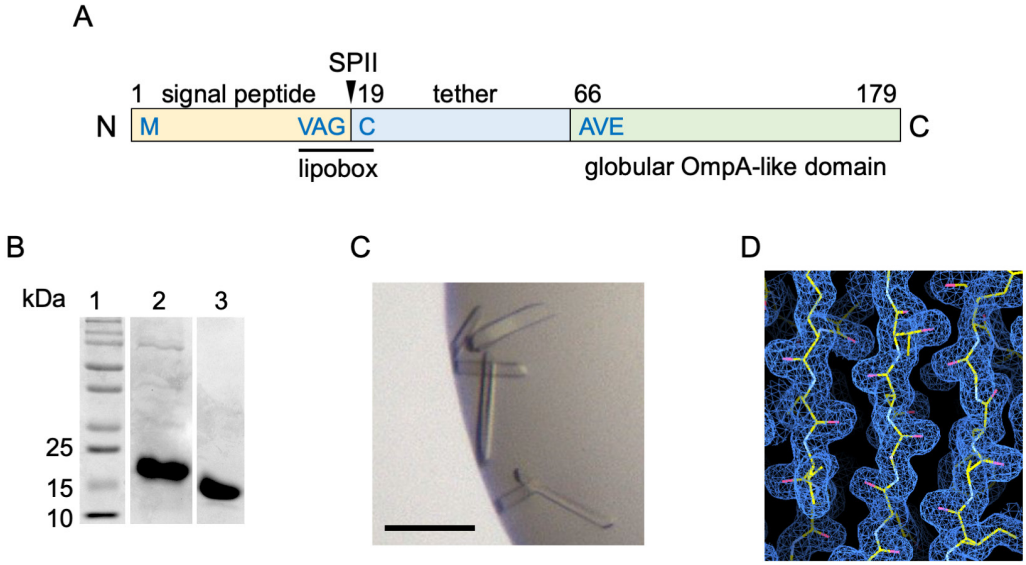

Figure 2. Production and preliminary crystallographic analysis of the C-terminal globular domain of *H. pylori* Pal (*Hp*Pal-C). (A) Schematics of full-length *H. pylori* Pal, showing N-terminal signal peptide, lipobox, site of cleavage by signal peptidase II (SPII), disordered tether and the C-terminal globular OmpA-like domain (residues 66-179) that was produced and crystallised in this study. **(B)** Coomassie Blue-stained 15% SDS-PAGE gel of Ni-NTA purified His-tagged *Hp*Pal-C (lane 2) and *Hp*Pal-C after tag cleavage and gel filtration chromatography (lane 3). **(C)** Crystals of *Hp*Pal-C. Scale bar corresponds to 0.1 mm. **(D)** Representative portion of the electron density map of the molecular replacement solution after preliminary XYZ, B refinement. The contour level is 1 σ.

Calculation of the Matthews coefficient (V_M) (*36*) suggested that the asymmetric unit most likely contains 2 molecules (V_M=2.24 Å^3/Da). In agreement with this, a molecular replacement (MR) search, performed using the structures of Pals from *B. cenocepacia*, *B. pseudomallei* and *A. baumannii* as search models, yielded solutions that contained 2 subunits. One round of XYZ, B refinement of the solution based on *A. baumannii* Pal (log likelihood gain function = 291) resulted in the largest decrease of R/Rfree values (to 0.365/0.408) of the three models. Inspection of the electron density map revealed good agreement with the partially refined MR solution (Figure 2D). Exhaustive refinement in Phenix with iterative model rebuilding in Coot (*37*) are in progress.

3.5. Discussion

The canonical Tol-Pal system in the bacterial cell wall comprises the cytoplasmic membrane proteins TolA, TolQ and TolR, the periplasmic protein TolB and the outer membrane protein Pal (*38*). Pal, bound *via* its N-terminal anchor to the outer membrane, and *via* its C-terminal OmpA-like domain to the peptidoglycan, is important for the integrity of the outer membrane. In some bacteria, including *E. coli*, the Tol-Pal system plays an important role in cell division, by promoting the constriction of the outer membrane (*39*) and peptidoglycan restructuring at the septum (*38*).

Although *H. pylori* Pal shares 38% amino acid sequence identity with the well-characterised Pal

component of the *E. coli* Tol-Pal system, *H. pylori* does not have homologs of the inner membrane components of this system (TolA, TolQ or TolR) (*35*). This suggests that *H. pylori* may possess a non-canonical TolB/Pal system that has a different primary function. A previous study of the Δ*pal* (HP1125) mutant of non-motile *H. pylori* strain 26695 (*35*) pointed to a possible association of Pal with the flagellar motor, although the results were not conclusive. However, recent reports of *E. coli pal* mutants with reduced motility in semi-solid agar (*21,22*) also pointed to the possible involvement of Pal in the regulation or function of the flagellar motor. In this study, we performed preliminary X-ray crystallographic analysis of Pal from *H. pylori* and evaluated its requirement for *H. pylori* motility in both liquid and semi-solid media. Under both conditions, inactivation of the *pal* gene produced flagellated cells with reduced motility. These results demonstrate the functional association of *Hp*Pal with the flagellar motor. We note that the motility defects were more prominent in semi-solid agar, and only a modest reduction in the linear swimming speed was observed in liquid medium. Although it remains to be established if *Hp*Pal is an integral component of the periplasmic scaffold of the *H. pylori* flagellar motor, our results suggest that *Hp*Pal plays a novel, non-canonical role by regulating the function of the motor in response to surface contact or increased viscosity. Our observation that, in contrast to other characterised Pals that are monomeric in solution (*40,41*), *Hp*Pal behaves as a dimer, may be related to this different role.

Pals have been studied extensively as potential targets for new therapeutics for several reasons. *i*) In some bacteria, *e.g. Caulobacter crescentus* (*42*), *pal* is essential. *ii*) A fraction of the Pal molecules become exposed on the surface of bacteria, which has been exploited in the design and evaluation of many vaccine candidates (*38,43*). *iii*) In *A. baumannii*, the surface-exposed Pal interacts with host fibronectin (*43*); blocking this interaction with small molecules may offer a new strategy to combat bacterial infections. *iv*) Pal was also shown to be important for production of biofilm (*43*). *v*) In addition, importance of Pal for persister cell formation during antibiotic treatment of *E. coli* has been demonstrated (*44*). *vi*) Furthermore, *E. coli* Pal was shown to be required for the production of the capsular polysaccharide and resistance to serum (*45*). *vii*) Finally, *A. baumannii* Pal was found to contribute to virulence by regulating the twitching motility (*43*). The latter finding about the role of Pal in the type IV pili-mediated motility is particularly interesting because the results of our study suggest that Pal can also regulate flagellar motor-mediated motility, which adds yet another facet to the role of this enigmatic protein. The purification, crystallisation and preliminary X-ray diffraction analysis of recombinant *Hp*Pal-C presented in this study is an important step towards elucidation of the non-canonic *Hp*Pal function and exploration of its therapeutic potential.

In conclusion, *H. pylori* SS1 Δ*pal* mutant strain showed a significant motility defect in semisolid agar. *The* Δ*pal* mutants were also unable to achieve WT linear swimming speeds in liquid media. Cloning, overexpression, purification and biochemical characterisation of the C-terminal globular domain of *H. pylori* Pal (*Hp*Pal-C) allowed us to perform its preliminary X-ray crystallographic analysis. The outcomes of this work pave the way to future studies aimed at elucidation of the role of *Hp*Pal in the regulation, or function of, the flagellar motor.

Acknowledgements

The authors would like to thank Houdaii Elhoussaini (Monash University) for preliminary expression analysis. Part of this research was undertaken on the MX2 beamline of the Australian Synchrotron, Victoria, Australia. We thank the AS staff for their assistance with data collection. We are also grateful to Dr. Geoffrey Kong at the Monash Macromolecular Crystallisation Platform for assistance with the robotic crystallization trials.

Funding: This work was supported by the Australian Research Council grant DP210103056 to A.R.

Conflict of Interest: The authors have no conflicts of interest to disclose.

References

1. Hooi JKY, Lai WY, Ng WK, Suen MMY, Underwood FE, Tanyingoh D, Malfertheiner P, Graham DY, Wong VWS, Wu JCY, Chan FKL, Sung JJY, Kaplan GG, Ng SC. Global prevalence of *Helicobacter pylori* infection: Systematic review and meta-analysis. Gastroenterology. 2017; 153:420-429.
2. Warren JR, Marshall B. Unidentified curved bacilli on gastric epithelium in active chronic gastritis. Lancet. 1983; 1:1273-1275.
3. The EUROGAST Study Group. An international association between *Helicobacter pylori* infection and gastric cancer. Lancet. 1993; 341:1359-1362.
4. Peek RM Jr, Blaser MJ. *Helicobacter pylori* and gastrointestinal tract adenocarcinomas. Nat Rev Cancer. 2002; 2:28-37.
5. de Martel C, Georges D, Bray F, Ferlay J, Clifford GM. Global burden of cancer attributable to infections in 2018: a worldwide incidence analysis. Lancet Glob Health. 2020; 8:e180-e190.
6. Sung H, Ferlay J, Siegel RL, Laversanne M, Soerjomataram I, Jemal A, Bray F. Global Cancer Statistics 2020: GLOBOCAN estimates of incidence and mortality worldwide for 36 cancers in 185 countries. CA Cancer J Clin. 2021; 71:209-249.
7. Evans DG, Queiroz DM, Mendes EN, Evans DJ Jr. *Helicobacter pylori cagA* status and *s* and *m* alleles of

vacA in isolates from individuals with a variety of *H. pylori*-associated gastric diseases. J Clin Microbiol. 1998; 36:3435-3437.
8. Tohidpour A, Gorrell RJ, Roujeinikova A, Kwok T. The middle fragment of *Helicobacter pylori* CagA induces actin rearrangement and triggers its own uptake into gastric epithelial cells. Toxins (Basel). 2017; 9:237.
9. Roujeinikova A. Phospholipid binding residues of eukaryotic membrane-remodelling F-BAR domain proteins are conserved in *Helicobacter pylori* CagA. BMC Res Notes. 2014; 7:525.
10. Krulwich TA, Sachs G, Padan E. Molecular aspects of bacterial pH sensing and homeostasis. Nat Rev Microbiol. 2011; 9:330-343.
11. Modak JK, Rut W, Wijeyewickrema LC, Pike RN, Drag M, Roujeinikova A. Structural basis for substrate specificity of *Helicobacter pylori* M17 aminopeptidase. Biochimie. 2016; 121:60-71.
12. Stent A, Every AL, Sutton P. *Helicobacter pylori* defense against oxidative attack. Am J Physiol Gastrointest Liver Physiol. 2012; 302:G579-G587.
13. Ud-Din AI, Liu YC, Roujeinikova A. Crystal structure of *Helicobacter pylori* pseudaminic acid biosynthesis N-acetyltransferase PseH: Implications for substrate specificity and catalysis. PLoS One. 2015; 10:e0115634.
14. Hanyu H, Engevik KA, Matthis AL, Ottemann KM, Montrose MH, Aihara E. *Helicobacter pylori* uses the TlpB receptor to sense sites of gastric injury. Infect Immun. 2019; 87:e00202-19.
15. Hu S, Ottemann KM. *Helicobacter pylori* initiates successful gastric colonization by utilizing L-lactate to promote complement resistance. Nat Commun. 2023; 14:1695.
16. Machuca MA, Johnson KS, Liu YC, Steer DL, Ottemann KM, Roujeinikova A. *Helicobacter pylori* chemoreceptor TlpC mediates chemotaxis to lactate. Sci Rep. 2017; 7:14089.
17. Qin Z, Lin WT, Zhu S, Franco AT, Liu J. Imaging the motility and chemotaxis machineries in *Helicobacter pylori* by cryo-electron tomography. J Bacteriol. 2017; 199:e00695-16.
18. Zhou X, Roujeinikova A. The structure, composition, and role of periplasmic stator scaffolds in polar bacterial flagellar motors. Front Microbiol. 2021; 12:639490.
19. Tachiyama S, Chan KL, Liu X, Hathroubi S, Peterson B, Khan MF, Ottemann KM, Liu J, Roujeinikova A. The flagellar motor protein FliL forms a scaffold of circumferentially positioned rings required for stator activation. Proc Natl Acad Sci USA. 2022; 119:e2118401119.
20. Reboul CF, Andrews DA, Nahar MF, Buckle AM, Roujeinikova A. Crystallographic and molecular dynamics analysis of loop motions unmasking the peptidoglycan-binding site in stator protein MotB of flagellar motor. PLoS One. 2011; 6:e18981.
21. Hirakawa H, Suzue K, Kurabayashi K, Tomita H. The Tol-Pal system of uropathogenic *Escherichia coli* is responsible for optimal internalization into and aggregation within bladder epithelial cells, colonization of the urinary tract of mice, and bacterial motility. Front Microbiol. 2019; 10:1827.
22. Hirakawa H, Suzue K, Takita A, Awazu C, Kurushima J, Tomita H. Roles of the Tol-Pal system in the Type III secretion system and flagella-mediated virulence in enterohemorrhagic *Escherichia coli*. Sci Rep. 2020; 10:15173.
23. Teufel F, Almagro Armenteros JJ, Johansen AR, Gíslason MH, Pihl SI, Tsirigos KD, Winther O, Brunak S, von Heijne G, Nielsen H. SignalP 6.0 predicts all five types of signal peptides using protein language models. Nat Biotechnol. 2022; 40:1023-1025.
24. Jones DT, Cozzetto D. DISOPRED3: precise disordered region predictions with annotated protein-binding activity. Bioinformatics. 2015; 31:857-863.
25. Woon AP, Tohidpour A, Alonso H, Saijo-Hamano Y, Kwok T, Roujeinikova A. Conformational analysis of isolated domains of *Helicobacter pylori* CagA. PLoS One. 2013; 8:e79367.
26. Bradford MM. A rapid and sensitive method for the quantitation of microgram quantities of protein utilizing the principle of protein-dye binding. Anal Biochem. 1976; 72:248-254.
27. Dawkins JV. Size Exclusion Chromatography. In: Comprehensive Polymer Science and Supplements (Allen G., Bevington JC, eds.). Pergamon, 1989, pp. 231-238.
28. Kabsch W. *XDS.* Acta Crystallogr D Biol Crystallogr. 2010; 66:125-132.
29. Evans PR, Murshudov GN. How good are my data and what is the resolution? Acta Crystallogr D Biol Crystallogr. 2013; 69:1204-1214.
30. Winn MD, Ballard CC, Cowtan KD, *et al.* Overview of the CCP4 suite and current developments. Acta Crystallogr D Biol Crystallogr. 2011; 67:235-242.
31. Capelli R, Matterazzo E, Amabili M, Peri C, Gori A, Gagni P, Chiari M, Lertmemongkolchai G, Cretich M, Bolognesi M, Colombo G, Gourlay LJ. Designing probes for immunodiagnostics: Structural insights into an epitope targeting *Burkholderi*a infections. ACS Infect Dis. 2017; 3:736-743.
32. Gourlay LJ, Peri C, Ferrer-Navarro M, *et al.* Exploiting the *Burkholderia pseudomallei* acute phase antigen BPSL2765 for structure-based epitope discovery/design in structural vaccinology. Chem Biol. 2013; 20:1147-1156.
33. McCoy AJ, Grosse-Kunstleve RW, Adams PD, Winn MD, Storoni LC, Read RJ. Phaser crystallographic software. J Appl Crystallogr. 2007; 40:658-674.
34. Liebschner D, Afonine PV, Baker ML, *et al.* Macromolecular structure determination using X-rays, neutrons and electrons: Recent developments in Phenix. Acta Crystallogr D Struct Biol. 2019; 75:861-877.
35. Turner L, Praszkier J, Hutton ML, Steer D, Ramm G, Kaparakis-Liaskos M, Ferrero RL. Increased outer membrane vesicle formation in a *Helicobacter pylori tolB* mutant. Helicobacter. 2015; 20:269-283.
36. Matthews BW. Solvent content of protein crystals. J Mol Biol. 1968; 33:491-497.
37. Emsley P, Cowtan K. Coot: Model-building tools for molecular graphics. Acta Crystallogr D Biol Crystallogr. 2004; 60:2126-2132.
38. Szczepaniak J, Press C, Kleanthous C. The multifarious roles of Tol-Pal in Gram-negative bacteria. FEMS Microbiol Rev. 2020; 44:490-506.
39. Petiti M, Serrano B, Faure L, Lloubes R, Mignot T, Duché D. Tol energy-driven localization of pal and anchoring to the peptidoglycan promote outer-membrane constriction. J Mol Biol. 2019; 431:3275-3288.
40. Parsons LM, Lin F, Orban J. Peptidoglycan recognition by Pal, an outer membrane lipoprotein. Biochemistry. 2006; 45:2122-2128.
41. Dennehy R, Romano M, Ruggiero A, Mohamed

YF, Dignam SL, Mujica Troncoso C, Callaghan M, Valvano MA, Berisio R, McClean S. The *Burkholderia cenocepacia* peptidoglycan-associated lipoprotein is involved in epithelial cell attachment and elicitation of inflammation. Cell Microbiol. 2017; 19:e12691.
42. Yeh YC, Comolli LR, Downing KH, Shapiro L, McAdams HH. The *Caulobacter* Tol-Pal complex is essential for outer membrane integrity and the positioning of a polar localization factor. J Bacteriol. 2010; 192:4847-4858.
43. Solanki V, Tiwari M, Tiwari V. Investigation of Peptidoglycan-Associated Lipoprotein of *Acinetobacter baumannii* and Its Interaction with Fibronectin to Find Its Therapeutic Potential. Infect Immun. 2023; 91:e0002323.
44. Sulaiman JE, Hao C, Lam H. Specific enrichment and proteomics analysis of *Escherichia coli* persisters from rifampin pretreatment. J Proteome Res. 2018; 17:3984-3996.
45. Diao J, Bouwman C, Yan D, Kang J, Katakam AK, Liu P, Pantua H, Abbas AR, Nickerson NN, Austin C, Reichelt M, Sandoval W, Xu M, Whitfield C, Kapadia SB. Peptidoglycan Association of murein lipoprotein is required for KpsD-Dependent group 2 capsular polysaccharide expression and serum resistance in a uropathogenic *Escherichia coli* isolate. mBio. 2017; 8:e00603-17.

Received October 26, 2023; Revised December 2, 2023; Accepted December 4, 2023.

**Address correspondence to:*
Anna Roujeinikova, Department of Microbiology, Infection and Immunity Program, Monash Biomedicine Discovery Institute; Department of Biochemistry and Molecular Biology, Monash University, Melbourne, Victoria, Australia.
E-mail: anna.roujeinikova@monash.edu

Released online in J-STAGE as advance publication December 8, 2023.

Correspondence

DOI: 10.5582/bst.2023.01303

Immunity debt: Hospitals need to be prepared in advance for multiple respiratory diseases that tend to co-occur

Ting Li[1,2], Cordia Chu[2], Biying Wei[1], Hongzhou Lu[1,*]

[1] Department of Infectious Diseases, National Clinical Research Center for Infectious Diseases, the Third People's Hospital of Shenzhen, Shenzhen, Guangdong, China
[2] Centre for Environment and Population Health, School of Medicine and Dentistry, Griffith University, Brisbane, Australia.

SUMMARY As SARS-CoV-2 transitions from a pandemic to an endemic presence, a significant rise in respiratory diseases such as influenza and Mycoplasma pneumonia is challenging healthcare systems weakened by the impact of COVID-19. This commentary examines the global resurgence of respiratory pathogens, heightened by the post-pandemic "immunity debt", through an analysis of WHO surveillance data and national health reports. Findings reveal a substantial increase in respiratory illnesses, notably among children, compounded by a shortage of pediatricians and growing antimicrobial resistance. This underscores the need to improve hospital preparedness, optimize clinical responses, and enhance public health strategies to effectively navigate the impending peak of concurrent respiratory infections.

Keywords immunity debt, influenza, mycoplasma pneumonia, respiratory infection, hospital preparedness

As the novel coronavirus SARS-CoV-2 (the cause of COVID-19) gradually transitions from a pandemic-causing pathogen to a common endemic virus, respiratory infectious pathogens such as influenza viruses, respiratory syncytial virus, and *Mycoplasma pneumoniae* have become prevalent again. Healthcare facilities already hit hard by the COVID-19 pandemic are now facing new challenges from the upsurge in respiratory illnesses.

Many countries are repaying their post-COVID-19 "immunity debt", and China is no exception

According to the predictions and assessments of numerous public health experts worldwide, non-pharmaceutical interventions (NPIs) during the COVID-19 pandemic have led to a widespread deficiency in adaptive immunity, which many scholars refer to as "immunity debt" or "immunity gap" (*1-3*). In other words, a lack of adaptive immunity in the population is very likely to lead to outbreaks of various respiratory diseases. This situation has already occurred in several countries, including the US, France, Australia, and Canada (*4*). The World Health Organization's (WHO's) surveillance data on global influenza clearly substantiates that contention; In contrast to the low prevalence of influenza during the COVID-19 pandemic(*5,6*), since the start of 2022, several countries have experienced at least two waves of influenza outbreaks, and the number of influenza cases is significantly higher than before the outbreak of COVID-19 in 2020 (Figure 1). At the same time, the prevalence of common respiratory viruses has greatly exceeded their baseline levels before the COVID-19 pandemic, leading to a rapid increase in cases in a short period of time (*7*).

Multiple respiratory diseases that tend to co-occur are the key problem

The seasonal flu epidemic is unquestionably coming in China. Some scholars proposed preparing in advance for the simultaneous epidemic of COVID-19 and influenza in 2022, but China is now facing multiple respiratory virus epidemics (*8*). Since mid-October of this year, the incidence of influenza-like illnesses in China has increased compared to the same period over the past three years, with a surge in pediatric visits to many hospitals. The daily outpatient volume has doubled, reaching more than 13,000 people at Tianjin Children's Hospital, with pediatric wards at full capacity and lines forming (*9*). Data obtained from The Third People's Hospital of Shenzhen, China shows that the number of children with a fever has increased by more than 50% in the past month, and more than 90% of children in hospital are infected with *Mycoplasma pneumoniae*. The weekly influenza surveillance report from the Chinese Center for Disease Control and Prevention for week 46 of 2023 shows that positivity according to

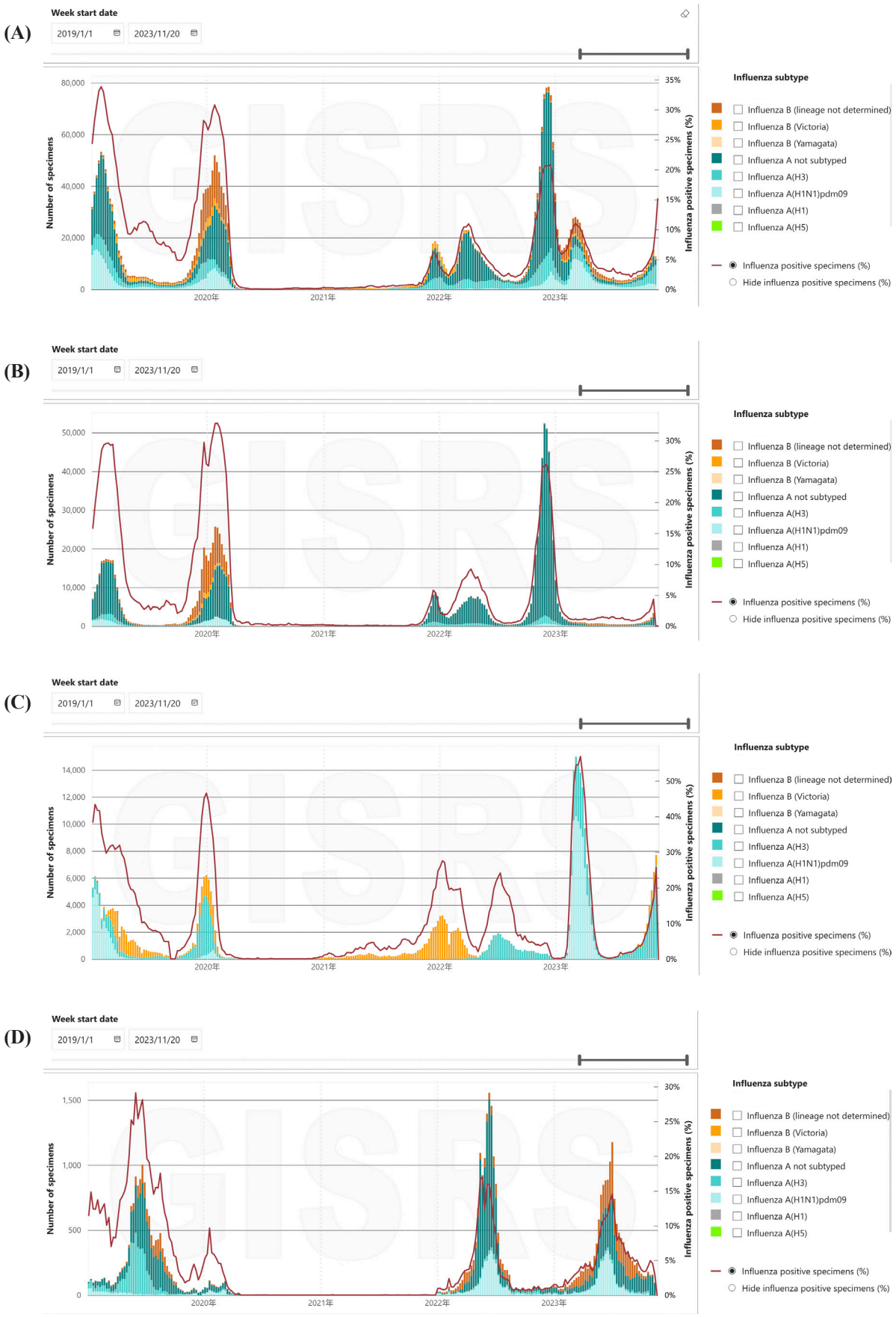

Figure 1. Status of current influenza infections from 01/2019 to 11/2023. (A), Global data on influenza infections from 01/2019 to 11/2023. **(B)** Data on influenza infections in the United States of America from 01/2019 to 11/2023. **(C)** Data on influenza infections in China from 01/2019 to 11/2023. **(D)** Data on influenza infections in Australia from 01/2019 to 11/2023. *Data source*: FluNet (*http://www.who.int/tools/flunet*) (*16*).

influenza virus testing continued to rise in November, predominantly involving the A(H3N2) subtype, followed by the B(Victoria) lineage. By November 19th, there were 205 reported outbreaks of influenza-like illnesses (ILI) nationwide. Sentinel hospitals in China's southern provinces reported that the percentage of ILI was 6.4%, which is higher than the previous week's level (5.5%). At the same time, sentinel hospitals in northern provinces reported that the percentage of ILI was 6.2%, which is higher than the previous week's level (5.0%) (*10*).

Announcements from Beijing, Tianjin, Changchun, and some southern cities in China have indicated that there has been a significant increase in the incidence of respiratory infectious diseases. The proportion of cases of Mycoplasma pneumonia in children with pneumonia has markedly increased, with many patients presenting with co-infections of multiple pathogens.

Respiratory diseases that overlap in prevalence put tremendous pressure on the administration of many hospitals

On November 22, the WHO requested that China provide detailed information regarding the increase in respiratory diseases and the cluster of pediatric pneumonia mentioned in related reports. The next day, the WHO stated that data from the Chinese Center for Disease Control and Prevention indicated that the current peak of pediatric pneumonia is attributed to known pathogens, including influenza viruses, *Mycoplasma pneumoniae*, and respiratory syncytial viruses (*11,12*). The National Health Commission of China released information predicting that influenza will peak nationwide during the winter and spring, and *Mycoplasma pneumoniae* infections will continue to occur at high rates in certain regions for some time. This winter and coming spring, China may face a situation where COVID-19, influenza, *Mycoplasma pneumoniae* infections, and other respiratory diseases overlap in prevalence (*13*).

Given the current pressure pediatric patients are placing on many Chinese hospitals, the shortage of pediatricians is a problem that needs to be urgently addressed. In addition, there is a widespread epidemic of *Mycoplasma pneumoniae* in children, and clinicians have warned that azithromycin resistance among children with mycoplasma pneumonia could be as high as 90%. This has once again made the public aware that incidence of macrolide-resistant Mycoplasma pneumoniae (MRMP) is so high that azithromycin has gradually been relegated to a second-line clinical drug. Even research published in JAMA in 2022 warned of a high incidence of MRMP globally (*13*). This was particularly true in the Western Pacific, where that incidence was 53.4%, but China had the highest rate of MRMP at 79.5%.

Prioritization of hospital preparedness for respiratory infections

The cooccurrence of multiple respiratory diseases due to several pathogens, the shortage of pediatricians, and increased drug resistance represent complex challenges to healthcare administration. According to our predictions, the peak period of overlapping multiple respiratory infections has not yet been reached, so preparations and responses by hospitals are the priorities.

Adaptability in clinical protocols: Clinical treatment regimens need to be tailored to the diverse etiologies of respiratory infections. Given that acute respiratory infections represent a significant cause of pediatric and geriatric morbidity and mortality worldwide, pre-emptive clinical intervention is imperative to forestall the progression to critical illness within these vulnerable cohorts.

Pharmacological sensitivity and efficacy: Emphasis must be placed on the judicious selection of antimicrobials in therapeutic management. Notwithstanding the prevalent use of azithromycin for pediatric co-infections with *Mycoplasma pneumoniae*, increasing resistance underscores the need for vigilant monitoring of drug efficacy.

Nosocomial infection control: Enhancing infection control protocols is essential to minimizing the incidence of iatrogenic infections, particularly during patient influxes. Upholding fundamental prophylactic standards and implementing strict contact isolation practices are critical to mitigating nosocomial transmission.

Resource allocation in response to the pathogen burden: The cooccurrence of multiple respiratory pathogens necessitates the pre-emptive allocation of medical personnel and the stockpiling of medicinal supplies and facilities to accommodate patients. Hospitals should formulate preemptive logistics and communication strategies to effectively manage the anticipated patient surge.

Future strategies for hospitals to manage respiratory infectious diseases

A robust mechanism for an effective response: Research on and improvements in emergency preparedness and response frameworks are required, and this includes vaccines and novel pharmacological treatments (*14*). The expeditious improvement of clinical infrastructure and the of comprehensive expansion of clinical treatment capacity are also of paramount importance.

Enhanced pathogen surveillance: Prior to the appearance of novel pathogenic entities, surveillance systems need to be continually improved, ensuring prompt pathogen identification. This involves continuous improvement of monitoring methodologies and the enhancement of early detection and warning capabilities.

Improved health education: Prioritizing health education is quintessential to alleviating public trepidation and the consequent overtaxing of healthcare systems (*15*). This initiative should incorporate the

provision of timely, accurate, and impartial information, along with interpretations of relevant policies, to facilitate communication with the general population.

Funding: This work was supported by a grant for Science and Technology Research Projects of Shenzhen (JSGG20220606141001003).

Conflict of Interest: The authors have no conflicts of interest to disclose.

References

1. Cohen R, Pettoello-Mantovani M, Somekh E, Levy C. European pediatric societies call for an implementation of regular vaccination programs to contrast the immunity debt associated to coronavirus disease-2019 pandemic in children. J Pediatr. 2022; 242:260-261.e263.
2. Messacar K, Baker RE, Park SW, Nguyen-Tran H, Cataldi JR, Grenfell B. Preparing for uncertainty:Endemic paediatric viral illnesses after COVID-19 pandemic disruption. The Lancet. 2022.
3. Cohen R, Levy C, Rybak A, Angoulvant F, Ouldali N, Grimprel E. Immune debt: Recrudescence of disease and confirmation of a contested concept. Infect Dis Now. 2023; 53:104638.
4. Cohen R, Rybak A, Werner A, Béchet S, Desandes R, Hassid F, André J-M, Gelbert N, Thiebault G, Kochert F. Trends in pediatric ambulatory community acquired infections before and during covid-19 pandemic support the immunity debt concept (pari study). Social Science Electronic Publishing.
5. Li Q, Wang J, Lv H, Lu H. Impact of China's COVID-19 prevention and control efforts on outbreaks of influenza. Biosci Trends. 2021; 15:192-195.
6. Sawakami T, Karako K, Song P, Sugiura W, Kokudo N. Infectious disease activity during the COVID-19 epidemic in Japan: Lessons learned from prevention and control measures. Biosci Trends. 2021; 15:257-261.
7. Pan American Health Organization. Epidemiological Alert - Influenza, respiratory syncytial virus and SARS-CoV-2 - 6 June 2023. *https://www.paho.org/en/documents/epidemiological-alert-influenza-respiratory-syncytial-virus-and-sars-cov-2-6-june-2023* (accessd November 27, 2023).
8. Li T, Asakawa T, Liu H, Chu C, Lu H. The role of influenza in the era of COVID-19: Can we forget it? Biosci Trends. 2022; 16:374-376.
9. 163.com. Is the recent overloading of paediatric consulting rooms really paying off the immunisation debt? It's not that simple. *https://m.163.com/dy/article_cambrian/IKATBQ4H0553BGSF.html* (accessd November 27, 2023).
10. Chinese National Influenza Center. Chinese Weekly Influenza Surveillance Report. *https://ivdc.chinacdc.cn/cnic/zyzx/lgzb/202311/t20231123_270811.htm* (accessd November 27, 2023).
11. World health Organisation. WHO statement on reported clusters of respiratory illness in children in northern China. *https://www.who.int/news/item/22-11-2023-who-statement-on-reported-clusters-of-respiratory-illness-in-children-in-northern-china* (accessd November 27, 2023).
12. World health Organisation. Upsurge of respiratory illnesses among children-Northern China. *https://www.who.int/emergencies/disease-outbreak-news/item/2023-DON494* (accessd November 27, 2023).
13. China NHCo. Transcript of the press conference of the National Health Commission of China on 24 November 2023. *http://www.nhc.gov.cn/cms-search/xxgk/getManuscriptXxgk.htm?id=4b4569ebb26f4d2583763780c85c7ba4* (accessd November 27, 2023).
14. Karako K, Song P, Chen Y, Karako T. Trends in managing COVID-19 from an emerging infectious disease to a common respiratory infectious disease: What are the subsequent impacts on and new challenges for healthcare systems? Biosci Trends. 2022; 16:381-385.
15. Luo M, Sun J, Gong Z, Wang Z. What is always necessary throughout efforts to prevent and control COVID-19 and other infectious diseases? A physical containment strategy and public mobilization and management. Biosci Trends. 2021; 15:188-191.
16. World health Organization. Global Influenza Programme. *http://www.who.int/tools/flunet* (accessd November 27, 2023).

Received Novermber 28, 2023; Revised December 5, 2023; Accepted December 7, 2023.

**Address correspondence to:*
Hongzhou Lu, Department of Infectious Diseases, National Clinical Research Center for Infectious Diseases, the Third People's Hospital of Shenzhen, 29 Buji Bulan Road, Shenzhen, Guangdong Province 518112, China.
E-mail: luhongzhou@fudan.edu.cn

Released online in J-STAGE as advance publication December 8, 2023.

Correspondence

DOI: 10.5582/bst.2023.01285

Development of a novel cholesterol tag-based system for transmembrane transport of protein drugs

Pengfei Zhao[1,3,4,§], Shuo Song[5,§], Zhuojun He[1,2,3,§],Guiqin Dai[1,3], Deliang Liu[1,3], Jiayin Shen[1,3], Tetsuya Asakawa[1,*], Mingbin Zheng[1,2,3,5,*], Hongzhou Lu[1,3,*]

[1] Institute of Neurology, National Clinical Research Center for Infectious Diseases, the Third People's Hospital of Shenzhen, Shenzhen, Guangdong, China;
[2] Key Laboratory for Nanomedicine, Guangdong Medical University, Dongguan, Guangdong, China;
[3] National Clinical Research Center for Infectious Disease, Shenzhen Clinical Medical Research Center for Tuberculosis, Institute for Hepatology, the Third People's Hospital of Shenzhen, Shenzhen, Guangdong, China;
[4] College of Physics and Optoelectronic Engineering, Shenzhen Key Laboratory of Photonics and Biophotonics, Key Laboratory of Optoelectronic Devices and Systems of the Ministry of Education and Guangdong Province, Shenzhen University, Shenzhen, China;
[5] Shenzhen Samii Medical Center, Shenzhen, Guangdong, China.

SUMMARY The main technological difficulties of developing an intracellular (transmembrane) transport system for protein drugs lie in two points: *i*) overcoming the barriers in the cellular membrane, and *ii*) loading enough protein drugs, and particularly high-dose proteins, into particles. To address these two technological problems, we recently developed a novel cholesterol tag (C-Tag)-based transmembrane transport system. This pilot study found that the C-Tag dramatically improved the cellular uptake of Fab (902-fold, *vs*. Fab alone) into living cells, indicating that it successfully achieved transmembrane transport. Moreover, C-Tag-mediated membrane transport was verified using micron-scale large unilamellar vesicles (LUVs, approximately 1.5 μm)-based particles. The C-Tagged Fab was able to permeate the liposomal bilayer and it greatly enhanced (a 10.1-fold increase *vs*. Fab alone) internalization of proteins into the LUV-based particles, indicating that the C-Tag loaded enough proteins into particles for use of high-dose proteins. Accordingly, we established a novel C-Tag-based transport system that has overcome the known technological difficulties of protein transmembrane delivery, and this might be a useful technology for drug development in the future.

Keywords protein drug, cell membrane, transmembrane transport, cholesterol tag, intraparticle delivery

1. The main difficulties in delivery of therapeutic protein drugs into the cytoplasm

Expression and regulation of proteins in living cells play a crucial role in biological processes, involving almost all forms of cellular physiology and disease progression (*1-4)*. In terms of diagnosis and treatment of some refractory diseases, a crucial task is to explore the cytosolic targets associated with cell necrocytosis, energy metabolism, and protein expression (*5*). During the development of a novel therapy, we sometimes need to deliver therapeutic proteins or drugs from extracellular fluid to the cytoplasm (*6*). However, cytosolic delivery of therapeutic proteins is usually hampered by cell membrane obstruction, endocytic sequestration, and lysosomal breakdown, which present notable barriers for approaching those intracellular targets (*7-9*). Hence, delivering therapeutic proteins/drugs into the cytoplasm is a challenge during the development of novel strategies to fight against these refractory diseases (*10,11*). Thus far, several physical technologies have been developed to address this problem. Approaches like direct microinjection of biologics into cytosols using a microinjector are plausible, but these approaches suffer from quite low throughput (*12*). High-throughput approaches, like squeezing and electroporation, have to punch transient pores at the cell membrane in order to establish temporary channels for material exchange between the extracellular and intracellular environments. However, these approaches suffer from uncontrollable material exchange, along with potential cell toxicity (*13,14*). Other intrinsic cellular mechanisms such as endocytosis have also been considered. Many chemical agents, such as liposomes, polymers, and cell-penetrating peptides (CPPs), are commonly delivered mostly into cells *via* endocytosis. Nevertheless, such endocytotic action is fundamentally regarded as a cellular self-defense mechanism, the basic function

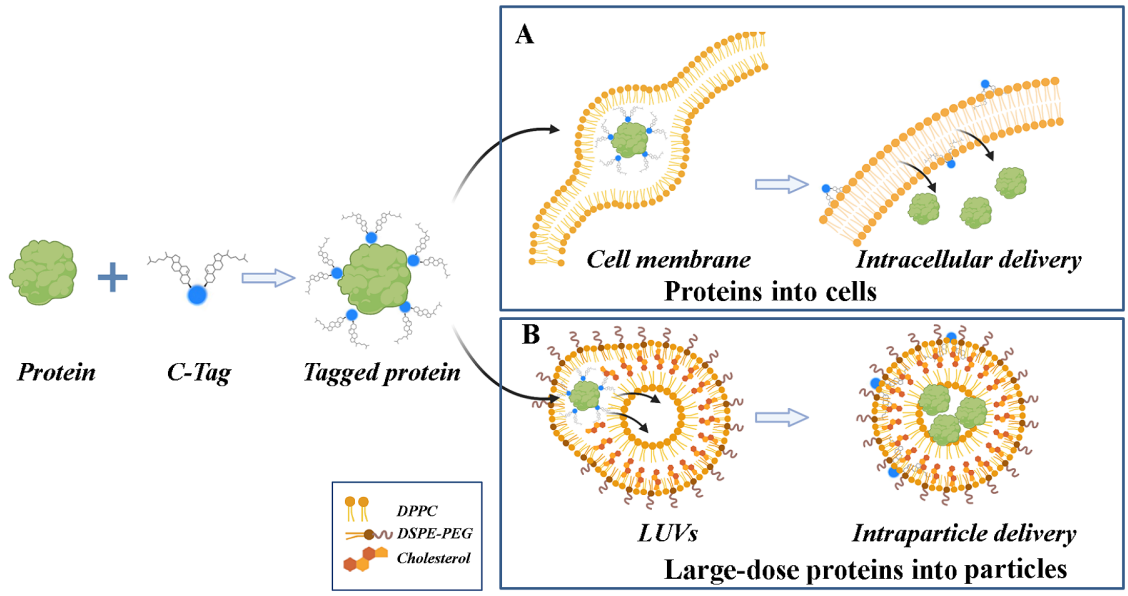

Figure 1. Schematic diagram of the novel C-Tag-based transmembrane transport system. The novel C-Tag-based transmembrane transport system addressed two technological difficulties: **(A)**. Transporting proteins into cells; **(B)**. Loading high-dose proteins into particles. The CB moiety of C-Tag non-covalently anchors onto the protein surface, and the cholesterol motif facilitates protein insertion into the hydrophobic lipid bilayers of cell membranes (or LUVs). Due to the noncovalent nature of C-Tag, the protein-tag complex embedded between the bilayers would separate, precluding the presence of the hydrophilic protein within the hydrophobic bilayer. Eventually, the proteins escape from the membrane and enter the cytoplasm (or LUV cavity), achieving protein transmembrane transport. Created with Biorender.com. CB: Coomassie blue; C-Tag: cholesterol tag; DPPC: 1,2-dipalmitoyl-sn-glycero-3-phosphocholine; DSPE-PEG: 1,2-distearoyl-sn-glycero-3-phosphoethanolamine-N-[carboxy(polyethylene glycol)-2000], LUVs: large unilamellar vesicles.

of which is to prevent intact foreign biomolecules from entering the cytoplasm (*15,16)*. Thus, inducing such endocytotic action might not be able to maintain the biological activity of the delivered drugs. Thus, such "endocytotic action" should be avoided when developing novel delivery vehicles/systems/strategies to transport active therapeutic proteins into cytosolic targets because of their "inactivation". Lipid-based vehicles are the most common class of FDA-approved micro-nano particles, and they have a simple formulation and involve self-assembly, biocompatibility, and bioavailability (*15*). By incorporating a stimuli-response and cationic design, such lipid-based particles might also facilitate endosomal escape and fulfill potent protein internalization, which might be conveniently used in the scenario of disease treatment (*17*). Nevertheless, conventional lipid-based nanoparticles cannot sufficiently encapsulate cargo proteins due to uncontrollable particle assembly and an amphiphilic protein structure, hence limiting their further use in cytosolic protein delivery and personalized precision medicine (*18*). Accordingly, the aforementioned technologies have certain drawbacks and are far from satisfactory. Development of a novel delivery system is an urgent task for treating some refractory diseases (*15,19*), but the main technological difficulties lie in two points: *i*) The difficulty of achieving satisfactory intracellular (transmembrane) transport (the problem of "Transporting proteins into cells") and *ii*) The difficulty of filling the delivery vehicle with high-dose proteins (the problem of "Loading particles with high-dose proteins"). To address these two technological problems, we recently developed a novel cholesterol tag (C-Tag)-based transmembrane transport system (Figure 1).

2. Establishment of a novel C-Tag-based transmembrane transport system

A novel C-Tag-based transmembrane transport system was developed to achieve transmembrane delivery of protein drugs into cytoplasm with complete biological activity, along with ability to fill the delivery vehicle with high-dose proteins.

To overcome the first technological problem to achieve intracellular delivery, a cholesterol-based protein delivery tag was established by conjugating a Coomassie blue (CB) molecule with two copies of cholesterol (Figure 2A). Cholesterol is a natural component of eukaryote cell membranes, and CB can non-covalently bind to the protein surface. As shown as in Figure 1, the C-Tag can anchor onto the protein surface and facilitate permeation of the protein directly into cells without generating any transient pores or reducing drug activity (*19*). C-Tag therefore can serve as a promising tool to pull linked proteins into the cell bilayer and eventually transported proteins into the cytoplasm rather than *via* endocytosis (Figure 1A). Our previous study suggested that compact proteins are highly amenable to transmembrane delivery, whereas large proteins tend to enter cells *via* endocytosis (*19,20*). Hence, the compact Fab fragments (~55 kDa) of

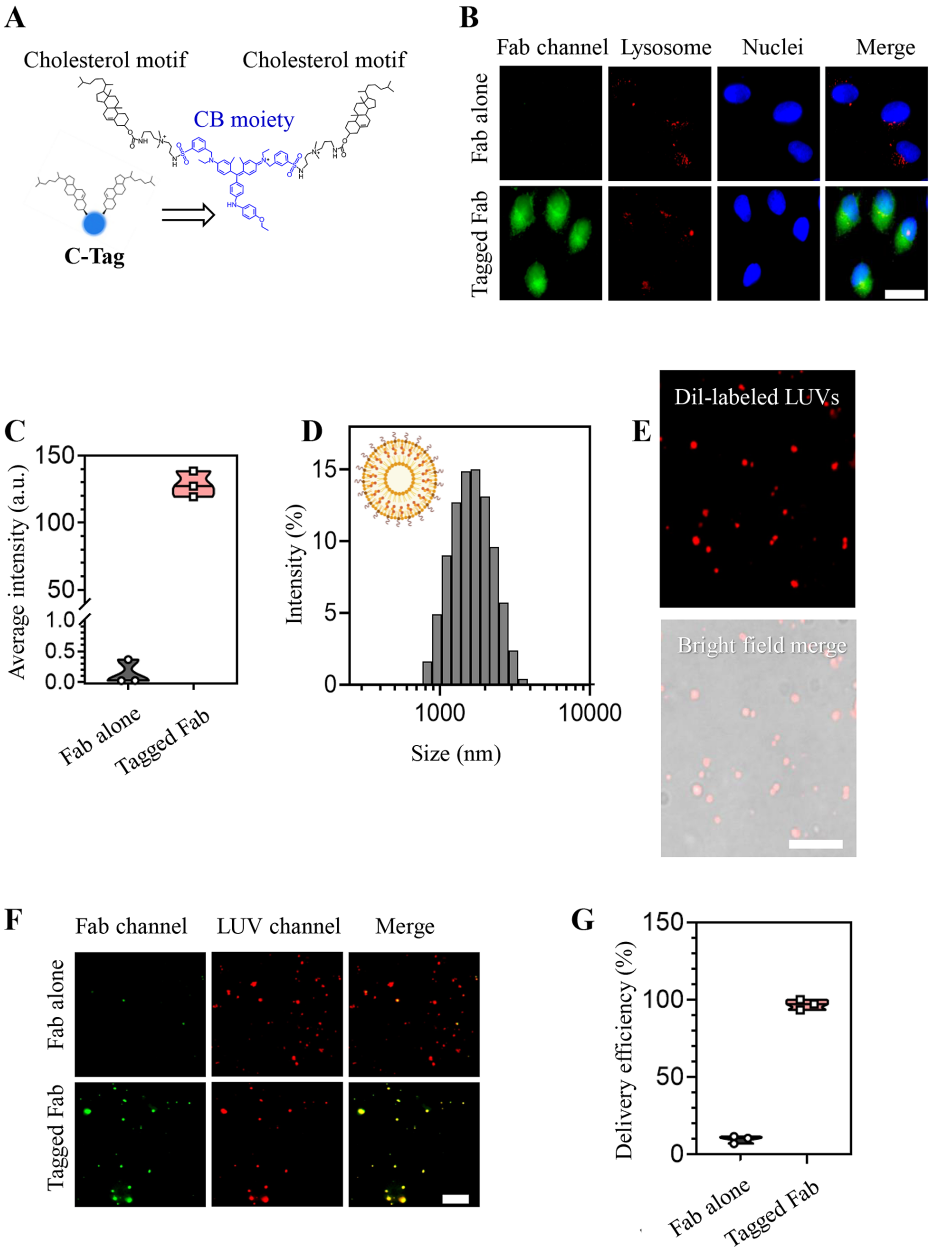

Figure 2. Verification of the C-Tag-based transmembrane transport system. (A). The structural formula of the noncovalent cholesterol tag (C-Tag). C-Tag consisted of a CB G250 and two copies of cholesterol molecules. **(B)** and **(C)**. Fluorescent images and quantitative analysis verified the efficiency of intracellular (transmembrane) transport of proteins in this system. HeLa cells (a human cervical carcinoma cell line) were used in experiments. Fab was labeled with Alexa Fluor488® (green), and lysosomes were stained with LysoTracker Red (red). Bar: 20 μm. **(D)**. Size and morphology of the micron-scale LUVs. **(E)**. The LUVs were stained with the lipophilic tracer Dil (red). Bar: 10 μm. **(F)** and **(G)**. Evaluating the efficiency of filling the LUVs with high-dose proteins. Fab was labeled with Alexa Fluor488® (green), and the LUVs were stained with Dil (red). Bar: 10 μm.

antibodies might be optimal candidates for the validation of C-Tag-mediated cytosolic delivery since Fab is known to engage in antigen recognition along with binding during the immune response. As shown in Figure 2B, the tagged Fab displayed bright and homogeneous intracellular fluorescence without apparent punctate bright spots or lysosome co-localization (manifestations of endocytosis, protein drugs may aggregate in the lysosome and be inactivated by enzymolysis). These results indicated a special pattern of Fab distribution within the cytoplasm *via* direct membrane permeation rather than endocytosis in the living cells. Importantly, the tagged Fab achieved a 902-fold increase in protein internalization (*vs*. Fab alone) and little Fab distribution in lysosomes, so endocytic sequestration and subsequent lysosomal hydrolysis were fundamentally avoided (Figure 2C). Thus, the C-Tag effectively avoids endocytosis and induces cytosolic delivery of proteins, thus providing a novel but useful pathway to achieve effective transmembrane transport of protein drugs while also, importantly, satisfactorily maintaining both the integrity and bioactivities of these protein drugs. In this

regard, C-Tag represents an advanced transmembrane technology to deliver protein drugs into cells for them to be efficacious by intervening in intracellular targets while avoiding endocytic sequestration.

The second technological problem is to achieve intraparticle delivery for high-dose proteins, and this can be addressed by designing a nano-particle that enables encapsulation of high-dose proteins to achieve satisfactory delivery efficiency and bioavailability (Figure 1B). Accordingly, micron-scale large unilamellar vesicles (LUVs) were prepared by thin film hydration followed by repeated extrusions. In brief, 1,2-dipalmitoyl-sn-glycero-3-phosphocholine (DPPC), 1,2-distearoyl-sn-glycero-3-phosphoethanolamine-N-[carboxy(polyethylene glycol)-2000] (DSPE-PEG), and cholesterol were dissolved in a chloroform solution, and a thin film was formed using a rotary evaporator. The film was subsequently hydrated in a 4% ethanol aqueous solution and sonicated and repeatedly extruded with a mini extruder (pore diameter = 1.0 μm). The bilayer LUVs had a hydrodynamic size of 1.5 ± 0.2 μm (Figure 2D). Observed with fluorescent microscopy, the LUVs (stained with Dil) exhibited excellent spherical morphology, a uniform size, and uniform dispersion in the aqueous solution (Figure 2E), indicating that the LUVs might be a satisfactory candidate for protein drug encapsulation. To investigate whether LUVs can encapsulate proteins *via* C-Tag-mediated protein transportation, the efficiency with which a given amount of Fab was internalized into LUVs *via* cholesterol tagging was evaluated. As shown as in Figures 2F and G, Fab alone barely co-localized with LUVs, indicating poor internalization of Fab into the cavity of LUVs. However, C-tagged Fab greatly enhanced (above 10-fold) internalization of proteins into LUVs (Figures 2F and G). Thus, the intraparticle delivery of high-dose proteins was achieved.

3. Insights and future perspectives

Reported here is a novel C-Tag-based transmembrane transport system that has addressed two existing technological difficulties. When this noncovalent cholesterol tagging technique was used, preliminary data proved that this C-Tag-based transmembrane tool provided effective transport of protein drugs into both the cytoplasm and the LUVs (particularly for loading high-dose protein). To the extent known, this is the first lipid-based transmembrane tool that has addressed these two technological difficulties. First, this novel technology enables the transport of proteins directly into cytosols and it avoids endocytic sequestration. When C-Tag mixes with proteins, the CB moiety of C-Tag non-covalently anchors onto the protein surface and facilitates protein insertion into the lipid bilayers of cell membranes. This allows proteins to dissociate from the bilayers and enter the cytoplasm rather than *via* endocytosis (Figure 1A). Hence, this technology has three advantages in terms of transmembrane transport: *i*) avoiding cell endocytosis, *ii*) sustaining cell integrity (no transient poles are required), *iii*) importantly, maintaining the protein bioactivity. Second, LUVs were used to create particles to verify the efficiency with which C-Tag filled particles with high-dose proteins (Figure 1B). Thanks to the concept of C-Tag technology, all technological difficulties were overcome, and transmembrane transport even of high-dose proteins was achieved. Overcoming the barriers in the cellular membrane and loading enough protein drugs into nanoparticles is important. Thus, this technology might provide a novel and powerful platform for medicine design. Due to the "refractory" nature of some diseases, intervention in intracellular targets, and particularly cytosolic targets, might be an ultimate solution (*vs*. conventional treatments). In this context, the technology described in this study may kindle the flame of hope to change the clinical outcomes for these patients from "incurable" to "treatable".

The clinical use of this C-Tag-based transmembrane transport system is highly anticipated, but its safety, efficacy, and indications are still unknown. A future study will focus on further verification of this system *in vitro* and *in vivo*. Even though thus is a promising platform for designing novel lipid-based micro-nano medicines, exploring its indications is also crucial.

Funding: This work was supported by the National Natural Science Foundation of China (nos. 82372271, 62005176, 82070420), the Shenzhen Science and Technology Program (nos. JCYJ20220530163005012, JCYJ20210324115611032), the Key Area Projects for Universities in Guangdong Province (2022DZX2022), the Shenzhen Scientific and Technological Foundation (nos. JSGG20220606141001003 and JSGG20220301090005007), the Third People's Hospital of Shenzhen Foundation (no. 22240G1001), and the Shenzhen High-level Hospital Construction Fund (No.23274G1001).

Conflict of Interest: The authors have no conflicts of interest to disclose.

References

1. Gudinas AP, Mai DJ. Polymeric protagonists for biological processes. Nat Chem. 2023; 15:751-752.
2. Yu S, Yang H, Li T, *et al*. Efficient intracellular delivery of proteins by a multifunctional chimaeric peptide *in vitro* and *in vivo*. Nat Commun. 2021; 12:5131.
3. Qin W, Shi Y, Chen W, Jia X, Asakawa T. Can kynurenine pathway be considered as a next-generation therapeutic target for Parkinson's disease? An update information. Biosci Trends. 2022; 16:249-256.
4. Vogel JW, Iturria-Medina Y, Strandberg OT, Smith R, Levitis E, Evans AC, Hansson O, Alzheimer's Disease Neuroimaging I, Swedish BioFinder S. Spread of pathological tau proteins through communicating neurons in human Alzheimer's disease. Nat Commun. 2020;

11:2612.
5. Wang X, Huang H, Zhu Y, Li S, Zhang P, Jiang J, Xi C, Wu L, Gao X, Fu Y, Zhang D, Chen Y, Hu S, Lai J. Metformin acts on the gut-brain axis to ameliorate antipsychotic-induced metabolic dysfunction. Biosci Trends. 2021; 15:321-329.
6. Huang Y, Liu Y, Li Y, Liu Y, Zhang C, Wen H, Zhao L, Song Y, Wang L, Wang Z. Role of key amino acids in the transmembrane domain of the Newcastle disease virus fusion protein. Biosci Trends. 2021; 15:16-23.
7. Raman V, Van Dessel N, Hall CL, Wetherby VE, Whitney SA, Kolewe EL, Bloom SMK, Sharma A, Hardy JA, Bollen M, Van Eynde A, Forbes NS. Intracellular delivery of protein drugs with an autonomously lysing bacterial system reduces tumor growth and metastases. Nat Commun. 2021; 12:6116.
8. Slastnikova TA, Ulasov AV, Rosenkranz AA, Sobolev AS. Targeted intracellular delivery of antibodies: The state of the art. Front Pharmacol. 2018; 9:1208.
9. Gong S, Ma J, Tian A, Lang S, Luo Z, Ma X. Effects and mechanisms of microenvironmental acidosis on osteoclast biology. Biosci Trends. 2022; 16:58-72.
10. Parolo C, Idili A, Ortega G, Csordas A, Hsu A, Arroyo-Curras N, Yang Q, Ferguson BS, Wang J, Plaxco KW. Real-time monitoring of a protein biomarker. ACS Sens. 2020; 5:1877-1881.
11. Harroun SG, Lauzon D, Ebert M, Desrosiers A, Wang X, Vallee-Belisle A. Monitoring protein conformational changes using fluorescent nanoantennas. Nat Methods. 2022; 19:71-80.
12. Wong FK, Haffner C, Huttner WB, Taverna E. Microinjection of membrane-impermeable molecules into single neural stem cells in brain tissue. Nat Protoc. 2014; 9:1170-1182.
13. Sherba JJ, Hogquist S, Lin H, Shan JW, Shreiber DI, Zahn JD. The effects of electroporation buffer composition on cell viability and electro-transfection efficiency. Sci Rep. 2020; 10:3053.
14. Sharei A, Zoldan J, Adamo A, *et al*. A vector-free microfluidic platform for intracellular delivery. Proc Natl Acad Sci U S A. 2013; 110:2082-2087.
15. Mitchell MJ, Billingsley MM, Haley RM, Wechsler ME, Peppas NA, Langer R. Engineering precision nanoparticles for drug delivery. Nat Rev Drug Discov. 2021; 20:101-124.
16. Qin Y, Wang G, Chen L, Sun Y, Yang J, Piao Y, Shen Y, Zhou Z. High throughput screening of surface engineered cyanine nanodots for active transport of therapeutic antibody into solid tumor. Adv Mater. 2023;e2302292.
17. Wang M, Zuris JA, Meng F, Rees H, Sun S, Deng P, Han Y, Gao X, Pouli D, Wu Q, Georgakoudi I, Liu DR, Xu Q. Efficient delivery of genome-editing proteins using bioreducible lipid nanoparticles. Proc Natl Acad Sci U S A. 2016; 113:2868-2873.
18. Shalek AK, Robinson JT, Karp ES, Lee JS, Ahn DR, Yoon MH, Sutton A, Jorgolli M, Gertner RS, Gujral TS, MacBeath G, Yang EG, Park H. Vertical silicon nanowires as a universal platform for delivering biomolecules into living cells. Proc Natl Acad Sci U S A. 2010; 107:1870-1875.
19. Tai W, Zhao P, Gao X. Cytosolic delivery of proteins by cholesterol tagging. Sci Adv. 2020; 6:eabb0310.
20. Zhao P, Liu S, Koriath AT, Gao X. Partial magneto-endosomalysis for cytosolic delivery of antibodies. Bioconjug Chem. 2022; 33:363-368.

Received November 1, 2023; Revised December 2, 2023; Accepted December 5, 2023.

[§]These authors contributed equally to this work.
**Address correspondence to:*
Tetsuya Asakawa and Mingbin Zheng, Institute of Neurology, National Clinical Research Center for Infectious Diseases, the Third People's Hospital of Shenzhen, 29 Bulan Road, Shenzhen, Guangdong 518112, China.
E-mail: asakawat1971@gmail.com (TA); mingbinzheng@126.com (MZ)

Hongzhou Lu, Department of Infectious Diseases, National Clinical Research Center for Infectious Diseases, the Third People's Hospital of Shenzhen, 29 Bulan Road, Shenzhen, Guangdong 518112, China.
E-mail: luhongzhou@fudan.edu.cn

Released online in J-STAGE as advance publication December 8, 2023.

DOI: 10.5582/bst.2023.E1

Corrigendum

Corrigendum to "Shufengjiedu capsules protect against neuronal loss in olfactory epithelium and lung injury by enhancing autophagy in rats with allergic rhinitis", *BioScience Trends*. 2019; 13(6):530-538. doi: 10.5582/bst.2019.01332.

This corrigendum corrects error that was inadvertently introduced in Figure 1D. The corrected Figure 1 shown below. This correction does not alter the conclusion of this article. The authors deeply apologize for the oversight and any inconvenience it may have caused.

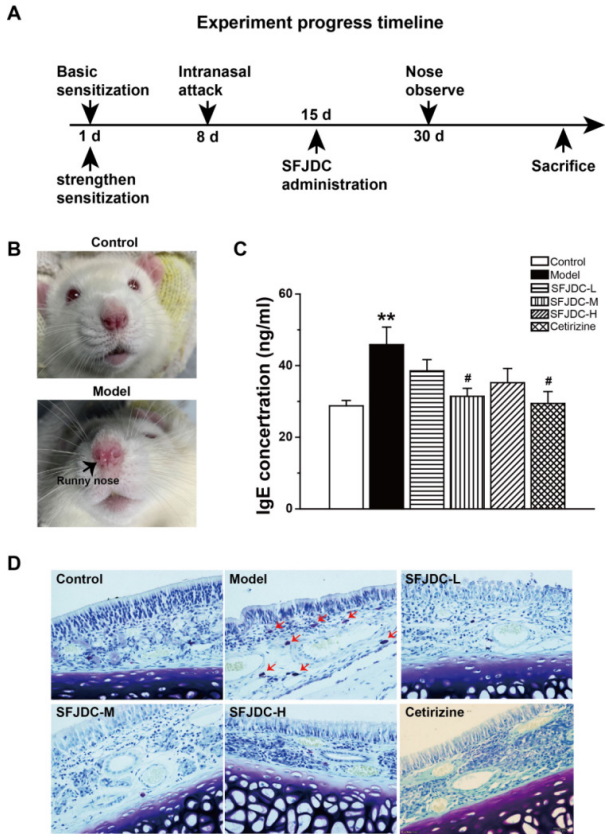

Figure 1. SFJDCs reduced levels of IgE and the number of mast cells in rats with AR. (A): Schematic overview of the study design. **(B)**: Watery rhinorrhea in the model group. **(C)**: Bar graph of the IgE level in serum according to ELISA. **(D)**: Toluidine blue staining of OE from different groups. Arrows indicate mast cells. Data are representative of at least three separate experiments. (**$p < 0.01$ *vs*. control group; #$p < 0.05$ *vs*. model group).

DOI: 10.5582/bst.2023.E2

Corrigendum

Corrigendum to "Hepatic stellate cell exosome-derived circWDR25 promotes the progression of hepatocellular carcinoma via the miRNA-4474-3P-ALOX-15 and EMT axes", *BioScience Trends*. 2022; 16(4):267-281. DOI: 10.5582/bst.2022.01281.

This corrigendum corrects error that was inadvertently introduced in Figure 6F (c) and (f). The corrected Figure 6 shown below. This correction does not alter the conclusion of this article. The authors deeply apologize for the oversight and any inconvenience it may have caused.

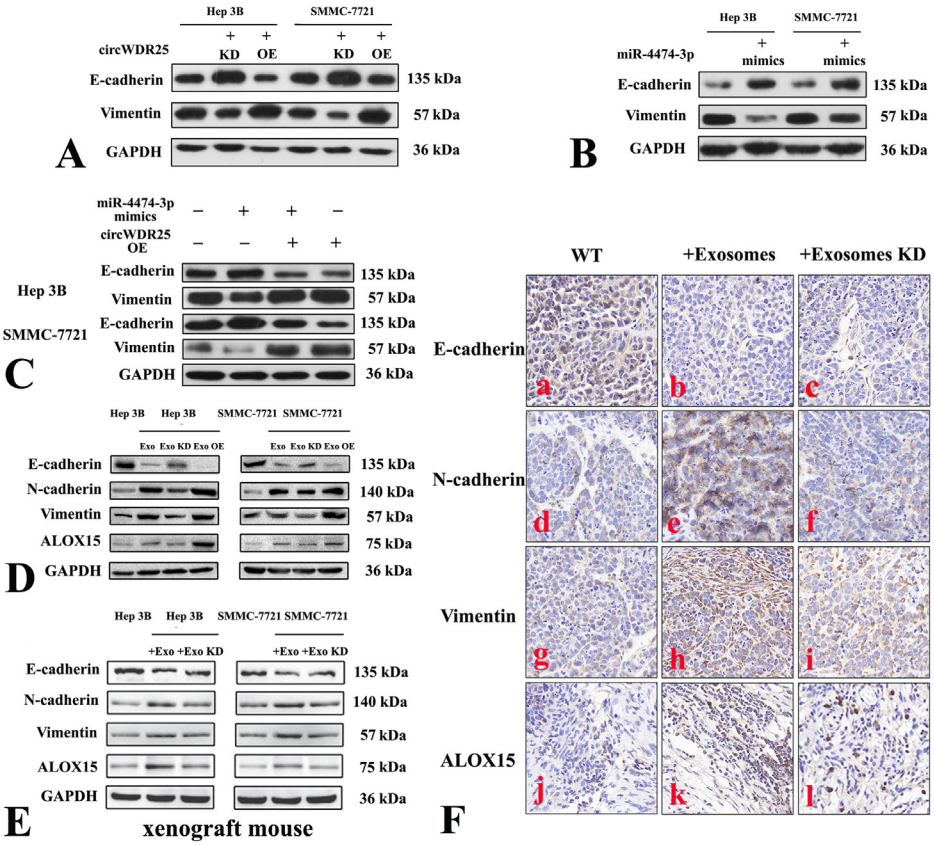

Figure 6. Exogenous and HSC exosome-derived circWDR25 induce epithelial-to-mesenchymal transition (EMT). A-B: The levels of expression of EMT marker proteins in HCC cells as were affected by circWDR25KD, circWDR25OE, or miR-4474-3p mimics were determined using Western blot analysis. **C:** The relative expression of EMT marker proteins in HCC cells as was affected by circWDR25KD, miR-4474-3p mimics, or a combination of the two. **D:** The levels of expression of EMT marker and ALOX15 proteins in HCC cells cultured with HSC-derived exosome circWDR25KD or circWDR25OE. **E:** The levels of expression of EMT marker and ALOX15 proteins in tumors of xenograft mice injected with HSC-derived exosomal circWDR25KD. **F:** Representative images of IHC staining of mouse tumors revealed the effects of exosomal circWDR25KD from HSCs on the EMT markers and ALOX15 (400× magnification).

BST
BioScience Trends

Guide for Authors

1. Scope of Articles

BioScience Trends (Print ISSN 1881-7815, Online ISSN 1881-7823) is an international peer-reviewed journal. *BioScience Trends* devotes to publishing the latest and most exciting advances in scientific research. Articles cover fields of life science such as biochemistry, molecular biology, clinical research, public health, medical care system, and social science in order to encourage cooperation and exchange among scientists and clinical researchers.

2. Submission Types

Original Articles should be well-documented, novel, and significant to the field as a whole. An Original Article should be arranged into the following sections: Title page, Abstract, Introduction, Materials and Methods, Results, Discussion, Acknowledgments, and References. Original articles should not exceed 5,000 words in length (excluding references) and should be limited to a maximum of 50 references. Articles may contain a maximum of 10 figures and/or tables. Supplementary Data are permitted but should be limited to information that is not essential to the general understanding of the research presented in the main text, such as unaltered blots and source data as well as other file types.

Brief Reports definitively documenting either experimental results or informative clinical observations will be considered for publication in this category. Brief Reports are not intended for publication of incomplete or preliminary findings. Brief Reports should not exceed 3,000 words in length (excluding references) and should be limited to a maximum of 4 figures and/or tables and 30 references. A Brief Report contains the same sections as an Original Article, but the Results and Discussion sections should be combined.

Reviews should present a full and up-to-date account of recent developments within an area of research. Normally, reviews should not exceed 8,000 words in length (excluding references) and should be limited to a maximum of 10 figures and/or tables and 100 references. Mini reviews are also accepted, which should not exceed 4,000 words in length (excluding references) and should be limited to a maximum of 5 figures and/or tables and 50 references.

Policy Forum articles discuss research and policy issues in areas related to life science such as public health, the medical care system, and social science and may address governmental issues at district, national, and international levels of discourse. Policy Forum articles should not exceed 3,000 words in length (excluding references) and should be limited to a maximum of 5 figures and/or tables and 30 references.

Communications are short, timely pieces that spotlight new research findings or policy issues of interest to the field of global health and medical practice that are of immediate importance. Depending on their content, Communications will be published as "Comments" or "Correspondence". Communications should not exceed 1,500 words in length (excluding references) and should be limited to a maximum of 2 figures and/or tables and 20 references.

Editorials are short, invited opinion pieces that discuss an issue of immediate importance to the fields of global health, medical practice, and basic science oriented for clinical application. Editorials should not exceed 1,000 words in length (excluding references) and should be limited to a maximum of 10 references. Editorials may contain one figure or table.

News articles should report the latest events in health sciences and medical research from around the world. News should not exceed 500 words in length.

Letters should present considered opinions in response to articles published in *BioScience Trends* in the last 6 months or issues of general interest. Letters should not exceed 800 words in length and may contain a maximum of 10 references. Letters may contain one figure or table.

3. Editorial Policies

For publishing and ethical standards, *BioScience Trends* follows the Recommendations for the Conduct, Reporting, Editing, and Publication of Scholarly Work in Medical Journals issued by the International Committee of Medical Journal Editors (ICMJE, *https://icmje.org/recommendations*), and the Principles of Transparency and Best Practice in Scholarly Publishing jointly issued by the Committee on Publication Ethics (COPE, *https://publicationethics.org/resources/guidelines-new/principles-transparency-and-best-practice-scholarly-publishing*), the Directory of Open Access Journals (DOAJ, *https://doaj.org/apply/transparency*), the Open Access Scholarly Publishers Association (OASPA, *https://oaspa.org/principles-of-transparency-and-best-practice-in-scholarly-publishing-4*), and the World Association of Medical Editors (WAME, *https://wame.org/principles-of-transparency-and-best-practice-in-scholarly-publishing*).

BioScience Trends will perform an especially prompt review to encourage innovative work. All original research will be subjected to a rigorous standard of peer review and will be edited by experienced copy editors to the highest standards.

Ethical Approval of Studies and Informed Consent: For all manuscripts reporting data from studies involving human participants or animals, formal review and approval, or formal review and waiver, by an appropriate institutional review board or ethics committee is required and should be described in the Methods section. When your manuscript contains any case details, personal information and/or images of patients or other individuals, authors must obtain appropriate written consent, permission and release in order to comply with all applicable laws and regulations concerning privacy and/or security of personal information. The consent form needs to comply with the relevant legal requirements of your particular jurisdiction, and please do not send signed consent form to *BioScience Trends* to respect your patient's and any other individual's privacy. Please instead describe the information clearly in the Methods (patient consent) section of your manuscript while retaining copies of the signed forms in the event they should be needed. Authors should also state that the study conformed to the provisions of the Declaration of Helsinki (as revised in 2013, *https://wma.net/what-we-do/medical-ethics/declaration-of-helsinki*). When reporting experiments on animals, authors should indicate whether the institutional and national guide for the care and use of laboratory animals was followed.

Reporting Clinical Trials: The ICMJE (*https:// icmje.org/recommendations/browse/publishing-and-editorial-issues/clinical-trial-registration.html*) defines a clinical trial as any research project that prospectively assigns people or a group of people to an intervention, with or without concurrent comparison or control groups, to study the relationship between a health-related intervention and a health outcome. Registration of clinical trials in a public trial registry at or before the time of first patient enrollment is a condition of consideration for publication in *BioScience Trends*, and the trial registration number will be published at the end of the Abstract. The registry must be independent of for-profit interest and publicly accessible. Reports of trials must conform to CONSORT 2010 guidelines (*https://consort-statement.org/consort-2010*). Articles reporting the results of randomized trials must include the CONSORT flow diagram showing the progress of patients throughout the trial.

Conflict of Interest: All authors are required to disclose any actual or potential conflict of interest including financial interests or relationships with other people or organizations that might raise questions of bias

in the work reported. If no conflict of interest exists for each author, please state "There is no conflict of interest to disclose".

Submission Declaration: When a manuscript is considered for submission to *BioScience Trends*, the authors should confirm that 1) no part of this manuscript is currently under consideration for publication elsewhere; 2) this manuscript does not contain the same information in whole or in part as manuscripts that have been published, accepted, or are under review elsewhere, except in the form of an abstract, a letter to the editor, or part of a published lecture or academic thesis; 3) authorization for publication has been obtained from the authors' employer or institution; and 4) all contributing authors have agreed to submit this manuscript.

Initial Editorial Check: Immediately after submission, the journal's managing editor will perform an initial check of the manuscript. A suitable academic editor will be notified of the submission and invited to check the manuscript and recommend reviewers. Academic editors will check for plagiarism and duplicate publication at this stage. The journal has a formal recusal process in place to help manage potential conflicts of interest of editors. In the event that an editor has a conflict of interest with a submitted manuscript or with the authors, the manuscript, review, and editorial decisions are managed by another designated editor without a conflict of interest related to the manuscript.

Peer Review: *BioScience Trends* operates a single-anonymized review process, which means that reviewers know the names of the authors, but the authors do not know who reviewed their manuscript. All articles are evaluated objectively based on academic content. External peer review of research articles is performed by at least two reviewers, and sometimes the opinions of more reviewers are sought. Peer reviewers are selected based on their expertise and ability to provide quality, constructive, and fair reviews. For research manuscripts, the editors may, in addition, seek the opinion of a statistical reviewer. Every reviewer is expected to evaluate the manuscript in a timely, transparent, and ethical manner, following the COPE guidelines (*https://publicationethics.org/files/cope-ethical-guidelines-peer-reviewers-v2_0.pdf*). We ask authors for sufficient revisions (with a second round of peer review, when necessary) before a final decision is made. Consideration for publication is based on the article's originality, novelty, and scientific soundness, and the appropriateness of its analysis.

Suggested Reviewers: A list of up to 3 reviewers who are qualified to assess the scientific merit of the study is welcomed. Reviewer information including names, affiliations, addresses, and e-mail should be provided at the same time the manuscript is submitted online. Please do not suggest reviewers with known conflicts of interest, including participants or anyone with a stake in the proposed research; anyone from the same institution; former students, advisors, or research collaborators (within the last three years); or close personal contacts. Please note that the Editor-in-Chief may accept one or more of the proposed reviewers or may request a review by other qualified persons.

Language Editing: Manuscripts prepared by authors whose native language is not English should have their work proofread by a native English speaker before submission. If not, this might delay the publication of your manuscript in *BioScience Trends*.

The Editing Support Organization can provide English proofreading, Japanese-English translation, and Chinese-English translation services to authors who want to publish in *BioScience Trends* and need assistance before submitting a manuscript. Authors can visit this organization directly at *https://www.iacmhr.com/iac-eso/support.php?lang=en*. IAC-ESO was established to facilitate manuscript preparation by researchers whose native language is not English and to help edit works intended for international academic journals.

Copyright and Reuse: Before a manuscript is accepted for publication in *BioScience Trends*, authors will be asked to sign a transfer of copyright agreement, which recognizes the common interest that both the journal and author(s) have in the protection of copyright. We accept that some authors (*e.g.*, government employees in some countries) are unable to transfer copyright. A JOURNAL PUBLISHING AGREEMENT (JPA) form will be e-mailed to the authors by the Editorial Office and must be returned by the authors by mail, fax, or as a scan. Only forms with a hand-written signature from the corresponding author are accepted. This copyright will ensure the widest possible dissemination of information. Please note that the manuscript will not proceed to the next step in publication until the JPA Form is received. In addition, if excerpts from other copyrighted works are included, the author(s) must obtain written permission from the copyright owners and credit the source(s) in the article.

4. Cover Letter

The manuscript must be accompanied by a cover letter prepared by the corresponding author on behalf of all authors. The letter should indicate the basic findings of the work and their significance. The letter should also include a statement affirming that all authors concur with the submission and that the material submitted for publication has not been published previously or is not under consideration for publication elsewhere. The cover letter should be submitted in PDF format. For an example of Cover Letter, please visit: *https://www.biosciencetrends.com/downcentre* (Download Centre).

5. Submission Checklist

The Submission Checklist should be submitted when submitting a manuscript through the Online Submission System. Please visit Download Centre (*https://www.biosciencetrends.com/downcentre*) and download the Submission Checklist file. We recommend that authors use this checklist when preparing your manuscript to check that all the necessary information is included in your article (if applicable), especially with regard to Ethics Statements.

6. Manuscript Preparation

Manuscripts are suggested to be prepared in accordance with the "Recommendations for the Conduct, Reporting, Editing, and Publication of Scholarly Work in Medical Journals", as presented at *https://www.ICMJE.org*.

Manuscripts should be written in clear, grammatically correct English and submitted as a Microsoft Word file in a single-column format. Manuscripts must be paginated and typed in 12-point Times New Roman font with 24-point line spacing. Please do not embed figures in the text. Abbreviations should be used as little as possible and should be explained at first mention unless the term is a well-known abbreviation (*e.g.* DNA). Single words should not be abbreviated.

Title page: The title page must include 1) the title of the paper (Please note the title should be short, informative, and contain the major key words); 2) full name(s) and affiliation(s) of the author(s), 3) abbreviated names of the author(s), 4) full name, mailing address, telephone/fax numbers, and e-mail address of the corresponding author; 5) author contribution statements to specify the individual contributions of all authors to this manuscript, and 6) conflicts of interest (if you have an actual or potential conflict of interest to disclose, it must be included as a footnote on the title page of the manuscript; if no conflict of interest exists for each author, please state "There is no conflict of interest to disclose").

Abstract: The abstract should briefly state the purpose of the study, methods, main findings, and conclusions. For articles that are Original Articles, Brief Reports, Reviews, or Policy Forum articles, a one-paragraph abstract consisting of no more than 250 words must be included in the manuscript. For Communications, Editorials, News, or Letters, a brief summary of main content in 150 words or fewer should be included in the manuscript. For articles reporting clinical trials, the trial registration number should be stated at the end of the Abstract. Abbreviations must be kept to a minimum and non-standard

abbreviations explained in brackets at first mention. References should be avoided in the abstract. Three to six key words or phrases that do not occur in the title should be included in the Abstract page.

Introduction: The introduction should provide sufficient background information to make the article intelligible to readers in other disciplines and sufficient context clarifying the significance of the experimental findings

Materials/Patients and Methods: The description should be brief but with sufficient detail to enable others to reproduce the experiments. Procedures that have been published previously should not be described in detail but appropriate references should simply be cited. Only new and significant modifications of previously published procedures require complete description. Names of products and manufacturers with their locations (city and state/country) should be given and sources of animals and cell lines should always be indicated. All clinical investigations must have been conducted in accordance Materials/ Patients and Methods.

Results: The description of the experimental results should be succinct but in sufficient detail to allow the experiments to be analyzed and interpreted by an independent reader. If necessary, subheadings may be used for an orderly presentation. All Figures and Tables should be referred to in the text in order, including those in the Supplementary Data.

Discussion: The data should be interpreted concisely without repeating material already presented in the Results section. Speculation is permissible, but it must be well-founded, and discussion of the wider implications of the findings is encouraged. Conclusions derived from the study should be included in this section.

Acknowledgments: All funding sources (including grant identification) should be credited in the Acknowledgments section. Authors should also describe the role of the study sponsor(s), if any, in study design; in the collection, analysis, and interpretation of data; in the writing of the report; and in the decision to submit the paper for publication. If the funding source had no such involvement, the authors should so state.

In addition, people who contributed to the work but who do not meet the criteria for authors should be listed along with their contributions.

References: References should be numbered in the order in which they appear in the text. Citing of unpublished results, personal communications, conference abstracts, and theses in the reference list is not recommended but these sources may be mentioned in the text. In the reference list, cite the names of all authors when there are fifteen or fewer authors; if there are sixteen or more authors, list the first three followed by *et al*. Names of journals should be abbreviated in the style used in PubMed. Authors are responsible for the accuracy of the references. The EndNote Style of *BioScience Trends* could be downloaded at **EndNote** (*https://ircabssagroup.com/examples/BioScience_Trends.ens*).

Examples are given below:

Example 1 (Sample journal reference):

Inagaki Y, Tang W, Zhang L, Du GH, Xu WF, Kokudo N. Novel aminopeptidase N (APN/CD13) inhibitor 24F can suppress invasion of hepatocellular carcinoma cells as well as angiogenesis. Biosci Trends. 2010; 4:56-60.

Example 2 (Sample journal reference with more than 15 authors):

Darby S, Hill D, Auvinen A, *et al*. Radon in homes and risk of lung cancer: Collaborative analysis of individual data from 13 European case-control studies. BMJ. 2005; 330:223.

Example 3 (Sample book reference):

Shalev AY. Post-traumatic stress disorder: Diagnosis, history and life course. In: Post-traumatic Stress Disorder, Diagnosis, Management and Treatment (Nutt DJ, Davidson JR, Zohar J, eds.). Martin Dunitz, London, UK, 2000; pp. 1-15.

Example 4 (Sample web page reference):

World Health Organization. The World Health Report 2008 – primary health care: Now more than ever. *http://www.who.int/whr/2008/whr08_en.pdf* (accessed September 23, 2022).

Tables: All tables should be prepared in Microsoft Word or Excel and should be arranged at the end of the manuscript after the References section. Please note that tables should not in image format. All tables should have a concise title and should be numbered consecutively with Arabic numerals. If necessary, additional information should be given below the table.

Figure Legend: The figure legend should be typed on a separate page of the main manuscript and should include a short title and explanation. The legend should be concise but comprehensive and should be understood without referring to the text. Symbols used in figures must be explained. Any individually labeled figure parts or panels (A, B, *etc*.) should be specifically described by part name within the legend.

Figure Preparation: All figures should be clear and cited in numerical order in the text. Figures must fit a one- or two-column format on the journal page: 8.3 cm (3.3 in.) wide for a single column, 17.3 cm (6.8 in.) wide for a double column; maximum height: 24.0 cm (9.5 in.). Please make sure that the symbols and numbers appeared in the figures should be clear. Please make sure that artwork files are in an acceptable format (TIFF or JPEG) at minimum resolution (600 dpi for illustrations, graphs, and annotated artwork, and 300 dpi for micrographs and photographs). Please provide all figures as separate files. Please note that low-resolution images are one of the leading causes of article resubmission and schedule delays.

Units and Symbols: Units and symbols conforming to the International System of Units (SI) should be used for physicochemical quantities. Solidus notation (*e.g.* mg/kg, mg/mL, mol/mm^2/min) should be used. Please refer to the SI Guide *www.bipm.org/en/si/* for standard units.

Supplemental data: Supplemental data might be useful for supporting and enhancing your scientific research and *BioScience Trends* accepts the submission of these materials which will be only published online alongside the electronic version of your article. Supplemental files (figures, tables, and other text materials) should be prepared according to the above guidelines, numbered in Arabic numerals (*e.g.*, Figure S1, Figure S2, and Table S1, Table S2) and referred to in the text. All figures and tables should have titles and legends. All figure legends, tables and supplemental text materials should be placed at the end of the paper. Please note all of these supplemental data should be provided at the time of initial submission and note that the editors reserve the right to limit the size and length of Supplemental Data.

5. Submission Checklist

The Submission Checklist will be useful during the final checking of a manuscript prior to sending it to *BioScience Trends* for review. Please visit Download Centre and download the Submission Checklist file.

6. Online Submission

Manuscripts should be submitted to *BioScience Trends* online at *https://www.biosciencetrends.com/login*. Receipt of your manuscripts submitted online will be acknowledged by an e-mail from Editorial Office containing a reference number, which should be used in all future communications. If for any reason you are unable to submit a file online, please contact the Editorial Office by e-mail at *office@biosciencetrends.com*

8. Accepted Manuscripts

Page Charge: Page charges will be levied on all manuscripts accepted for publication in *BioScience Trends* (Original Articles / Brief Reports / Reviews / Policy Forum / Communications: $140 per page for black white pages, $340 per page for color pages; News / Letters: a total cost of $600). Under exceptional circumstances, the author(s) may apply to the editorial office for a waiver of the publication charges by stating the reason in the Cover Letter when the manuscript online.

Misconduct: *BioScience Trends* takes seriously all allegations of potential misconduct and adhere to the ICMJE Guideline (*https://icmje.org/recommendations*) and COPE Guideline (*https://publicationethics.org/files/Code_of_conduct_for_journal_editors.pdf*). In cases of suspected research or publication misconduct, it may be necessary for the Editor or Publisher to contact and share submission details with third parties including authors' institutions and ethics committees. The corrections, retractions, or editorial expressions of concern will be performed in line with above guidelines.

(As of December 2022)

BioScience Trends
Editorial and Head Office
Pearl City Koishikawa 603,
2-4-5 Kasuga, Bunkyo-ku,
Tokyo 112-0003, Japan.
E-mail: office@biosciencetrends.com